

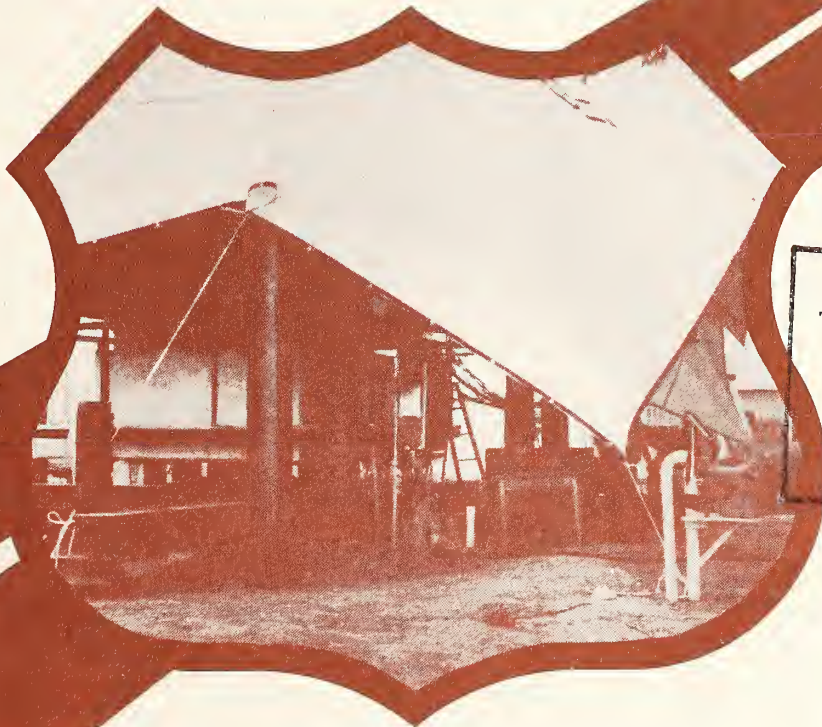
PB 81 249145

TE
662
.A3
no.
FHWA-
RD-
81-002

rt No. FHWA/RD-81/002

LD STUDY OF PILE GROUP ACTION

March 1981
Final Report



DEPARTMENT OF
TRANSPORTATION
MAY 11 1982
LIBRARY

Document is available to the public through
the National Technical Information Service,
Springfield, Virginia 22161



Prepared for
FEDERAL HIGHWAY ADMINISTRATION
Offices of Research & Development
Materials Division
Washington, D.C. 20590

FOREWORD

This report presents the results of a comprehensive research program to investigate the behavior of a vertically loaded pile group in stiff clay. The study included the development and verification of a mathematical model for pile group analysis, extensive pile and ground instrumentation, and 17 pile load tests to failure on single piles and pile groups.

The work reported resulted from FCP Project 4H Study, "A Field Study of Pile Group Action," conducted by Raymond International Builders, Inc. The research was performed under DOT-FH-11-9526 during the period October 1, 1978, to November 18, 1980.

In addition to the final report supporting documents are available upon request in the form of appendices to the final report, an interim report which describes the mathematical model chosen for detailed analysis and presents a priori analysis of group behavior, and a report on the analysis of dynamic measurements taken during driving the 11 test piles.

Copies of the final report are being distributed by the Materials Division, Office of Research, to other researchers and to appropriate members of the FCP Project 4H team.


Charles F. Schettley
Director, Office of Research
Federal Highway Administration

NOTICE

This document is disseminated under the sponsorship of the Department of Transportation in the interest of information exchange. The United States Government assumes no liability for its contents or use thereof.

The contents of this report reflect the views of the authors who are responsible for the facts and the accuracy of data presented herein. The contents do not necessarily reflect the official view of the Department of Transportation. This report does not constitute a standard, specification, or regulation.

The United States Government does not endorse products or manufacturers. Trade or manufacturers' names appear herein only because they are considered essential to the object of this document.

662
 .A3
 no.
 FHWA -
 RD -
 81-002

1. Report No. FHWA/RD-81/002		2. Government Accession No.		3. Recipient's Catalog No.	
4. Title and Subtitle FIELD STUDY OF PILE GROUP ACTION				5. Report Date March 1981	
				6. Performing Organization Code	
				8. Performing Organization Report No.	
7. Author(s) M. W. O'Neill, R. A. Hawkins, and L. J. Mahar					
9. Performing Organization Name and Address RAYMOND INTERNATIONAL BUILDERS, INC. 2801 SOUTH POST OAK RD HOUSTON, TEXAS 77027				10. Work Unit No. (TRAIS) FCP 34H2-012	
				11. Contract or Grant No. DOT-FH-11-9526	
				13. Type of Report and Period Covered Final Report	
12. Sponsoring Agency Name and Address OFFICES OF RESEARCH AND DEVELOPMENT FEDERAL HIGHWAY ADMINISTRATION U.S. DEPARTMENT OF TRANSPORTATION WASHINGTON, D.C. 20590				14. Sponsoring Agency Code M/0671	
15. Supplementary Notes FHWA Contract Manager: Mr. Carl Ealy (HRS-21) Principal Investigator: Dr. Michael W. O'Neill, University of Houston Project Manager: Mr. Richard A. Hawkins, Raymond Technical Facilities, Inc.					
16. Abstract <p>This report is the final report for a study involving the static vertical load testing of a full scale, instrumented pile group. The test group consisted of nine pipe piles instrumented for settlement, load transfer, pore pressures, total pressures and inclination. Two similarly instrumented reference (control) piles were also installed. Two smaller subgroups within the main group were also tested, and uplift tests were conducted on several of the individual piles. The soils at the test site consisted of clays that were overconsolidated by desiccation. It was determined that the efficiency of the main group and of the subgroups was essentially unity. Settlement ratios in the working load range were found to vary from about 1.2 to about 1.7, depending on the number of piles that were loaded. Failure was observed to be by plunging of the individual piles. Unit side load transfer varied essentially linearly with depth. Some dependence of load transfer patterns on residual stresses that remained after driving the piles was observed. The measured behavior of the group and subgroups was modeled by the "hybrid" algorithm, by means of Program PILGP1, which was developed for this study and documented in Appendixes A and B. Good agreement between computed and measured results were achieved when the unit load transfer curves from the reference piles were used and when the soil modulus of deformation was appropriately adjusted to account for pile reinforcement of the soil and the presence of very small strains in the mass of soil around the group.</p> <p>A description of the mathematical model, the rationale for its selection and a prior analysis of group behavior is presented in FHWA/RD-81/001. An analysis of dynamic measurements taken during driving the 11 test piles is in FHWA/RD-81/009. Analyses and data obtained during the conduct of this study are in Appendixes A-F, FHWA/RD-81/003-008.</p>					
17. Key Words Piles, Clay soils, Pile groups, computer model, pile driving			18. Distribution Statement This document is available to the public through the National Technical Information Service, Springfield, VA. 22161		
19. Security Classif. (of this report) Unclassified		20. Security Classif. (of this page) Unclassified		21. Na. of Pages 217	22. Price

DEPARTMENT OF
 TRANSPORTATION
 FHWA/RD-81/001
 MAY 11 1982
 LIBRARY

CONVERSION FACTORS, U. S. CUSTOMARY TO METRIC (SI)
UNITS OF MEASUREMENT

U. S. customary units of measurement used in this report can be converted to metric (SI) units as follows:

Multiply	By	To Obtain
Angstroms	0.0000001 (10^{-7})	millimetres
inches	2.54	centimetres
feet	0.3048	metres
miles (U. S. statute)	1.609344	kilometres
square inches	0.00064516	square metres
square feet	0.09290304	square metres
cubic feet	0.02831685	cubic metres
cubic yards	0.7645549	cubic metres
grams	0.001	kilograms
pounds (mass)	0.4535924	kilograms
tons (2000 pounds)	907.1847	kilograms
pounds (mass) per cubic foot	16.01846	kilograms per cubic metre
pounds (mass) per cubic yard	0.59327631	kilograms per cubic metre
pounds (force)	4.448222	newtons
pounds (force) per square inch	6894.757	pascals
pounds (force) per square foot	4.882428	kilograms per square metre
miles per hour	1.609344	kilometres per hour
degrees (angle)	0.01745329	radians
Fahrenheit degrees	5/9	Celsius degrees or Kelvins*

* To obtain Celsius (C) temperature readings from Fahrenheit (F) readings, use the following formula: $C = (5/9)(F - 32)$. To obtain Kelvin (K) readings, use: $K = (5/9)(F - 32) + 273.15$.

TABLE OF CONTENTS

	Page
Summary	xi
Chapter 1 - Test Pile Installation	1
Introduction	1
Soil Conditions at Test Site	2
Test Piles	4
Ground Instrumentation	11
Loading and Testing Sequence	11
Pile Driving	13
Soil Displacements During Driving	25
Pore Water Pressures	27
Assessment of Soil Disturbance	34
As-Driven Locations of Piles	34
Residual Loads Developed in Piles Due to Driving	40
Chapter 2 - Pile and Soil Performance Under Load	45
General	45
Load-Settlement Behavior	45
Distribution of Loads to Piles	67
Variation of Capacity with Time	67
Settlement Ratios	76
Induced Settlements	78
Efficiencies	81
Pore Water, Total, and Effective Pressures	
Developed During Load Tests	89
Ground Movements During Tests	112
Chapter 3 - Load Transfer	127
General	127
Load Transfer Patterns for Reference Piles and for	
Group Piles by Position	127
Apparent Peak Load Transfer by Soil Layer	141
Progressive Failure Patterns	143
Effects of Residual Stresses on Load Transfer	143

TABLE OF CONTENTS (Continued)

	Page
Unit Load Transfer Curves	151
Load Transfer Correlations	159
Variability of Load Transfer	165
Load Transfer Correlation Factors at Pile Tips	165
 Chapter 4 - Reanalysis of Performance	
Using Hybrid Model	169
Introduction	169
Tests Modeled	170
Geometric Inputs	170
Loadings	174
Structural Properties	174
Soil Inputs	174
Results - Single Pile	180
Results - Pile Groups	180
Observations	186
 Chapter 5 - Recommendations for Future Study	194
 Appendix A	
Appendix B	
Appendix C	
Appendix D	
Appendix E	
Appendix F	

LIST OF FIGURES

Figure		Page
A.	Calibration of Piles	xvii
B.	Driving of Test Piles	xvii
C.	Pile Group Before Installing Cap	xviii
D.	Reaction and Reference Frames	xviii
E.	Jacks and Load Cells	xix
F.	Electronic Data Acquisition System	xix
1.1	Stratigraphy at Test Site	3
1.2	Indicated Shear Strengths	5
1.3	Indicated Young's Moduli	6
1.4	At Rest Earth Pressure Coefficient and OCR Variation	7
1.5	Instrumentation of Test Piles (Schematic)	9
1.6	Ground Instrumentation Plan	10
1.7	Ground Instrumentation (East Elevation)	12
1.8	Approximate Locations of All Test and Reaction Piles and Sequence of Driving	15
1.9	Force-Time Traces for One Blow on Piles 2 and 4	19
1.10	Force-Time Traces for One Blow on Piles 1 and 5	20
1.11	Measured and Calculated Pile Forces and Wave Equation Model	22
1.12	Measured and Computed Force-Time Relationships for Pile 4	23
1.13	Observed Soil Movements During Pile Installation	26
1.14	Observed Soil Pore Water Pressures Preceding Pile Installation	28
1.15	Pore Water Pressure vs. Time at 19 ft (5.8 m) Depth	29
1.16	Pore Water Pressure vs. Time at 34 ft (10.4 m) Depth	30
1.17	Pore Water Pressure vs. Time at 50 ft (15.3 m) Depth	31
1.18	Measured Effective Earth Pressure Coefficients Against Piles Four Days After Installation	35
1.19	Pore Pressure Profile Section Lines	36
1.20	Ground Pore Pressure Profiles: Before and at Conclusion of Driving	37
1.21	As-Constructed Locations and Alignments of Group Piles	38
1.22	As-Constructed Locations and Alignments of Reference Piles	41
1.23	Residual Loads in Reference Piles After Driving	42
1.24	Residual Loads in Typical Group Pile After Installation	43

LIST OF FIGURES (Continued)

Figure		Page
1.25	Comparison of Residual Loads (Per Pile) in Reference and Group Piles	44
2.1	Reference Pile Load-Settlement Relationships for Test No. 1	46
2.2	Reference Pile Load-Settlement Relationships for Test No. 2	48
2.3	Reference Pile Load-Settlement Relationships for Test No. 3	49
2.4	Cumulative Load-Settlement Curve for Reference Pile Tests	50
2.5	Load-Settlement Relationships for 9-Pile Group, Test 1	51
2.6	Cap Movements at Approximately One-Half of Failure Load, Test 1	52
2.7	Cap Movements at Approximately 90 Percent of Failure Load, Test 1	53
2.8	Cap Movements at Failure, Test 1	54
2.9	Cap Movements Upon Removal of Load, Test 1	55
2.10	Load-Settlement Curves for Individual Piles on North Row, Test 1	57
2.11	Load-Settlement Curves for Individual Piles on Center Row, Test 1	58
2.12	Load-Settlement Curves for Individual Piles on South Row, Test 1	59
2.13	Load-Settlement Curves for Second and Third 9-Pile Group Tests	60
2.14	Cumulative Load-Settlement Curve for 9-Pile Group Tests	61
2.15	Load-Settlement Relationships for Subgroup Tests	63
2.16	Normalized Load-Settlement Relationships	64
2.17	Butt Load-Uplift Relationships	65
2.18	Tip Load-Uplift Relationships	66
2.19	Load Distribution to Pile Heads-Subfailure; Group Test 1	68
2.20	Load Distribution to Pile Heads-Failure and Unloaded; Group Test 1	69
2.21	Variation in Peak Capacity with Time	75
2.22	Settlement Ratios for Nine-Pile Group Tests	77
2.23	Measured and Theoretical Settlement Ratios for Nine-, Five-, and Four-Pile Group Tests	79
2.24	Settlements in Unloaded Piles Versus Load Per Loaded Pile (above); Settlement Differences in Corner Piles Between 5- and 4-Pile Subgroup Tests (below)	83
2.25	Pore and Total Pressure Changes on Piles at 9-Foot (2.7 m) Depth	91
2.26	Pore and Total Pressure Changes on Piles at 19-Foot (5.8 m) Depth	92

LIST OF FIGURES (Continued)

Figure		Page
2.27	Pore and Total Pressure Changes on Piles at 34-Foot (10.4 m) Depth	93
2.28	Pore and Total Pressure Changes on Piles at 41-Foot (12.4 m) Depth	94
2.29	Horizontal Variation in Pore Pressure in Soil on Pile 1 Prior to Reference Tests	96
2.30	Horizontal Variation in Pore Pressure in Soil and on Group Piles Prior to 9-Pile Tests	97
2.31	Horizontal Variation in Pore Pressure in Soil and on Group Piles Prior to Subgroup Tests	98
2.32	Horizontal Variation in Pore Pressure During Reference Pile Tests	99
2.33	Horizontal Variation in Pore Pressure During 9-Pile Tests	100
2.34	Horizontal Variation in Pore Pressure During Subgroup Tests	101
2.35	Vertical Variation in Pore Pressure on Reference Pile 1	103
2.36	Vertical Variation in Average Pore Pressure on Group Piles; 9-Pile Tests	104
2.37	Vertical Variation in Average Pore Pressure on Group Piles; Subgroup Tests	105
2.38	Vertical Variation in Pore Pressure on Piles During Uplift Tests	107
2.39	Vertical Variation in Total Lateral Pressure on Reference Pile 1	108
2.40	Vertical Variation in Average Total Lateral Pressure on Group Piles (2,3,4,5)	109
2.41	Vertical Variation in Average Total Pressure on Piles in Subgroup Tests (2,3,5)	110
2.42	Vertical Variation in Total Pressure for Uplift Tests	111
2.43	Vertical Variation in Lateral Effective Stress on Reference Pile 1	113
2.44	Vertical Variation in Average Lateral Effective Stress on Group Piles (2,3,4,5)	114
2.45	Vertical Variation in Average Lateral Effective Stress in Subgroup Tests (Piles 2,3,5)	115
2.46	Vertical Variation in Lateral Effective Stress for Uplift Tests	116
2.47	Surface Soil Movements Near Pile 1; Reference Tests	118
2.48	Surface Soil Movements for 9-Pile Group Tests	119
2.49	Surface Soil Movements for Average of Subgroup Tests	120
2.50	Soil Movements; 300 inch (7.6 m) Depth: 9-Pile Group Tests	121

LIST OF FIGURES (Continued)

Figure		Page
2.51	Soil Movements; 300 inch (7.6 m) Depth; Average of Subgroup Tests	122
2.52	Soil Movements; 516 inch (13.1 m) Depth; 9-Pile Group Tests	123
2.53	Soil Movements; 516 inch (13.1 m) Depth; Average of Subgroup Tests	124
2.54	Soil Movements; 600 inch (15.3 m) Depth; 9-Pile Group Tests	125
3.1	Load Distribution and f-d Diagrams; Subfailure; 9-Pile Test 1	128
3.2	Load Distribution and f-d Diagrams; Failure; 9-Pile Test 1	129
3.3	Load Distribution and f-d Diagrams; Subfailure; 9-Pile Test 2	130
3.4	Load Distribution and f-d Diagrams; Failure; 9-Pile Test 2	131
3.5	Load Distribution and f-d Diagrams; Subfailure; 9-Pile Test 3	132
3.6	Load Distribution and f-d Diagrams; Failure; 9-Pile Test 3	133
3.7	Load Distribution and f-d Diagrams; Subfailure; 5-Pile Test	134
3.8	Load Distribution and f-d Diagrams; Failure; 5-Pile Test	135
3.9	Load Distribution and f-d Diagrams; Subfailure; 4-Pile Test	136
3.10	Load Distribution and f-d Diagrams; Failure; 4-Pile Test	137
3.11	Progressive Failure in Reference Piles; Test 1	144
3.12	Progressive Failure in Group Piles; 9-Pile Test 1	145
3.13	Residual Loads in Reference Piles; Test 1	146
3.14	F-d Relationships for Reference Piles; Test 1	147
3.15	Average Residual Loads in Group Piles; Test 1	149
3.16	Average f-d Relationships for Group Piles; Test 1	150
3.17	Average Apparent and Adjusted Load Distribution Diagrams at Failure for Reference Piles	152
3.18	Average Apparent and Adjusted Load Distribution Diagrams at Failure for Group Piles 2,4,5 and 9	153
3.19	F-z Curves; Soil Zones A and B; Reference Piles; Test 1	155
3.20	F-z Curves; Soil Zones C and D; Reference Piles; Test 1	156
3.21	F-z Curves; Soil Zones A and B; Group Piles; Test 1	157
3.22	F-z Curves; Soil Zones C and D; Group Piles; Test 1	158

LIST OF FIGURES (Continued)

Figure		Page
3.23	Q-z Curves for Test 1; Reference Piles (above); Group Piles (below)	160
4.1	Pile Head Coordinates for PILGP1 Analysis	171
4.2	Direction Angles	172
4.3	Jack Coordinates	175
4.4	F-z Curves for PILGP1 Input	176
4.5	Q-z Curve for PILGP1 Input	177
4.6	Computed and Measured Mean Pile Head Load Settlement Curves; Reference Piles; Test 1; PILGP1	181
4.7	Computed and Measured Mean Distribution of Load; Reference Piles; Test 1; PILGP1	182
4.8	Measured and Computed Load-Settlement Curves; 9-Pile Test 1	183
4.9	Measured and Computed Settlement Ratios; 9-Pile Test 1	185
4.10	Measured and Computed Distributions of Loads Along Piles; 9-Pile Test 1; Load = 581.4 K	188
4.11	Measured and Computed Distribution of Loads Along Piles; 9-Pile Test 1; Load = 1274.7 K	189
4.12	Measured and Computed Load-Settlement Curves; Subgroup Tests	190
4.13	Measured and Computed Distributions of Loads Along Piles; 5-Pile Test; Load = 278.9 K	191
4.14	Measured and Computed Distribution of Loads Along Piles; 4-Pile Test; Load = 287.6 K	192

LIST OF TABLES

Tables	Page
A. Summary of Gross Test Results	xiv
B. Summary of Load Distribution Data:	
First Nine-Pile Group Test Series	xv
1.1 Chronology of Major Field Events	14
1.2 Pile Driving Data: Blow Counts in Blows/Foot	17
1.3 Computed Peak Pile Forces During Driving As Function of Side Damping, J_s	24
1.4 Pile Head and Jack Coordinates for 9-Pile Test No. 1	39
2.1 Distribution of Loads to Pile Heads: 9-Pile Group Test	70-72
2.2 Distribution of Loads to Pile Heads: Subgroup Tests	73-74
2.3 Settlement Ratios for Pile Tips for Test 1	80
2.4 Induced Settlements	82
2.5 Summary of Failure Loads and Efficiencies for 9-Pile Group Tests	84
2.6 Summary of Failure Loads and Efficiencies for Subgroup Tests	86
2.7 Overall Efficiency by Geometric Position and Average Shaft and Tip Efficiencies	87
2.8 Overall Pile Group Efficiencies for Test Program	88
3.1 Variation of Depth of Median Side Load Transfer Among Tests	140
3.2 Variation of Peak Unit Side Load Transfer Based on Pretest Zeros	142
3.3 Adjusted and Unadjusted Peak Load Transfer in psf by Soil Layer for Compression and Uplift Tests	154
3.4 Side Resistance Correlation Factors, 9-Pile Test 1	161
3.5 Interpreted Peak Cohesion (c) and Angle of Internal Friction (ϕ) Values Used for Load Transfer Correlations	163
3.6 Factors (δ) for Computing α Corelation for Individual Piles and Layers, 9-Pile Test 1	166
3.7 Average End Bearing Capacity Factors for Reference and Group Piles	167
4.1 Pile Geometry for PILGP1 Reanalysis	173
4.2 F-z Curves for PILGP1 Solutions: Reanalyzed and Criteria	178
4.3 Q-z Curves for PILGP1 Solutions	179
4.4 Distribution of Loads to Piles From PILGP1 Analyses	187

Summary

The purposes of the study described in this report were to obtain field data that are useful in interpreting fundamental phenomena that control the behavior of groups of driven piles in overconsolidated clay and that are appropriate for verification of mathematical models for predicting the response of pile groups to applied vertical, static loads. In order to develop the data, eleven instrumented full-sized pipe piles were driven: two as isolated, reference piles and nine in a square group. These piles were load tested to failure at various times after driving as individual piles, as a nine-pile group with a three-diameter spacing, and as five- and four-pile subgroups with variable spacings. A comprehensive in-situ and laboratory soil investigation program was undertaken, and piezometers and movement monuments were placed in the soil.

A specific mathematical model, the "hybrid" model, was selected for detailed study. That model and other models are described in the Interim Report. A digital computer version of the hybrid model, Program PILGP1, was developed during the study and is described and documented in Appendix A and Appendix B of this report.

Gross field results are summarized succinctly in Tables A and B. The term "SP" in the former table refers to "single pile."

The following principal observations were made:

1. Significant pore water pressures were developed during driving adjacent to the reference (isolated) pile that was studied for this effect and in the soil within and surrounding the pile group. Pore pressures dissipated rapidly thereafter such that pore pressures were nearly hydrostatic within about 20 days after driving within the group and around the reference pile. The rapid pore pressure dissipation is thought to be due largely to the presence of a secondary structure network and to continuous sand partings in the soil layers and to the high coefficient of consolidation associated with the overconsolidated soils. Very small positive changes in pore pressure occurred during loading.

2. The distribution of soil resistance along the piles during the driving process was dissimilar to that observed during static loading. During driving, essentially no dissipation of compression wave amplitude occurred over the top half of the piles at full penetration. This suggests that no shear stress transfer took place in the top half of the piles during driving, possibly resulting from a small annular space between piles and soil that may have developed because of lateral motion of the piles. Significant transfer of load occurred in this zone during

TABLE A. SUMMARY OF GROSS TEST RESULTS (1 k = 4.45 kN, 1 in = 25.4 mm)

Test (a)	Failure Mode	Plunging Failure Load (k) (b)	Settlement at 50% of Plunging Load (in)	Efficiency	Settlement Ratio at 50% of Plunging Load
SP 1 (15 days)	Plunging	168	0.068		
SP 11 (15 days)	Plunging	133	0.048		
9-Pile (20 days)	Plunging of Individual Piles w/ Tip-pling of Group	1332	0.094	0.99	1.62
SP 1 (78 days)	Plunging	187	0.080		
SP 11 (78 days)	Plunging	170	0.067		
9-Pile (82 days)	Plunging of Individual Piles	1532	0.113	0.98	1.54
SP 1 (105 days)	Plunging	177	0.080		
SP 11 (105 days)	Plunging	181	0.077		
9-Pile (110 days)	Plunging of Individual Piles	1541	0.116	0.96	1.48
5-Pile (113 days)	Plunging of Individual Piles	832	0.096	0.93	1.31
4-Pile (116 days)	Plunging of Individual Piles	661	0.085	0.92	1.19

(a) Times between pile installation and test shown in parentheses

(b) Includes cap weight and weight of loading accessories

TABLE B. SUMMARY OF LOAD DISTRIBUTION DATA: FIRST NINE-PILE GROUP TEST SERIES (1 k = 4.45 kN)

Pile Position	Avg. Load per Pile (k) at Approximately One-Half Plunging Failure Load			Avg. Load per Pile (k) at Plunging Failure Load		
	Pile Head	Shaft Load	Tip Load	Pile Head	Shaft Load	Tip Load
Center	59.9	51.8	8.1	153.2	119.3	33.9
Edge	64.0	57.4	6.6	138.9	112.5	26.4
Corner	66.4	58.2	8.2	141.5(a)	113.8	27.7
Control	63.1	60.3	2.8	149.5	127.0	22.5

NOTE: Shaft and tip loads are apparent loads that do not consider residual stresses produced by installation.

(a) Corner Pile 8 failed prior to failure of group as a whole.

static testing, implying that the annular space may have been closed due to lateral soil expansion after driving.

3. Effective lateral stresses measured in the piles several days after driving were greater than the in-situ lateral pressures, especially in the bottom halves of the piles.

4. Shear strength of soil within the area of the pile group but some distance away from the immediate vicinity of the pile faces, as measured by the static cone resistance after testing, changed negligibly from pre-drive strength.

5. Observed butt heave on piles already in place in the group never exceeded 0.05 in. (1.3 mm) due to driving of the remaining piles. Maximum soil surface heave was approximately 1 in. (25.4 mm) adjacent to the 9-pile group, diminishing to 0.1 in. (2.54 mm) 28 ft. (8.54 m) from the center of the group.

6. Small, variable residual loads were observed in the reference piles after installation. Residual loads were somewhat lower in the group piles at the same time. Static load testing to failure in both the group and reference piles produced a significant increase in residual loads which had to be considered in order to assess set-up effects.

7. Appreciable "apparent" set-up occurred between the first and second sets of loads tests (lapse period of 62 days) in both the reference piles and group piles. This effect could not be attributed to increased side resistance caused by pore pressure reductions, which were very minor during the lapse period. Instead, they were deduced to be largely the result of increased tip capacity resulting from the effects of the earlier loading.

8. The efficiency of the pile groups (9, 5, and 4 piles) was essentially 1.0 when the weight of the pile cap was included as applied load. Shaft efficiency was slightly less than 1.0, and tip efficiency was greater than 1.0. Since failure was essentially "brittle," shaft failure preceded tip failure, whereafter shaft relaxation occurred in both reference and group piles. Therefore, the peak capacity of any individual pile was slightly less than the sum of its peak side and tip capacities.

9. Failure of the 9-pile group and of the subgroups was by plunging of the individual piles and not by failure of the groups as blocks.

10. The settlement ratios at subfailure loads in the 9-pile group and in the subgroups were considerably lower than the settlement ratios predicted by elastic solid models when the soil modulus was constant or uniformly increasing with depth in a strained layer that is infinitely thick. Several factors could account for this effect, including the

reinforcement of the soil provided by the piles and the relatively strong influence of the stiffer soils that were present beneath the pile tips that were not modeled properly with the procedures considered.

11. The mean measured shear strain amplitudes in the soil immediately adjacent to the group were very small at loads up to and including the failure load. This fact suggests that elastic modulus to be used in analytical models for predicting short-term settlement response of pile groups should be taken to correspond to very low strain amplitudes and should be measured in-situ whenever possible.

12. The loads were relatively evenly distributed to the pile heads. Within the working load range in the 9-pile group the center pile carried the least load and the corner piles carried the greatest load. These loads differed by about 10 per cent. Larger differences are generally predicted by elastic solid models. (See Interim Report.)

13. Progressive failure was experienced in the soil at the test site. In an individual group or reference pile, shaft failure progressed generally from the top and bottom of the pile toward the middle, beginning at an applied load of about 85 percent of plunging failure load. During the first group load test slightly eccentric loading caused tipping of the pile cap, which induced plunging failure in the northeast corner pile that then progressed to other piles in the group. In the other group and subgroup tests, where loading was more concentric, failure was essentially non-progressive among the piles.

14. Graphs of peak developed unit side resistance versus depth showed a distinct trend toward linear increase in unit side resistance with depth. This fact, coupled with the small measured pore pressure changes observed during loading, suggests that a frictional or effective stress approach to assessment of shaft capacity is feasible for soils of the type in which the tests were conducted.

15. The best overall direct correlations of load transfer, both at the tips and along the shafts of the piles, were with the in-situ static cone, although some variability in the side resistance correlation factors existed among the various soil layers. The general effective stress method (GESM) also yielded correlation factors near, but consistently below 1.0 (indicating unconservative predictions) below a depth of 10 ft. (3.05 m). Correlation of measured maximum unit side load transfer with soil shear strength calculated from peak effective stress parameters measured in laboratory triaxial compression and from the measured lateral effective stresses on the piles were less accurate, due partially to the difficulties in interpreting total normal stresses (Item 17) and the questionable applicability of peak triaxial parameters to represent soil shear strength. Indirect correlation methods, such as the α method, yielded factors consistent with those obtained in numerous single pile tests in stiff, overconsolidated clay.

16. No conclusions can be drawn with respect to the comparison of behavior of a reference pile tested according to the "quick test" method and one tested according to the "standard" one-hour load increment method used in this study. Apparently, the pile that was subjected to the quick test was enveloped by soil with higher undissipated pore pressures at the time the comparative tests were carried out than the pile subjected to the standard test, resulting in its unexpectedly lower capacity. This is speculated to be due to the result of driving the pile subjected to the quick test in a pilot hole that was partially filled with water.

17. The instrumentation and data acquisition systems (described in detail in the Interim Report) performed adequately, except that some ground piezometers did not function properly and the temperature sensitivity and small geometric irregularities in the total lateral pressure cells made interpretation of total pressure data difficult. In this regard, the total and effective stresses shown in Chapter 2 should be considered as representative of trends and not of exact values.

18. Program PILGP1 satisfactorily replicated the behavior of the piles during the first 9-pile group test and the 5- and 4-pile subgroup tests. Unit load transfer curves from the first set of reference pile tests were used as inputs, and the soil was treated as incompressible (Poisson's ratio = 0.5) and given a Young's modulus about twice that measured by the self-boring pressuremeter in the soil at a level immediately below the pile tips. This value of Young's modulus also corresponds to an E/c of 1400, where c is the average undrained cohesion, as indicated by UU triaxial compression tests, between the ground surface and the depth of the pile tips.

19. The experimental results obtained in this study are directly applicable only to small groups of moderately spaced driven displacement piles in soil of the type encountered at the test site. Application of the results to sites with other soil types or to larger groups or groups with more closely spaced piles in any type of soil must be done through sound judgment. One use of the hybrid model (or other mathematical model) would be to assist a designer in making that judgment.

20. Stress contours in the soil in around the piles were not measured. However, displacements were measured at several points in the soil, and stresses induced in unloaded piles were also measured. It may be possible to use indirect analytical methods to infer approximate stress contours from these data, but such analyses are beyond the scope of this report.

Photographes of several aspects of the field work are shown in Figs. A-F.



FIGURE A. CALIBRATION OF PILES



FIGURE B. DRIVING OF TEST PILES

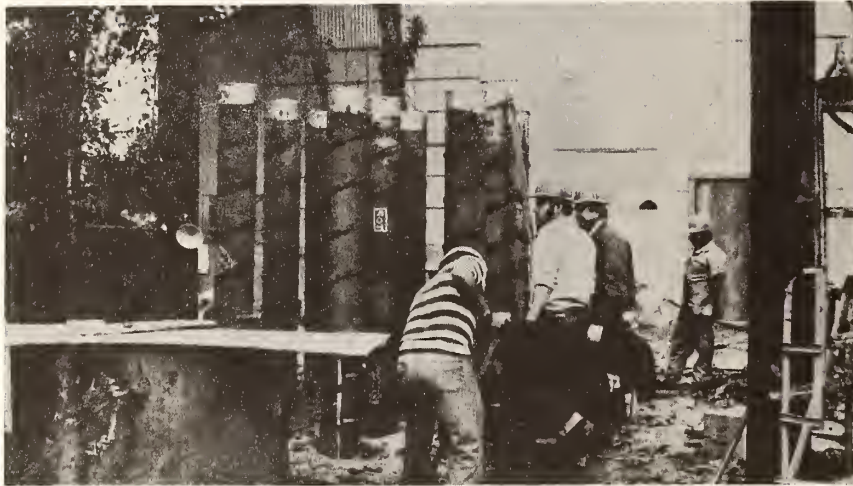


FIGURE C. PILE GROUP BEFORE INSTALLING CAP

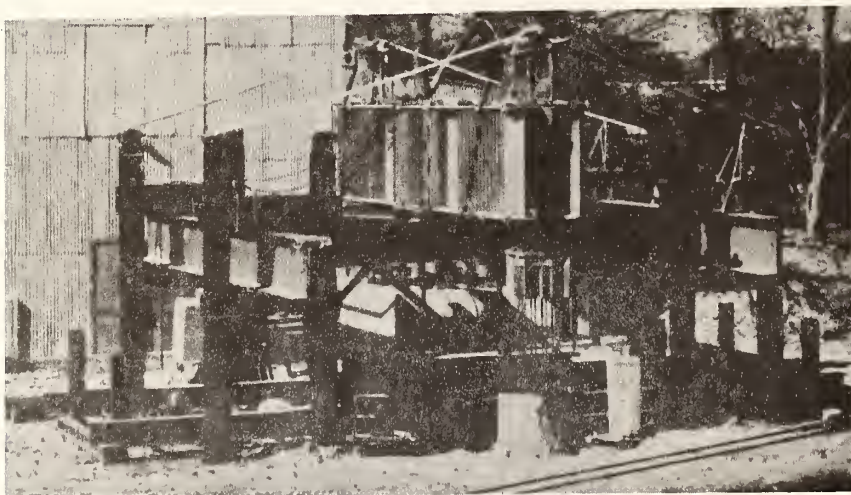


FIGURE D. REACTION AND REFERENCE FRAMES

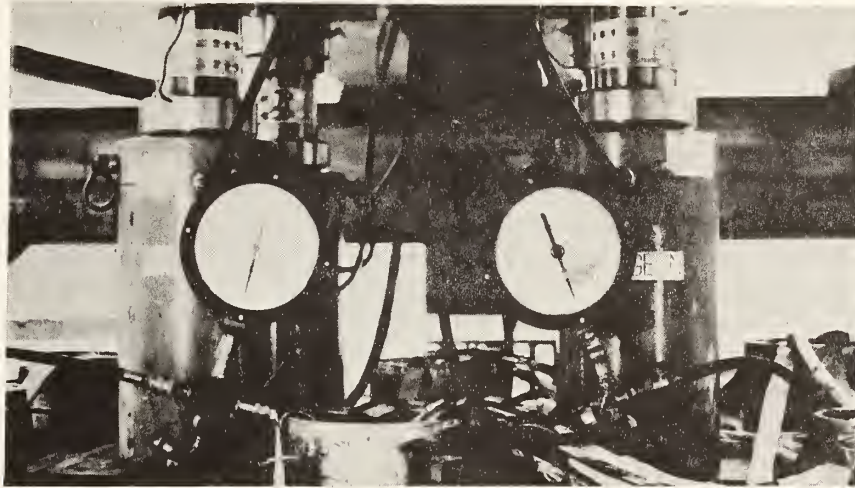


FIGURE E. JACKS AND LOAD CELLS



FIGURE F. ELECTRONIC DATA ACQUISITION SYSTEM

Chapter 1. Test Pile Installation

Introduction

This report describes the results of measurements made during the installation and vertical load testing of eleven instrumented test piles in overconsolidated clay at a test site on the University of Houston Central Campus. The overall objectives of the study were: (1) to evaluate mathematical models for pile groups; (2) to choose one model to predict the behavior of a three by three group of piles that would be tested in over-consolidated clay; (3) to design a test program, based on the aforementioned mathematical solution, that would be capable of verifying the model; (4) to install and conduct load tests on the pile group and two reference (control) piles, acquiring such data as needed to check the mathematical model and other data relevant to the fundamental understanding of pile group response under vertical loading; (5) to remodel the load test using the chosen model in order to calibrate the model to the soil conditions encountered at the test site.

The Interim Report for the study, dated March, 1979, was concerned with Items 1-3, above. Procedures for modeling the pile group mathematically have been described in the Interim Report. That report also contains details of the pile and soil instrumentation systems employed, the pile driving system, geotechnical conditions, testing procedures, and structural details of the reaction and reference systems and the cap. This report is concerned with Items 4 and 5.

This report, while factual, necessarily reflects some degree of interpretation of data and phenomena by the authors. So that other investigators may conduct independent analyses, a complete set of raw and partially reduced data has been transmitted to the Federal Highway Administration, Offices of Research and Development, Washington, D.C. 20590. Supporting documentation and data (principally in reduced form) for this report are contained in several appendices, as follows:

(1) Appendix A: User's Guide for Program PILGP1. This digital computer program is the algorithm for the hybrid mathematical model chosen for use on this project. The hybrid model characterizes soil response by combining unit load transfer curves and elastic theory. The hybrid model is described in the User's Guide.

(2) Appendix B: Documentation for Program PILGP1. This appendix contains flow charts, descriptions of primary variable names, etc., used in Program PILGP1. A complete listing of the FORTRAN IV computer code is also provided.

(3) Appendix C: Geotechnical Investigation. Appendix C contains the geotechnical data for the site. (A distillation and an interpretation of the geotechnical conditions are given in Chapter 5

of the Interim Report.) Information contained in this appendix includes results from static cone soundings obtained before and after driving the piles, pressuremeter tests, seismic crosshole tests, standard penetration tests, water level measurements, classification tests, torvane and hand penetrometer tests, moisture content and dry density tests, unconfined compression tests, undrained triaxial compression tests with pore pressure measurements, and drained direct shear tests. Locations of the test borings are noted, and detailed logs of boring are provided.

(4) Appendix D: Detailed Graphical Presentation of Reduced Data. This appendix contains selected representative computer-produced graphs of load-settlement, load distribution, and load transfer data for all tests except the first test, which is described in detail in the main text.

(5) Appendix E: Evaluation of Instrumentation. Appendix E describes in detail problems encountered with the various pile and soil instrumentation systems, documents transducer performance, describes pile calibration, and describes the procedure used for fitting strain gage data. Sources and evaluation of errors in deformation measurements are also considered.

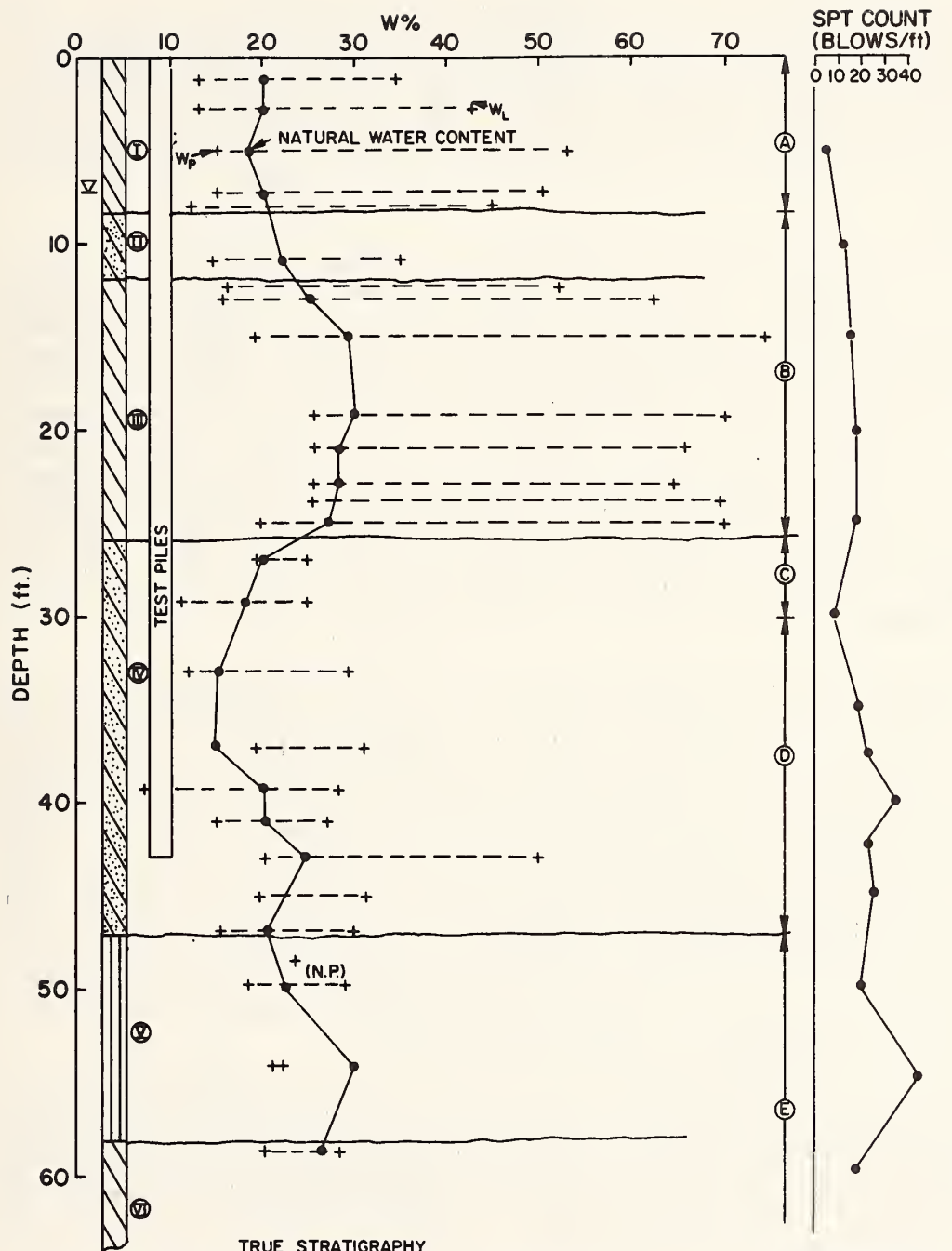
(6) Appendix F: Supplementary Information. Certain repetitive supplementary reduced data, such as graphical presentation of cap motion, load distribution diagrams, and total and pore pressure tabulations are contained in Appendix F.

Soil Conditions at Test Site

While numerical descriptions of soil properties are given in both the Interim Report and in Appendix C of this report, a short description of the soil conditions at the test site is given here.

Two principal geological formations were identified at the site: (1) the Beaumont formation, from the ground surface to a depth of 26 ft. (7.9 m); and (2) the Montgomery formation, sometimes described locally as the Upper Lissie formation, below a depth of 26 ft. (7.9 m). Both of these formations are deltaic Pleistocene terraces, with the underlying Montgomery formation having been deposited during the Sangamon Interglacial Stage and the Beaumont formation having been deposited during the Peorian Interglacial Stage. Both deposits consist primarily of clay that was preconsolidated by means of desiccation when the level of the nearby Gulf of Mexico was several hundred feet below its present level.

The site topography is essentially flat. The stratigraphy consists of 1.5 ft. (0.5 m) of clay fill, below which is found approximately 6 ft. (2 m) of weathered Beaumont clay. A detailed stratigraphic schematic is shown in Fig. 1.1. Stratum C, the upper 4 ft. (1.2 m) of the



- | | | |
|---|---|--|
| <p>① VERY STIFF GRAY AND TAN CLAY (CL-CH)</p> <p>② STIFF GRAY AND TAN SANDY CLAY WITH SAND SEAMS (CL)</p> <p>③ STIFF TO VERY STIFF RED AND LIGHT GRAY CLAY (CH)</p> <p>④ STIFF TO VERY STIFF LIGHT GRAY AND TAN SANDY CLAY WITH SAND POCKETS (CL)</p> | <p>⑤ DENSE RED AND LIGHT GRAY SILT WITH CLAYEY SILT AND SAND LAYERS (ML)</p> <p>⑥ VERY STIFF RED AND LIGHT GRAY CLAY (CL)</p> | <p>IDEAL STRATIGRAPHY (FOR CORRELATIONS)</p> <p>ZONE (A) - STRATUM ①</p> <p>ZONE (B) - STRATA ② & ③</p> <p>ZONE (C) - STRATUM ④ (UPPER)</p> <p>ZONE (D) - STRATUM ④ (LOWER)</p> <p>ZONE (E) - STRATA ⑤, ⑥ & BELOW</p> |
|---|---|--|

FIGURE 1.1. STRATIGRAPHY AT TEST SITE (1 ft = 0.305 m)

Montgomery formation, was noticeably softer than underlying soil. Note that the free water level in observation wells remained at approximately 7 ft. (2.1 m) below site grade throughout the study. Piezometric studies, described later in this chapter, indicate that this water level closely represents the piezometric head in all soils down to a depth of 50 ft. (15.3 m), which is 7 ft. (2.1 m) below the tips of the test piles.

Figure 1.2 expresses the variation of shear strength as indicated by several methods. The static cone penetrometer values are averages based on three soundings made prior to pile installation. Inconsistencies among methods are readily apparent. Most are believed to be associated with the strong secondary structure of the Beaumont formation and of the relatively high sand content of the Montgomery formation (often present in small lenses and partings), which produce scatter in parameters obtained through laboratory tests and probably result in a bias toward unrepresentatively low laboratory strengths, especially in the sandy clay soil below a depth of 35 ft. (10.7 m), where the content of the sand increases to almost 50 per cent. Further explanation of the test results reported in Fig. 1.2 is given in the Interim Report.

Since it will be necessary to refer to the Young's modulus of the soil during the mathematical analysis of the tests described in Chapter 4, Fig. 1.3 is reproduced from the Interim Report to express the variation of Young's modulus with depth by several test methods. The moduli reported for the laboratory triaxial test are arbitrarily defined as secant moduli to the principal stress difference-major principal strain curve at twenty per cent of the peak principal stress difference. It is evident that the associated strain level in the triaxial test is much higher than that produced by crosshole seismic testing. Again, the variability of data is obvious. Part of this variability is associated with the definition of strain level at which the modulus is defined; part is also undoubtedly due to the effects of sampling disturbance, rendering the laboratory values unrepresentatively low.

Figure 1.4, which was also extracted from the Interim Report, presents graphs showing the measured variations of in-situ at-rest earth pressure coefficient and overconsolidation ratio (OCR) with depth. Note that the at-rest earth pressure coefficient is very high in the depth range of 15 - 20 ft. (4.6 - 6.1 m). This range may have coincided with an ancient evaporation surface.

Test Piles

The test piles were steel pipes, 10.75 in. (273 mm) in outside diameter, with wall thicknesses of 0.365 in. (9.27 mm). They were closed on the bottom end with 1 in. (25.4 mm) thick steel boot plates and sealed at the top (after driving) with airtight cover plates through

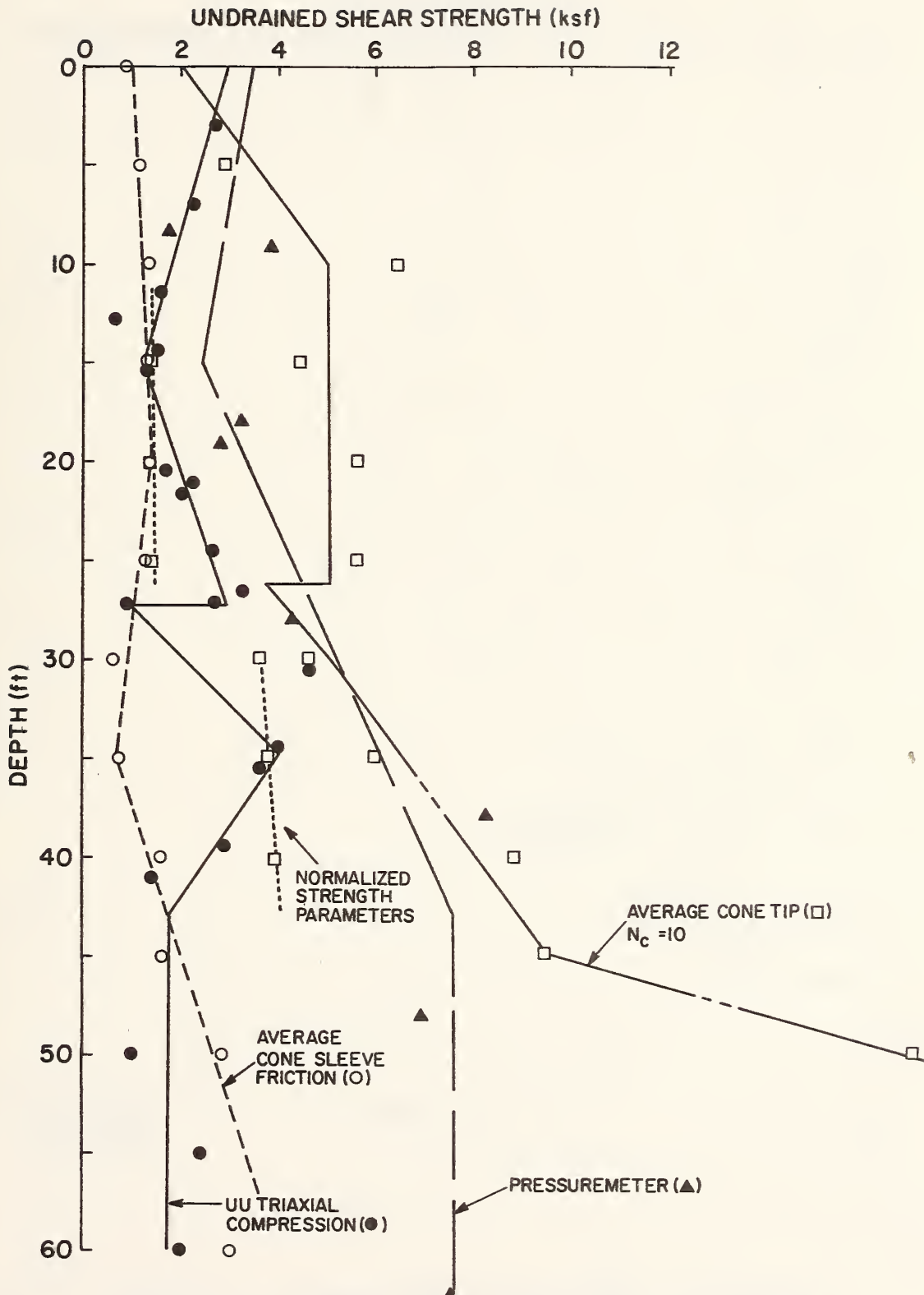


FIGURE 1.2. INDICATED SHEAR STRENGTHS (1 ft = 0.305 m; 1 ksf = 47.9 kN/m²)

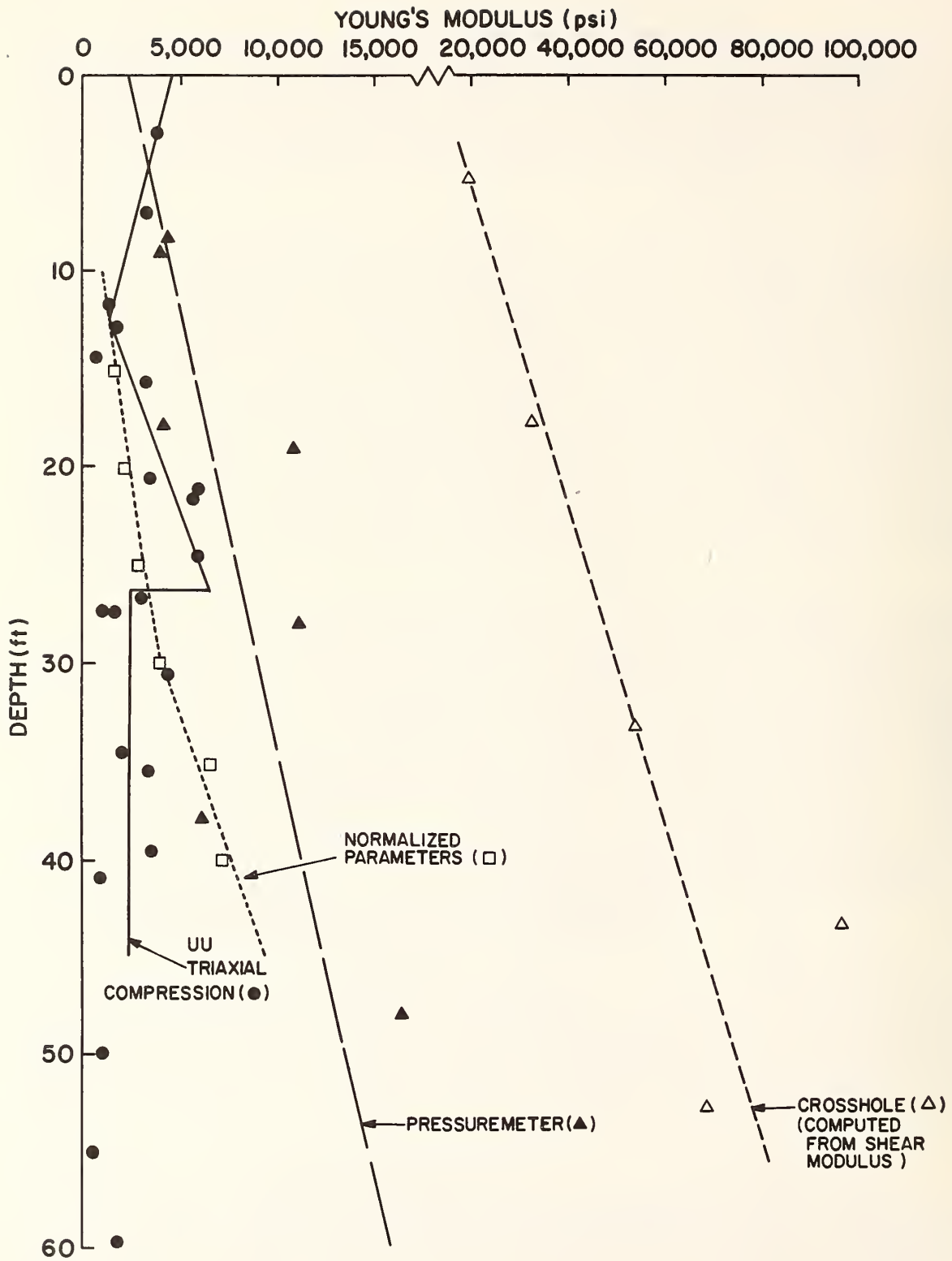


FIGURE 1.3. INDICATED YOUNG'S MODULI (1 ft = 0.305 m;
1 psi = 6.89 kN/m²)

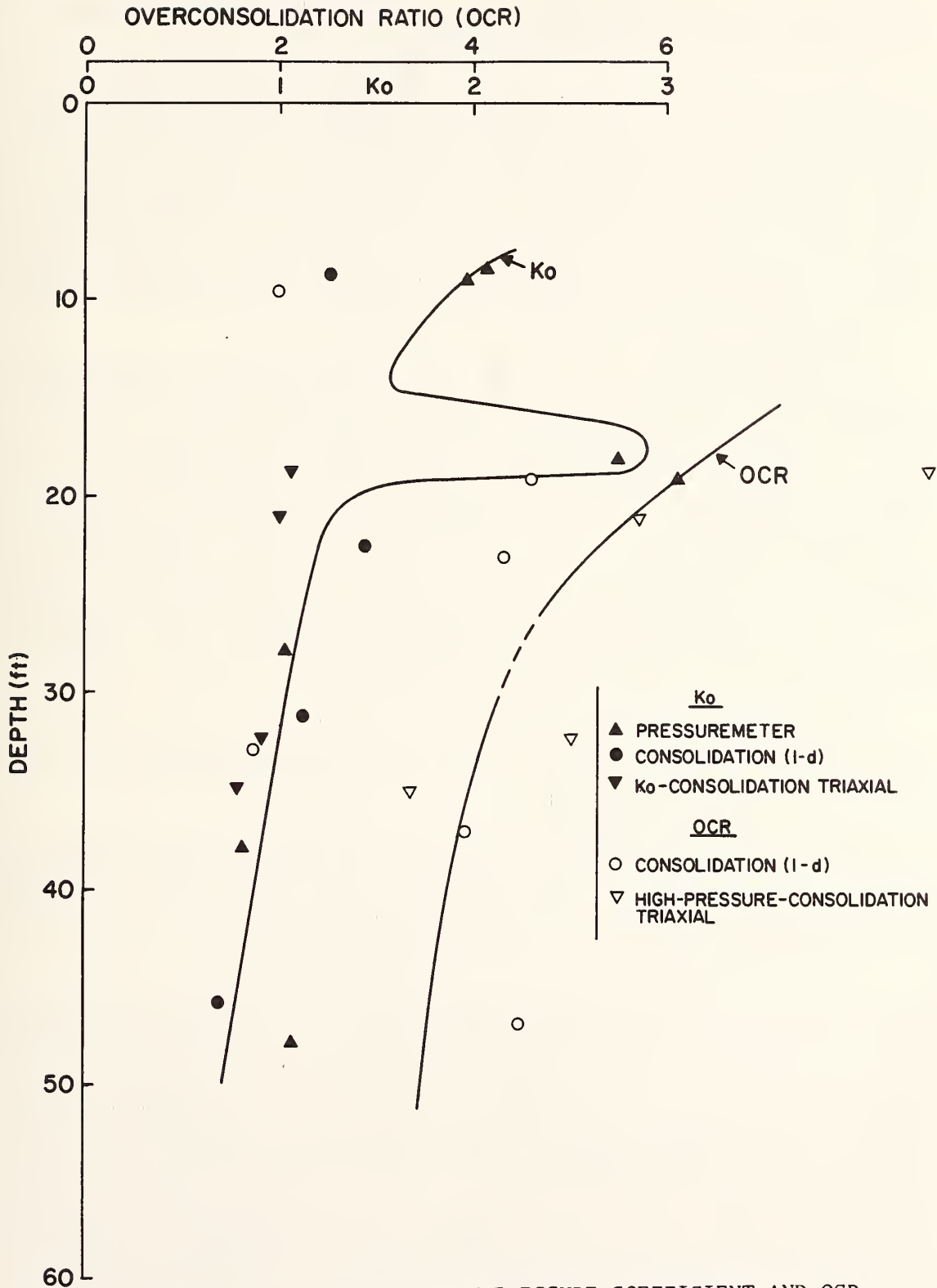


FIGURE 1.4. AT REST EARTH PRESSURE COEFFICIENT AND OCR VARIATION (1 ft = 0.305 m)

which dry nitrogen was passed in the periods between tests to preserve the integrity of the electrical instruments.

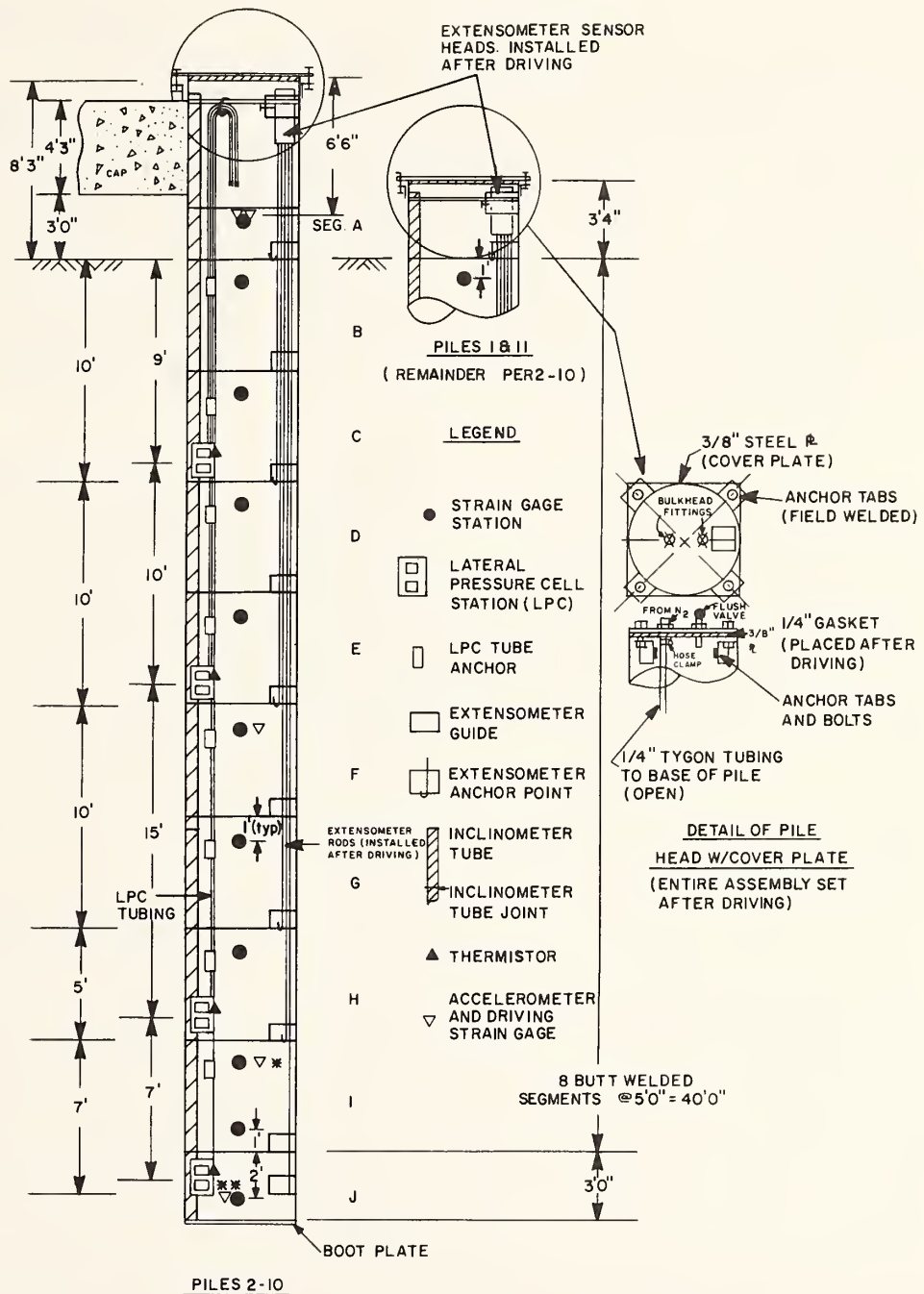
Nine of the piles were driven in a square group, nominally three diameters on centers. These piles penetrated to a depth of 43 ft. (13.1 m) and protruded 8.25 ft. (2.5 m) above the ground surface. The piles were rigidly connected to each other with a 4.25-ft.- (1.30 m) thick reinforced concrete cap. A 3.0-foot (0.92 m) free space was left between the bottom of the cap and the soil surface. Two other piles were driven as isolated reference (control) piles 12 ft. (3.66 m) to the south and north of the center of the 9-pile group, respectively. These piles were identical to the group piles except that they were not capped and extended only 3.3 ft. (1.0 m) above grade.

The instrumentation carried by the various test piles is summarized schematically on Fig. 1.5. All eleven test piles contained full-bridge, precalibrated strain gage circuits placed at approximately 5 ft. (1.5 m) depth intervals. Before driving, each pile was subjected to an "exercising" procedure followed by calibration of each gage circuit to an axial load of 150 tons (1335 kN). Details of the calibration procedure are given in Appendix E. The second highest levels of strain gages in the group piles served as load transducers for measuring load distributed to the head of each pile, with the uppermost level (just beneath the base of the pile cap) serving as a backup load transducer in case of a malfunction of the primary transducer. The remaining strain circuits were used to measure load transfer between the piles and the soil.

The pile numbering scheme is shown in Fig. 1.6. The group piles were designated with numbers 2-10, while the reference piles were assigned numbers 1 and 11.

Load applied to the pile group and to the reference piles was also measured by a series of independent electronic load cells, and loads were also monitored by reading hydraulic jack pressures. All of the electronic instrumentation was monitored with a microcomputer-based data acquisition system, described in the Interim Report.

Other pile instrumentation consisted of mechanical extensometers to serve as a backup to the strain gage system in the event of electronic system malfunction, lateral earth pressure (total and pore water pressure) cells at four locations on five of the test piles, and an inclinometer tube to be used after installation to determine the exact orientation of the piles in the ground. A separate strain gage system, consisting only of single gages, was installed and monitored during the driving of four of the piles (Nos. 1, 2, 4, and 5). This "dynamic" system was used to obtain force-time traces for the purpose of comparing the results of an E.A.L. Smith wave equation model analysis with measured behavior. This wave equation analysis, described later in this chapter, was used to evaluate the appropriate values of side damping and distribution of static resistance for isolated and group piles at this test site.



ITEMS NOT SHOWN: RIBBON CABLE, ACCELEROMETER CABLE, THERMISTOR WIRE.
SEE INDIVIDUAL DRAWINGS FOR DETAILED DIMENSIONS. ABOVE DIMENSIONS ARE NOMINAL.

LPC'S, LPC ANCHORS, LPC TUBING, THERMISTORS OMITTED ON PILES 6-11
ACCELEROMETER AND DRIVING STRAIN GAGES OMITTED ON ALL PILES EXCEPT 1, 2, 4, 5.

* POSITION ON PILES 4 & 5 ** POSITION ON PILES 1 & 2

FIGURE 1.5. INSTRUMENTATION OF TEST PILES (SCHEMATIC)
(1 ft = 0.305 m; 1 in = 25.4 mm)

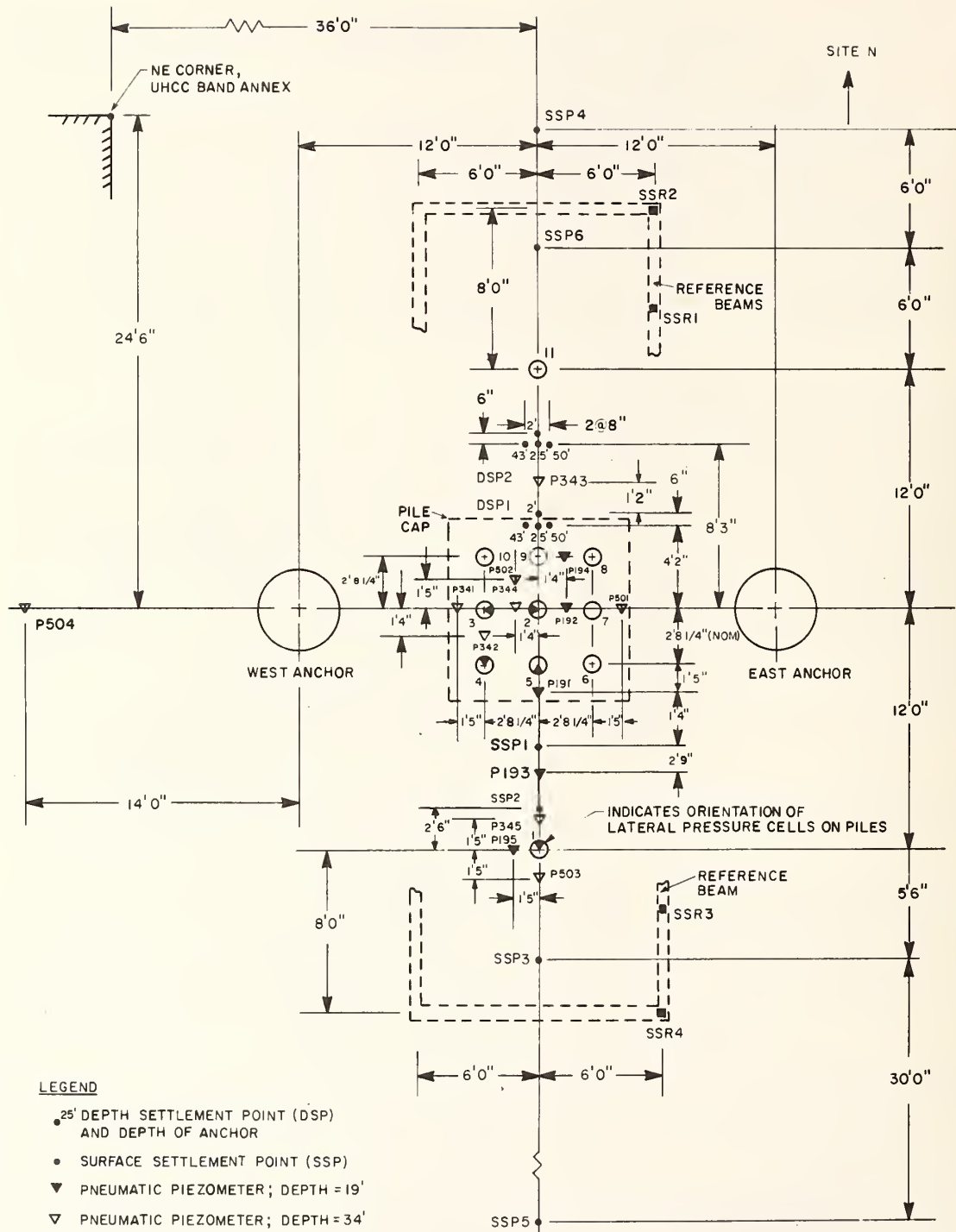


FIGURE 1.6. GROUND INSTRUMENTATION PLAN
(1 ft = 0.305 m; 1 in = 25.4 mm)

Ground Instrumentation

Figure 1.6 depicts the layout of the test site and also describes the location of ground instrumentation in plan view. Ground instrumentation consisted of two principal systems: (1) pneumatic piezometers, and (2) Borros-type heave-settlement points. Figure 1.7 shows the east elevation of the ground instrumentation, indicating the depths at which the various instruments were situated. Both systems were installed several weeks before the test piles were driven and were monitored during test pile installation. The settlement points were monitored by means of a microhead level during installation and by dial gages suspended from the reference beams during load testing. Exact as-built positions of the settlement points nearest the piles are shown in Fig. 1.20.

Loading System and Testing Sequence

The pile group was loaded vertically by a system of four hydraulic jacks hooked to a common pressure manifold and reacting against two plate griders. The plate griders were anchored by vertical Dywidag bars that were secured to the bases of two concrete anchor caissons approximately 105 ft. (32.0 m) below grade. These anchors are described in detail in the Interim Report. The resulting reaction system, consisting of the girders and flexible bars was essentially articulated, rendering it free to translate or to rotate with the pile cap.

The reference piles were loaded by single jacks reacting against beams which were each supported by four H - piles driven to a penetration of 25 ft. (7.6 m). Cross beams were placed between the reference pile reaction systems to provide a rest for the group reaction girders when they were not being loaded.

All load tests (with one exception, described later) were conducted by applying a small increment of compression load (about one-eighth of the failure load) each hour. Most instruments were read 5 minutes, 30 minutes and 55 minutes after each load was applied. Loading was monotonic and continued until failure occurred, after which load was removed in several decrements (except in the uplift tests, where all load was removed in one decrement). The total length of time required for each test was on the order of 12 hours.

The 9-pile group was tested to failure three times: at 20, 82, and 110 days after the completion of installation, in order to assess the effects of set-up. Approximately five days prior to each nine-pile group test, the two reference piles were tested simultaneously. The first test on Reference Pile No. 11 was a "quick" test in which load increments were applied every 2.5 minutes instead of every hour.

Following completion of the three 9-pile group tests and associated reference pile tests, the corner piles (denoted Piles 4,6,8, and 10 on

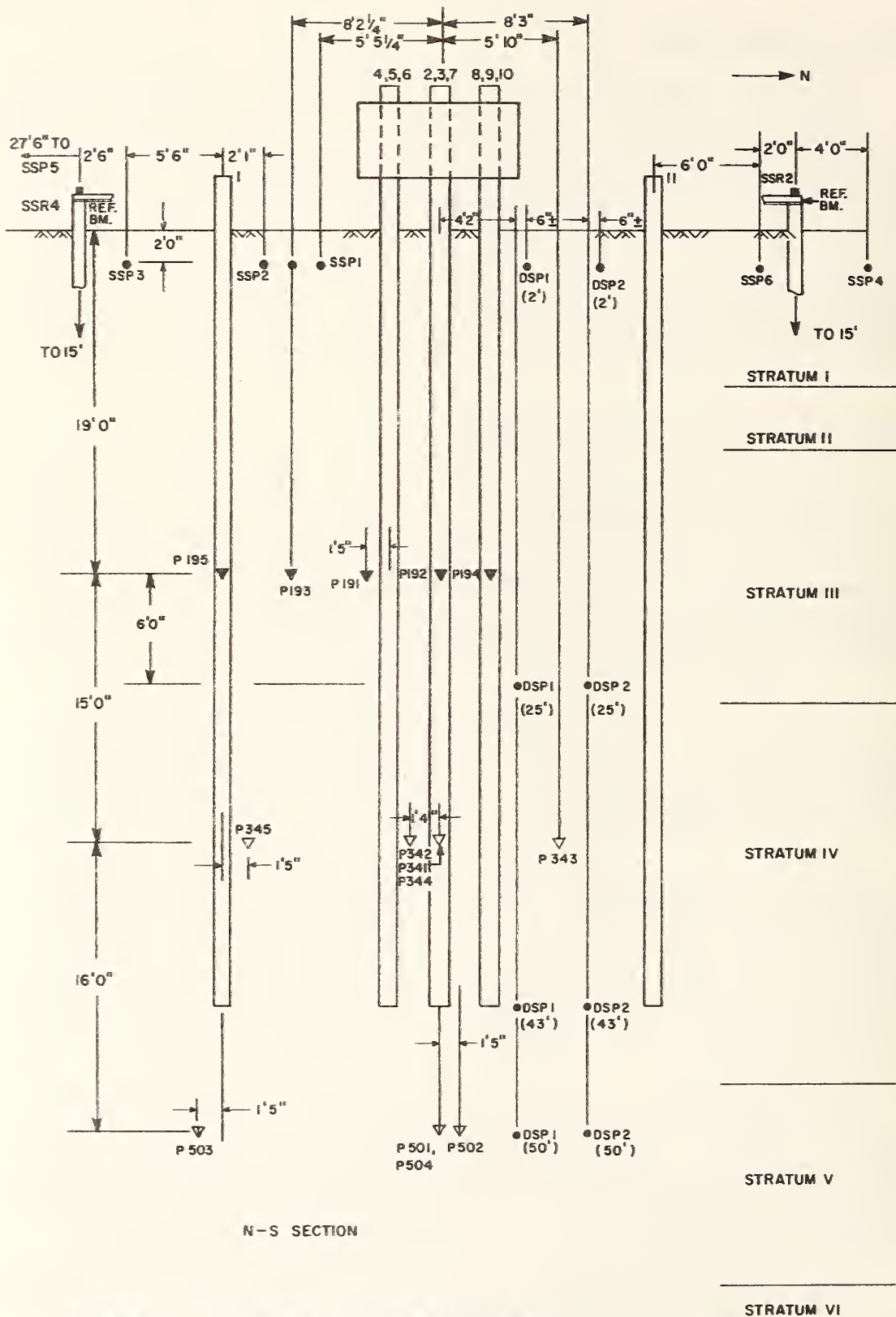


FIGURE 1.7. GROUND INSTRUMENTATION (EAST ELEVATION)
 (1 ft = 0.305 m; 1 in = 25.4 mm)

Fig. 1.6) were detached from the pile cap and the remaining five piles were tested as a subgroup. Immediately following the 5-pile subgroup test the center pile (denoted Pile 2) was detached from the cap and the remaining four piles were tested as a subgroup. Following the 4-pile subgroup test the cap was completely removed, the reaction system rearranged, and six of the piles (both reference piles and four group piles) were subjected to individual uplift, or tension, tests. The chronology of the tests and other significant field events is presented in Table 1.1.

Vertical deflections of each pile in every test were measured by two dial gages mounted diametrically opposite each other approximately one ft. (0.3 m) off the ground. The dial gages were suspended from common reference beams. Backup vertical deflections were also obtained by means of a microhead level sighting on scales placed on the pile cap and backsighting on a bench mark on a structure outside the zone of influence of the piles.

Twelve dial gages were also mounted at the lower corners of the cap to monitor cap rotation and translation in six degrees of freedom and to verify cap rigidity.

In order to minimize errors associated with thermal effects the entire test site was covered with a canvas shroud. In order to minimize errors associated with moisture content changes in the near-surface soils, the testing was carried out in the late fall, winter and early spring (wet season at the test site).

During the first load test on the 9-pile group, tipping of the cap toward the north was observed. This is believed to be due partially to the fact that the reaction girders were not centered exactly over the center of reaction of the piles when the Dywidag bars were vertical. Since it was necessary to position the jacks essentially under the webs of the girders, the jacks themselves were slightly displaced (perhaps 50 mm) from the center of reaction. To alleviate this problem on subsequent tests the girders and jacks were moved so that the resultant jack load would be at the calculated center of pile reaction from the first test. This necessitated moving the girders several inches south. In order to prevent their translation back to the north in subsequent tests, lateral braces were installed on the cross "resting" beams. These braces permitted vertical movement but effectively restrained horizontal translation of the reaction girders.

Pile Driving

General. The reaction piles for the reference test piles (H-piles) and reference beam support piles (also H-piles) and the eleven test piles were driven in the sequence described in Fig. 1.8. Approximately one week was required to install all 23 piles and to retap five of the

TABLE 1.1. CHRONOLOGY OF MAJOR FIELD EVENTS

<u>EVENT</u>	<u>DATE</u>
Initial Site Investigations	15 Jan 79 - 30 Mar 79
Installation of Anchor Caissons	27 Aug 79 - 5 Sep 79
Installation of Ground Instruments	6 Sep 79 - 25 Sep 79
Installation of H-Pile Anchors	26 Oct 79
Predrilling of Pilot Holes	26 Oct 79
Installation of Test Piles	29 Oct 79 - 1 Nov 79
Retapping of Test Piles	2 Nov 79
Erection of Cap, Reaction and Reference Frames	5 Nov 79 - 14 Nov 79
Reference Pile Tests No. 1	16 Nov 79
9-Pile Group Test No. 1	21 Nov 79
Reference Pile Tests No. 2	18 Jan 80
9-Pile Group Test No. 2	22 Jan 80
Reference Pile Tests No. 3	14 Feb 80
9-Pile Group Test No. 3	19 Feb 80
5-Pile Subgroup Test	26 Feb 80
4-Pile Subgroup Test	29 Feb 80
Uplift Test: Pile 1	19 Mar 80
Uplift Test: Pile 11	21 Mar 80
Uplift Test; Pile 2	27 Mar 80
Uplift Test; Pile 9	28 Mar 80
Uplift Test: Pile 5	1 Apr 80
Uplift Test: Pile 4	3 Apr 80
Final Soil Soundings and Site Closure	8 Apr 80 - 18 Apr 80

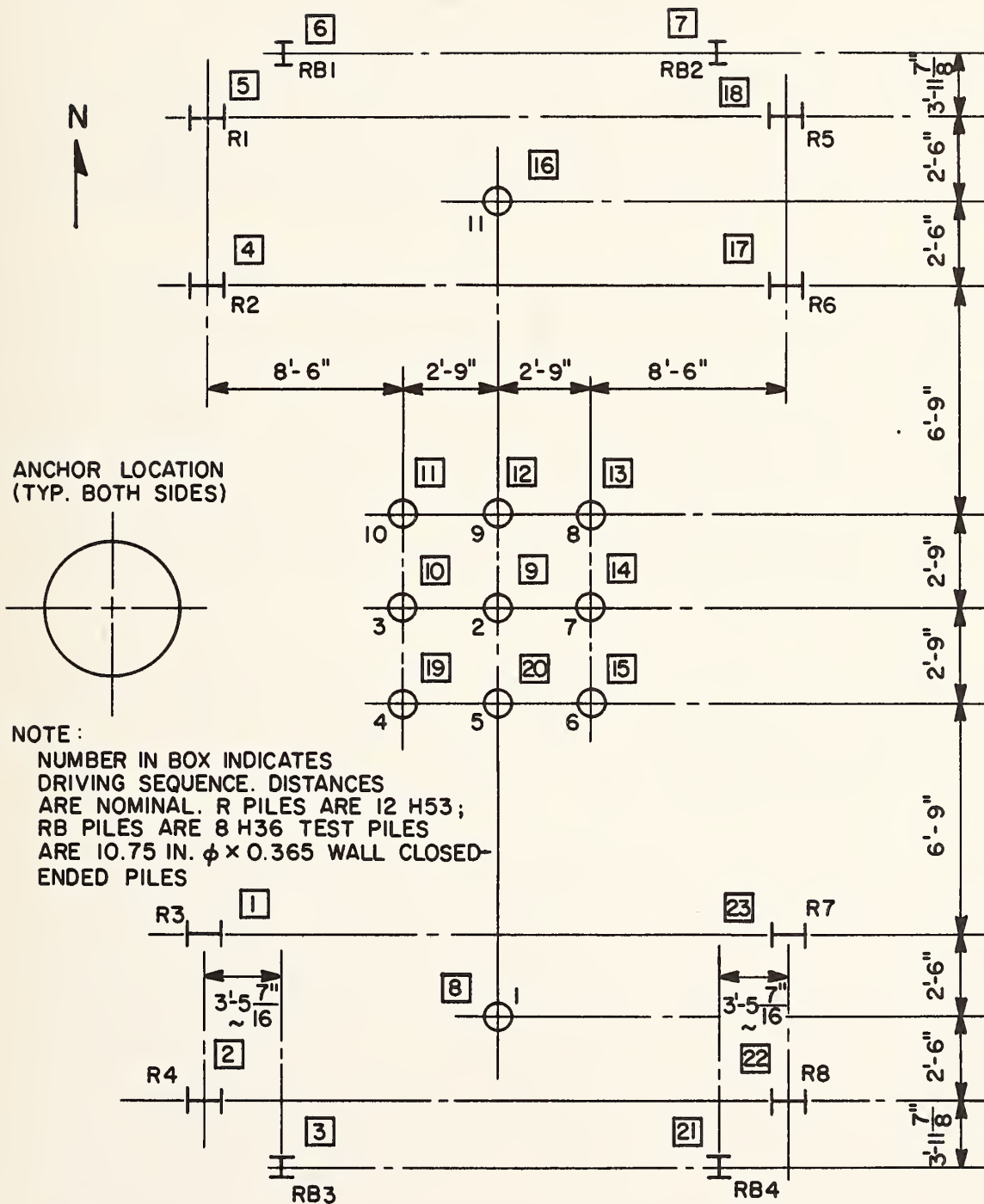


FIGURE 1.8. APPROXIMATE LOCATIONS OF ALL TEST AND REACTION PILES AND SEQUENCE OF DRIVING (1 ft = 0.305 m; 1 in = 25.4 mm)

test piles. Each of the test piles was driven in an 8-inch (200 mm) diameter by 10 ft. (3.1 m) deep pilot hole in order to ensure proper positioning and vertical alignment. All of the pilot holes were drilled at one time, 3 days before the first test pile was driven. The site was inundated with a heavy thunderstorm on the night of October 30, 1979, following the driving of Pile No. 9 (12th pile in the sequence). This left the pilot holes for the remaining test piles containing some free water which the construction crew attempted to remove. This effort was only partially successful. The presence of free water in the pilot hole for Pile 11 may explain the anomalous behavior experienced by this pile during the first load test, described later.

All 23 piles were driven by a Raymond 1S hammer, which is a single acting steam hammer with a rated energy of 19,500 ft-lbs. (26,500 m-N) per blow. The steel driving cap for the test piles fit over the outside of the piles. Cushioning, in the form of a 16.5-in. (404 mm) thick stack of alternating pads of aluminum and micarta was employed between the hammer and the driving cap. There was no cushion between the driving cap and the pile heads. The hammer was supported on hanging leads without a spotter beam. Driving records for all 23 piles are presented in Table 1.2. Note that Piles 1,2,4,8, and 11 were initially driven slightly short of their intended penetration and then retapped to final penetration at varying times after initial driving. These "retaps" were intended to serve as a qualitative guide to short-term set-up.

Quantitative data on actual energy delivered to the pile heads and on short-term set-up were acquired by means of the "Goble Pile Driving Analyzer" by others during installation. The reader is referred to the FHWA report "Dynamic Pile Driving Measurements for University of Houston Pile Group Study" by A.R. Dover, G.E. Locke, and J.M.E. Audibert, dated December, 1979, for that information.

Some comments on the above report appear appropriate here. A review of that report reveals that actual energy accepted by the pile heads varied from about 4,000 ft-lbs (5,400 m-N) per blow for Pile 9 to about 8,000 ft-lbs (10,900 m-N) per blow for Pile 11. These values had very little dependence on tip penetration. Short-term set-up, based on retap data and Analyzer results requires the assumption of a damping factor, denoted J. Prior experience by the authors of the above-referenced report suggests that the appropriate J-factor is that which applies to the soil type near the pile tip. In this case (sandy clay) J should be in the range of 0.45 - 0.70. Analysis of the predicted rate of set-up over a period of four days (lapse period for the retaps) with $J = 0.6$, at the approximate midpoint of the time range (Fig. 13 of the above-referenced report) suggests that the static pile capacity during driving was likely between 50 and 100 kips (220 and 450 kN) and that the static capacity approximately four days after driving was 150 to 200 kips (670 to 890 kN) for Piles 1 and 2. The implications of these data, if a constant J-factor is realistic, are that almost all of the

set-up of both the center group pile (No. 2) and the isolated reference pile (No. 1) occurred within four days of driving, since the capacities of Piles 1 and 2 were in the range of 150 to 170 kips (670 to 760 kN) at the time of Test No. 1, approximately three weeks after driving. This result appears to be consistent with the rapid rate of pore water pressure dissipation observed at this test site following driving. Pore pressure effects are described in detail later.

Measurement of Compression Wave Attenuation. Representative traces of dynamic force vs. time during driving are presented in Figs. 1.9 and 1.10. Figure 1.9 shows force-time traces at the tops, near the middles, and near the bottoms of Pile 2 and Pile 4 for one hammer blow at essentially full penetration during initial driving. Exact locations of transducers are noted on the figure. Two transducers were placed at opposite ends of a diameter at the top locations to allow the bending effect produced by an uneven blow to be accounted for (by averaging the traces for the two gages). At the lower levels only one transducer was placed because it was assumed that effects of eccentricity of the stress wave would be damped out by the soil by the time the wave reached those locations. The average force-time trace for the top transducers, as well as all individual force-time traces are shown with respect to a common time base for each pile. Two facts are evident in these traces: (1) very little force attenuation occurred over the first 21 ft. (6.4 m) of embedment, and (2) considerable force was transmitted to the vicinity of the pile tips. These observations imply that virtually all of the soil resistance developed during driving was in the form of side shear over the bottom half of the pile and of tip resistance. This inference is in general agreement with the wave return measurements made at the pile heads by Dover, et al, using the Goble Pile Driving Analyzer.

For purposes of further analysis, it may be assumed that Pile 2 behaved as an "isolated" pile during driving, since it was the first pile driven in the group, and that Pile 4 behaved as a "group" pile, since it was one of the last piles driven in the group.

Similar driving traces are shown in Fig. 1.10 for Piles 1 and 5. Pile 5 data are shown for a partial penetration of 28 ft. (8.5 m). Beyond that penetration one of the top gages and the bottom gage yielded a flat response, probably due to a broken wire or connection. Pile 5 is also a "group" pile, as it was the last pile driven. The partial penetration data for Pile 5 indicated a significant reduction in transmitted force in the upper 22 ft. (6.7 m) of soil, unlike the essentially non-existent reduction in the upper 21 ft. (6.4 m) of soil in Piles 2 and 4 at full penetration. The same general effect was observable for Piles 2 and 4 for partial penetrations. This suggests that effects of driving may have degraded the contact between the pile wall and the soil in the upper approximately 20 ft. (6.1 m) as the piles were being driven from about 28 ft. (8.5 m) of penetration to 43 ft. (13.1 m) of penetration. Subsequent load testing, however, indicated relatively high load transfer

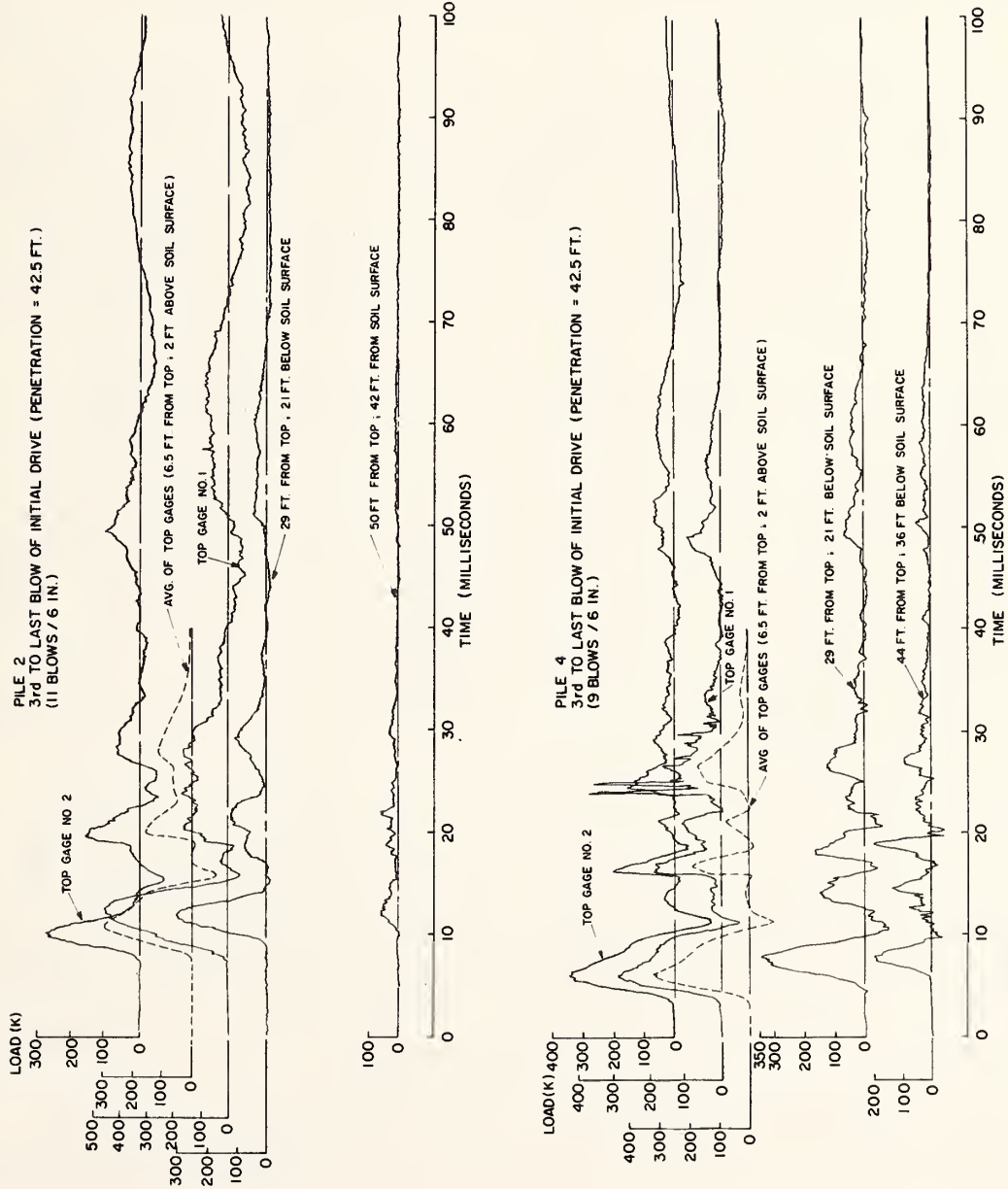


FIGURE 1.9. FORCE-TIME TRACES FOR ONE BLOW ON PILES 2 and 4 (1 k = 4.45 kN; 1 ft = 0.305 m; 1 in = 25.4 mm)

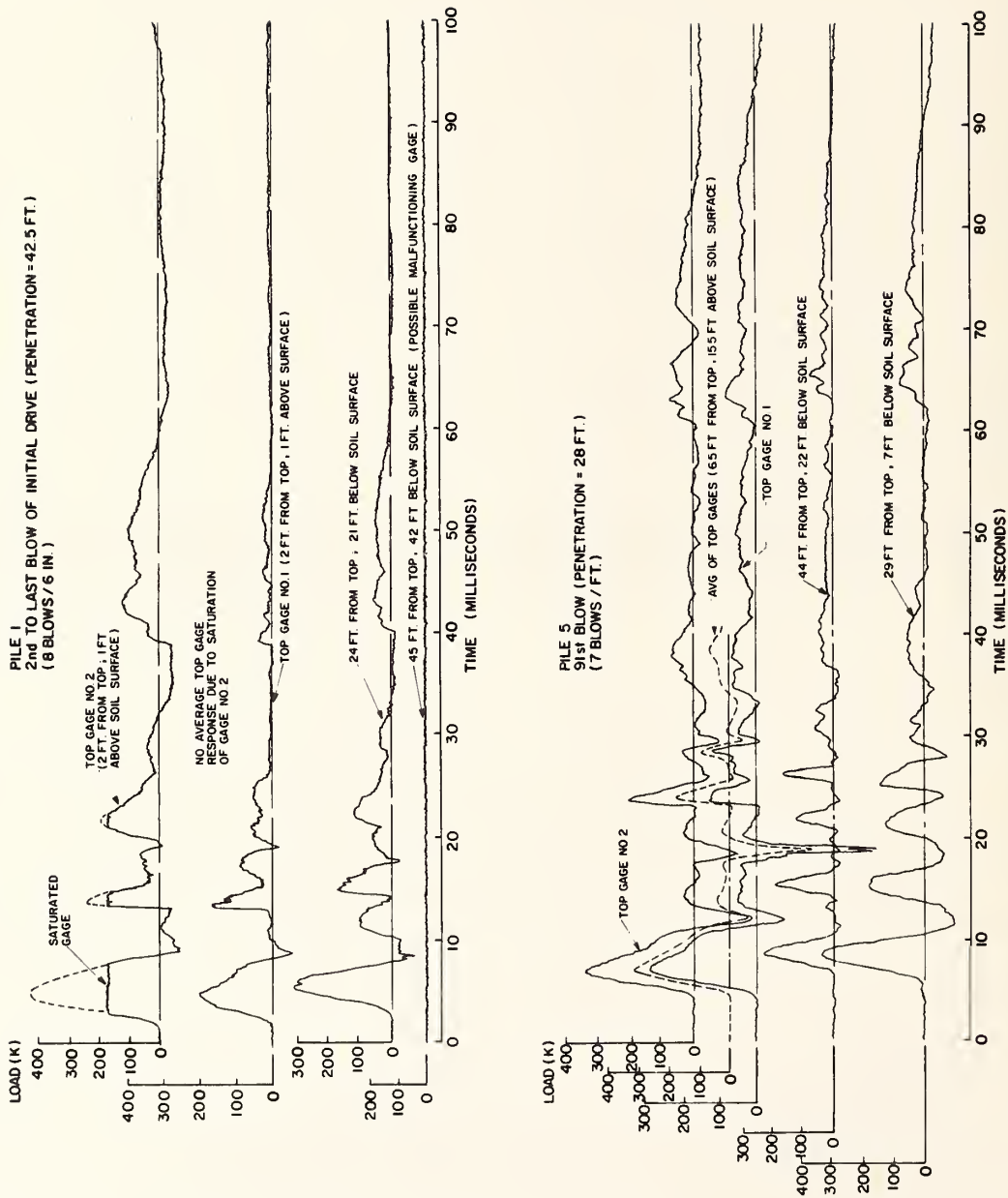


FIGURE 1.10. FORCE-TIME TRACES FOR ONE BLOW ON PILES 1 AND 5 (1 k = 4.45 kN; 1 ft = 0.305 m; 1 in = 25.4 mm)

in the upper 20 ft. (6.1 m), suggesting that the soil in this zone may have developed a very small annular space with respect to the pile wall during driving after which the soil rapidly swelled laterally into contact with the pile wall.

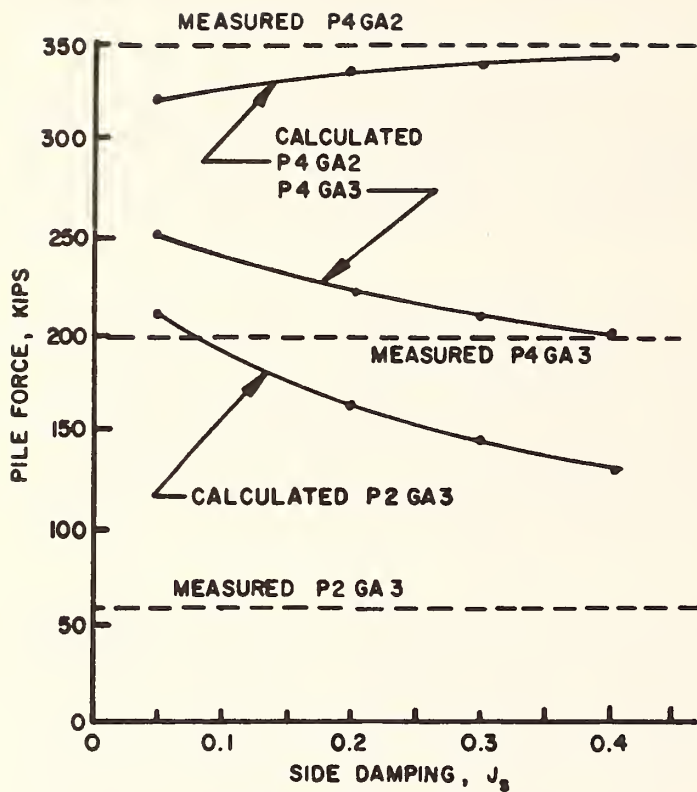
The data for Pile No. 1 are incomplete. One of the top gages saturated electrically because of an improper amplifier setting. The bottom gage yielded a flat response. This gage was later found to be faulty. The scheme of establishment of dynamic gages with respect to bending was identical on Piles 1 and 5 to the scheme described for Piles 2 and 4.

Wave Equation Analyses. Force measurements made during pile installation at three locations on instrumented piles indicate some attenuation or reduction in pile shaft force between gage stations two (GA 2) and three (GA 3) (Fig. 1.11c) for readings made just prior to final penetration. Wave equation modeling was attempted for Piles 2 and 4. Various values of Smith side damping were examined to determine what comments could be made relative to appropriate values for use in analysis of a single pile (Pile 2) versus a group pile (Pile 4).

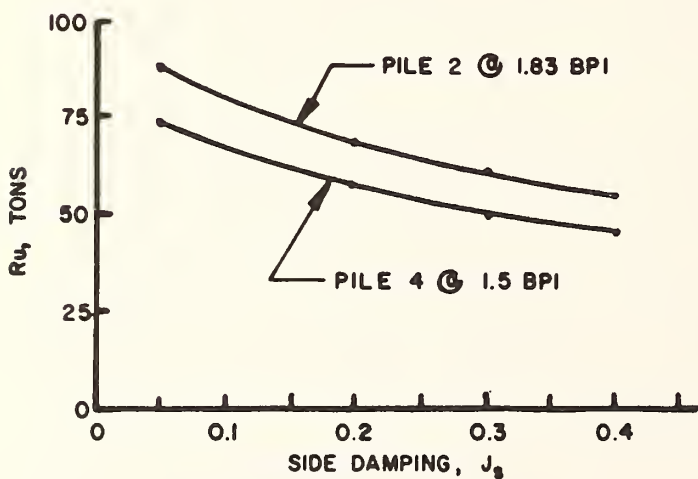
Recorded driving resistance for Pile 2 was 1.83 blows per inch (0.072 blows /mm), and the pile force was observed to drop from 300 kips (1330 kN) at GA 2 to 60 kips (267 kN) at GA 3. Recorded driving resistance for Pile 4 was 1.5 blows per inch (0.059 blows/mm), and the pile force was observed to drop from 350 kips (1560 kN) at GA 2 to 200 kips (890 kN) at GA 3. Evaluation of the force-time records indicate that approximately 40 per cent of the static pile capacity developed during driving occurred at the tip and the remaining capacity occurred in side friction over approximately the bottom one half of the penetration length. These proportions were used in the wave equation study. The wave equation program used is the program developed by E.A.L. Smith while he was Chief Mechanical Engineer for Raymond International.

The results of the study are indicated on Figs. 1.11 and 1.12 and in Table 1.3. The best match of measured versus calculated pile force was obtained for Pile 4 using a uniform friction distribution and a J-side of 0.4. Comparison of measured versus calculated pile force (Fig. 1.12a) indicates that for Pile 4 the measured forces were approached asymptotically by the calculated forces as J-side was increased, indicating that reasonably larger values of J-side would not further enhance the comparison. Similarly, this figure also indicates that the measured force at GA 3 for Pile 2 would never be reached using the R_u distribution under study.

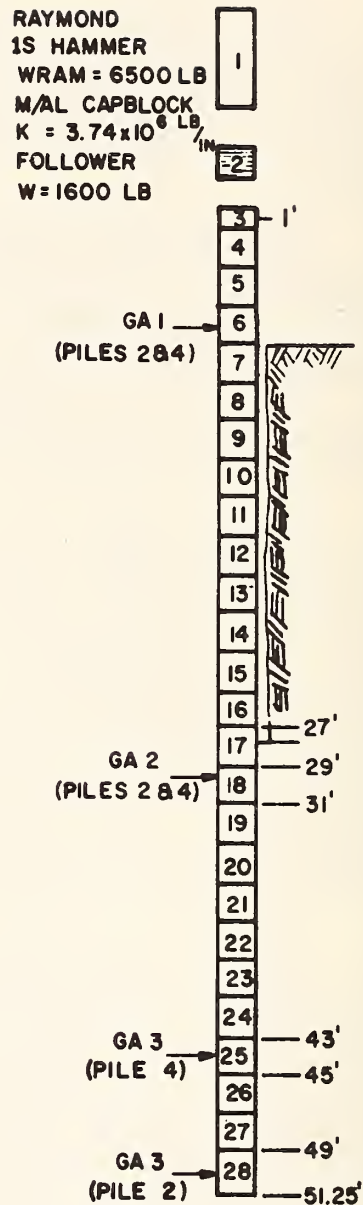
Conclusions which can be drawn from this comparison of measured and calculated forces are (1) for the distribution under study a J-side of 0.4 appears appropriate for group Pile 4, and (2) either a different



(a) MEASURED AND CALCULATED PILE FORCE



(b) DYNAMIC RESISTANCE vs. J_s



(c) WAVE EQUATION MODEL
PILES 2 & 4

FIGURE 1.11. MEASURED AND CALCULATED PILE FORCES AND WAVE EQUATION MODEL (1 k = 4.45 kN; 1 ton = 8.9 kN; 1 ft = 0.305 m; 1 lb = 4.45 N; 1 in = 25.4 mm)

PILE 4

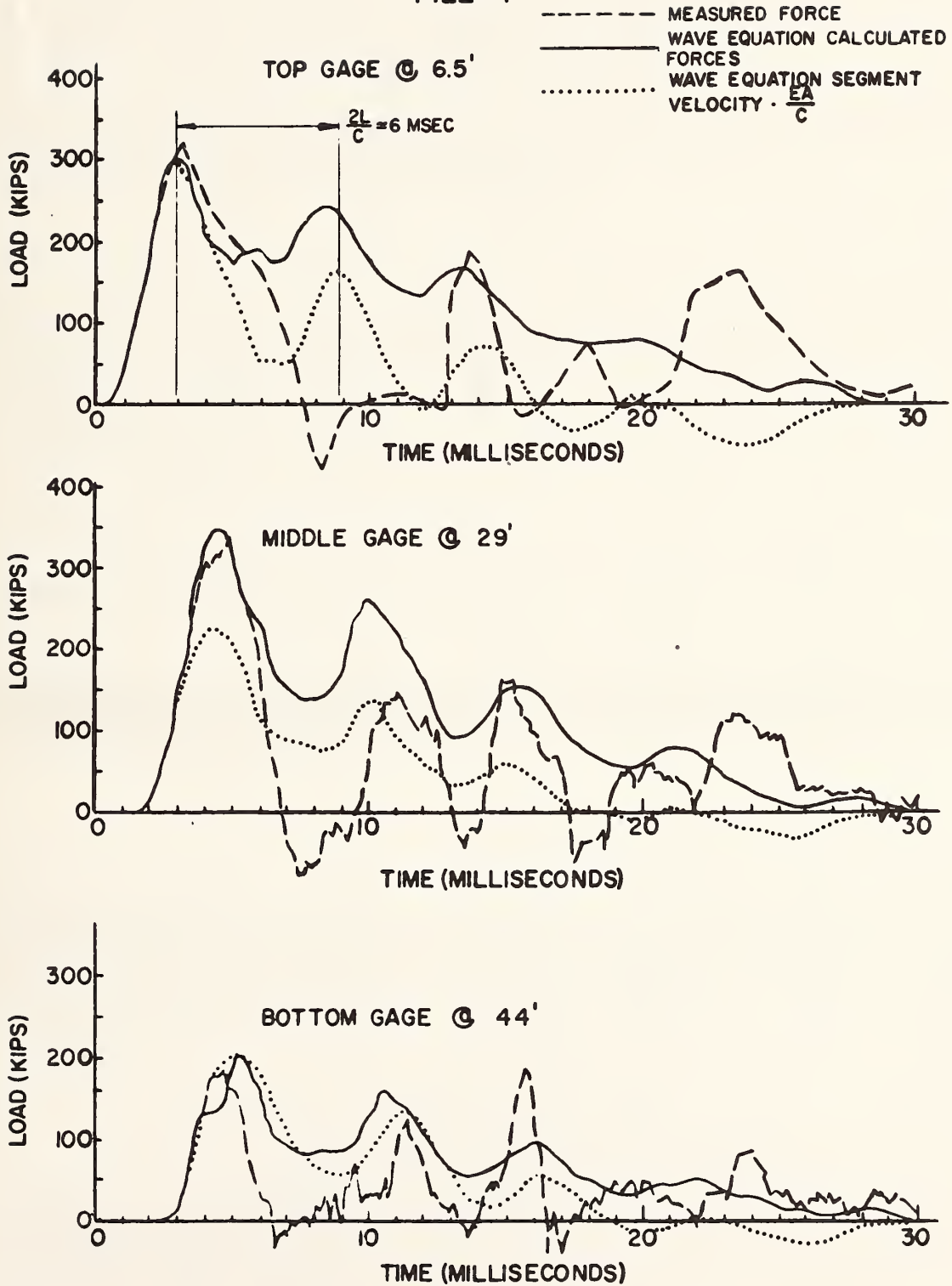


FIGURE 1.12. MEASURED AND COMPUTED FORCE-TIME RELATIONSHIPS FOR PILE 4 (1 k = 4.45 kN; 1 ft = 0.305 m)

TABLE 1.3. COMPUTED PEAK PILE FORCES DURING DRIVING AS
 FUNCTION OF SIDE DAMPING, J (1 k = 4.45 kN;
 1 t = 8.9 kN; 1 ft = 0.305 m; 1 in = 25.4 mm;
 1 ft-lb = 1.36 m-N; 1 BPI = 1 blow / 25.4 mm)

		MAXIMUM PILE FORCE, KIPS				
		@6'-6"	@29'3"	@ 44'	@ 50'-3"	
Pile 4 Measured		300 K	350 K	200 K		
Pile 2 Measured		300 K	300 K		60 K	
40% Point, Triangular Friction Distribution Lower 23'						
Pile	R _u	J _s	GA 1	GA 2	GA 3	GA 3
4	75 T	0.05	299.3	318.4	282.2	
2	88 T	0.05	299.3	321.7		320.2
4	58 T	0.20	299.3	328.4	269.1	
2	70 T	0.20	299.3	334.2		180.2
4	52 T	0.30	299.3	333.8	265.6	
2	63 T	0.30	299.3	340.8		165.1
4	46 T	0.40	299.3	337.3	262.1	
2	57 T	0.40	299.3	345.6		153.8
40% Point, Uniform Friction Distribution Lower 23'						
Pile	R _u	J _s	GA 1	GA 2	GA 3	GA 3
4	75 T	0.05	299.3	322.9	251.0	
2	89 T	0.05	299.3	327.2		209.5
4	59 T	0.20	299.3	335.0	222.1	
2	70 T	0.20	299.3	340.8		162.7
4	51 T	0.30	299.3	339.4	210.0	
2	62 T	0.30	299.3	346.6		144.8
4	46 T	0.40	299.3	343.3	201.5	
2	56 T	0.40	299.3	351.0		132.0

NOTES: 1. Pile 4 driven to 1.5 BPI, Pile 2 to 1.83 BPI
 2. Hammer impact velocity = 12.81 ft/sec or energy delivered by hammer = 16,575 ft-lbs.
 3. Side quake & Point quake = 0.10, and Point damping = 0.15 for all runs.

R_u distribution existed at Pile 2 or significantly higher damping occurred during installation of this pile. Examination of the R_u curves of Figure 1.11b indicates that for the distribution studied, Piles 2 and 4 had a minimum capacity at the time of driving of approximately 57 and 46 tons, respectively. These values also seemed to be approaching a limit as J-side was increased. Damping associated with transverse vibration of the pile could have been active during driving, but such damping is not modeled in the one-dimensional wave equation.

The maximum pile forces reported by the Pile Analyzer equipment at a point approximately three feet (1 m) above GA 1 for Piles 2 and 4 at approximately the same penetration are 157 and 256 kips (699 and 1139 kN), respectively, while measurements made for this study consistently indicate 300 kips (1335 kN). Similarly, maximum energy transferred to the piles as calculated by the integral of force times velocity over time for Piles 2 and 4 were, respectively, 4400 and 6500 foot-pounds (6000 and 8840 m-N). Matching of wave equation analysis to the measured 300 kips (1335 kN) pile head force indicates an effective required hammer energy of 16,575 foot-pounds (22,540 m-N). Calculation of energy delivered to the pile, as opposed to energy accepted by the pile (and presumably dissipated into the soil), using the measured velocity for Piles 2 and 4 from the Pile Analyzer and the hammer ram weight in the expression $E = \frac{1}{2} M V^2$ yields a delivered energy of 7640 and 10,296 foot-pounds (10,390 and 14,000 m-N), respectively, for Piles 2 and 4. These values seem low, but they may offer a more realistic basis for hammer evaluation than does the energy transferred to the pile given directly by the Analyzer.

Soil Displacements During Driving

The surface and depth settlement points ("SSP" and "DSP," respectively) were monitored during test pile installation by means of a microhead level. This level was realistically capable of resolving movements of 0.05 in. (1 mm) or greater. The results of this monitoring are summarized in Fig. 1.13, in which the progression of soil movement along a north-south line is shown at various stages of driving. The maximum heave of the soil surface was about 1 in. (25 mm) near the outer perimeter of the group, reducing to about 0.1 in. (2.5 mm) at a distance of 28 ft. (8.5 m) from the center of the group. The reference piles were driven along this north-south line, and they appear to have magnified the heave in the soil some distance from the group.

Below-surface vertical movements were generally small except at a depth of 25 ft. (7.6 m), where about 1 in. (25 mm) of settlement was noted in the settlement point nearest Pile 9 (DSP1). This phenomenon is probably a result of one of the spread anchors for the point being in the zone of shear drag for this pile. Farther from the group perimeter, at DSP2, slight heaving of the soil was observed. The observations imply a vertical extension of the soil near the perimeter of the group in the upper 25 ft. (7.6 m). Very little net movement was observed at

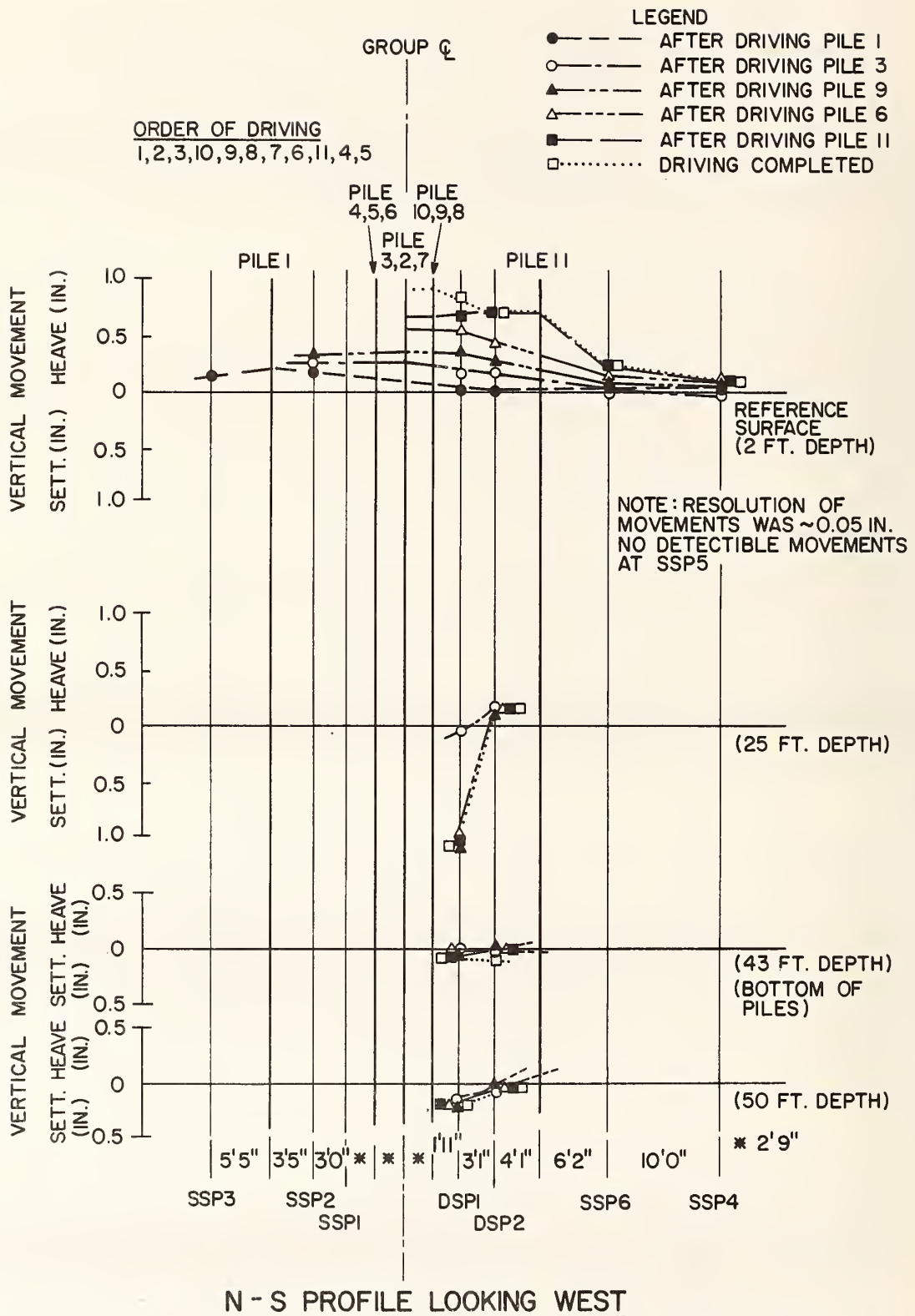


FIGURE 1.13. OBSERVED SOIL MOVEMENTS DURING PILE INSTALLATION
(1 ft = 0.305 m; 1 in = 25.4 mm)

DSP1 and DSP2 at a depth of 43 ft. (13.1 m), although it should be recalled that these points were positioned outside the perimeter of the group. Slightly greater movements (settlements) were observed at the 50 ft. (15.3 m) depth.

The observed surface heave accounted for approximately 30 per cent of the theoretical volume of displaced soil from the 11 test piles, assuming the displacements were symmetric; that is, displacement measured along the north-south line would apply to any other section through the group.

Pore Water Pressures

Figures 1.14-1.17 present the pore water pressure history, as measured by the pneumatic ground and pile piezometers from prior to the time of installation through the first load test. The free-field response of 11 of the 14 ground piezometers for the 30-day period prior to pile installation is shown in Fig. 1.14. All but 3 of these piezometers reached essentially a steady state condition prior to pile installation. The three that did not reach steady state drifted toward higher indicated pressure readings rather than lower readings. One of these piezometers, P503, eventually returned to a reasonable reading. The other two (P343 and P504) continued to drift upwards in reading throughout the test program and are considered by the authors to have yielded unrepresentative values of pore pressure. Two other piezometers, P194 and P341, gave zero pore pressure readings, (flat response) throughout the test program. Thus, it appears that 10 of the 14 ground piezometers yielded reasonable results through all or part of the testing program. The performance of both the pile and ground piezometers is discussed further in Appendix E.

The pile piezometers lost saturation upon driving. Therefore, pore pressure readings against the pile faces immediately after driving could not be made. The pile piezometers were resaturated during and immediately after the period of pile installation through special tubing that had been installed for that purpose. The first valid reading on the various pile piezometers after resaturation is denoted by the character "S" on Figs. 1.15-1.17. These figures do not show the pressure-time relationships for the 9 ft. (2.7 m) and 41 ft. (12.5 m) pile piezometers. The 9 ft. (2.7 m) piezometers registered essentially zero response and the 41 ft. (12.5 m) piezometers responded in a manner similar to the 34 ft. (10.4 m) piezometers. Numerical values for these levels are given in a different form later in this report.

Several observations from Figs. 1.15-1.17 are noted. First, the ground piezometers yielded free-field pore pressures (before installation of piles) that could be approximated with a piezometric surface at a depth of about 7 ft. (2.1 m). The average hydrostatic piezometer reading before pile installation at each level was as follows:

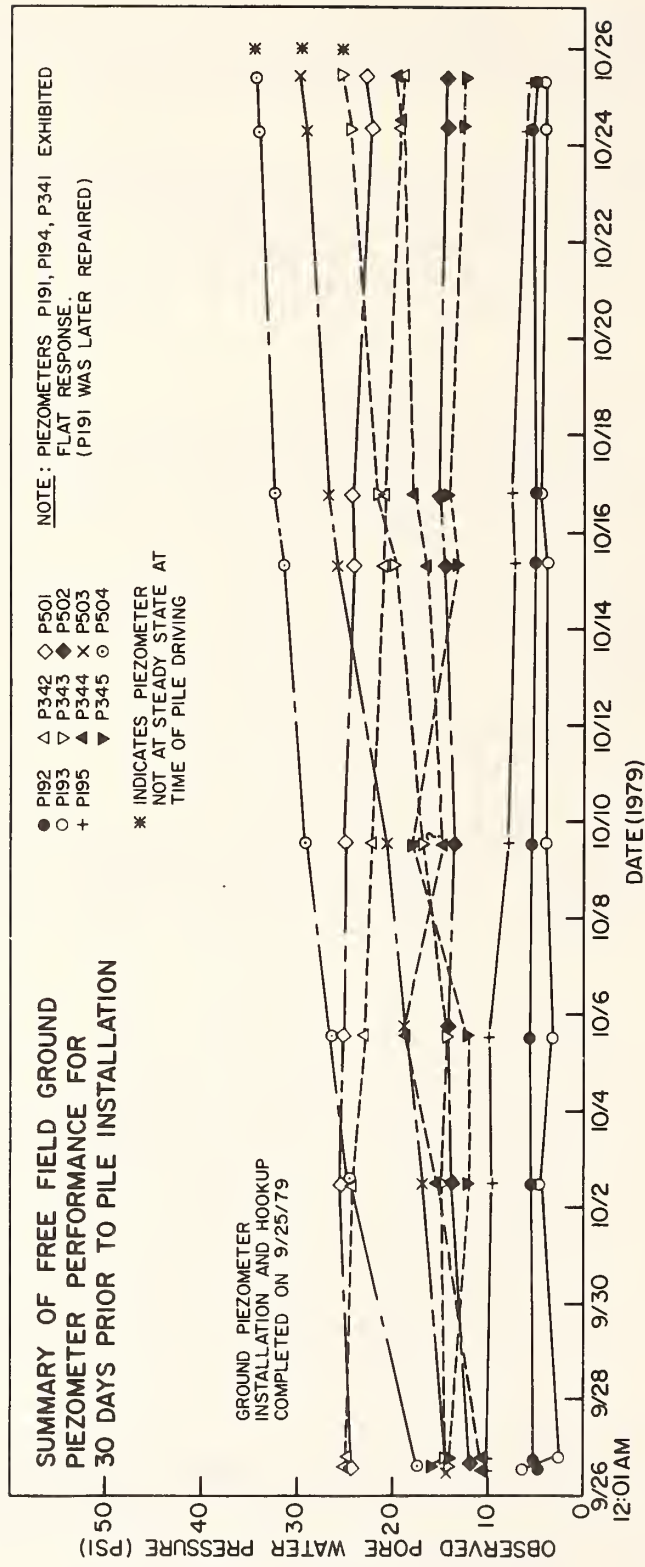


FIGURE 1.14. OBSERVED SOIL PORE WATER PRESSURES PRECEDING PILE INSTALLATION
(1 psi = 6.89 kN/m²)

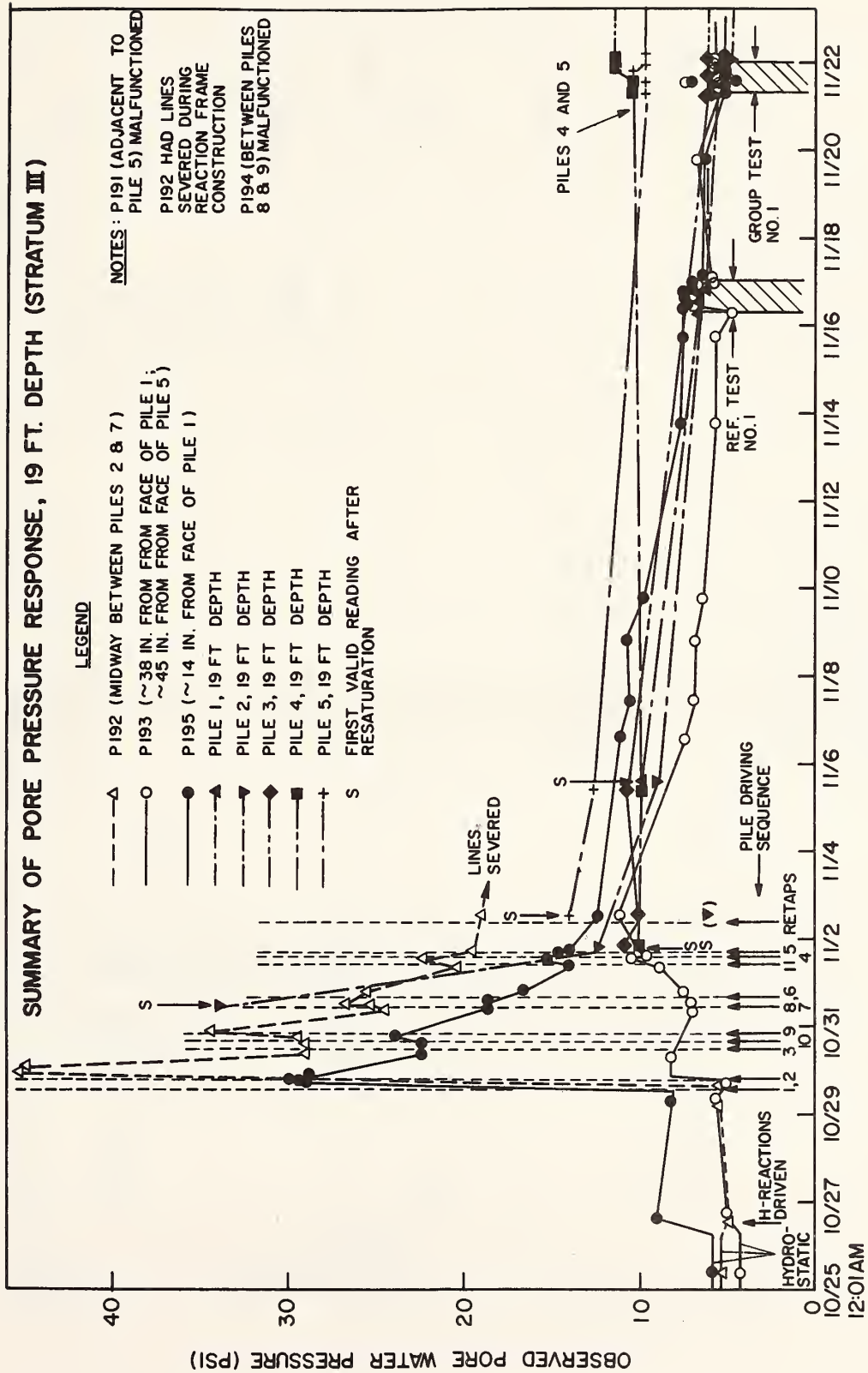


FIGURE 1.15. PORE WATER PRESSURE VS. TIME AT 19 FT (5.8 M) DEPTH
 (1 ft = 0.305 m; 1 psi = 6.89 kN/m²)

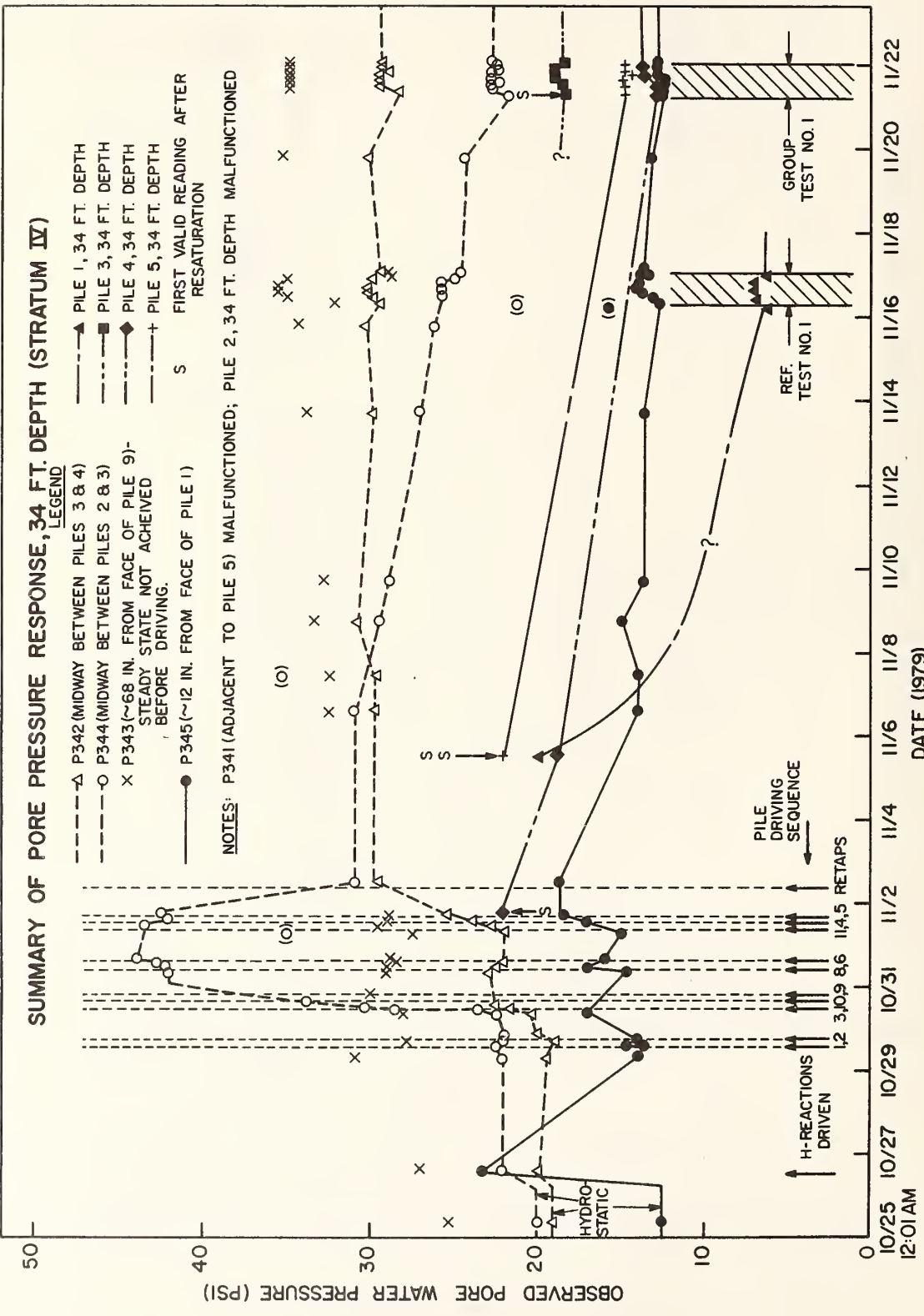


FIGURE 1.16. PORE WATER PRESSURE VS. TIME AT 34 FT (10.4 M) DEPTH
 (1 ft = 0.305 m; 1 psi = 6.89 kN/m²)

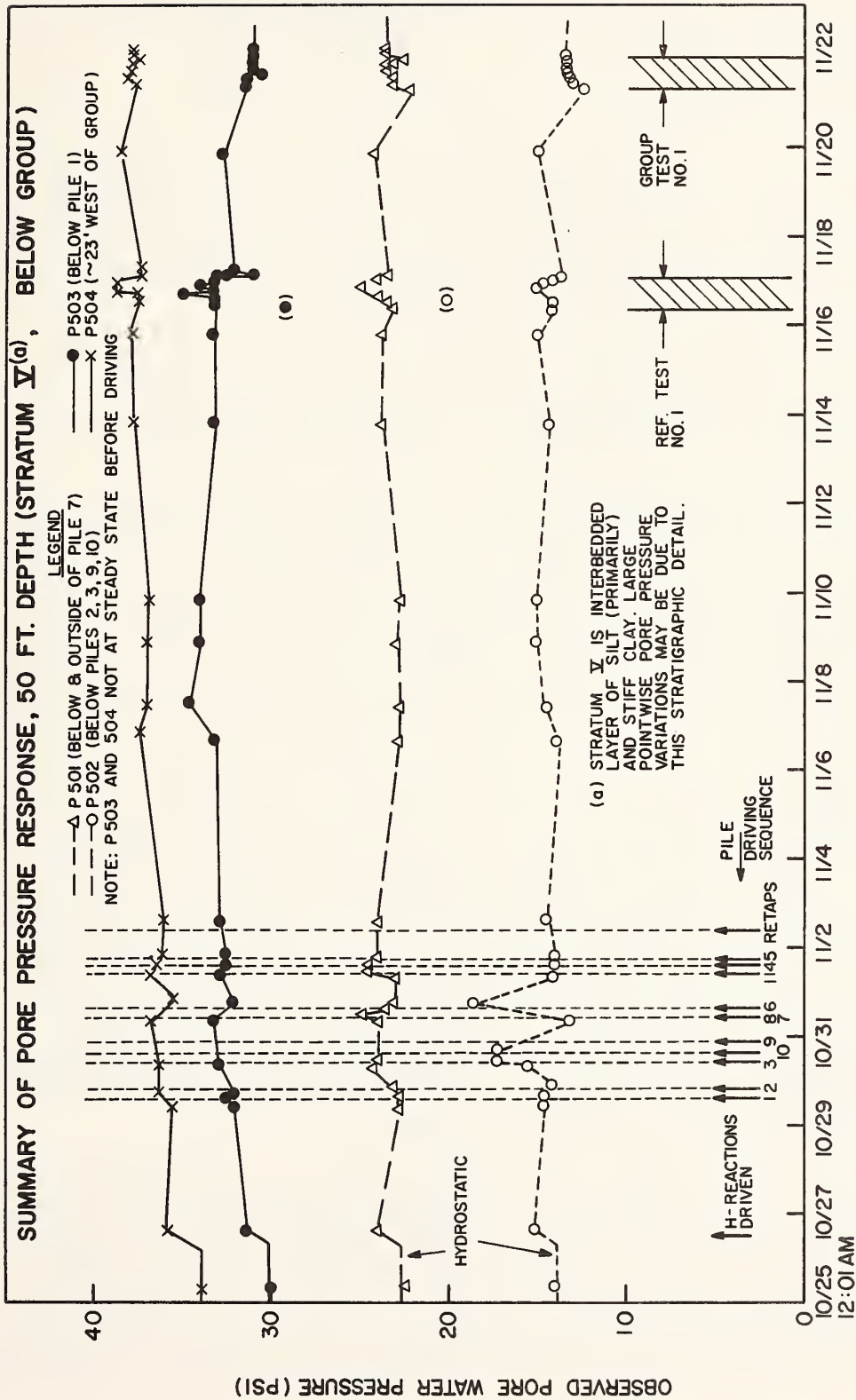


FIGURE 1.17. PORE WATER PRESSURE VS. TIME AT 50 FT (15.3 M) DEPTH
 (1 ft = 0.305 m; 1 psi = 6.89 kN/m²)

<u>Piezometer Depth</u>	<u>Depth of Hydrostatic Head Level Below Site Grade</u>
9 ft (2.7 m)	8.0 ft (2.4 m)
19 ft (5.8 m)	7.5 ft (2.3 m)
34 ft (10.4 m)	-4.8 ft (-1.5 m)
50 ft (15.3 m)	7.3 ft (2.2 m)

The negative value at the third level indicates that the appropriate hydraulic head line was above grade. This value is believed to be anomalous and unrepresentative due to one high reading. Some scatter in the hydrostatic pressure values at a given level can be observed. This scatter is believed to be the result of local variations in soil properties and their effect on piezometer response.

Second, the action of driving the "non-displacement" H-type reaction piles elevated the pore water pressures, especially at P345, near Pile 1. These pressures were largely dissipated three days after the H-piles were driven and prior to driving the test piles.

Third, pore pressure response to test pile installation in the soil mass showed that in general rather large excess pore pressures were generated by pile installation and that these excess pressures dissipated rapidly. The functional ground piezometer at the 19 ft. (5.8 m) level within the pile group (P192) experienced a peak pressure of 44 psi (303 kN/m²), 39 psi (269 kN/m²) of which was excess. The peak developed excess pore pressure may be expressed as a ratio to the existing vertical in-situ effective stress. This ratio, hereafter called the pore pressure ratio, was 3.3 for P192 immediately after the installation of Pile 2. The pore pressure at P192 dissipated rapidly but responded sharply again when Piles 9 and 7 (near the piezometer) were driven. These later responses were not as strong as the response associated with the installation of Pile 2. The peak readings, expressed as pore pressure ratios, were 2.5 upon installing Pile 9 and 1.9 upon driving Pile 7. The corresponding piezometer adjacent to Pile 1 (P195) responded similarly to the driving of Pile 1, with a peak pore pressure ratio of 2.0. The effects of driving other piles were less pronounced at P195 than at P192, which was inside the group. P193, which was situated between the group and Pile 1 responded less intensely to the installation of the test piles, exhibiting a gradual buildup of pore pressure during installation of the group rather than sharp response to the installation of any single pile. The maximum pore pressure ratio was 0.6 and occurred after the completion of the retaps.

At the 34 ft. (10.4 m) level, somewhat less consistent behavior occurred. The two functional ground piezometers within the group responded somewhat differently. P344, between Piles 2 and 3 did not respond when Pile 2 was driven but did respond to the driving of Pile 3. The pore pressure ratio was 0.6 after Pile 3 was driven. Pore pressures at this location continued to increase until after Pile 6 was driven, at which time the pore pressure ratio was 1.2. Thereafter,

rapid dissipation occurred until the first group test, at which time the excess pressure was about 3 psi (21 kN/m²). P342, between Piles 3 and 4, responded only slightly to the installation of Piles 3 and 4. Instead, a general increase in pore pressure occurred during installation of the test piles. A maximum pore pressure ratio of 0.6 was achieved after the final retap. However, this piezometer did not exhibit any dissipation of the excess pore pressure after the retaps, such that about 12 psi (83 kN/m²) of excess pore pressure existed at the time of the first group test. This is inconsistent with the behavior of other ground piezometers and is thought to be associated with a soil anomaly in the immediate vicinity of the piezometer. P345, adjacent to Pile 1, also failed to respond appreciably to the installation of Pile 1 but did exhibit a slight pore pressure buildup during installation of group piles, followed by rapid dissipation back to the hydrostatic level.

Pore pressure changes in the soil beneath the level of the pile tips were minor. The peak pore pressure ratio at P502, situated essentially beneath the center of the group at a depth of 50 ft. (15.3 m), was 0.2 and occurred just after driving Pile 6. Reestablishment of hydrostatic pressures occurred in the functional piezometers at the 50 ft. (15.3 m) level within 1 to 4 days after completion of driving.

Several of the ground piezometers were monitored while piles were in the process of being driven. Piezometers near driven piles that responded during driving of the piles did so as the pile tips approached the depths of the piezometers. After the tips passed, very little further pore pressure change occurred.

Fourth, the piezometric changes in the soil mass during load testing were very minor compared to those created by pile installation. (While the absolute values of the drifting piezometers, P343, P 503, and P 504, may be incorrect, the registered changes in pore pressures during the course of a load test are thought to be valid.) This fact suggests that the soil was behaving in essentially a drained manner.

Fifth, the response of the pile piezometers, once they had been resaturated, exhibited a trend similar to the ground piezometers in that pore pressures, both on the reference and group piles, decreased rapidly after driving and that excess pore pressures generated during load testing were very small.

The rapid pore pressure dissipation observed at this site is believed to be due to the high hydraulic diffusivity of the soil produced by fissure and slickenside planes in the Beaumont soil, by apparently continuous sand partings in the underlying Montgomery soil, and by the apparent inability of the pile to induce lateral pressures sufficient to transform the soils near the surface to a state of normal consolidation.

Total pressure cells on the piles were also read after pile installation. A rapid temperature drop on the cells during the first few

hours after driving rendered interpretation of the data for this event questionable. Further discussion of total pressure will be deferred until Chapter 2; however, for completeness with respect to pile installation, Fig. 1.18 is shown here, which depicts the average measured earth pressure coefficients against the reference and group pile walls compared with the in-situ values. The low value at 19 ft. (5.8 m) in the reference pile is due to an unrepresentatively low total pressure reading.

Figure 1.19 depicts section lines through various soil and pile pressure cells. These sections will be referenced later in this report when detailed descriptions of pore and total pressure changes are discussed. Meanwhile, Fig. 1.20 shows three of the sections along with a spatial comparison of measured pore pressure distributions one day before driving began and one day after driving was concluded.

Assessment of Soil Disturbance

At the conclusion of the tests that will be described in Chapter 2, approximately 5 months after the piles were installed, a final series of static cone soundings was made. The locations of these soundings, as well as the detailed results, are described in Appendix C. No evidence of shear strength reduction in the soil within the pile group could be found at that time. The penetrometer was not capable, however, of making precise measurements of shear strength in the zone immediately adjacent to the pile walls.

As-Driven Locations of Piles

After the piles had been driven and the cap secured, the locations of the heads of all of the group piles were located relative to a point of reference on the pile cap by survey techniques. The alignment of piles below the pile tops was measured by using a sensitive miniature electrical inclinometer, which was run down the inclinometer tubes (affixed to the interior of the piles) on two perpendicular tracks. The results of these measurements are shown on Fig. 1.21. That figure also shows the exact position of certain of the ground settlement points relative to the piles and of the loading jacks at the time of testing.

Note that none of the piles was exactly vertical, although only minor bending was observed. The average batter was about 1.5 per cent of the pile length, or slightly less than the inside diameters of the piles. The highest batter was in Pile 8 (18 in. (0.46 m)). There was a slight preference for a batter to the northeast or southwest, which was generally perpendicular to the plane containing the driving leads and the boom of the crane carrying the leads.

Table 1.4 gives numerical values for the locations of the centers of the pile heads and jack bases at the top of the cap relative to the geometric center of the top of the cap.

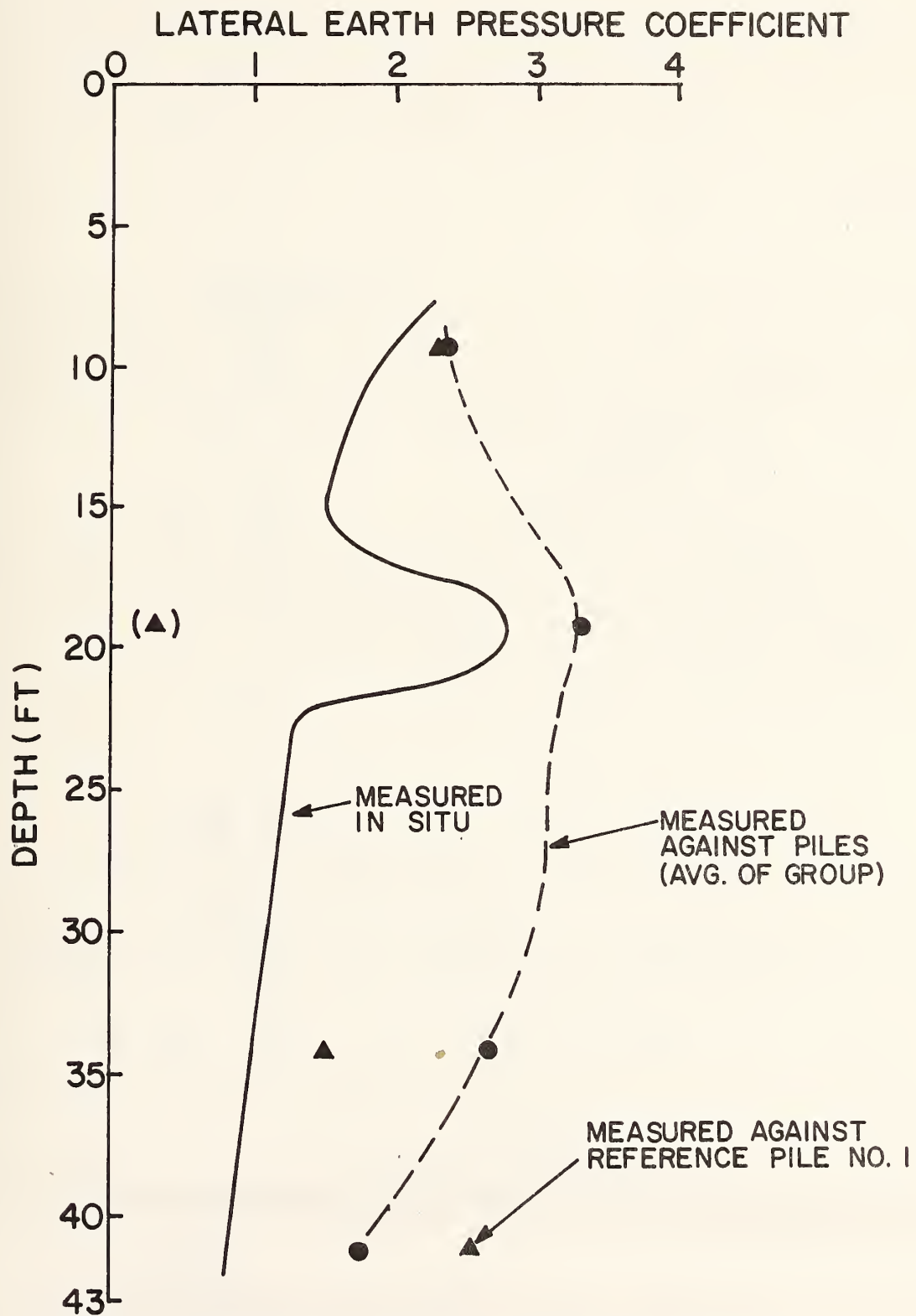
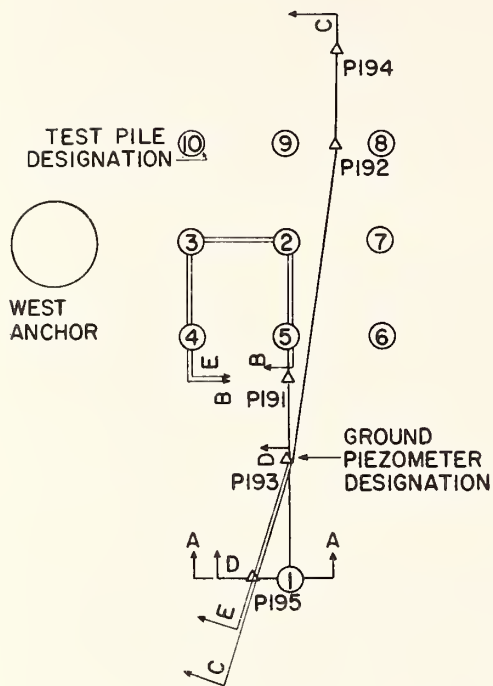
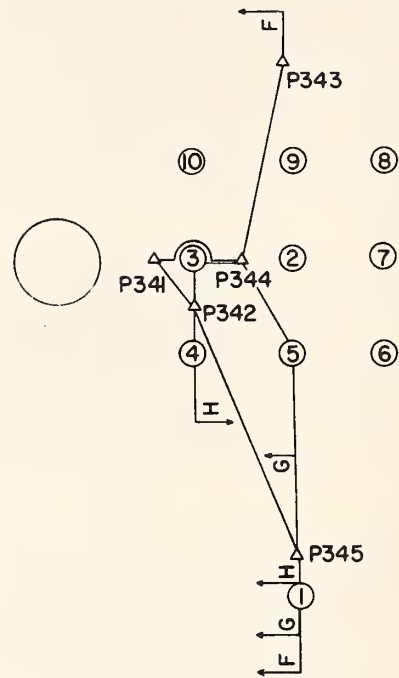


FIGURE 1.18. MEASURED EFFECTIVE EARTH PRESSURE COEFFICIENTS AGAINST PILES FOUR DAYS AFTER INSTALLATION (1 ft = 0.305 m)

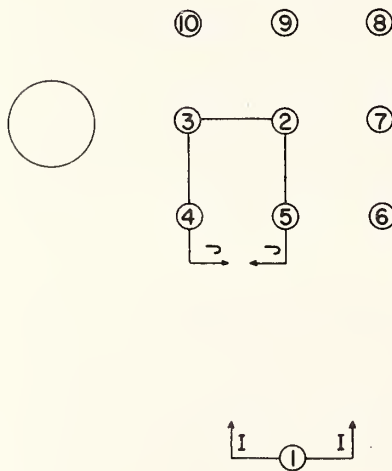
9- and 19-FOOT LEVELS



34-FOOT LEVEL



41-FOOT LEVEL



50-FOOT LEVEL

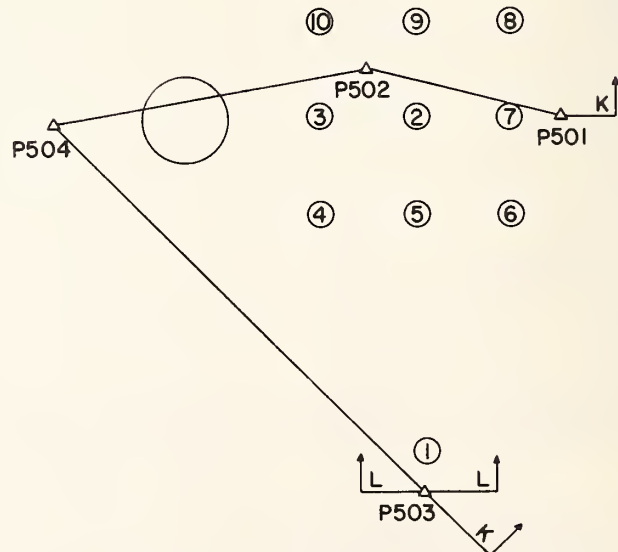


FIGURE 1.19. PORE PRESSURE PROFILE SECTION LINES (1 ft = 0.305 m)

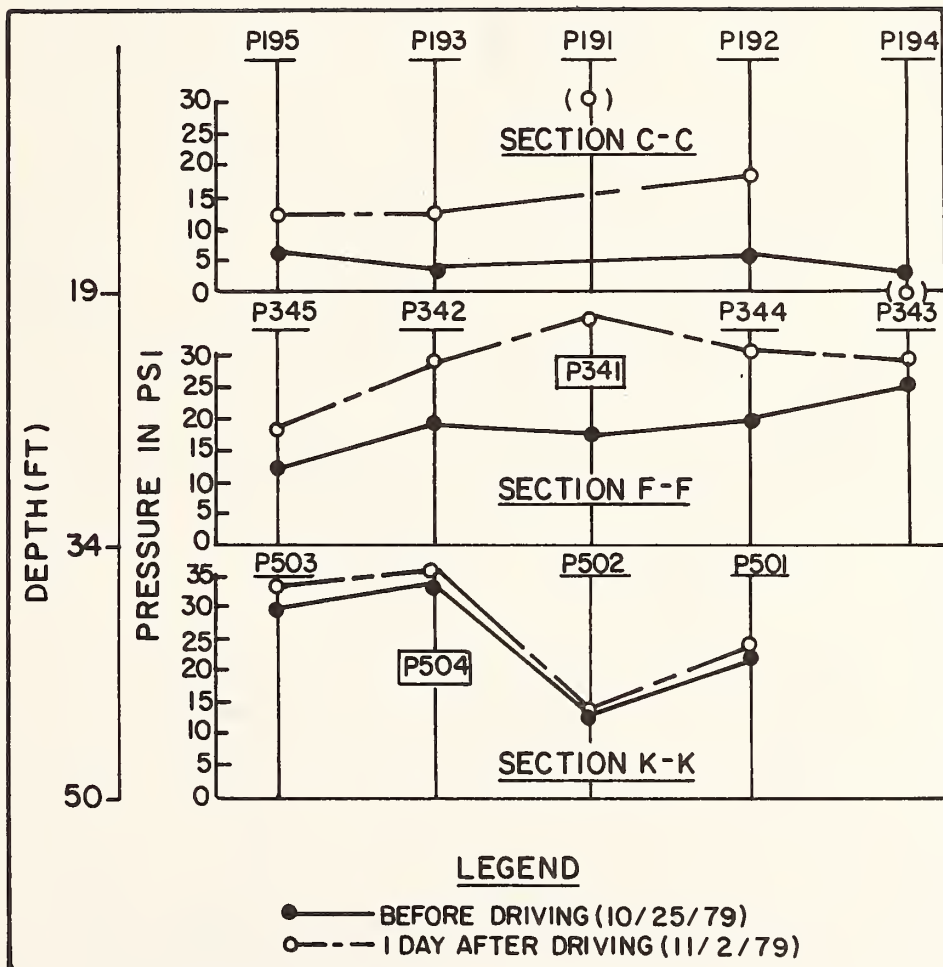
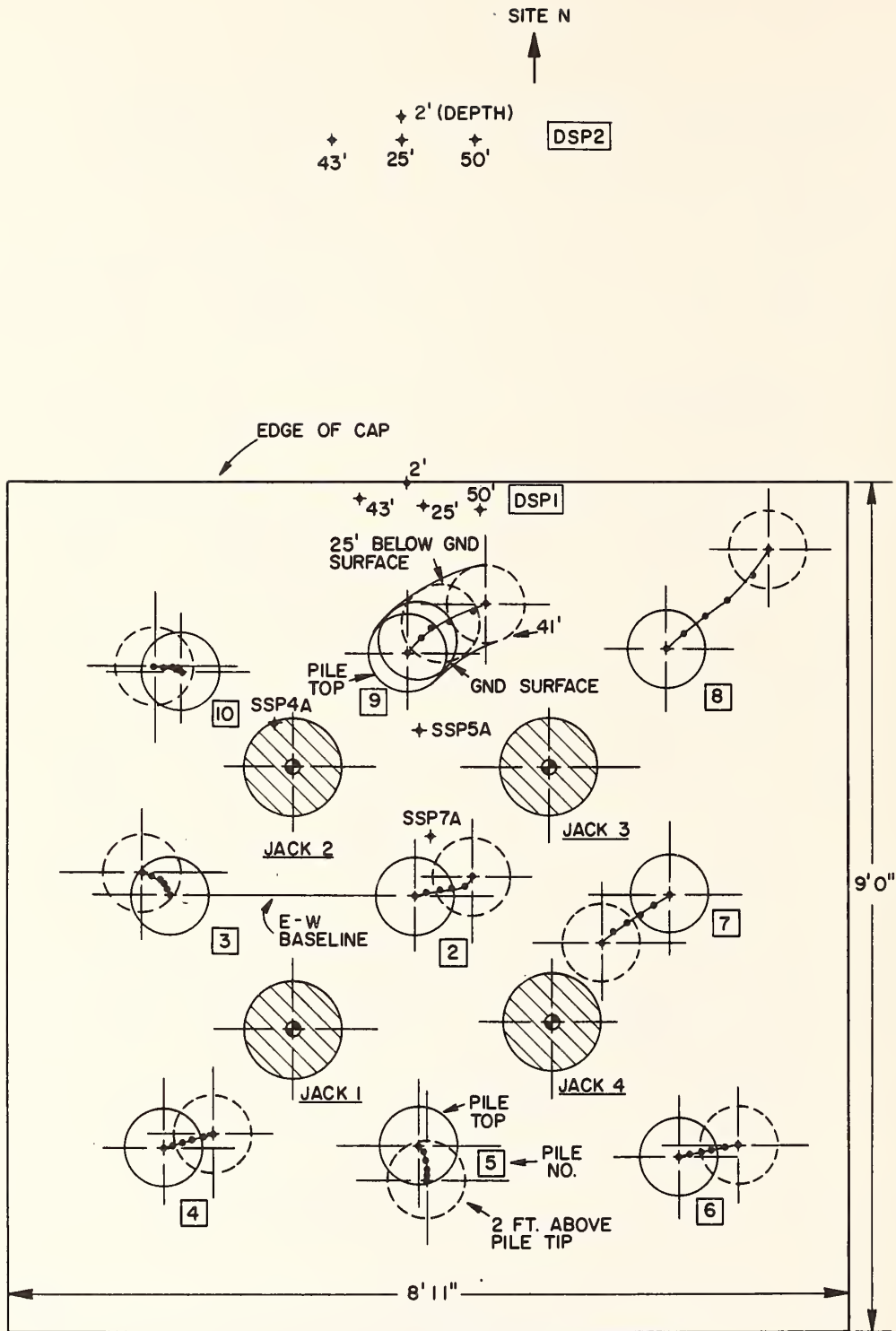


FIGURE 1.20. GROUND PORE PRESSURE PROFILES: BEFORE AND AT CONCLUSION OF DRIVING (1 ft = 0.305 m; 1 psi = 6.89 kN/m²)



NOTE: INSIDE DIAMETERS OF PILES ARE SHOWN. ϕ POINTS SHOWN AT 10 FT. INTERVALS.

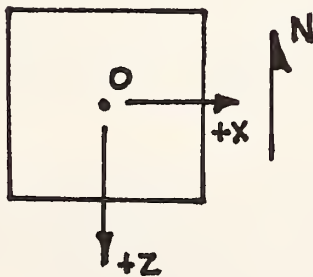
NOTE: SSP4A, 5A, AND 7A WERE NOT POSITIONED UNTIL AFTER FIRST GROUP TEST.

FIGURE 1.21. AS-CONSTRUCTED LOCATIONS AND ALIGNMENTS OF GROUP PILES
(1 ft = 0.305 m; 1 in = 25.4 mm)

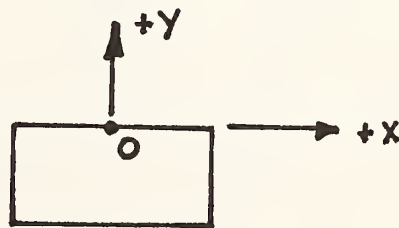
TABLE 1.4. PILE HEAD AND JACK COORDINATES FOR
9-PILE TEST NO. 1 (1 in. = 25.4mm)

PILE NO.	X (in.)	Y (in.)	Z (in.)
2	- 0.8	0	- 1.8
3	-32.0	0	- 1.8
4	-33.0	0	+30.0
5	- 0.5	0	+29.8
6	+33.0	0	+31.0
7	+32.0	0	- 2.0
8	+31.8	0	-33.5
9	- 2.0	0	-33.0
10	-30.9	0	-30.4
JACK NO. 1	-16.6	0	+15.0
JACK NO. 2	-16.4	0	-18.4
JACK NO. 3	+16.4	0	-18.2
JACK NO. 4	+16.8	0	+14.0

NOTES: JACKS 2, 3, 4 MOVED 3.5 IN. SOUTH (+Z) FOR TEST 2. JACK 1
MOVED 3.0 IN. SOUTH (+Z) FOR TEST 2. ALL JACKS MOVED 1.5
NORTH (-Z) FROM TEST 2 POSITION FOR TEST 3.



TOP VIEW



SOUTH ELEVATION

Finally, the exact locations and alignments of the reference piles are shown graphically in Fig. 1.22.

Residual Loads Developed in Piles Due to Driving

Zero readings were made on the strain gage circuits when the piles were in the calibration bed in an unstrained state and were checked again in the field just prior to driving each pile. Once each pile was driven a new set of strain circuit readings was made on each of the piles in the ground in an attempt to determine patterns of development of residual loads in the group piles compared to those in the reference piles. Readings taken during the installation process were largely unusable, due to instabilities in the data acquisition system, as explained in Appendix E. Stable readings were obtained, however, prior to the first load tests. These readings are shown graphically for the reference piles in Fig. 1.23. The largest residual loads were developed in Pile 1. Pile 11 exhibited low residual loads, perhaps because the presence of free water in the pilot hole for Pile 11 caused greater lubrication of that pile. The observed residual load pattern requires that negative side resistance (directed downward on the pile) be present above a depth of 25 ft. (7.6 m) and that positive side resistance exist below that depth. The average compressive residual tip load due to driving the reference piles was about 7 kips (31.2 kN).

The residual load pattern in the group piles was extremely complex. No pattern with respect to geometric position could be positively identified, therefore, the authors have chosen to average all of the residual load readings and thereby consider a typical group pile. The average residual load in the group piles and the measured upper and lower bounds are shown in Fig. 1.24. Some of the extreme readings may be the result of zero shifts in several of the circuits. Since the circuits were wired with random polarity among the piles, errors of this type tend to be cancelled when averages are taken.

The residual loads thus obtained in the group piles were generally lower than those in the reference piles, as demonstrated in Fig. 1.25. This is an expected phenomenon. The pattern of load distribution along the typical group pile was somewhat different from the pattern in the reference piles. Positive side resistance was encountered down to a depth of 15 ft. (4.6 m), presumably due to the load imparted by the cap (57 kips (254 kN) to 9 piles). Below that depth, side resistance was negative to a depth of 35 ft. (10.7 m) after which it again became positive. The residual tip load in the typical group pile was 3 kips (13.4 kN).

The effect of residual loads on the development of load transfer will be considered further in Chapter 3. Due to electrical drift it was not possible to maintain predrive zeros beyond the first load test. Specific reasons for this problem are discussed in Appendix E.

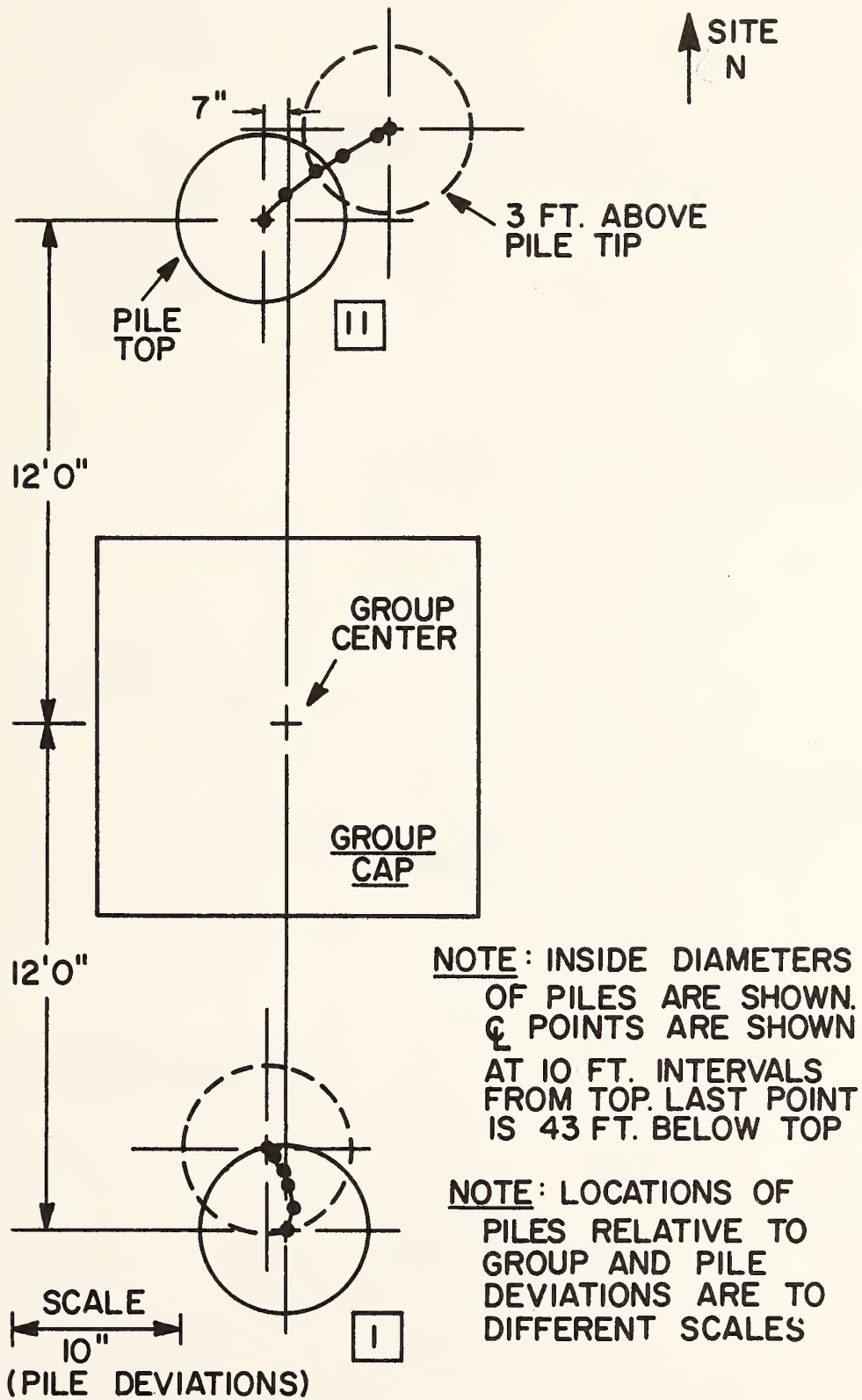


FIGURE 1.22. AS-CONSTRUCTED LOCATIONS AND ALIGNMENTS OF REFERENCE PILES
 (1 ft = 0.305 m; 1 in = 25.4 mm)

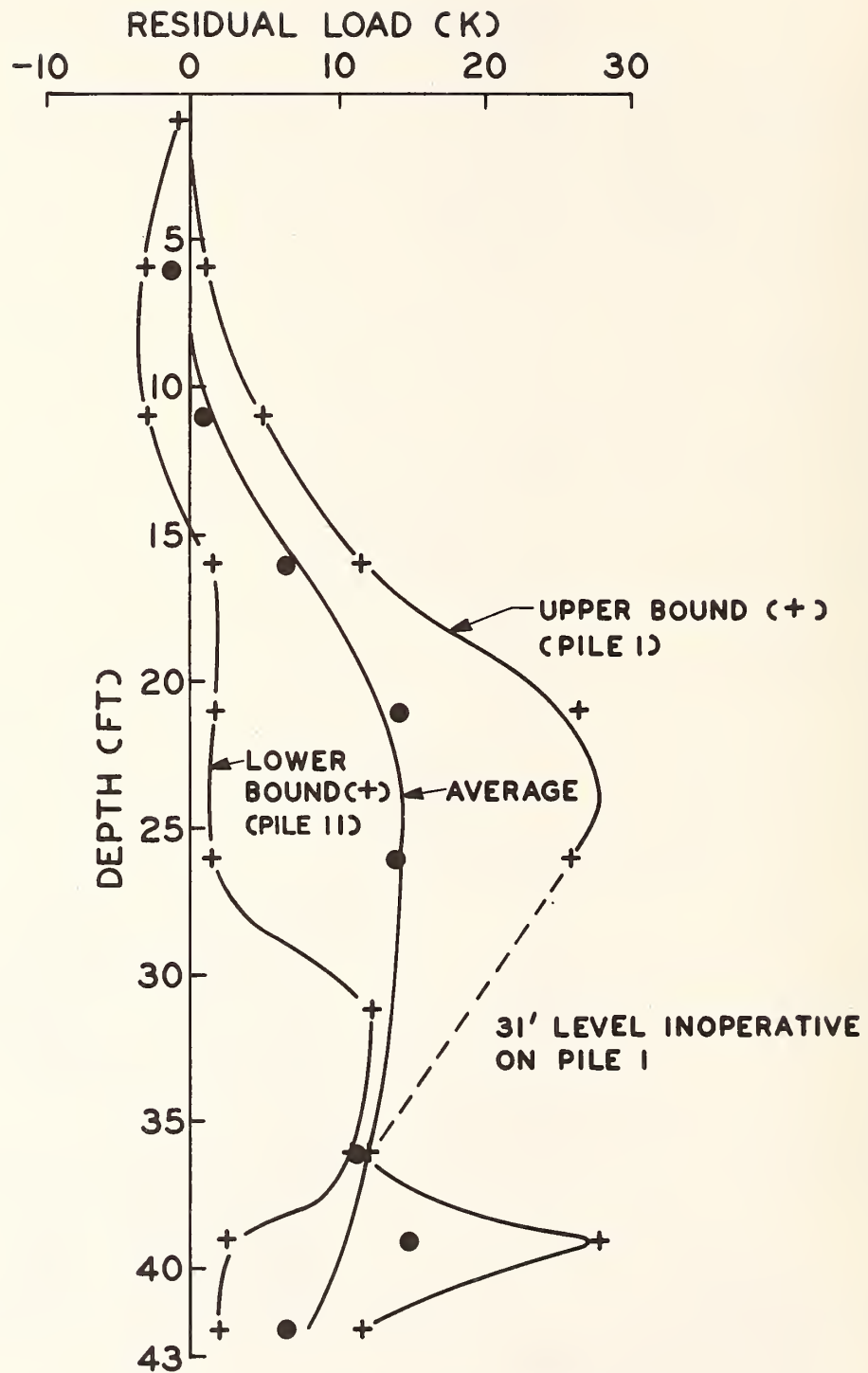


FIGURE 1.23. RESIDUAL LOADS IN REFERENCE PILES AFTER INSTALLATION
 (1 ft = 0.305 m; 1 k = 4.45 kN)

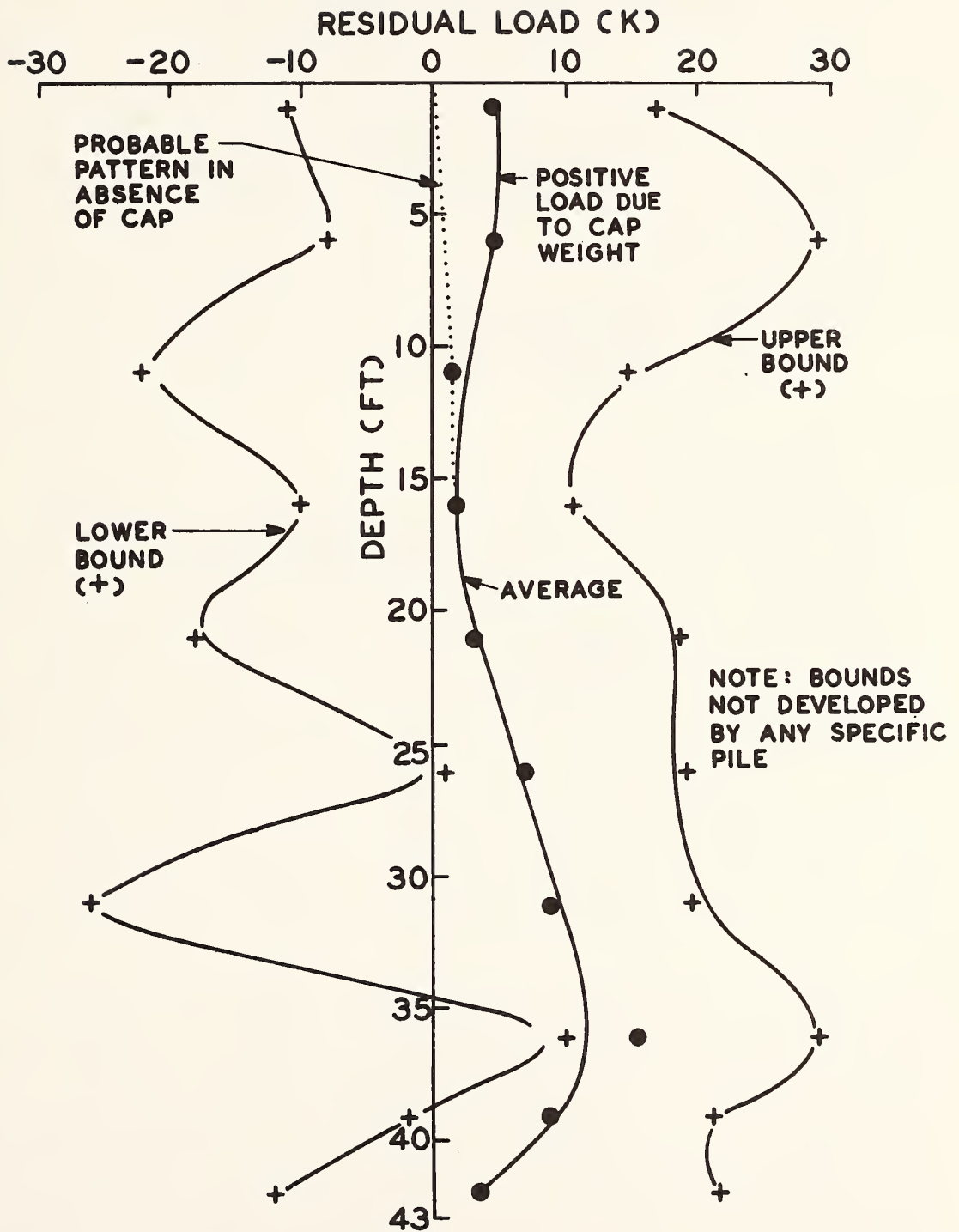


FIGURE 1.24. RESIDUAL LOADS IN TYPICAL GROUP PILE AFTER INSTALLATION
(1 ft = 0.305 m; 1 k = 4.45 kN)

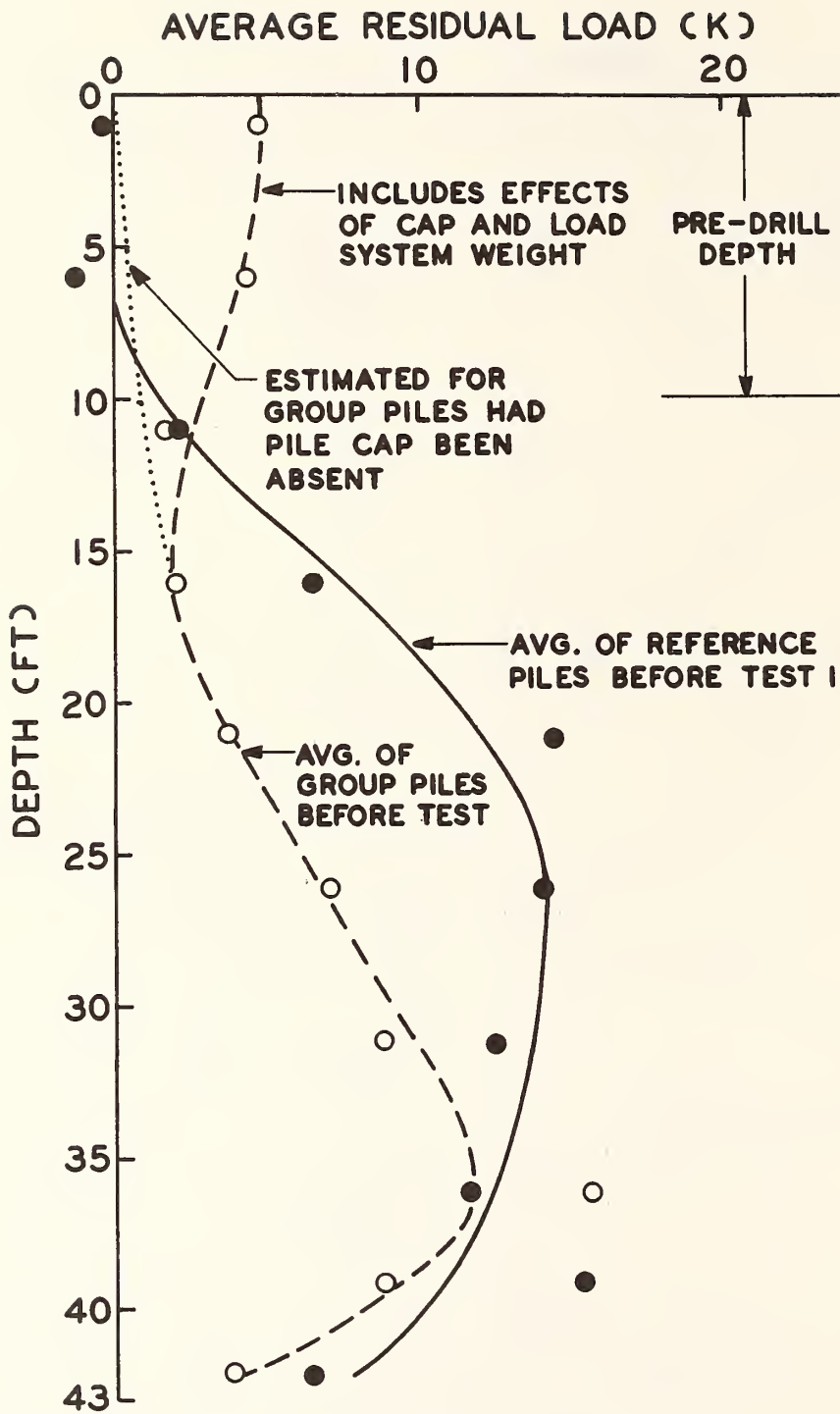


FIGURE 1.25. COMPARISON OF RESIDUAL LOADS (PER PILE) IN REFERENCE AND GROUP PILES (1 ft = 0.305 m; 1 k = 4.45 kN)

Chapter 2. Pile and Soil Performance Under Load

General

This chapter contains partial test results for the seventeen static load tests conducted as outlined in Table 1.1. Test results specifically pertaining to load transfer are deferred to Chapter 3. The various interpretations shown here in graphical and tabular form are based upon readings made 5 minutes after each increment of load was applied, except for the first test on Pile 11, where 30 second readings were used, and where otherwise noted. All reported settlements are as-read values that are uncorrected (except where noted) for reference system movements, and all loads are the loads indicated by the second highest level of strain gages (or sum thereof in group tests) on the piles, as verified by load cell and jack pressure measurements.

Load-Settlement Behavior

Reference Piles. Three tests were conducted on each reference pile, preceding by four to five days each 9-pile group test. The results of reference pile tests which immediately preceded a given group test were used to assess settlement ratio and efficiency (defined later) for that test. Separate reference pile tests were not conducted in association with the subgroup tests; therefore, the set of reference pile tests conducted in conjunction with the third and final 9-pile test was also used as a baseline for the subgroup tests. Figure 2.1 depicts the load-settlement behavior of Piles 1 and 11 (the reference piles) during the first load test, conducted 15 days after the completion of driving. It should be recalled that Pile 11 was subjected to a quick test, whereas Pile 1 was subjected to a standard one-hour-increment test. It is observed that both piles failed by plunging, followed by relaxation as further deformation developed. Failure in each case occurred abruptly, after a near-linear response, at a butt settlement of about 0.15 in. (3.8 mm). This type of "brittle" failure was typical of all failures in compression for both group and reference piles throughout the test program.

The tip loads depicted in Fig. 2.1 are based on pretest zeros and do not reflect the residual loads present prior to loading. Complete failure at the tip occurred at a downward movement of the tip of about 0.2 in. (5 mm), or about 2 per cent of the pile diameter. (All "tip" loads referred to in this report are actually loads measured by a strain circuit approximately 1 ft. (0.305 m) above the tip.) It should be noted that the tip deformation required to mobilize full end bearing capacity exceeded the relative deformation between the shaft and the soil needed to mobilize maximum shaft resistance. Because of pile flexibility, shaft failure preceded tip failure. Since some relaxation of shaft resistance occurred after shaft-soil failure, the peak pile capacity was less than the sum of the peak shaft and tip capacities.

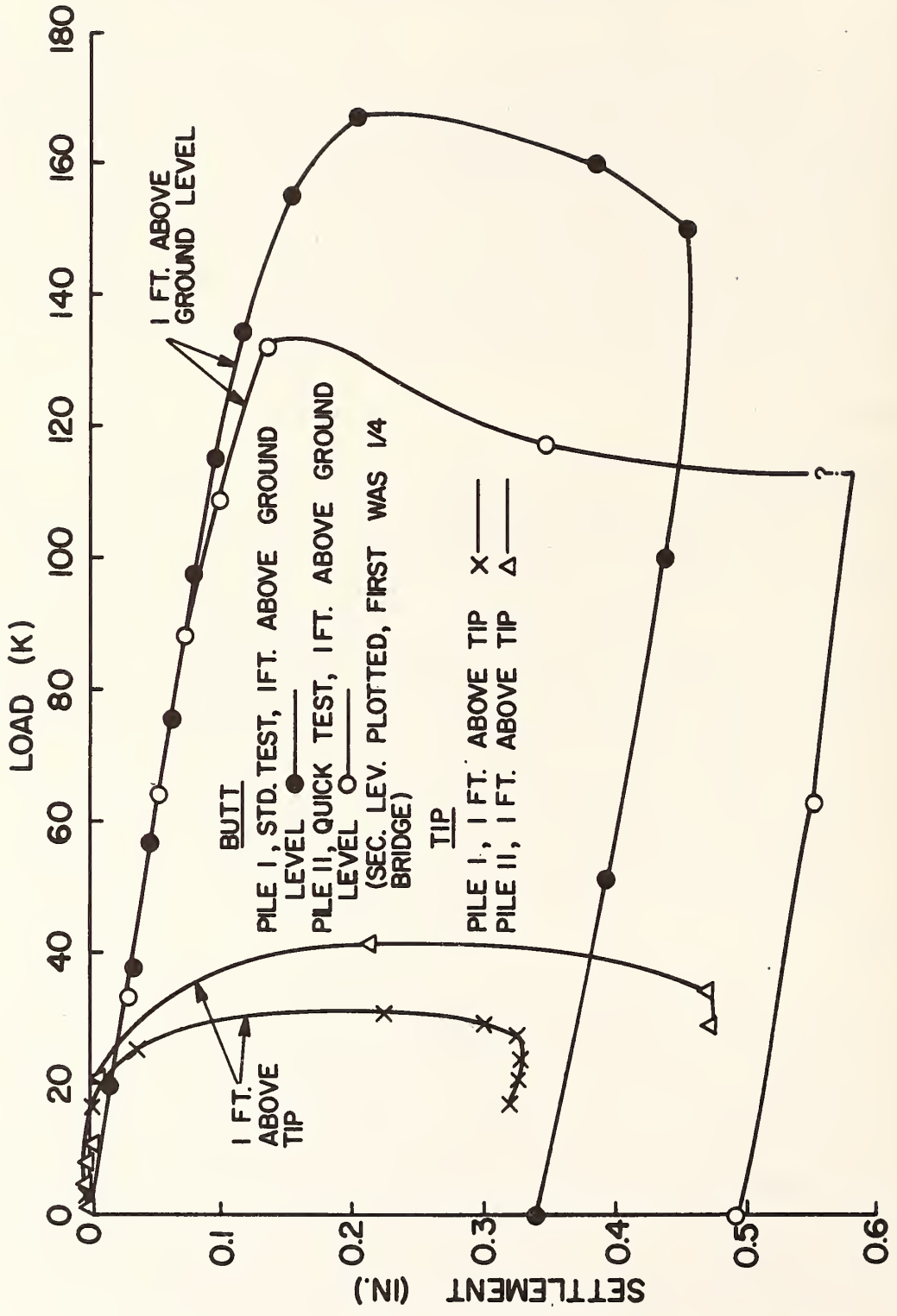


FIGURE 2.1. REFERENCE PILE LOAD-SETTLEMENT RELATIONSHIPS FOR TEST NO. 1
 (1 k = 4.45 kN; 1 ft = 0.305 m; 1 in = 25.4 mm)

Pile 11 failed at an applied load of about 35 kips (156 kN) less than Pile 1. This may be due to the effects of undissipated pore water pressures that may have been generated when Pile 11 was driven in a partially water-filled pilot hole. Because of the early failure of Pile 11, the only comment that can be made on the comparison of the results of quick and standard tests is that both yielded nearly identical load-settlement curves in the working load range. The data suggest that factors such as the condition of the pilot hole are probably more important than the effects of testing method (for the two methods considered) in the soil at the test site. It is noted, however, that no basis exists for excluding Pile 11 data from the reference baseline, since some group piles may have behaved more like Pile 11 than Pile 1.

The butt and tip load-settlement curves for the second load tests on the reference piles, conducted 78 days after completion of driving, are shown in Fig. 2.2. That figure also shows the butt load-settlement curves for Test 1 to provide a basis for comparison. Again, the tip curves are based upon pretest zeros. It is evident that both the butt and tip load-settlement behavior were more nearly identical between the two reference piles by this time and that appreciable apparent set-up had occurred. Plunging occurred at a butt settlement of about 0.2 in. (5 mm), and maximum tip load was also developed at a tip displacement of about 0.2 in. (5 mm).

Figure 2.3 depicts the butt and tip load-settlement curves for the final reference pile load tests, conducted 105 days after completion of driving. Tip curves are again based on pretest zeros. That figure also shows the peak butt loads developed in the previous two tests. Note that at this time the capacity of Piles 1 and 11 were almost identical and that some loss in capacity was actually observed between Tests 2 and 3 for Pile 1.

Cumulative load-settlement curves for the reference piles are given in Fig. 2.4.

Groups. Load-settlement curves for the first 9-pile group test are given in Fig. 2.5. The load axis does not include the weight of the pile cap, which was 57 kips (254 kN). This figure compares the results of readings taken 5, 30, and 55 minutes after each loading increment was applied. The differences were insignificant up to about 75 per cent of the plunging failure load. The pile cap experienced considerable tipping toward the north (Piles 8, 9, and 10) as failure approached. This phenomenon is illustrated in Figs. 2.6-2.9, which diagram the attitude of the cap at various stages of loading. Separate load-settlement curves have therefore also been plotted on Fig. 2.5 for the north and south rows of piles. A maximum differential settlement of approximately 0.3 in. (8 mm) was experienced across the piles at maximum applied load. Previous calculations had indicated that further rotation of the cap could induce plastic hinges in the piles at the base of the pile cap. The test was therefore terminated at this time. It is evident that in a gross sense (i.e., average pile settlement vs. average pile load, as depicted on Fig. 2.5) failure of the plunging type

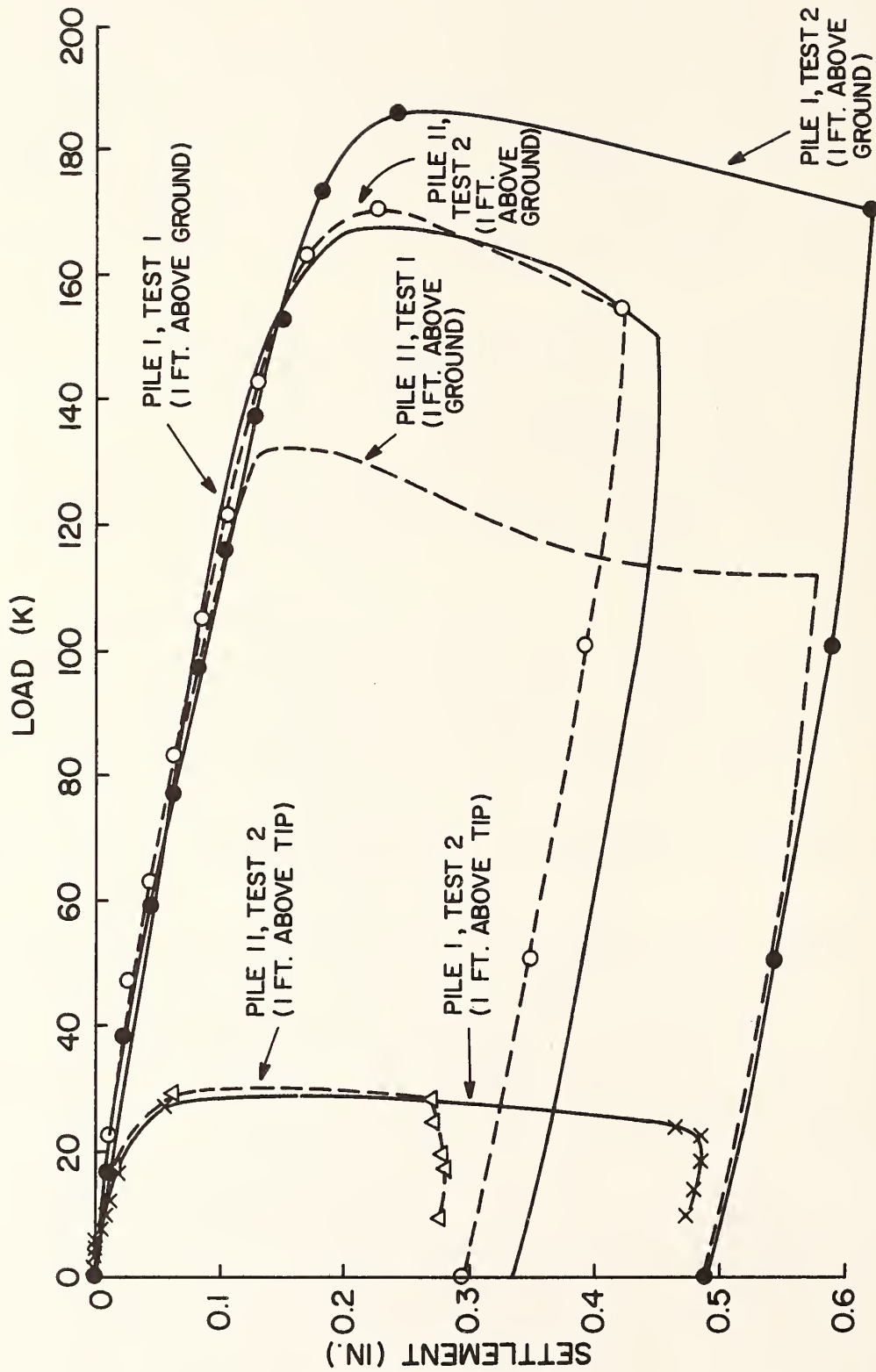


FIGURE 2.2. REFERENCE PILE LOAD-SETTLEMENT RELATIONSHIPS FOR TEST NO. 2
 (1 k = 4.45 kN; 1 ft = 0.305 m; 1 in = 25.4 mm)

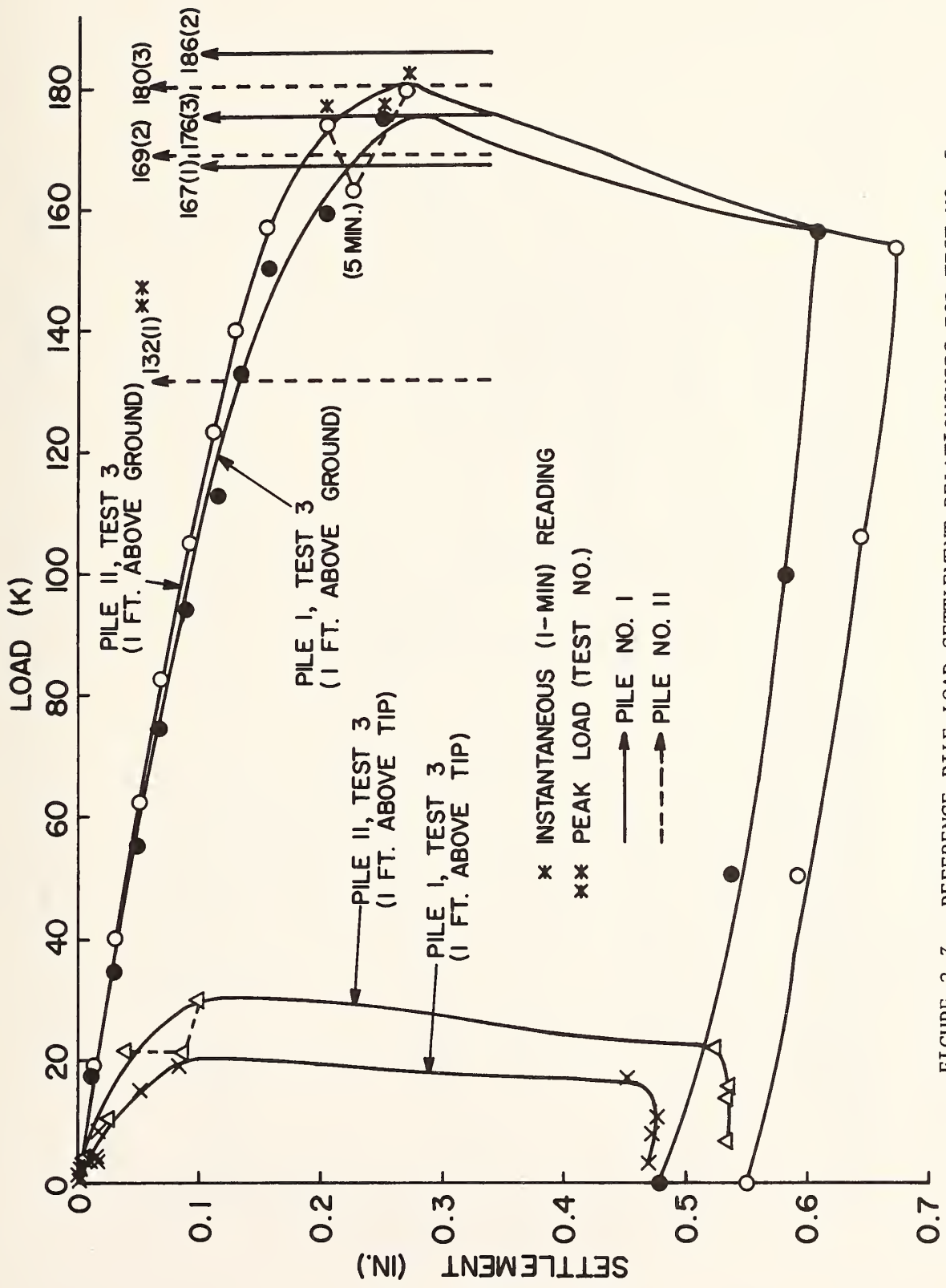


FIGURE 2.3. REFERENCE PILE LOAD-SETTLEMENT RELATIONSHIPS FOR TEST NO. 3
 (1 k = 4.45 kN; 1 ft = 0.305 m; 1 in = 25.4 mm)

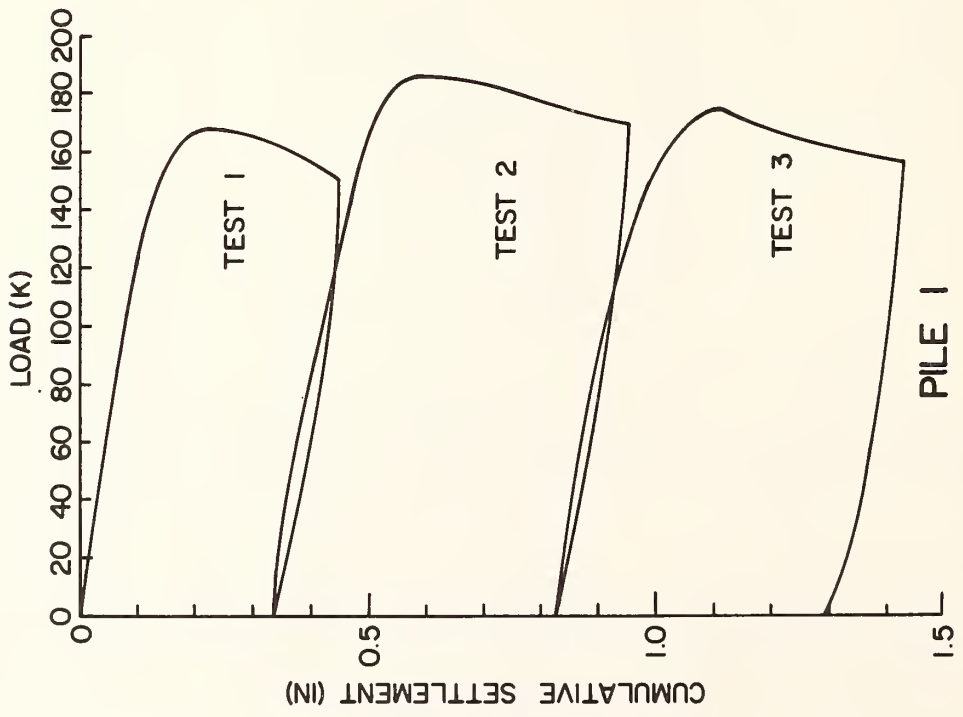
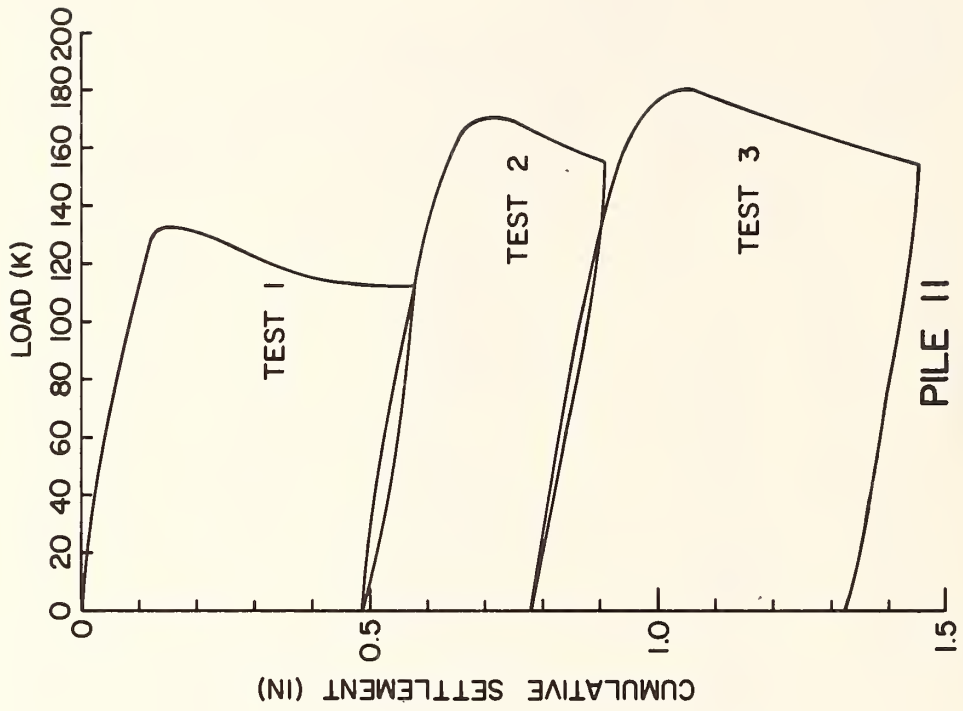


FIGURE 2.4. CUMULATIVE LOAD-SETTLEMENT CURVES FOR REFERENCE PILE TESTS
 (1 k = 4.45 kN; 1 ft = 0.305 m; 1 in = 25.4 mm)

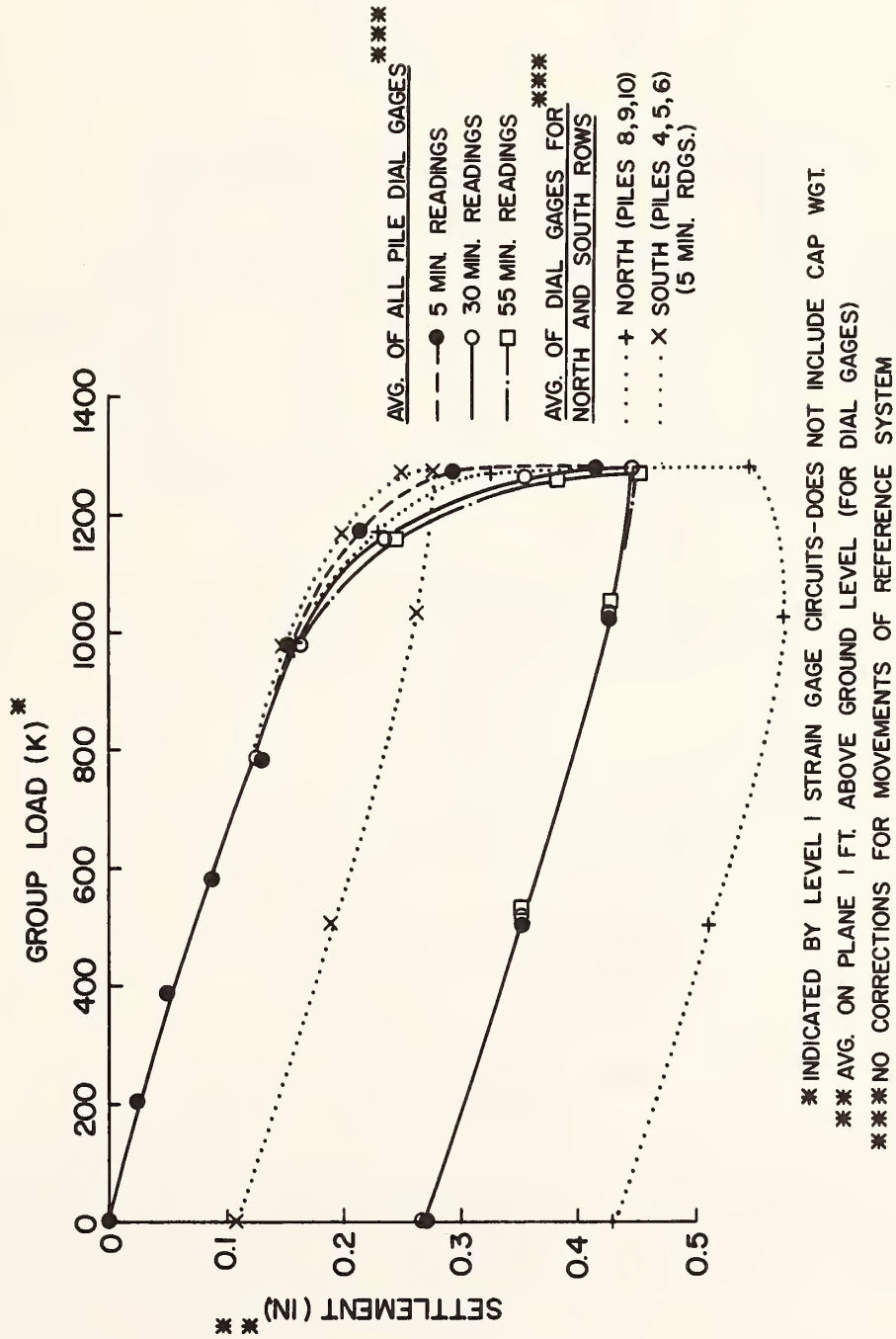


FIGURE 2.5. LOAD-SETTLEMENT RELATIONSHIPS FOR 9-PILE GROUP, TEST 1
 (1 k = 4.45 kN; 1 ft = 0.305 m; 1 in = 25.4 mm)

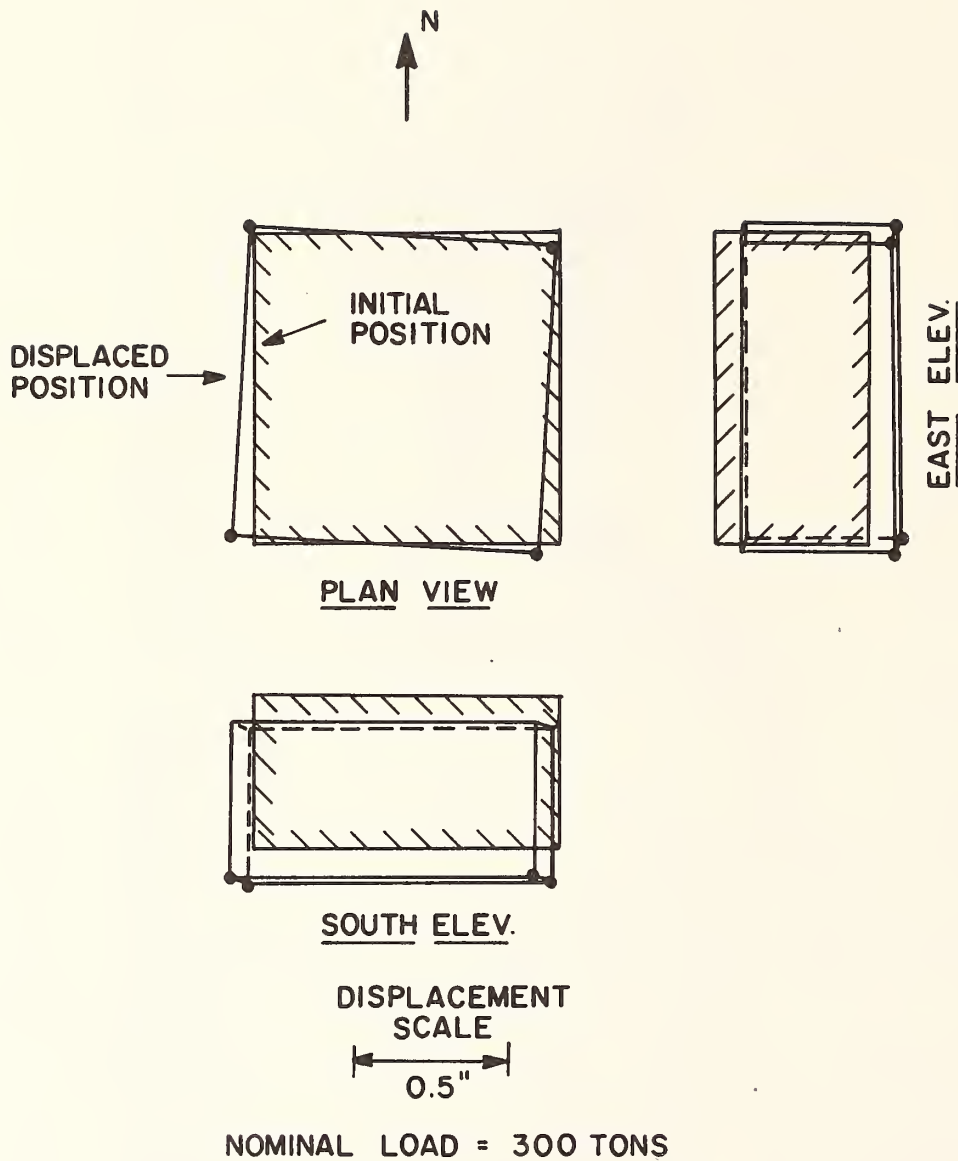


FIGURE 2.6. CAP MOVEMENTS AT APPROXIMATELY ONE-HALF OF FAILURE LOAD, TEST 1 (1 ton = 8.9 kN; 1 in = 25.4 mm)

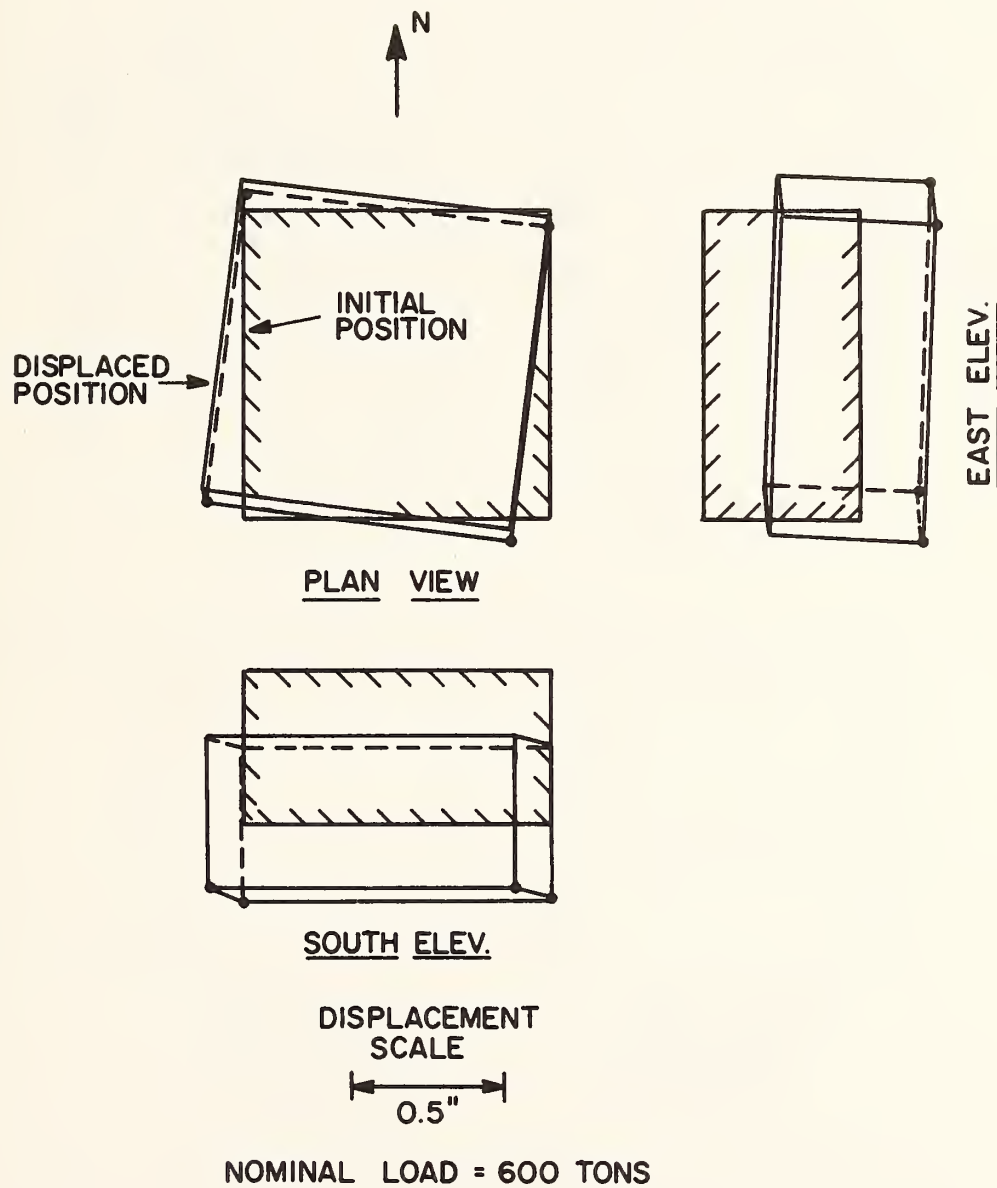


FIGURE 2.7. CAP MOVEMENTS AT APPROXIMATELY 90 PER CENT OF FAILURE LOAD, TEST 1 (1 ton = 8.9 kN; 1 in = 25.4 mm)

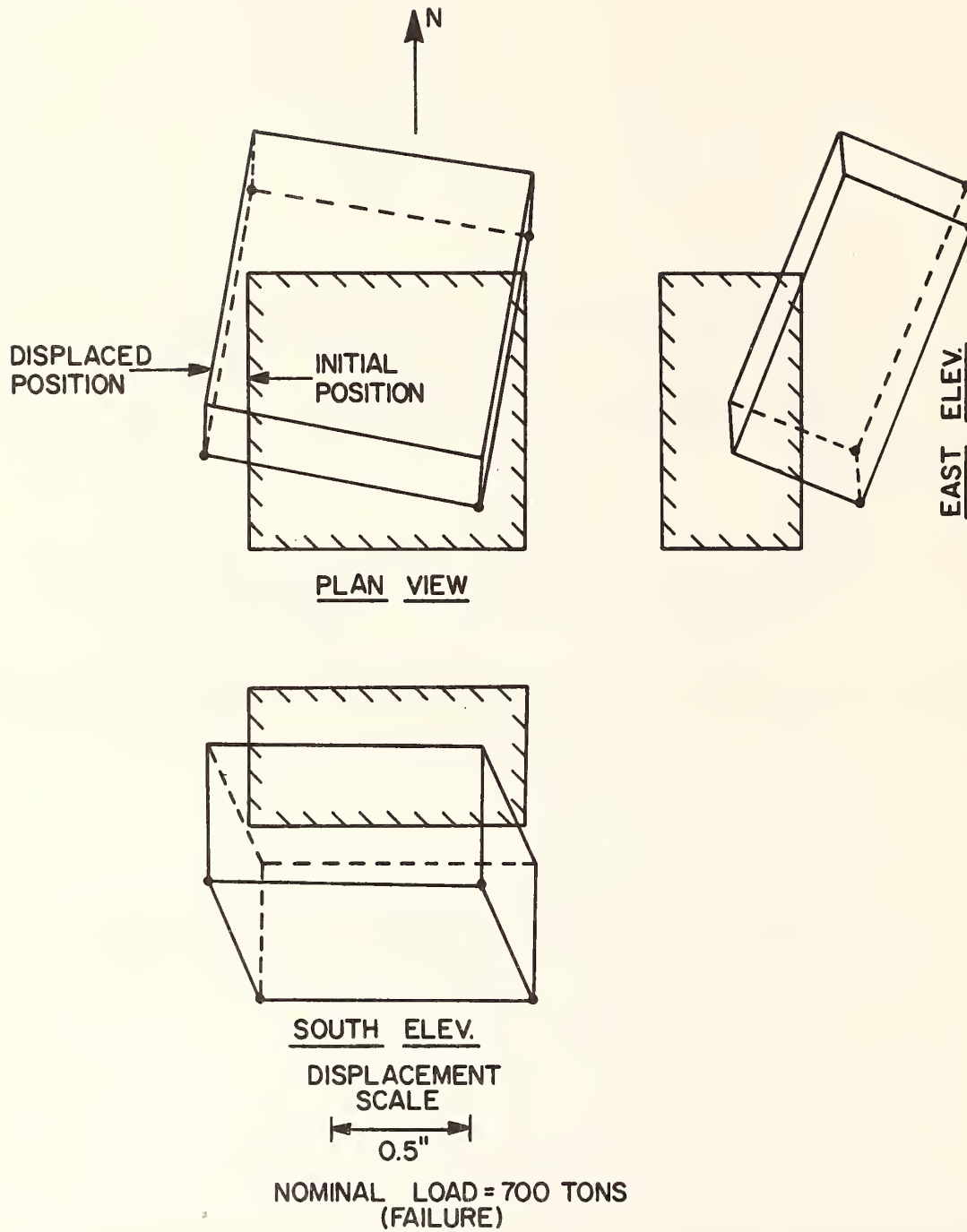


FIGURE 2.8. CAP MOVEMENTS AT FAILURE, TEST 1 (1 ton = 8.9 kN;
1 in = 25.4 mm)

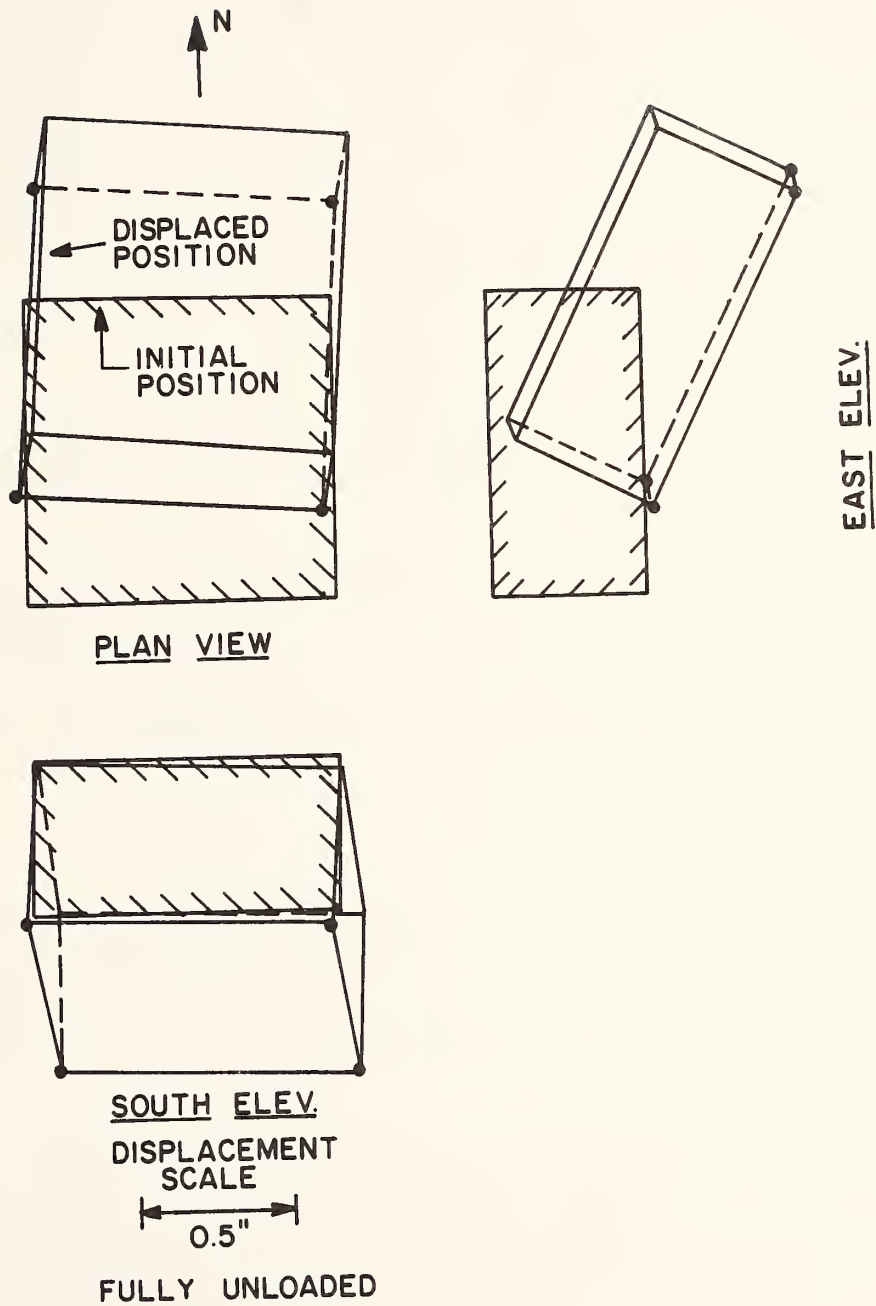


FIGURE 2.9. CAP MOVEMENTS UPON REMOVAL OF LOAD, TEST 1
 (1 ton = 8.9 kN; 1 in = 25.4 mm)

occurred in the group at the maximum applied load. However, examination of the individual pile load-settlement curves (Figs. 2.10-2.12) reveals that, because of the cap rotation, all of the piles did not fail simultaneously. Clearly, Piles 2,3,7,8,9, and 10 (on the central and northern rows) had failed by the time maximum load was reached, and Pile 6, on the southern row was in a state of impending failure. Piles 4 and 5, also on the southern row, had not failed but were apparently near failure, based on observations of load-settlement curves of piles that had failed. The gross failure pictured in Fig. 2.5, then, is the result of the achievement of plunging failure in some piles followed by relaxation, while other piles (notably 4 and 5) were still attracting load. Therefore, even though the group failed in a gross sense (could not carry more load without settlement of the center of the cap increasing in an unlimited way), complete failure of every pile was not achieved in the first test.

Complete tip failure was achieved in only a few of the piles. The locked-in tip loads at the end of the first group test were lower than those for the reference piles, presumably due to incomplete tip failure.

The characteristic shape of the 5-minute load-settlement curve for the group, as well as the shapes of the load-settlement curves for the individual group piles, is similar to that for the reference piles, except for the greater deflections required to mobilize failure in the group and for the lack of relaxation or "deformation softening" in the group load-settlement curve. The latter effect was produced by non-simultaneous failures of individual piles that were themselves deformation softening.

Considerably more attention will be directed toward the comparison of reference pile and group behavior later in this chapter.

Load-settlement curves for the second and third 9-pile group tests are shown in Fig. 2.13. Individual pile load-settlement curves and cap movement diagrams for these tests may be found in Appendices D and F, respectively, of this report. The failure load and load-settlement relationships for Tests 2 and 3 were nearly identical, although the group capacity in each test exceeded that in the first test by about 200 kips (890 kN).

Movement of the jacks approximately 3 in. (75 mm) to the south produced a more nearly vertical push in these tests. This resulted in complete failure for all piles, including complete tip failure. Because of the vertical push, all piles failed approximately simultaneously in these two tests, with the result that the deformation softening experienced by the individual piles can be observed in the group load-settlement curves.

The entire load-settlement history of the three 9-pile group tests is shown in the cumulative load-settlement graph in Fig. 2.14.

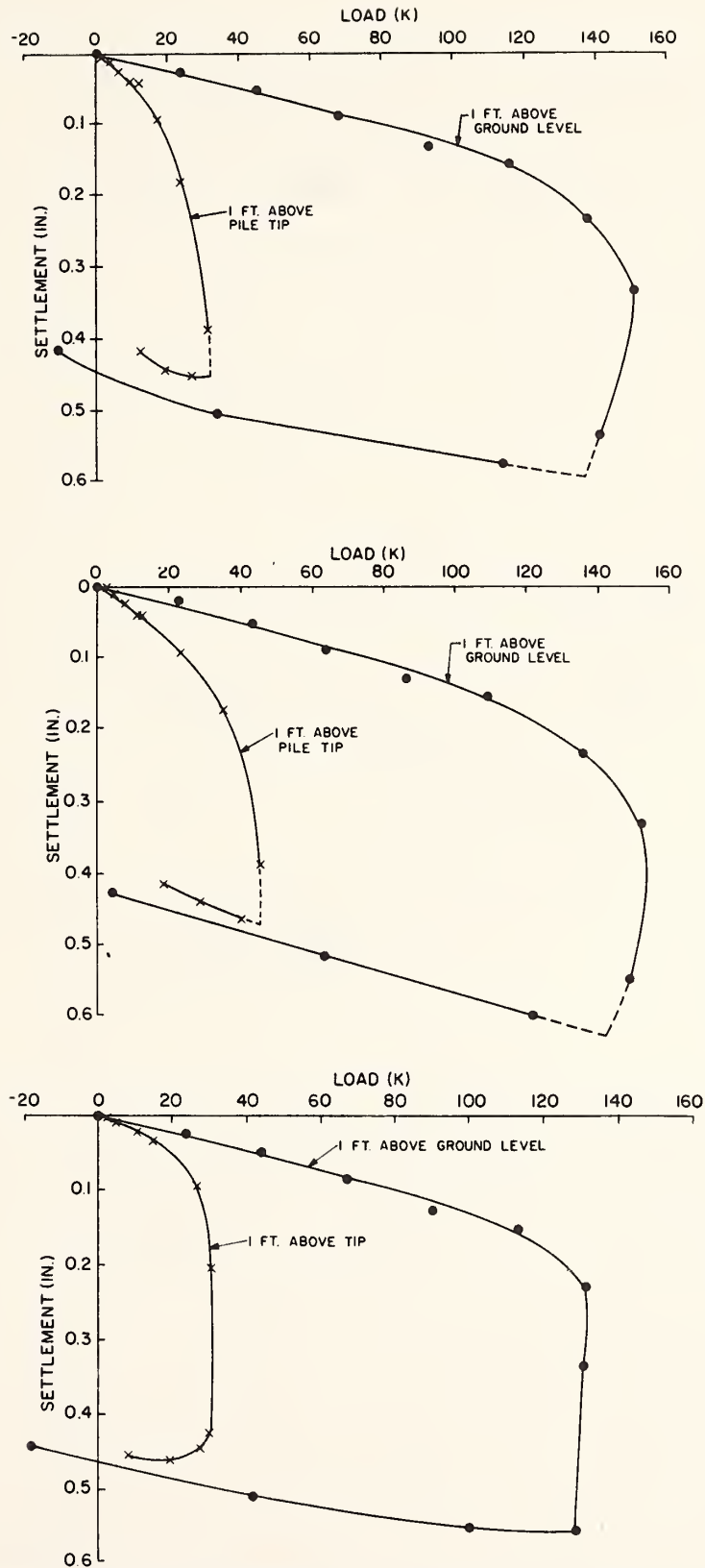


FIGURE 2.10. LOAD-SETTLEMENT CURVES FOR INDIVIDUAL PILES ON NORTH ROW, TEST 1 (TOP: PILE 10; MIDDLE: 9; BOTTOM: 8) (1 k = 4.45 kN; 1 ft = 0.305 m; 1 in = 25.4 mm)

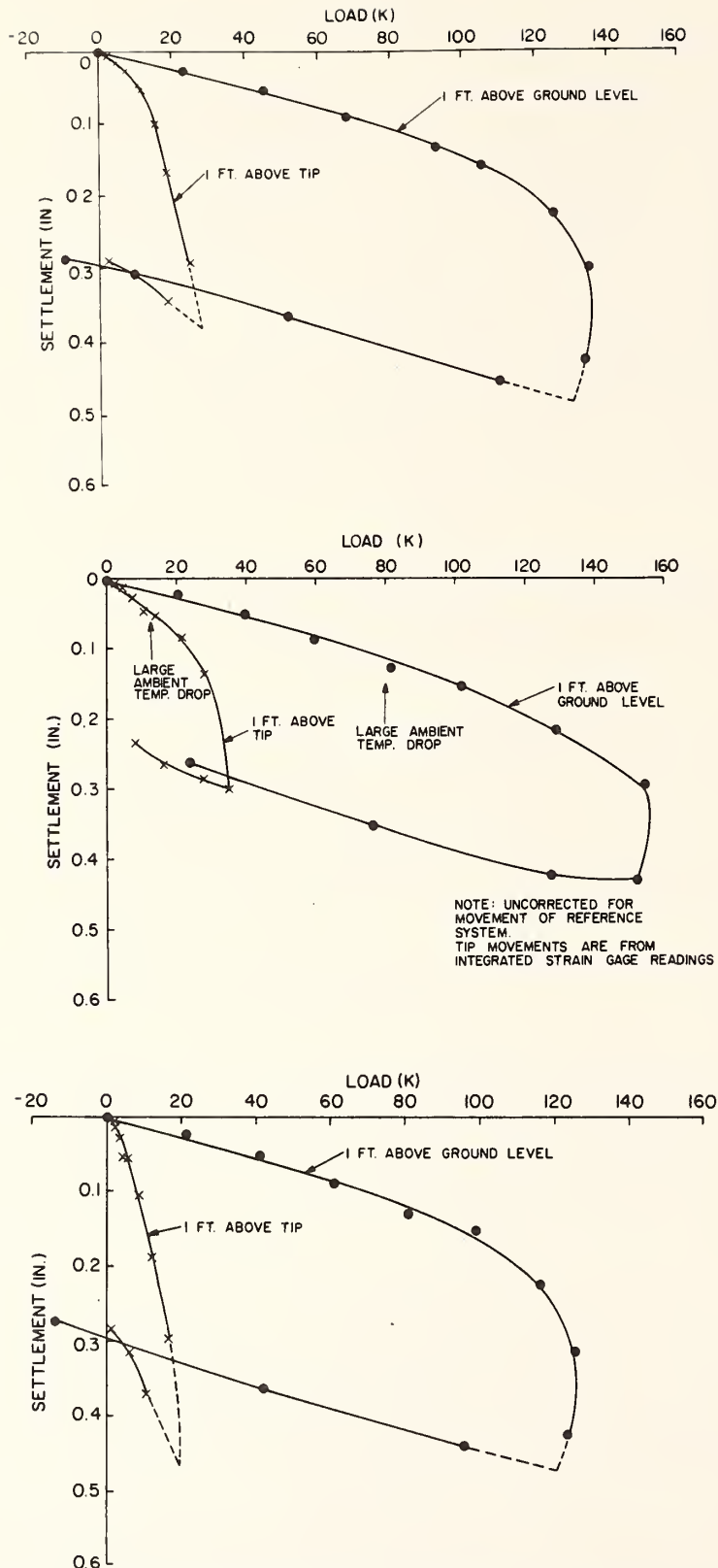


FIGURE 2.11. LOAD-SETTLEMENT CURVES FOR INDIVIDUAL PILES ON CENTER ROW, TEST 1 (TOP: PILE 3; MIDDLE: 2; BOTTOM: 7) (1 k = 4.45 kN; 1 ft = 0.305 m; 1 in = 25.4 mm)

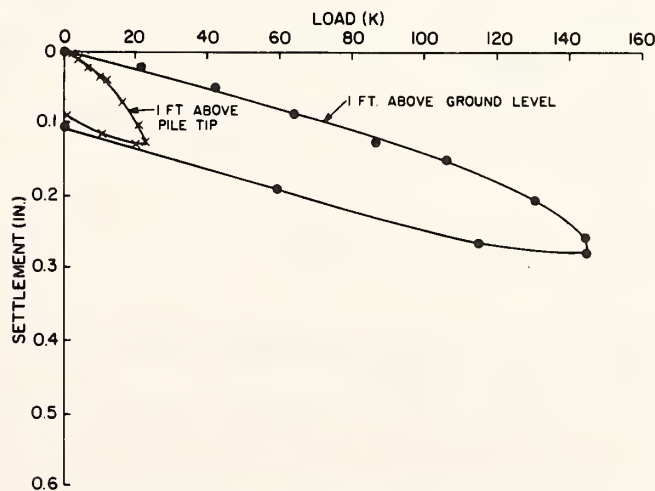
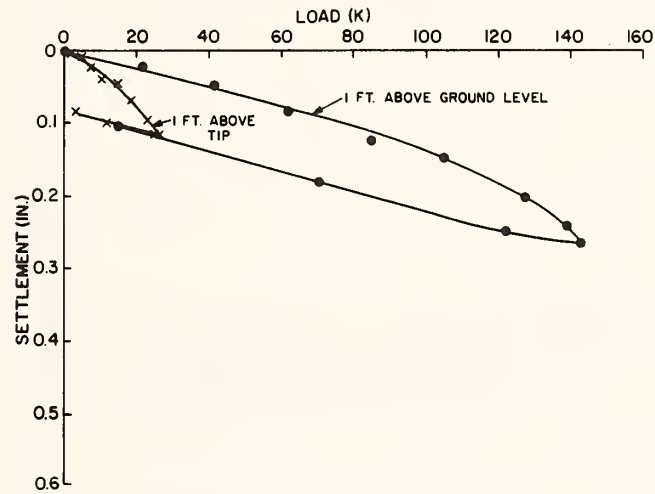
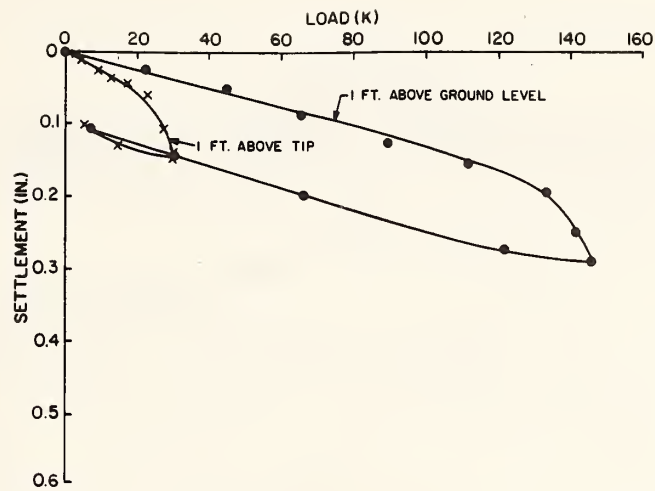
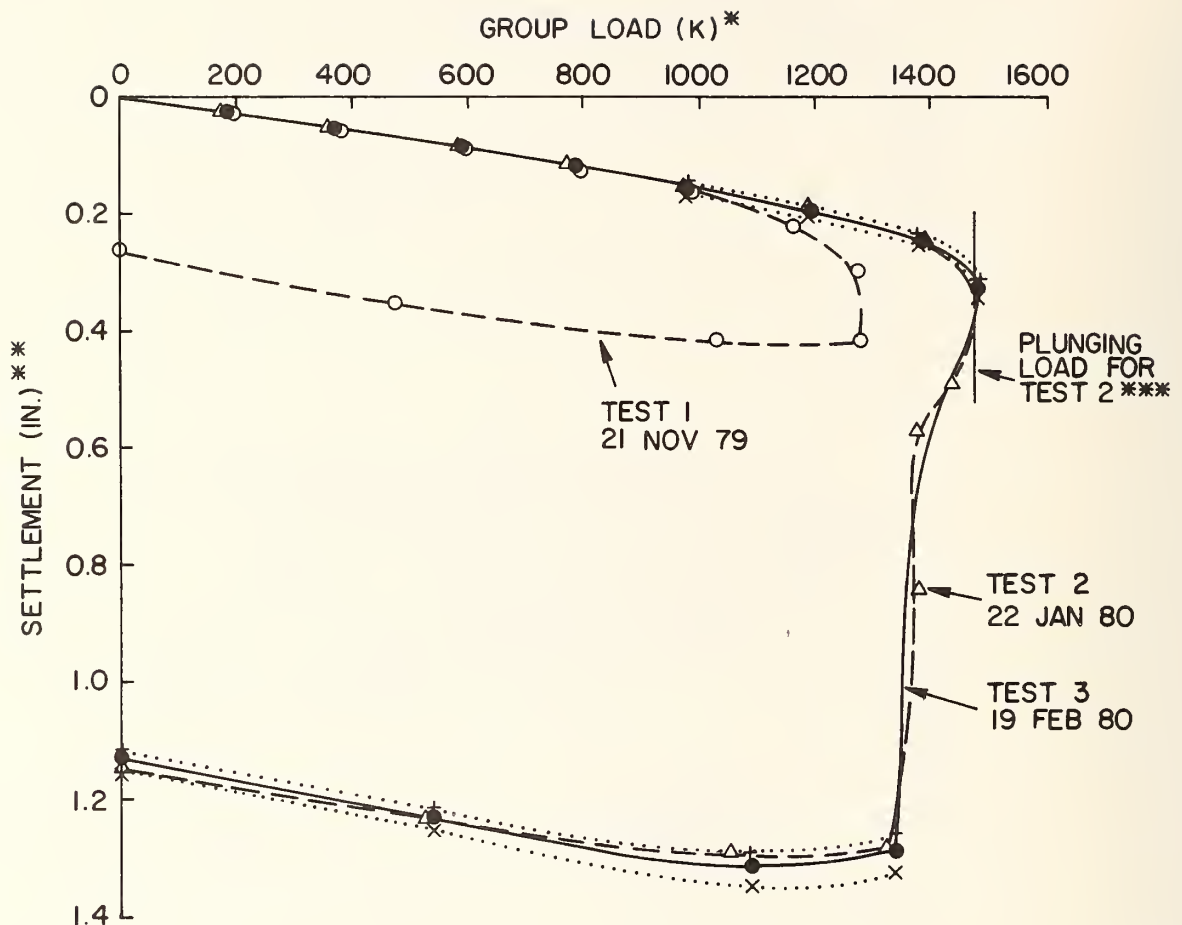


FIGURE 2.12. LOAD-SETTLEMENT CURVES FOR INDIVIDUAL PILES ON SOUTH ROW, TEST 1 (TOP: PILE 4; MIDDLE: 5; BOTTOM: 6)
 (1 k = 4.45 kN; 1 ft = 0.305 m; 1 in = 25.4 mm)



* AS INDICATED BY LEVEL I STRAIN GAGE CIRCUITS - DOES NOT INCLUDE CAP WGT.

** AVG. ON PLANE 1 FT. ABOVE GROUND LEVEL (FOR DIAL GAGES)

*** 1475 K REACHED WHEN PUMPING TO NEXT LOAD (INDICATED LOAD FROM LOAD CELLS)

○ TEST 1 }
 △ TEST 2 } AVG. OF ALL PILE DIAL GAGE READINGS,
 ● TEST 3 } 5 MIN. READINGS

+..... AVG. OF DIAL GAGES ON NORTH ROW (PILES 8,9,10) - TEST 3, 5-MIN RDGS.

x..... AVG. OF DIAL GAGES ON SOUTH ROW (PILES 4,5,6) - TEST 3, 5-MIN RDGS.

FIGURE 2.13. LOAD-SETTLEMENT CURVES FOR SECOND AND THIRD 9-PILE GROUP TESTS (1 k = 4.45 kN; 1 ft = 0.305 m; 1 in = 25.4 mm)

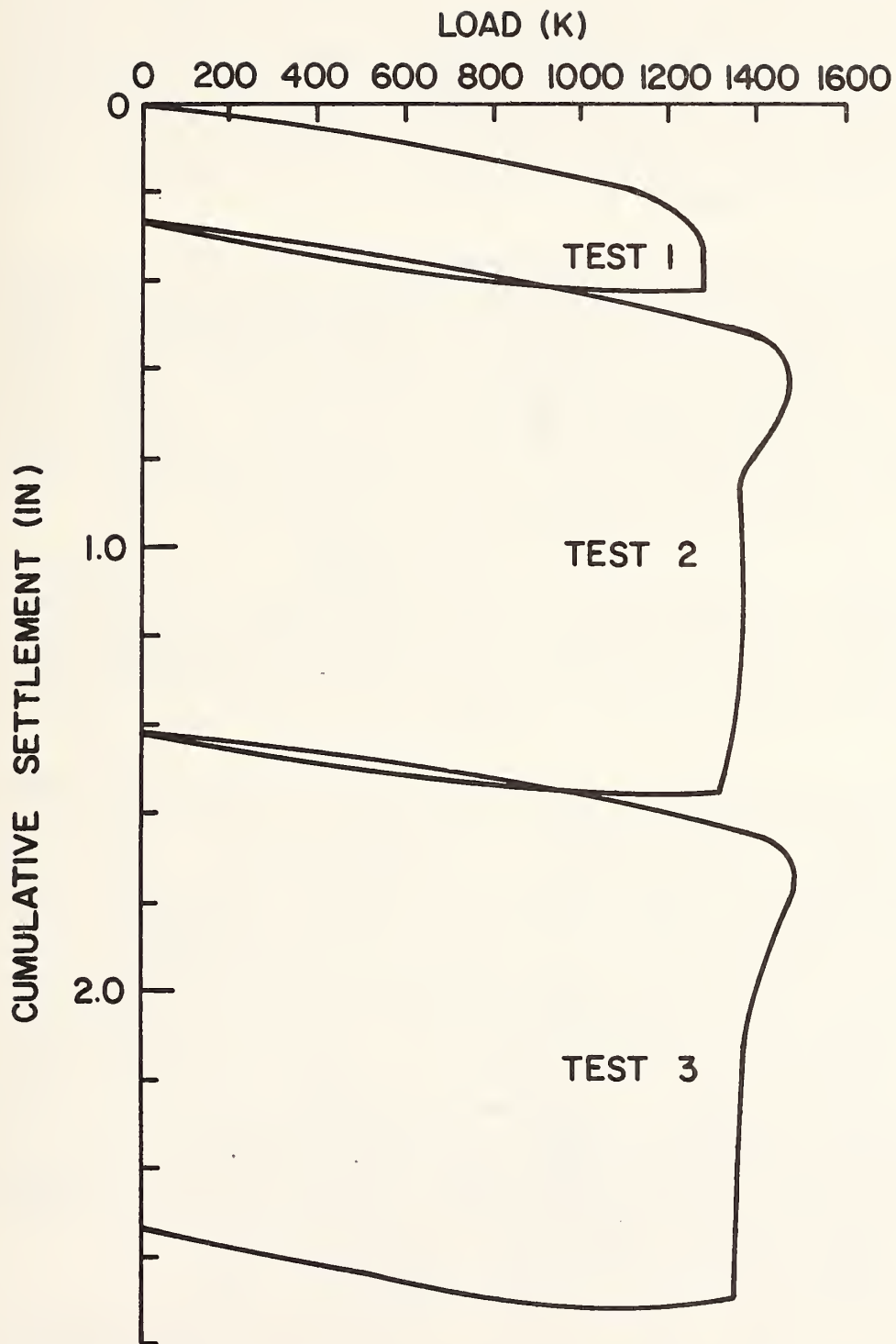


FIGURE 2.14. CUMULATIVE LOAD-SETTLEMENT CURVE FOR 9-PILE GROUP TESTS
 (1 k = 4.45 kN; 1 ft = 0.305 m; 1 in = 25.4 mm)

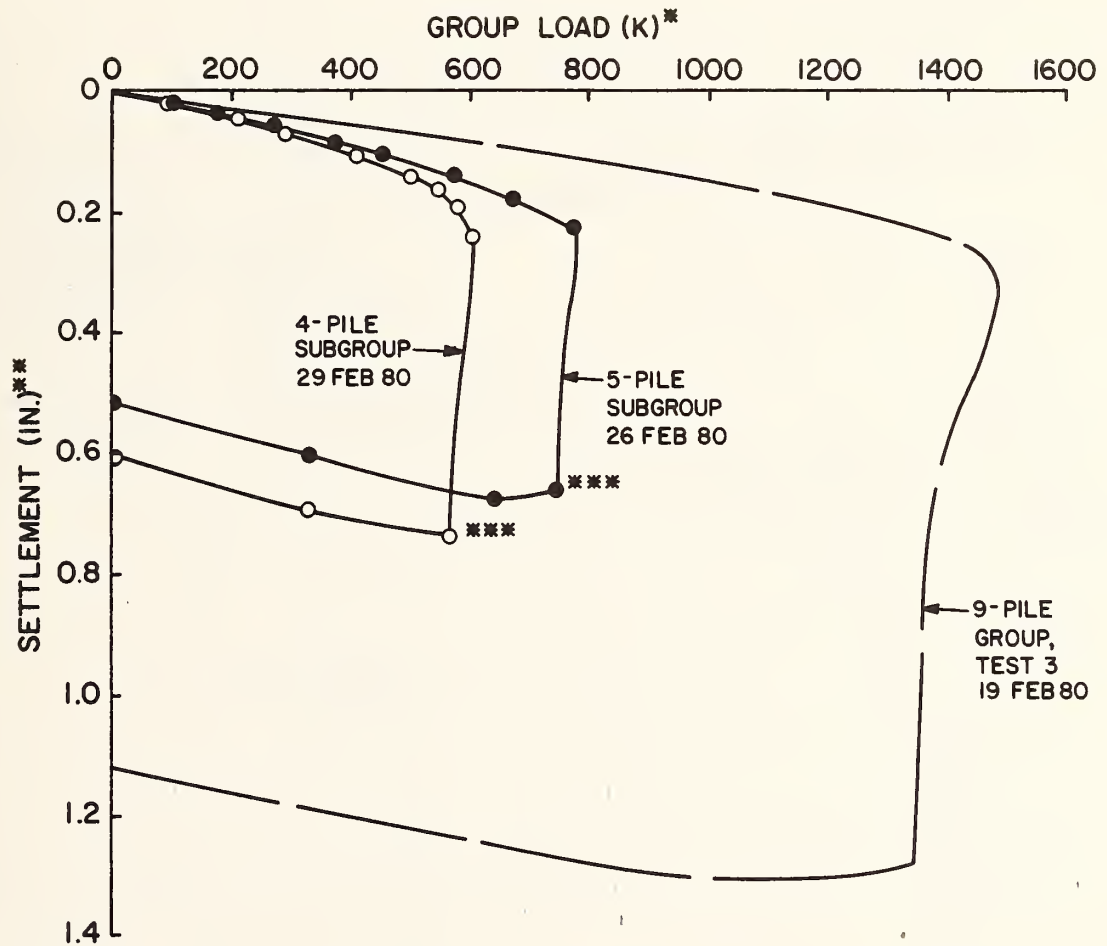
The load-settlement curves for the subgroup tests are shown in comparison with the third 9-pile test curve in Fig. 2.15. Relative capacity in each test was approximately in direct proportion to the number of loaded piles, and relative settlement at any given sub-failure load was approximately inversely proportional to the number of loaded piles. Detailed load-settlement plots for the individual piles in the subgroup tests can be found in Appendix D, and diagrams of cap motion are given in Appendix F.

Comparative behavior of the reference piles, subgroups and the 9-pile group is depicted in a normalized fashion in Fig. 2.16. It can be seen in that figure that the settlement corresponding to a given average load per pile increases with an increasing number of loaded piles in the group. The differences in capacities between the three group tests shown in Fig. 2.16 probably reflect statistical effects of removal of certain "strong" piles from the group tested earlier, but they also indicate that some degradation of soil resistance occurred with each successive test and that the interval of time between tests was too short to permit thixotropic or chemical healing of the soil fabric.

Uplift Tests. The butt load-uplift curves for the two reference piles and four group piles subjected to individual uplift tests are shown in Fig. 2.17. Superimposed on that figure is the average load-settlement graph for the reference piles in their final compression test. Significant differences between the uplift and compression tests are evident:

(1) The average failure load in uplift was approximately 112 kips (498 kN), compared with an average failure load in compression in the reference piles of approximately 178 kips (792 kN). Since the theoretical suction on the tips of the test piles is less than 1 kip (4.45 kN), it is apparent that the differences in capacities between uplift and compression testing reflect the maximum true compression loads developed on the tips of the test piles when they were loaded in compression. In this regard the load-uplift curves for the pile tips, based on pretest zeros, are plotted in Fig. 2.18. Negative tip loads at failure in the order of 40 to 50 kips (178 to 223 kN) are observed. These are not true loads but represent the removal of residual loads that were present at the end of the last compression loading. Fig. 2.18 also shows the average compressive tip load-settlement curve for the last loading of the reference piles, zeroed before the test. The sum of the maximum value on that curve and the average of the maximum (negative) values for the uplift curves for Piles 1 and 11 should yield the true compression tip capacity for the reference piles.

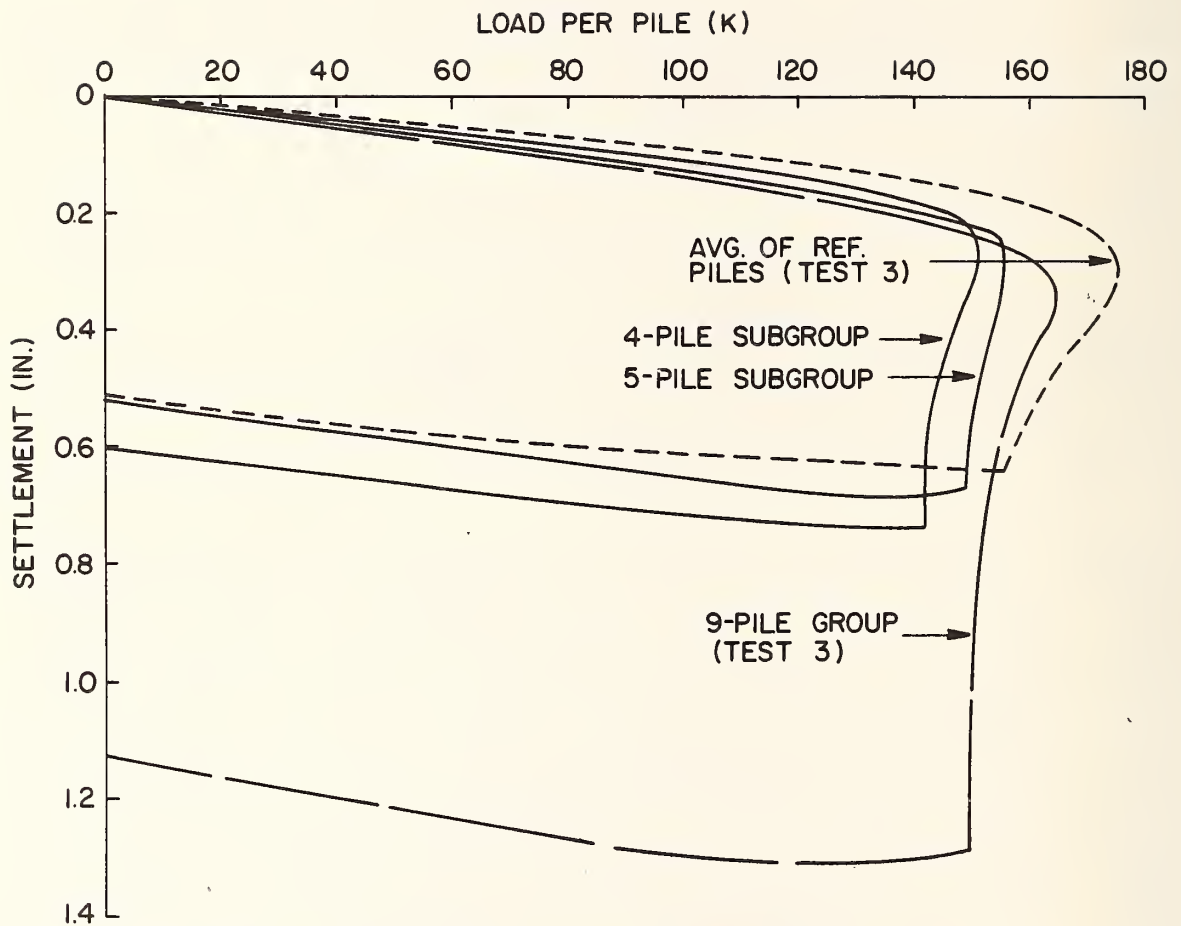
(2) The load-uplift curves were much more nonlinear than the load-settlement curves. This, again, is an expression of the release of residual loads in the piles and possibly the alteration of soil fabric around the piles as the direction of shear stress was reversed.



* AS INDICATED BY LEVEL I STRAIN GAGE CIRCUITS-DOES NOT INCLUDE CAP WGT.
 ** AVG. ON PLANE 1 FT. ABOVE GROUND LEVEL (FOR DIAL GAGES)
 *** 30-MIN READING. ALL OTHERS ARE 5-MIN READINGS

SOME MINOR TIPPING TO SOUTH AND EAST OCCURRED DURING THE 5-PILE SUBGROUP TEST AND THE 4-PILE SUBGROUP TEST

FIGURE 2.15. LOAD-SETTLEMENT RELATIONSHIPS FOR SUBGROUP TESTS
 (1 k = 4.45 kN; 1 ft = 0.305 m; 1 in = 25.4 mm)



NORMALIZED BUTT LOAD-SETTLEMENT CURVES
FOR THIRD REFERENCE AND 9-PILE GROUP TEST
AND FOR 5- AND 4-PILE SUBGROUP TESTS

FIGURE 2.16. NORMALIZED LOAD-SETTLEMENT RELATIONSHIPS
(1 k = 4.45 kN; 1 in = 25.4 mm)

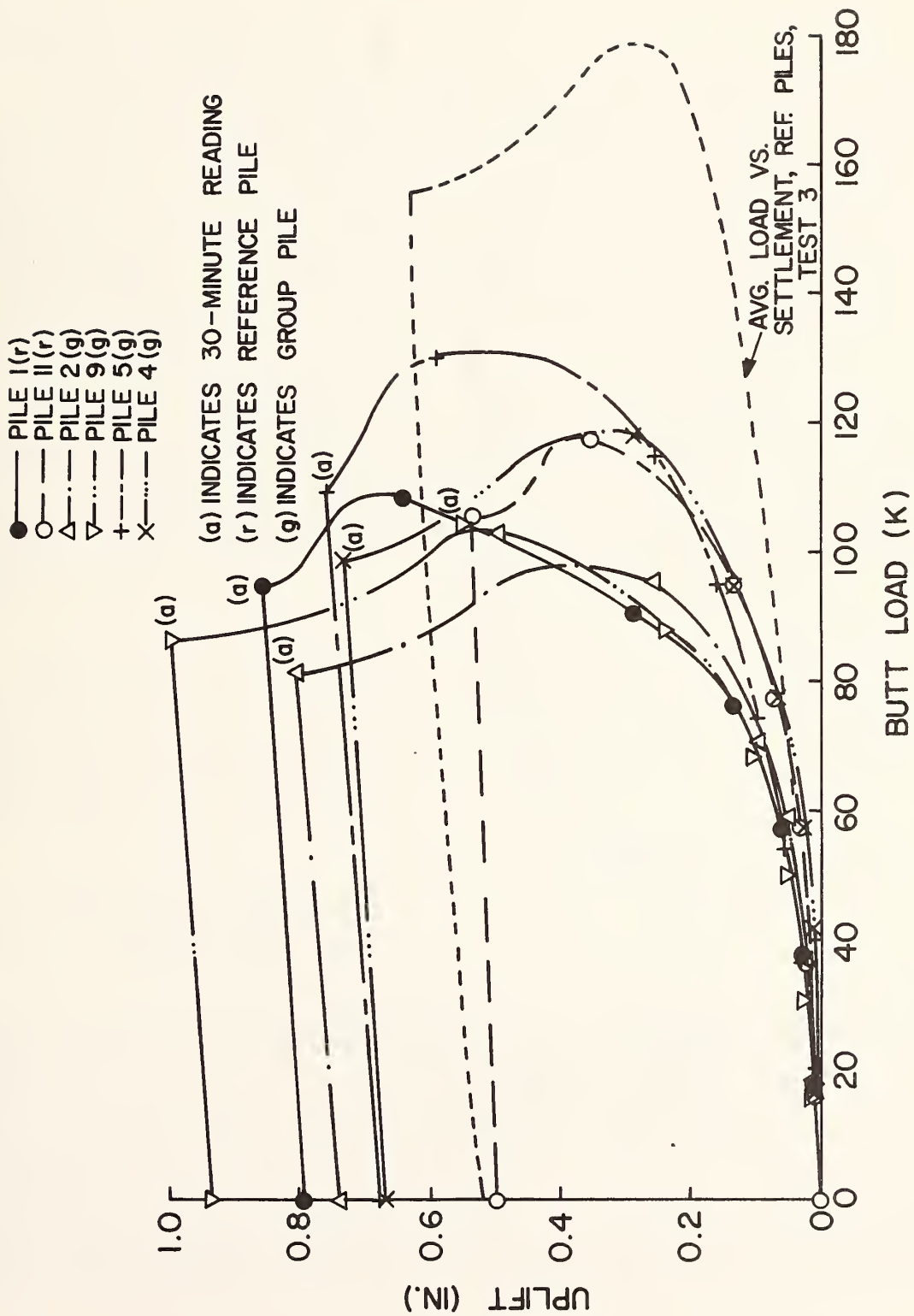
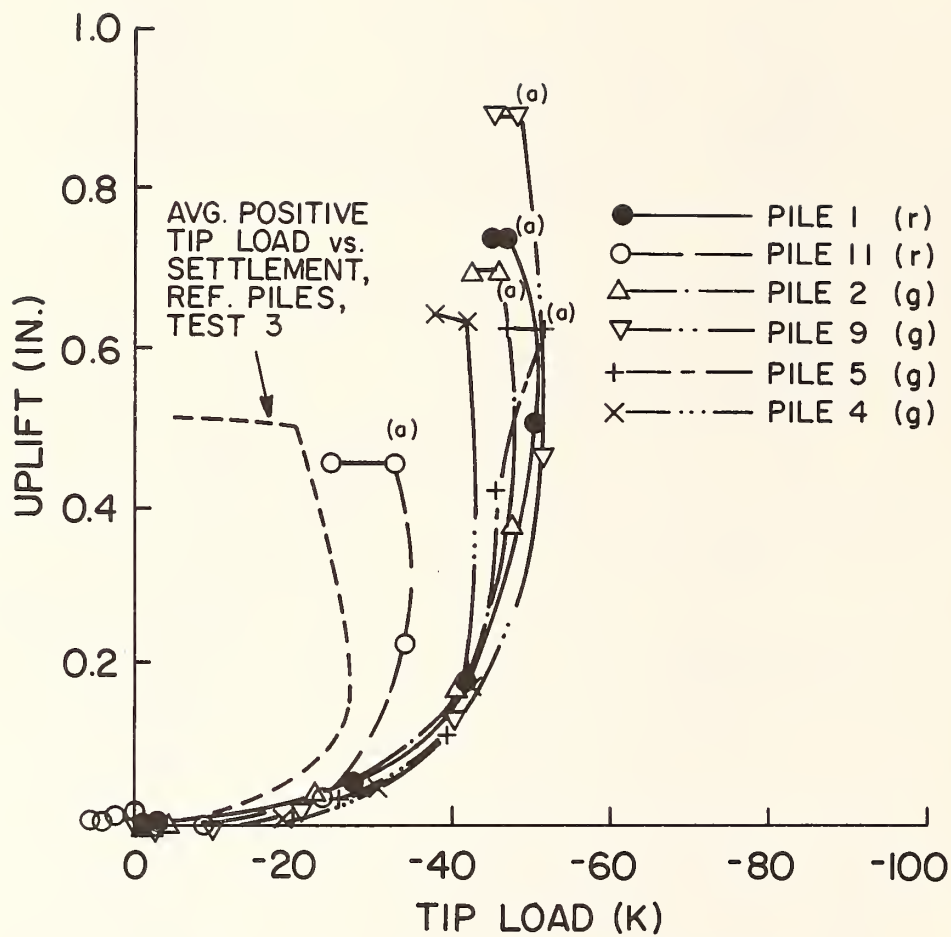


FIGURE 2.17. BUTT LOAD-UPLIIFT RELATIONSHIPS (1 k = 4.45 kN; 1 in = 25.4 mm)



(a) INDICATES 30-MINUTE READING
 (g) INDICATES GROUP PILE
 (r) INDICATES REFERENCE PILE

FIGURE 2.18. TIP LOAD-UPLIFT RELATIONSHIPS (1 k = 4.45 kN; 1 in = 25.4 mm)

(3) There was a higher degree of variability of load-uplift response than of load-settlement response.

Distribution of Loads to Piles

The distribution of applied loads to the various piles in the first 9-pile group test and pile settlements are depicted graphically in Figs. 2.19 and 2.20 for several values of load. Graphical depictions for other tests may be found in Appendix F. Tables 2.1 and 2.2 summarize numerically the pile head load distribution results for all group compression tests. It is apparent that the loads remained relatively uniform throughout the working load range in both the 9-pile group and the subgroups. The corner piles received about 10 per cent more load than the center pile, and the edge piles received an intermediate value in the first (virgin) 9-pile test. These loads do not include the effect of the cap weight.

At failure in the first 9-pile test the center pile attracted the largest load in the group. This effect could be partly due to the progressive nature of pile failure for this test, such that at the precise time the pile gages were read peak resistance may have existed in Pile 2 but not in the other piles, and not a general phenomenon to be associated with the failure of pile groups. Subsequent tests did not indicate that the center pile attracted higher loads at failure than the remaining piles.

Because of the tilting mechanism described earlier and because the piles did not fail simultaneously, considerable variations in the pile loads existed when the group was unloaded after Test 1. Tensile loads existed on the exterior piles that failed first (8,10,7,3), and significant compressive load remained on the center pile (2) and on Piles 4 and 5, which did not fail. Piles 9 and 6 had relatively small compressive loads upon removal of the applied load.

Similar variations can be observed for the other group and subgroup tests in Appendix F.

Variation of Capacity with Time

The variation of the average peak capacity of the reference piles and the average gross peak capacity of the 9-pile group for the three sets of compression tests are shown as functions of time plotted on a logarithmic scale in Fig. 2.21. There exists an apparent set-up in both the reference piles and the group, with set-up occurring at approximately the same rate in each system. The total set-up between the first and third tests, in the order of 30 kips (130 kN) per pile, is approximately equal to the difference in average residual tip load between the post-drive condition (Figs. 1.22 and 1.23) and the last compressive loading, suggested by the negative tip load values in Fig. 2.18. This fact implies that the capacity increase was not a result of

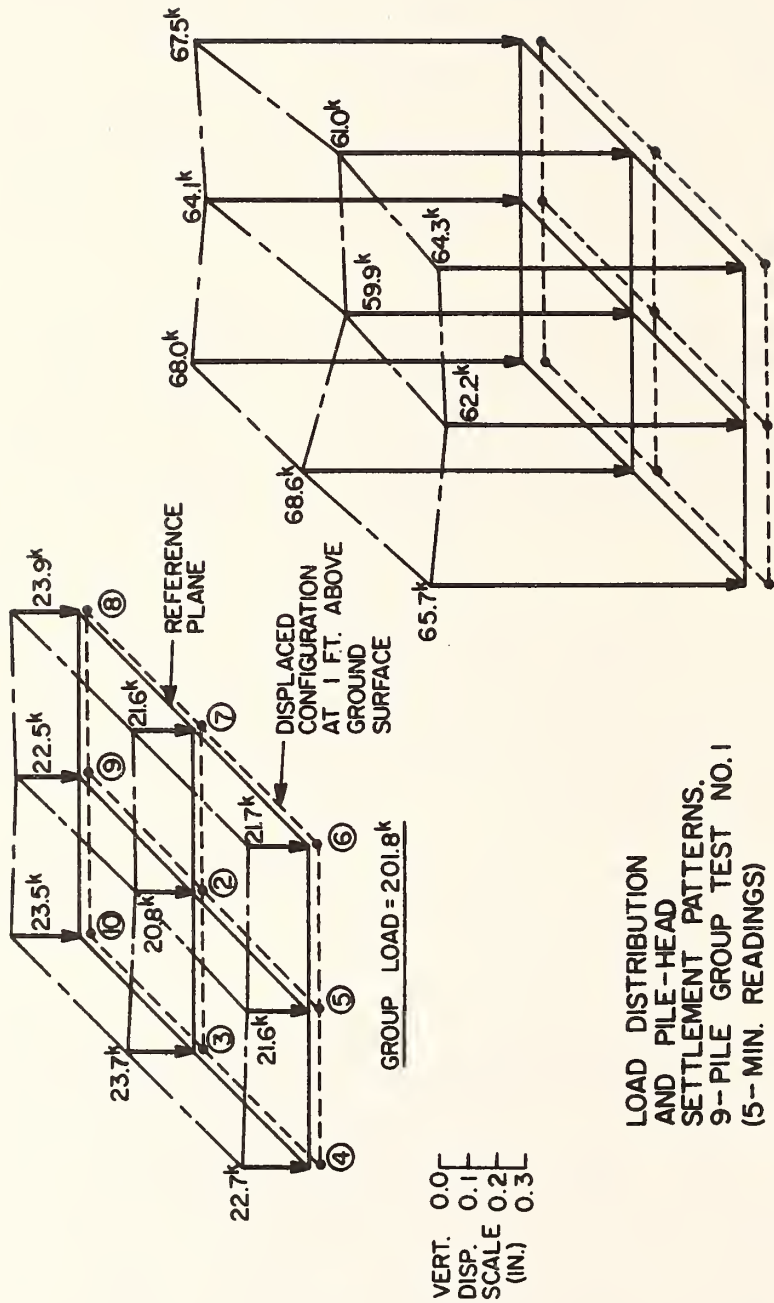
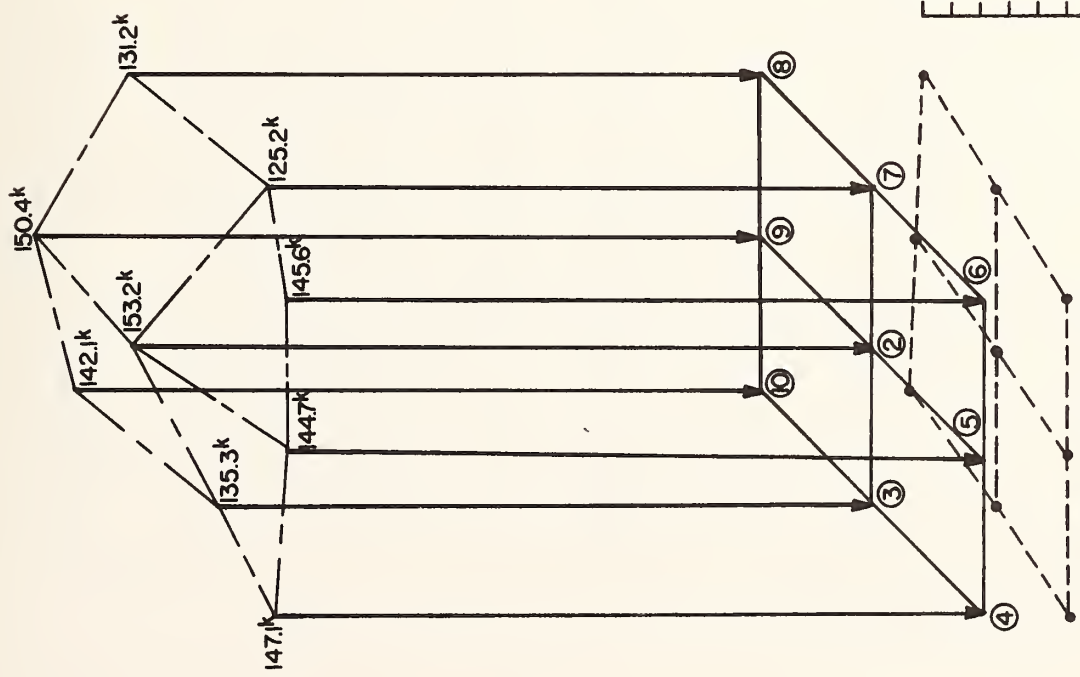
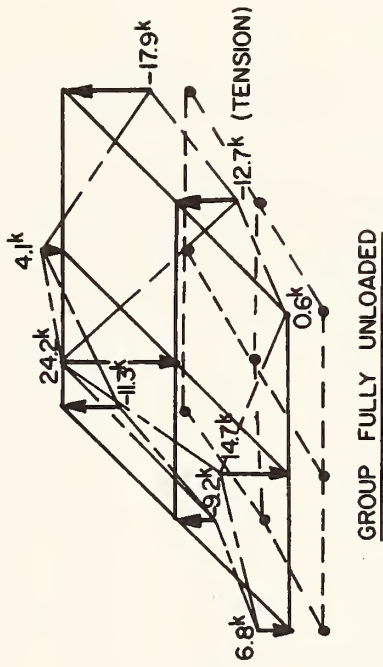


FIGURE 2.19. LOAD DISTRIBUTION TO PILE HEADS-SUBFAILURE; GROUP TEST 1
(1 k = 4.45 kN; 1 ft = 0.305 m; 1 in = 25.4 mm)



GROUP LOAD = 1274.9k
(MAXIMUM LOAD APPLIED)



GROUP FULLY UNLOADED

LOAD DISTRIBUTION AND
PILE-HEAD SETTLEMENT
PATTERNS, 9-PILE GROUP
TEST NO. 1 (5-MIN RDGS, CONT'D).

VERT.
DISP.
SCALE
(IN.)
0.0
0.2
0.4
0.6

FIGURE 2.20. LOAD DISTRIBUTION TO PILE HEADS-FAILURE AND UNLOADED; GROUP TEST NO. 1
(1 k = 4.45 kN; 1 in = 25.4 mm)

TABLE 2.1. DISTRIBUTION OF LOADS TO PILE HEADS:
9-PILE GROUP TESTS (1 k = 4.45 kN)

NOMINAL GROUP LOAD (k)	PILE	PILE HEAD LOAD (k)			AVERAGE PILE HEAD LOAD (k)
		TEST 1	TEST 2	TEST 3	
200	2	20.8	16.6	18.8	CE 1: CENTER (TEST 1): 20.8 (10.3) ¹
	3	23.7	18.1	19.7	ED 1: EDGE (TEST 1): 22.4 (11.1)
	4	22.7	22.6	22.9	CO 1: CORNER (TEST 1): 23.0 (11.4)
	5	21.6	20.8	21.9	CE 2: CENTER (TEST 2): 16.6 (9.5)
	6	21.7	23.5	24.6	ED 2: EDGE (TEST 2): 18.9 (10.8)
	7	21.6	19.1	19.8	CO 2: CORNER (TEST 2): 20.8 (11.9)
	8	23.9	18.1	19.7	CE 3: CENTER (TEST 3): 18.8 (10.3)
	9	22.5	17.4	17.6	ED 3: EDGE (TEST 3): 19.8 (10.9)
	10	23.5	18.9	16.7	CO 3: CORNER (TEST 3): 21.0 (11.6)
		Sum	201.8	174.8	181.8
400	2	40.2	34.6	37.6	CE 1: 40.2 (10.4)
	3	45.6	39.9	42.0	ED 1: 42.8 (11.0)
	4	44.9	46.8	43.6	CO 1: 44.3 (11.4)
	5	41.3	42.9	41.8	CE 2: 34.6 (9.6)
	6	42.4	45.5	47.1	ED 2: 39.4 (10.9)
	7	40.6	37.9	39.6	CO 2: 42.5 (11.7)
	8	44.2	38.0	42.0	CE 3: 37.6 (10.2)
	9	43.6	36.7	37.9	ED 3: 40.3 (11.0)
	10	45.7	39.7	36.2	CO 3: 42.2 (11.5)
		Sum	388.3	362.1	367.6
600	2	59.9	56.3	59.8	CE 1: 59.9 (10.3)
	3	68.6	67.2	67.2	ED 1: 64.0 (11.0)
	4	65.7	74.4	67.9	CO 1: 66.4 (11.4)
	5	62.2	70.4	67.3	CE 2: 56.3 (9.6)
	6	64.3	73.9	74.1	ED 2: 64.5 (11.0)
	7	61.0	61.8	62.3	CO 2: 67.4 (11.5)
	8	67.5	60.9	65.0	CE 3: 59.8 (10.2)
	9	64.1	58.6	59.4	ED 3: 64.1 (11.0)
	10	68.0	60.5	61.0	CO 3: 67.0 (11.5)
		Sum	581.3	583.9	583.9
800	2	81.5	75.0	81.8	CE 1: 81.5 (10.4)
	3	92.9	86.7	89.1	ED 1: 86.3 (11.0)
	4	89.6	98.5	91.8	CO 1: 90.0 (11.4)
	5	84.7	92.9	90.5	CE 2: 75.0 (9.7)
	6	86.5	98.0	98.0	ED 2: 84.6 (11.0)
	7	81.0	81.6	84.3	CO 2: 89.6 (11.6)
	8	90.1	80.4	87.0	CE 3: 81.8 (10.4)
	9	86.6	77.1	80.1	ED 3: 86.0 (11.0)
	10	93.7	81.3	82.6	CO 3: 89.9 (11.5)
		Sum	786.6	771.4	785.0

1 () indicates per cent of total.

TABLE 2.1. DISTRIBUTION OF LOADS TO PILE HEADS:
 9-PILE GROUP TEST (CONT'D) (1 k = 4.45 kN; 1 in. = 25.4 mm)

NOMINAL GROUP LOAD (k)	PILE	PILE HEAD LOAD (k)			AVERAGE PILE HEAD LOAD (k)
		TEST 1	TEST 2	TEST 3	
1000	2	102.3	94.9	100.2	CE 1: 102.3 (10.5) ED 1: 104.9 (10.8) CO 1: 112.1 (11.6) CE 2: 94.9 (9.7) ED 2: 106.6 (10.9) CO 2: 113.3 (11.6) CE 3: 100.2 (10.2) ED 3: 107.1 (10.9) CO 3: 112.7 (11.5)
	3	106.0	108.6	112.4	
	4	112.0	124.3	115.3	
	5	105.2	116.7	111.7	
	6	106.8	122.6	122.8	
	7	99.3	101.8	105.0	
	8	113.7	101.4	109.2	
	9	109.2	99.2	99.2	
	10	115.9	105.0	103.4	
	Sum	970.3	974.3	979.1	
1200	2	128.8	117.0	121.9	CE 1: 128.8 (11.0) ED 1: 126.1 (10.8) CO 1: 133.2 (11.4) CE 2: 117.0 (9.8) ED 2: 130.3 (11.0) CO 2: 137.5 (11.6) CE 3: 121.9 (10.2) ED 3: 131.4 (11.0) CO 3: 137.3 (11.5)
	3	124.6	132.9	136.7	
	4	132.8	151.3	140.3	
	5	127.3	144.2	139.2	
	6	130.5	148.4	148.2	
	7	116.6	123.7	127.9	
	8	131.8	124.2	132.4	
	9	135.8	120.5	121.7	
	10	137.8	126.2	128.3	
	Sum	1166.1	1188.3	1196.6	
1400 (Failure for Test 1- Settlement= 0.295 in.)	2	154.4	135.7	141.2	CE 1: 154.4 (12.1) ED 1: 138.2 (10.8) CO 1: 141.9 (11.1) CE 2: 135.7 (9.8) ED 2: 151.6 (11.0) CO 2: 160.4 (11.6) CE 3: 141.2 (10.2) ED 3: 152.5 (11.0) CO 3: 159.9 (11.5)
	3	135.1	154.3	159.6	
	4	140.9	171.4	163.3	
	5	139.4	170.4	162.4	
	6	144.9	174.2	172.4	
	7	126.0	141.4	144.5	
	8	131.0	144.8	153.0	
	9	152.2	140.4	143.3	
	10	150.9	151.2	150.7	
	Sum	1274.7	1383.8	1391.0	
1400 (May Settlement for Test 1 = 0.420 in.)	2	153.2			CE 1: 153.2 ED 1: 138.9 CO 1: 141.5
	3	135.3			
	4	147.1			
	5	144.7			
	6	145.6	-----	-----	
	7	125.2			
	8	131.2			
	9	150.4			
	10	142.1			
	Sum	1274.9			

TABLE 2.1. DISTRIBUTION OF LOADS TO PILE HEADS:
 9-PILE GROUP TEST (CONT'D) (1 k = 4.45 kN; 1 in. = 25.4 mm)

NOMINAL GROUP LOAD (k)	PILE	PILE HEAD LOAD (k)			AVERAGE PILE HEAD LOAD (k)
		TEST 1	TEST 2	TEST 3	
1600 (Failure for Test 2-Sett=0.48 in.) (Failure for Test 3-Sett=0.33 in.)	2		144.0	153.4	CE 2: 144.0 (10.1) ED 2: 158.5 (11.1) CO 2: 162.3 (11.4) CE 3: 153.4 (10.3) ED 3: 163.9 (11.0) CO 3: 168.8 (11.4)
	3		155.6	173.6	
	4		145.7	176.8	
	5		158.5	176.5	
	6	-----	174.8	181.5	
	7		149.1	155.3	
	8		169.9	159.4	
	9		170.9	150.0	
	10		158.6	157.5	
	Sum		1427.0	1483.9	
1600 (Max. Sett. for 5 min RDG for Test 2=1.29 in.) (Max. Sett. for 5 min RDG for Test 3=1.29 in.)	2		131.4	137.6	CE 2: 131.4 (9.9) ED 2: 146.7 (11.1) CO 2: 150.9 (11.4) CE 3: 137.6 (10.3) ED 3: 146.8 (11.0) CO 3: 151.6 (11.4)
	3		143.1	159.6	
	4		139.9	155.0	
	5		151.4	152.2	
	6	-----	159.6	158.3	
	7		141.8	138.9	
	8		153.6	147.4	
	9		150.6	136.6	
	10		150.4	145.8	
	Sum		1321.9	1331.3	
0 Unloaded	2	24.2	- 2.3	2.6	CE 1: 24.2 ED 1: -4.6 CO 1: -5.5 CE 2: -2.3 ED 2: 0.5 CO 2: -2.3 CE 3: 2.6 ED 3: -1.6 CO 3: -0.7
	3	- 9.2	-12.0	3.4	
	4	6.8	-17.0	-0.4	
	5	14.7	4.7	2.4	
	6	0.6	- 0.2	-3.0	
	7	-12.7	0.6	-2.5	
	8	-17.9	4.5	-1.4	
	9	4.1	8.5	-1.2	
	10	-11.3	3.5	-1.6	
	Sum	- 0.8	- 9.8	-1.6	

NOTE: Failure in Test 1 produced tendency for equalization of loads. Failure in Test 2 did not. Possibly due to progressive failure effects induced by cap rotation at failure, combined with lack of ability to read gages on all piles simultaneously.

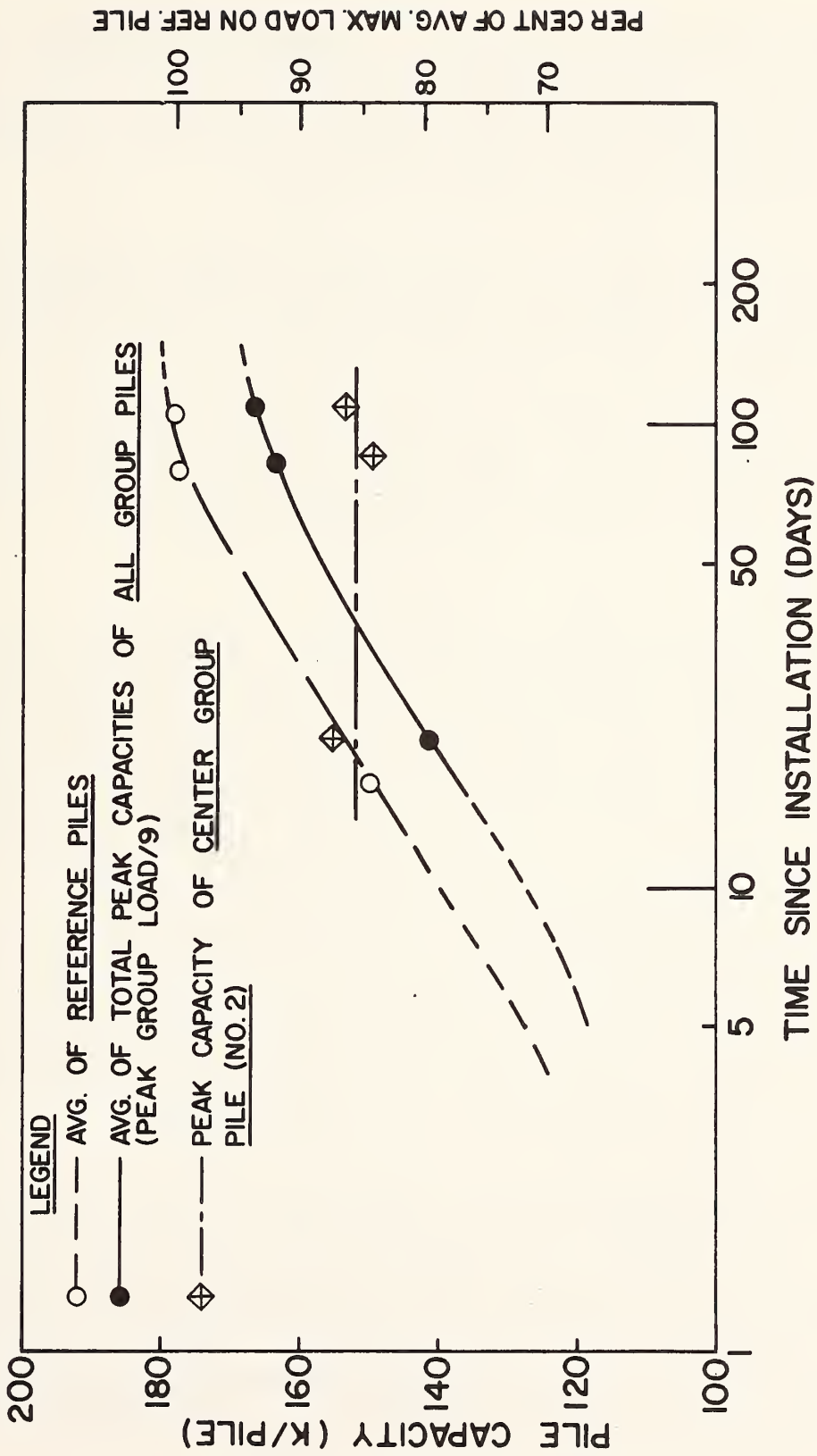
TABLE 2.2. DISTRIBUTION OF LOADS TO PILE HEADS:
SUBGROUP TESTS (1 k = 4.45 kN)

NOMINAL GROUP LOAD (k)	PILE	PILE HEAD LOAD (k)		AVERAGE PILE HEAD LOAD (k)
		5-PILE SUBGROUP	4-PILE SUBGROUP	
100	2	19.4	----	CE 5: 19.4 (18.8) ¹ (Center, 5 Pile Group) CO 5: 21.0 (20.3) (Corner, 5 Pile Group) CO 4: 24.6 (25) (Corner, 4 Pile Group)
	3	19.3	25.7	
	5	17.8	28.8	
	7	23.1	25.0	
	9	23.7	18.7	
	Sum	103.3	98.2	
200	2	30.5	----	CE 5: 30.5 (17.8) CO 5: 35.1 (20.5) CO 4: 52.6 (25)
	3	32.5	55.0	
	5	34.2	55.4	
	7	39.1	51.9	
	9	34.7	47.9	
	Sum	170.9	210.2	
300	2	50.5	----	CE 5: 50.5 (18.4) CO 5: 55.9 (20.4) CO 4: 71.9 (25)
	3	58.2	76.5	
	5	55.9	75.4	
	7	56.2	71.2	
	9	53.4	64.7	
	Sum	274.2	287.8	
400	2	69.3	----	CE 5: 69.3 (18.6) CO 5: 75.9 (20.4) CO 4: 102.4 (25)
	3	77.9	106.8	
	5	76.6	108.9	
	7	75.6	99.7	
	9	73.5	94.2	
	Sum	372.9	409.6	
500	2	84.7	----	CE 5: 84.7 (18.7) CO 5: 92.2 (20.3) CO 4: 126.4 (25)
	3	93.1	131.7	
	5	94.0	134.0	
	7	93.7	123.5	
	9	88.1	116.5	
	Sum	453.7	505.7	
600	2	106.7	----	CE 5: 106.7 (18.4) CO 5: 118.5 (20.4) CO 4: 137.7 (25)
	3	119.6	143.1	
	5	122.1	146.8	
	7	119.1	135.4	
	9	113.0	125.4	
	Sum	580.4	550.7	

1 () indicates per cent of total.

TABLE 2.2. DISTRIBUTION OF LOADS TO PILE HEADS: SUBGROUP TESTS (CONT'D)
 (1 k = 4.45 kN)

NOMINAL GROUP LOAD (k)	PILE	PILE HEAD LOAD (K)		AVG. PILE HEAD LOAD (k)
		5-PILE SUBGROUP	4-PILE SUBGROUP	
700	2	125.1	-----	CES: 125.1 (18.3) COS: 139.3 (20.4) CO4: 145.2 (25)
	3	141.5	151.9	
	5	144.0	153.3	
	7	137.6	141.6	
	9	134.1	133.9	
	SUM	682.2	580.7	
800	2	142.1	-----	CES: 142.1 (18.3) COS: 158.2 (20.4) CO4: 151.0 (25)
	3	166.6	157.0	
	5	167.0	158.9	
	7	149.5	148.7	
	9	149.6	139.6	
	SUM	774.9	604.1	
0 (unloaded)	2	-2.2	-----	CES: -2.2 COS: 1.1 CO4: 0.0
	3	7.0	2.0	
	5	2.6	-1.1	
	7	-5.0	-0.2	
	9	-0.4	-0.6	
	SUM	2.0	0.1	



PER CENT OF AVG. MAX. LOAD ON REF. PILE

FIGURE 2.21. VARIATION IN PEAK CAPACITY WITH TIME (1 k = 4.45 kN)

increased side resistance but rather a function of increasing tip capacity produced by cyclic loading of the soil beneath the pile tips. The residual tip loads which developed after each test apparently consolidated and strengthened the soil beneath the pile tips, rendering an increased total tip capacity (based on the unloaded condition, not the pretest condition) for each successive loading.

The center pile, Pile 2, maintained an approximately constant peak capacity in the presence of increasing residual tip load, indicating that average usable side resistance actually decreased with each successive loading. Further consideration to timewise decreases and increases in unit side resistance in the various soil layers is given in Chapter 3.

It must be concluded that the results of multiple load tests on the same pile or pile group in this soil (a strain-softening, rapidly draining, overconsolidated clay) do not yield accurate information on the gain of capacity with time that would be experienced by a typical pile or pile group, which would normally experience failure only once.

Settlement Ratios

One useful means of depicting group action is to express the ratio of butt settlement of a group of piles at a given average load per pile to that of a single, isolated pile under the same load. This ratio, termed the settlement ratio, describes how much more the group will settle than the isolated pile under similar loading conditions (short-term static loading in the case of this study). Settlement ratios at various percentages of group failure load (cap weight neglected) are shown graphically in Fig. 2.22 for the three 9-pile group tests. Settlements were considered at 1 ft. (0.305 m) above the ground surface for all piles, and the appropriate isolated pile settlement was taken as the average reference pile settlement for the particular set of tests (first, second, or third) being considered. The three sets of tests yielded consistent settlement ratios over a wide range of loads except for a low value at the low end of the load scale for Test 1. This low value is believed to be due to experimental errors associated with the very small settlements encountered at low load values and not to any physical phenomenon. It is also observed that the settlement ratio was essentially constant in all tests over a wide range of loads.

Errors associated with making settlement readings are discussed and evaluated in Appendix E. The ratios depicted in Fig. 2.22 and in the figures and tables which follow are based on as-read settlement readings. These readings are believed to be essentially correct for the reference piles but to be slightly low for the group piles due to small movements in the 40 ft. (12.2 m) long reference system produced by strains induced in the soil by the loaded piles. However, theoretical considerations, as well as back-up readings made using the microhead level, indicate that the reported settlement ratios are probably no more than 20 per cent too low.

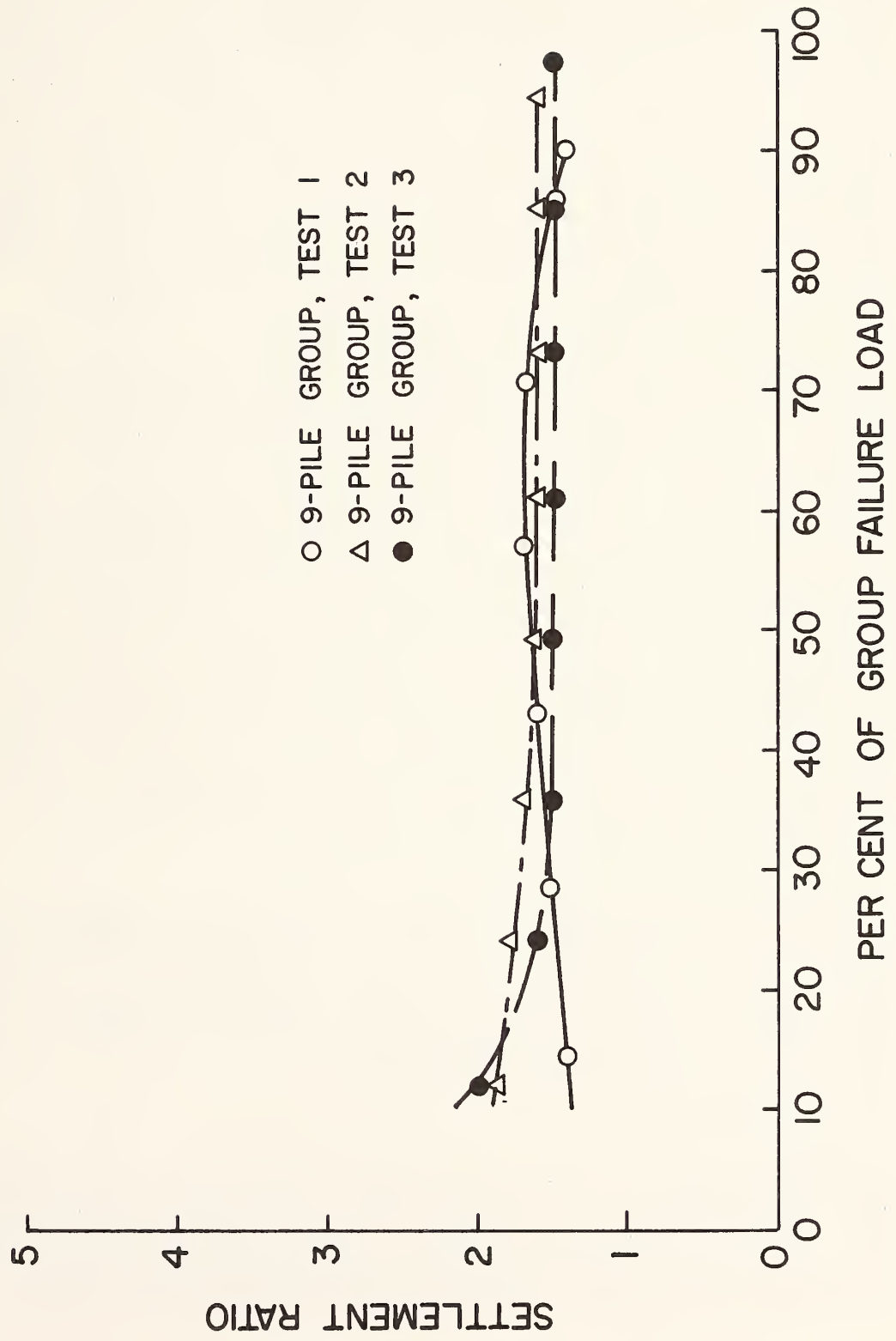


FIGURE 2.22. SETTLEMENT RATIOS FOR NINE-PILE GROUP TESTS

Figure 2.23 shows the average settlement ratios for the three 9-pile tests and the settlement ratios measured for the 5-pile and 4-pile subgroup tests. These latter ratios are based on the set of reference pile tests associated with the third 9-pile group test. Except at very low loads the settlement ratios for the smaller groups are lower than for the 9-pile group, in the order of 1.2 to 1.3, with the 4-pile group yielding the smallest values. It should be recalled that the nominal center-to-center spacing of the loaded piles was 3 diameters for the 5-pile group and 4.2 diameters for the 4-pile group; hence, Fig. 2.23 should be understood to represent the effects of both the number of loaded piles and of pile spacing. It is the authors' opinion that the loading history effects discussed in the previous section were relatively minor between the third 9-pile test and the final subgroup test, so that the settlement ratios in Fig. 2.23 represent a valid comparison.

Figure 2.23 also shows the settlement ratios that are predicted for the various groups by the elastic solid model (see Interim Report), assuming flexible piles and assuming two depthwise variations of soil modulus for an incompressible soil. It is evident that the "Gibson" soil (Young's modulus increasing linearly from zero at the soil surface to the modulus indicated by the pressuremeter at the pile tips) yields results closer to the measured values than does representation of the soil as a semi-infinite halfspace (constant modulus equal to the pressuremeter value at the mid-depths of the piles), although both soil representations yield settlement ratios that are consistently too high. This observation suggests that the stiffness of the soil in the zone beneath the pile tips may be more important than that above the pile tips in controlling short-term settlements and that the reinforcing effect of the piles, not considered by the elastic solid or hybrid models, may effectively stiffen the load-settlement response. For these reasons it appears that selection of soil moduli that are in excess of the in-situ modulus determined through high quality field or laboratory tests in the soil zone from two to three group widths below the pile tips would be most appropriate as inputs to the hybrid model.

The settlement ratios for the pile tips were greater than those for the pile butts, as indicated for Test 1 in Table 2.3. Common reference and group pile tip loads for making the calculations did not include residual loads, so that the ratios with respect to true, or absolute, loads would be slightly higher than those reported in Table 2.3. These data suggest that group action influenced tip settlements to a greater extent than it influenced pile compression.

Induced Settlements

Performance of the subgroup tests provided an opportunity to assess the effects of the loaded piles on the unloaded piles that had been detached from the pile cap. Settlement effects are described here, while load transfer effects are described in Chapter 3. The measured induced effects give some insight into mechanical group

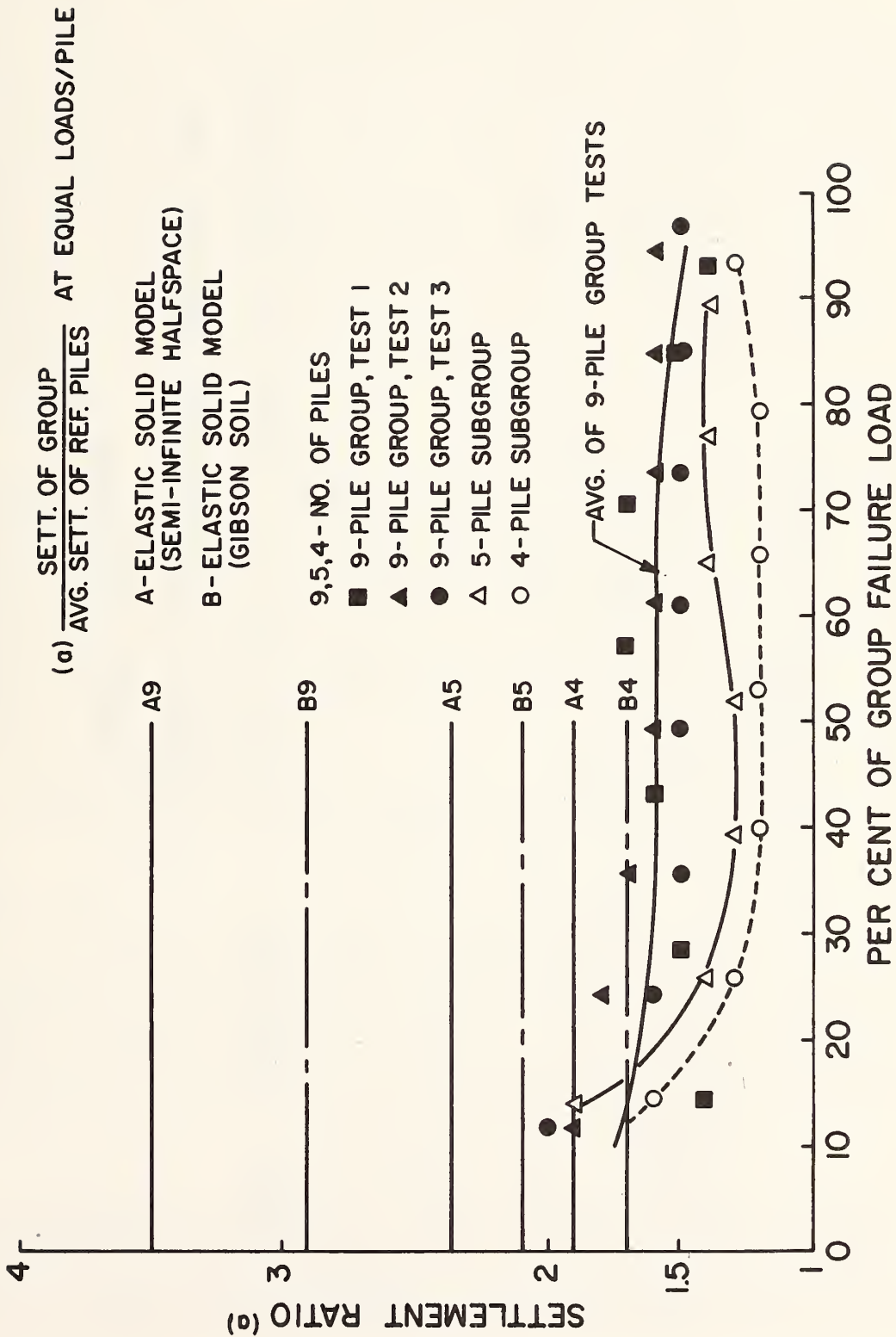


FIGURE 2.23. MEASURED AND THEORETICAL SETTLEMENT RATIOS FOR NINE-, FIVE-, AND FOUR-PILE GROUP TESTS

TABLE 2.3. SETTLEMENT RATIOS FOR PILE TIPS FOR TEST 1

TIP SETTLEMENT RATIOS
TEST 1

TIP LOAD/PILE (KIPS)	TIP SETTLEMENT (IN.)		TIP SETTLEMENT RATIO
	AVG. OF REF. PILES	AVG. OF GROUP PILES	
10	0.012	0.036	3.0
20	0.028	0.094	3.4
25	0.040	0.155	3.9

NOTE : BASED ON : (1) CORRECTED Q-Z CURVE FOR REFERENCE PILES.
 (2) CURVES THAT NEGLECT RESIDUAL TIP LOAD.
 (3) 5 MINUTE READINGS.

behavior and provide data for further fundamental investigations of mathematical models.

Table 2.4 summarizes the butt settlements of the unloaded corner piles (outside of the subgroups of loaded piles: Piles 4,6,8, and 10 from the 9-pile group) as ratios of butt settlements of the loaded piles (Piles 3,5,7, and 9) for various values of applied load in both the 4- and 5-pile subgroups. Likewise, the ratios of the settlement of the unloaded center pile (Pile 2) in the 4-pile test to the average settlement of the loaded piles is also shown. The unloaded corner piles can be seen to have settled somewhat more in the 5-pile test than in the 4-pile test for values of load less than about 75 per cent of failure of the loaded group. The unloaded center pile can also be seen to have settled more than the unloaded corner piles in the 4-pile test. These results are not unexpected, but the magnitudes of these effects are relatively smaller than can be inferred by most elastic solid model algorithms.

If the mean settlements of the unloaded corner piles are plotted as functions of average load per pile applied to the loaded piles for both subgroup tests, the differences in the plots should approximately represent the settlement effect produced by the center pile (loaded in the 5-pile test but not loaded in the 4-pile test) on the typical corner pile 4.2 diameters away. The result would be essentially a two-pile elastic interaction effect except for the presence of the neighboring piles and the effects of load history. Such a plot is given in Fig. 2.24 along with a graph of settlement differences versus single pile load. The latter relationship is essentially linear up to about one-half of the failure load, whereupon induced settlement does not increase further with additional applied load. The lack of induced settlement response at higher loads may be a result of experimental error in measuring settlements, and a possible correction to the curve is suggested in Fig. 2.24.

Efficiencies

A second principal means of expressing group action is by the ratio of the failure load of the pile group to the average failure load of the reference piles times the number of loaded piles in the group. This ratio is defined as the "efficiency" of the group. Efficiency is a characteristic often used by designers to size pile groups based on estimated or measured capacities of single piles. The term "failure" throughout this section will refer to the plunging load of a pile or pile group.

Table 2.5 presents a comprehensive summary of total peak capacities of every pile in each of the first three sets of tests (all reference pile tests and 9-pile group tests). It also gives peak side, or shaft, capacities and maximum tip loads measured on every pile. Based on the average peak shaft, tip, and total capacities for the two

TABLE 2.4. INDUCED SETTLEMENTS (1 k = 4.45 kN; 1 in = 25.4 mm)

SUMMARY OF SETTLEMENTS INDUCED IN UNLOADED PILES : SUBGROUP TESTS.

AVG. LOAD PER LOADED PILE (K) (APPROX.)	SETTLEMENT OF PILE 2 (IN.)		
	AVG. SETTLEMENTS OF PILES 3,5,7,9 (IN.)		
	5-PILE SUBGROUP	4-PILE SUBGROUP	
25	-	$\frac{0.005}{0.0201} = 0.25$	$\frac{0.006}{0.0201} = 0.30$
35	$\frac{0.0159}{0.0390} = 0.41$	-	-
75	$\frac{0.0376}{0.0939} = 0.40$	$\frac{0.0225}{0.0734} = 0.31$	$\frac{0.0265}{0.0734} = 0.36$
135	$\frac{0.055}{0.186} = 0.30$	-	-
145 (IMPENDING FAILURE : 4-PILE GP.)	-	$\frac{0.0478}{0.196} = 0.24$	$\frac{0.054}{0.196} = 0.28$
155 (IMPENDING FAILURE : 5-PILE GP.)	$\frac{0.056}{0.287} = 0.20$	-	-

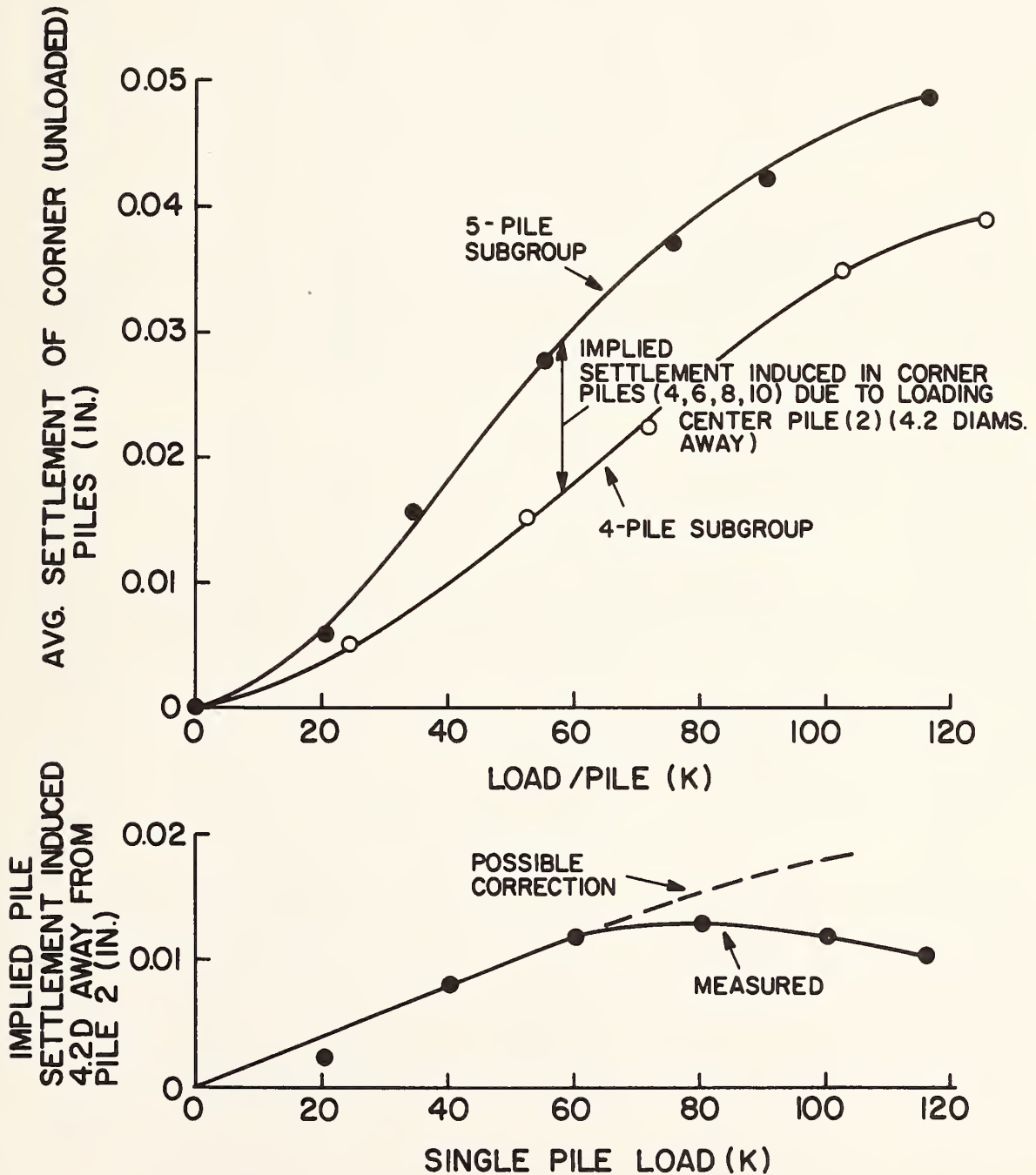


FIGURE 2.24. SETTLEMENTS IN UNLOADED PILES VERSUS LOAD PER LOADED PILE (ABOVE); SETTLEMENT DIFFERENCES IN CORNER PILES BETWEEN 5- AND 4-PILE SUBGROUP TESTS (BELOW) (1 k = 4.45 kN; 1 in = 25.4 mm)

TABLE 2.5. SUMMARY OF FAILURE LOADS AND EFFICIENCIES FOR 9-PILE GROUP TESTS
(1 k = 4.45 kN; 1 ton = 3.9 kN)

PILE	TOTAL PEAK SHAFT CAPACITY (K)			TOTAL TIP CAPACITY (K)			SHAFT (a) EFFICIENCY			TIP (a) EFFICIENCY			TOTAL (b) OVERALL PEAK CAPACITY (K)			TOTAL (c) OVERALL EFFICIENCY		
	TEST 1	2	3	TEST 1	2	3	TEST 1	2	3	TEST 1	2	3	TEST 1	2	3	TEST 1	2	3
I(ref)	142	159	157	31	27	19	—	—	—	—	—	—	167	186	176	—	—	—
II(ref)	112	141	153	41	28	30	—	—	—	—	—	—	132	169	180	—	—	—
2	126	116	123	35	41	30	0.99	0.77	0.79	1.49	1.22	1.22	155	149	153	1.04	0.84	0.86
3	117	136	139	(25)	35	35	0.92	0.91	0.90	(0.69)	1.27	1.43	135	162	174	0.90	0.91	0.98
4	(116)	143	142	(30)	40	35	(0.91)	0.95	0.92	(0.84)	1.45	1.43	(146)	171	177	(0.98)	0.96	0.99
5	(116)	149	140	(27)	41	36	(0.91)	0.99	0.90	(0.75)	1.49	1.47	(143)	176	177	(0.96)	0.99	0.99
6	122	155	145	(23)	42	38	0.96	1.03	0.94	(0.64)	1.53	1.55	145	182	182	0.97	1.03	1.02
7	114	143	135	(17)	21	21	0.90	0.95	0.87	(0.47)	0.76	0.86	126	157	155	0.84	0.88	0.87
8	105	152	124	31	33	42	0.83	1.01	0.80	0.86	1.20	1.71	132	178	159	0.88	1.00	0.89
9	117	149	121	46	41	35	0.92	0.99	0.78	1.28	1.49	1.43	152	179	150	1.02	1.01	0.84
10	127	144	132	(32)	34	36	0.99	0.96	0.85	(0.89)	1.24	1.47	151	167	157	1.01	0.94	0.88

NOTES: AVG. OF REF. PILES: TEST 1: PEAK SHAFT CAPACITY=127K; TIP CAPACITY = 36K; TOTAL OVERALL CAPACITY = 149.5K
TEST 2 " " " = 150K; " " = 27.5K; " " = 177.5K
TEST 3 " " " = 155K; " " = 24.5K; " " = 178.0K

(a) BASED ON AVG. OF 2 REF. PILE TESTS (b) PILE SHAFT + TIP CAPACITIES DO NOT NECESSARILY EQUAL TOTAL CAPACITY, SINCE SHAFT RELAXED AS TIP CONTINUED TO LOAD, ESP. IN GROUP TESTS. () INDICATES "NOT FAILED"

NOTE: EFFECT OF CAP AND LOADING ACCESSORY WEIGHTS AND OF RESIDUAL LOADS NOT INCLUDED IN THIS TABLE.

NOTE: FOR TEST 2, THE PEAK TOTAL CAPACITIES ARE ESTIMATED PEAK INSTANTANEOUS LOADS AND CORRESPONDING TIP LOADS ARE AVG OF PREFAILURE AND POSTFAILURE READINGS (FOR PURPOSE OF CALCULATING PEAK SHAFT CAPACITIES). ALL TOTAL LOADS ARE LOADS INDICATED BY TOP LEVEL OF STRAIN GAGES IN PILE.

FOR PILES 4 AND 5, PEAKS WERE ACHIEVED AT A DISCRETE LOAD RDG (700 TON NOMINAL).

FOR TESTS 1 AND 3, ALL VALUES CORRESPOND TO THE MAXIMUM VALUES READ.

reference pile tests that were associated with each group test, shaft, tip, and total efficiency for each group pile in each of the three 9-pile tests was calculated and tabulated in Table 2.5. The tabulated shaft and tip loads do not include the residual loads nor do they include the effect of cap weight. It is readily evident that the average shaft efficiency was slightly less than unity and the average tip efficiency was greater than unity, especially during the last tests. The high indicated tip efficiencies are believed to be partly due to lower residual tip loads in the group piles. The low indicated tip efficiency for Pile 7 may be due to a measurement error associated with the presence of a quarter bridge strain gage circuit at the tip of that pile.

It should again be noted that the shaft and tip efficiencies relate to maximum loads that were not developed at compatible pile deflections, so that the total efficiency of any pile is less than the sum of the products of shaft efficiency and reference shaft capacity and tip efficiency and reference tip capacity. Furthermore, the peak total pile loads do not necessarily sum to the group capacity for a given test since the peak loads were not all developed simultaneously.

Corresponding efficiency tabulations for the subgroup tests are presented in Table 2.6. Baseline reference pile values are those from the set of tests conducted prior to the third 9-pile group test. Shaft efficiencies were somewhat lower in the subgroup tests than in the 9-pile group tests, possibly due to a lack of healing time between the final 9-pile test, the 5-pile test, and the 4-pile test. Tip efficiencies were generally lower for the 5-pile test than for the final 9-pile test and lower in the 4-pile test than in the 5-pile test. This effect is believed to be due to the continued buildup of residual tip loads on the piles subjected to the subgroup tests to the point where, in the final (4-pile) test, the pretest residual loads were at such a magnitude that the tip loads mobilized during load testing in excess of the pretest residual loads were generally less than the corresponding mobilized loads in excess of pretest residual loads for the reference pile tests, conducted prior to the third 9-pile test.

Total or overall efficiency based on geometric position in the group is tabulated in Table 2.7. In general, the corner piles tended to be slightly more efficient than the edge piles, which, in turn, were slightly more efficient than the center pile. In the first 9-pile test, the center pile was the most efficient by a small margin. Table 2.7 also gives the average shaft and tip efficiencies for all group piles by test. The lowered efficiencies in the subgroup tests are due to statistical effects of removing slightly "stronger" piles from the original group and to the load history effects, including insufficient healing time, discussed earlier.

Finally, the overall efficiencies for the five group tests are evaluated in Table 2.8. In this table efficiency has been defined in four ways which comprise all combinations of the following two criteria:

TABLE 2.6. SUMMARY OF FAILURE LOADS AND EFFICIENCIES FOR SUBGROUP TESTS
(1 k = 4.45 kN)

PILE	TOTAL PEAK CAPACITY (K)		TOTAL TIP CAPACITY (K)		SHAFT (a) EFFICIENCY		TIP (a) EFFICIENCY		TOTAL PEAK CAPACITY (K)		TOTAL (a) OVERALL EFFICIENCY	
	5-PILE TEST	4-PILE TEST	5-PILE TEST	4-PILE TEST	5-PILE TEST	4-PILE TEST	5-PILE TEST	4-PILE TEST	5-PILE TEST	4-PILE TEST	5-PILE TEST	4-PILE TEST
2	107	—	35	—	0.69	—	1.43	—	142	—	0.80	—
3	139	134	29	26	0.90	0.86	1.18	1.06	167	157	0.94	0.88
5	136	138	31	22	0.88	0.89	1.27	0.90	167	159	0.94	0.89
7	132	138	17	12	0.85	0.89	0.69	0.49	149	149	0.84	0.84
9	121	120	29	19	0.78	0.77	1.18	0.78	150	140	0.84	0.79

(a) BASED ON AVG. OF REF. PILES FOR 9-PILE GROUP TEST 3 : PEAK SHAFT CAPACITY = 155 K ;
PEAK TIP CAPACITY = 24.5 K ; TOTAL OVERALL CAPACITY = 178.0 K

(b) PILE SHAFT + TIP CAPACITIES DO NOT NECESSARILY EQUAL TOTAL CAPACITY

NOTE : EFFECT OF CAP AND LOADING ACCESSORY WEIGHTS AND OF RESIDUAL LOADS NOT INCLUDED IN THIS TABLE

TABLE 2.7. OVERALL EFFICIENCY BY GEOMETRIC POSITION AND AVERAGE SHAFT AND TIP EFFICIENCIES

OVERALL
EFFICIENCY BASED ON
GEOMETRIC POSITION IN GROUP^(a)

TEST	CENTER PILE (2)	AVG. OF EDGE PILES(3,5,7,9)	AVG. OF CORNER PILES(4,6,8,10)
1	1.04	0.93	0.96
2	0.84	0.95	0.98
3	0.86	0.92	0.95
5-PILE SUB-GROUP	0.80	0.89	—
4-PILE SUB-GROUP	—	0.85	—

AVERAGE
SHAFT AND TIP
EFFICIENCIES^(a)

TEST	AVG. SHAFT EFFICIENCY	AVG. TIP EFFICIENCY
1	0.93	NOT ADEQUATELY DEFINED
2	0.95	1.32
3	0.86	1.40
5-PILE SUBGROUP	0.82	1.15
4-PILE SUBGROUP	0.85	0.81

(a) NEGLECTING WGT. OF CAP AND LOADING ACCESSORIES

TABLE 2.8. OVERALL PILE GROUP EFFICIENCIES FOR TEST PROGRAM
(1 k = 4.45 kN)

TEST	GROSS (a) NEGLECTING WGT. OF CAP AND LOADING ACCESSORIES	AVERAGE (b) NEGLECTING WGT. OF CAP AND LOADING ACCESSORIES	GROSS (c) INCLUDING WGT. OF CAP AND LOADING ACCESSORIES	AVERAGE (d) INCLUDING WGT. OF CAP AND LOADING ACCESSORIES
1	0.95	0.96	0.98	0.99
2	0.92	0.95	0.95	0.98
3	0.93	0.92	0.96	0.96
4(e)	0.87	0.87	0.93	0.93
5(f)	0.85	0.85	0.92	0.92

GROUP CAP WGT. = 57.5 K
WGT. OF JACK AND LOAD
HEAD FOR REF. PILES = 1.2K

- (a) (PEAK INSTANTANEOUS GROUP LOAD ÷ NO. OF PILES)/AVG. PEAK INSTANTANEOUS REF. PILE LOAD
- (b) AVERAGE OF EFFICIENCIES OF INDIVIDUAL PILES (PROBABLE IDEAL EFFICIENCY OF GROUP HAD PURE VERTICAL MOTION EXISTED)
- (c) SAME AS (a), BUT CAP WGT. ADDED TO NUMERATOR AND JACK AND LOAD HEAD WGT. ADDED TO DENOMINATOR
- (d) SAME AS (b), BUT COMPUTED BY ADDING (1/NO. OF PILES) TIMES TOTAL CAPACITY OF EACH GROUP PILE AND WGT. OF LOAD HEAD PLUS JACK AND DIVIDING BY AVG. TOTAL CAPACITY OF REFERENCE PILES
- (e) 5 - PILE SUBGROUP (f) 4 - PILE SUBGROUP

(1) failure defined by (a) load required to produce plunging failure of the center of the pile cap ("gross" failure), or (b) the sum of the plunging or maximum loads in each of the loaded piles comprising the group ("average" failure) and (2) failure load consisting of (a) applied load only, or (b) applied load plus the weight of the pile cap and loading accessories. For the condition of either average or gross failure, where the failure load included the weight of the cap, the overall efficiency was between 0.95 and 0.99 for the three 9-pile tests and was 0.92 to 0.93 for the subgroup tests.

It can therefore be concluded that the efficiency of a full-scale pile group of 4 to 9 piles at this site is essentially unity. It should be emphasized that these results are in conflict with the various design-type efficiency models described in the Interim Report, which either assume that the group will fail in a "block" mode, thus enhancing efficiency (at this site; in other soil types efficiency can be less than unity with the block model), or that some capacity reduction factor should be applied to each pile based on geometric effects (e.g., Feld's Rule). This is not to argue that such effects would not exist in other soil profiles or in groups in the same soil with a significantly larger number of piles or at closer spacings than were employed in this study.

Pore Water, Total and Effective Pressures Developed During Load Tests

Synoptic tabulations of pore and total pressure readings made on the piles during the load tests are presented in Appendix F. Because of the sensitivity of the total pressure cells to temperature, documented in Appendix E, a means of correcting the total pressure readings also had to be developed. This procedure, which was partially subjective, is also described in Appendix F. All of the total pressure readings reported in this chapter are corrected readings. Since effective stresses were determined as the differences in total and pore water stresses, effective stress values are also "corrected" values. Pore water pressure values are the raw values that were read during the tests.

Considerable scatter occurred among the total pressure cells. The reader can readily observe the scatter in the stress tables in Appendix F, and some thoughts concerning the reasons for the scatter are offered in Appendix E. Unknown temperatures in the sensing fluid, surface irregularities on the piles in the vicinity of the pressure cells, the use of flat sensor faces (as opposed to the cylindrical surface of the piles), and soil property variations are thought to be the primary causes of the scatter.

For this reason, it was not possible to discern differences in total or effective stress patterns on the various group piles. Therefore, data are presented in this chapter in terms of average total and effective stresses on the four group piles that were instrumented for lateral pressure and separately for the single reference pile (Pile 1) that was so instrumented.

Reference is made to Figs. 1.15-1.17, which indicated that significant excess pore pressures were developed during pile installation but that those pressures dissipated very rapidly thereafter to a level near the hydrostatic level by the beginning of the first set of load tests. Figure 1.18 depicted the general changes in lateral effective stresses at the pile surface produced by pile installation (but not by loading) in terms of effective earth pressure coefficients. Corrected, rather than raw, values of total pressure were used to produce the relationship shown in that figure. Measured lateral effective earth pressure coefficients after installation at the faces of the piles can be seen to be about 1.2 times the in-situ earth pressure coefficients at the 9 and 19 ft. (2.7 and 5.8 m) levels and 2.4 times the in-situ values at the 34 and 41 ft. (10.4 and 12.5 m) levels. Very little difference between the average indicated effective stress on the group piles and measured effective stress on the reference piles existed at the upper level or at the lower two levels. No definitive statement can be made about the second level due to the unrealistically low pressure coefficient observed there on the reference pile.

Attention is called to the fact that essentially no load transfer occurred over the top halves of the piles during the driving process (Figs. 1.9 and 1.10), yet approximately four days after driving (the time represented in Fig. 1.18) the effective lateral earth pressure coefficients in the top halves of the piles approximated the in-situ coefficients. From these measurements it is inferred that an annular space ("gap zone") may have developed between the pile and soil during driving over the top approximately one-half of the embedded portion of the pile at full penetration which later closed due to lateral expansion of the soil.

Pressure Changes During Loading. Plots of total and pore pressure changes that occurred during load testing on representative lateral pressure cells at the first through fourth levels are shown in Figs. 2.25 through 2.28. Changes in pore pressures at the pile face are seen to have been small during loading, generally in the order of + 2 psi (14 kN/m²) or less. Some small negative changes were noted at the 41 ft. (12.5 m) depth.

Total pressure changes were also generally small, although large changes can be observed after large relative movement occurred between the pile and soil for some cells, (e.g., Pile 4, 34 ft. (10.4 m) depth) These large changes, furthermore, were observed to be functions of the direction of loading, typically being positive for compression tests and negative for uplift tests. This phenomenon appears to have resulted from non-vertical alignment of the cells, produced by inadvertent battering of the piles and by initial placement of the cells on the piles such that the tops of the sensor plates protruded slightly beyond the bottoms. The need for this placement is discussed in Appendix E. Total stresses corresponding to failure were taken as the values just preceding the large increases or decreases, where such large changes occurred.

TOTAL AND PORE PRESSURE CHANGES DURING LOAD TESTING

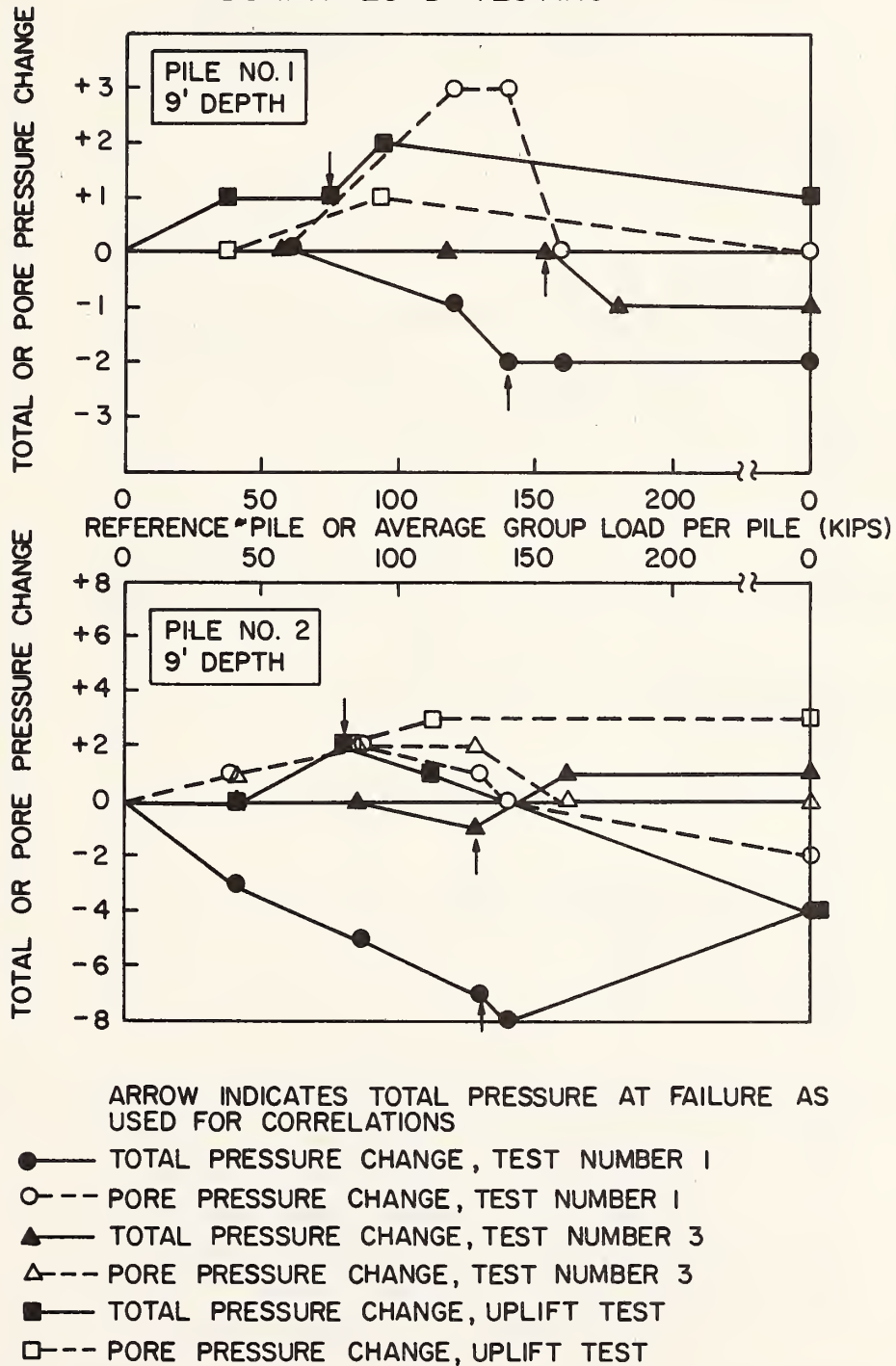


FIGURE 2.25. PORE AND TOTAL PRESSURE CHANGES ON PILES AT 9-FOOT (2.7 M) DEPTH (1 k = 4.45 kN; 1 psi = 6.89 kN/m²)

TOTAL AND PORE PRESSURE CHANGES DURING LOAD TESTING

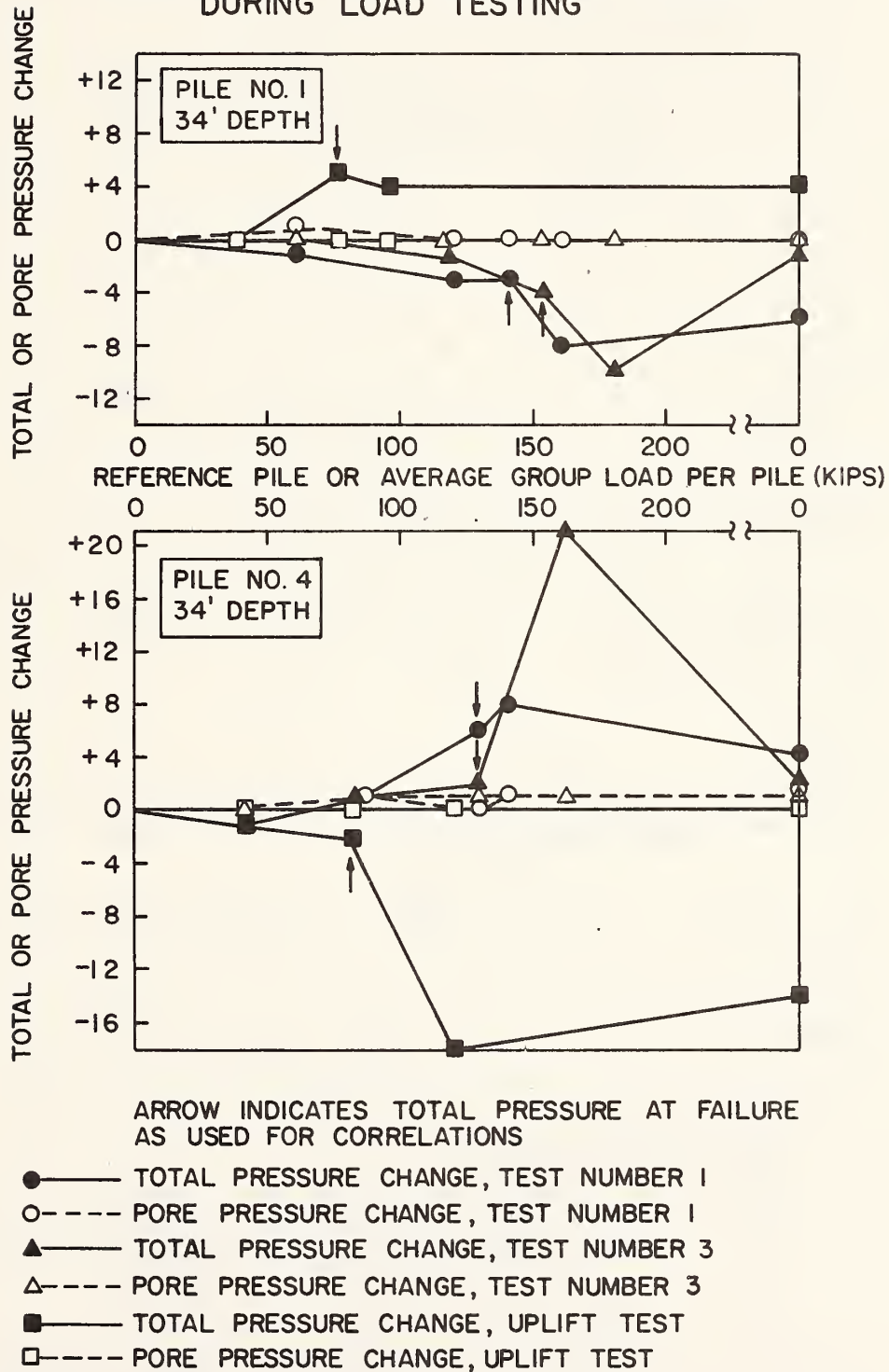
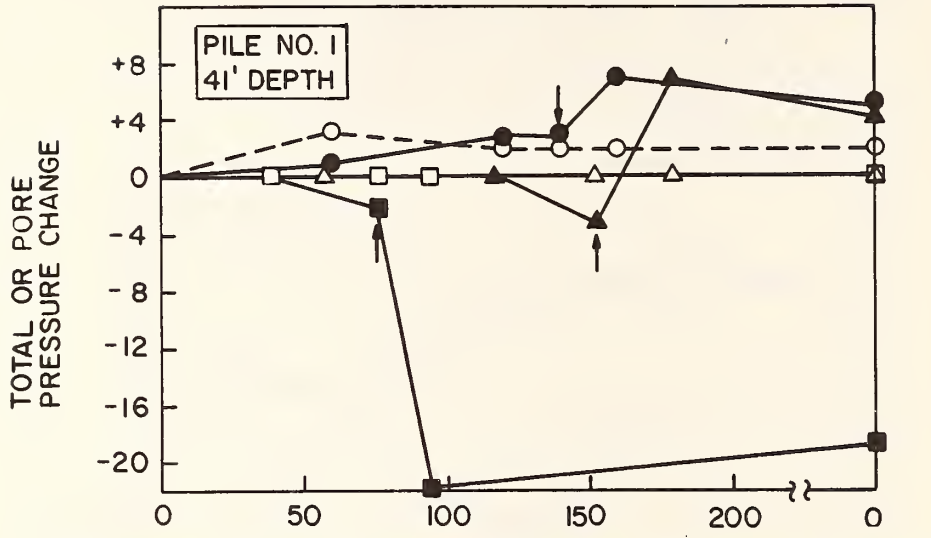
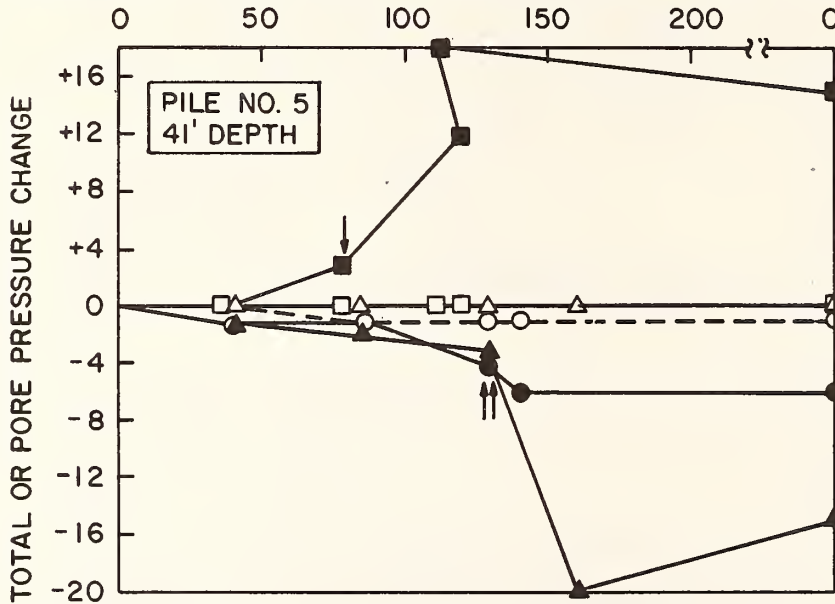


FIGURE 2.27. PORE AND TOTAL PRESSURE CHANGES ON PILES AT 34-FOOT (10.4 M) DEPTH (1 k = 4.45 kN; 1 psi = 6.89 kN/m²)

TOTAL AND PORE PRESSURE CHANGES DURING LOAD TESTING



REFERENCE PILE OR AVERAGE GROUP LOAD PER PILE (KEDS)



ARROW INDICATES TOTAL PRESSURE AT FAILURE AS USED FOR CORRELATIONS

- TOTAL PRESSURE CHANGE, TEST NUMBER 1
- PORE PRESSURE CHANGE, TEST NUMBER 1
- ▲——— TOTAL PRESSURE CHANGE, TEST NUMBER 2
- △----- PORE PRESSURE CHANGE, TEST NUMBER 2
- TOTAL PRESSURE CHANGE, UPLIFT TEST
- PORE PRESSURE CHANGE, UPLIFT TEST

FIGURE 2.28. PORE AND TOTAL PRESSURE CHANGES ON PILES AT 41-FOOT (12.5 M) DEPTH (1 k = 4.45 kN; 1 psi = 6.89 kN/m²)

It should be pointed out that the surface along which the pore pressures and total stresses were measured may not have been the actual failure surface, which may have developed at some slight distance into the soil. It is the opinion of the authors that since the pore pressure measurements were made very close to the failure surface in a saturated soil that the reported pore pressures developed during loading are very close to the values on the failure surface. The small changes in pore pressures along the shafts of the piles during loading suggest that the soil can possibly be treated as a frictional material for purposes of computing unit side resistance, and the small observed pore pressure changes coupled with the large observed increase in lateral effective earth pressure coefficient due to installation of the piles, in the bottom approximately one-fourth of the piles, suggests that the soil that was undergoing failure near the bottoms of the piles may have also been at or near the "critical state." This speculation is substantiated by the generally minor strain softening (relaxation) that occurred in the unit side shear-relative deformation (f-z) curves in the 30 to 40 ft. (9.2-12.2 m) depth range (described in Chapter 3 and in Appendix D). More significant strain softening occurred below 40 ft. (12.2 m), possibly due to a reduction in confining pressures caused by downward movement of the pile tips, and is not necessarily an indication that the soil undergoing failure was not at the critical state. The existence (or absence) of critical stress states is an important consideration for applying new advanced design procedures for pile capacities which are predicated on critical state soil mechanics theory.

The absence of significant increases in lateral effective earth pressure coefficients observed at the top two levels of earth pressure cells (roughly top one-half of the piles, where the soil was highly overconsolidated) suggests that the failing soil may not have achieved the critical state at those levels.

Horizontal Variations in Pore Water Pressure. Figures 2.29-2.34 present graphical summaries of pore pressure variations (not excess pressures) along the profile lines described in Fig. 1.19. The purpose of these graphs is to provide a comparison between pore pressures measured on the surfaces of the piles and those measured in the soil mass and to show variations among the piles and through the soil. The single numeral following the letter P designates a pile piezometer (e.g., P1 designates Pile 1, a reference pile, P2 designates Pile 2, a group pile, etc.), while a series of three numerals following the letter P designates a ground, or soil mass, piezometer (e.g., P345 designates a ground piezometer at a depth of 34 ft. (10.4 m) at position 5; see Figs. 1.6 and 1.7). The pore pressures shown during testing are those values read five minutes after a load application.

Figures 2.29-2.31 present pore water pressure readings prior to the beginning of each compression test. Figure 2.29 pertains to the reference pile tests and contains values only for the reference pile instrumented for lateral pressure (Pile 1); Figure 2.30 pertains to the

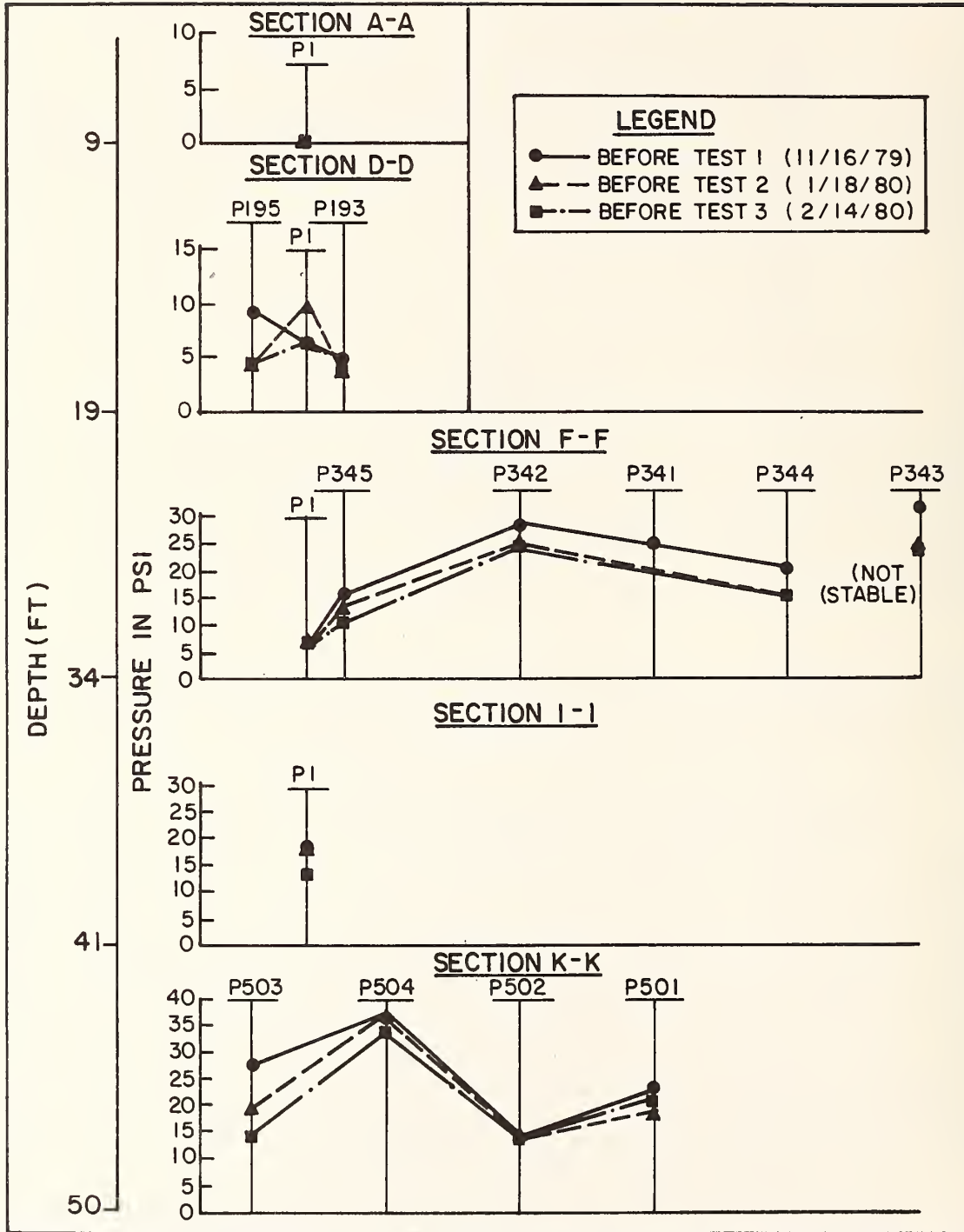


FIGURE 2.29. HORIZONTAL VARIATION IN PORE PRESSURE IN SOIL AND ON PILE 1 PRIOR TO REFERENCE TESTS (1 ft = 0.305 m; 1 psi = 6.89 kN/m²)

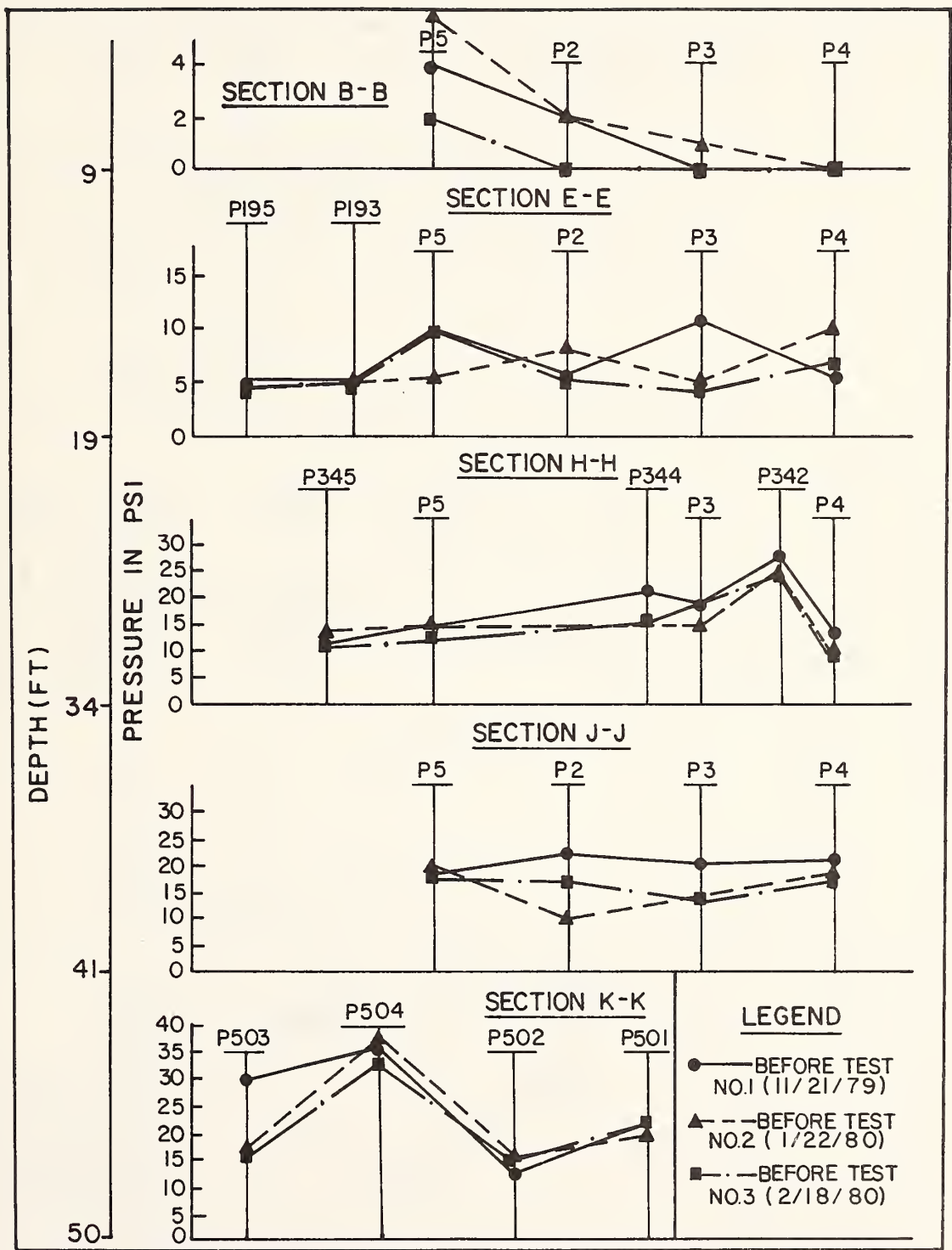


FIGURE 2.30. HORIZONTAL VARIATION IN PORE PRESSURE IN SOIL AND ON GROUP PILES PRIOR TO 9-PILE TESTS (1 ft = 0.305 m; 1 psi = 6.89 kN/m²)

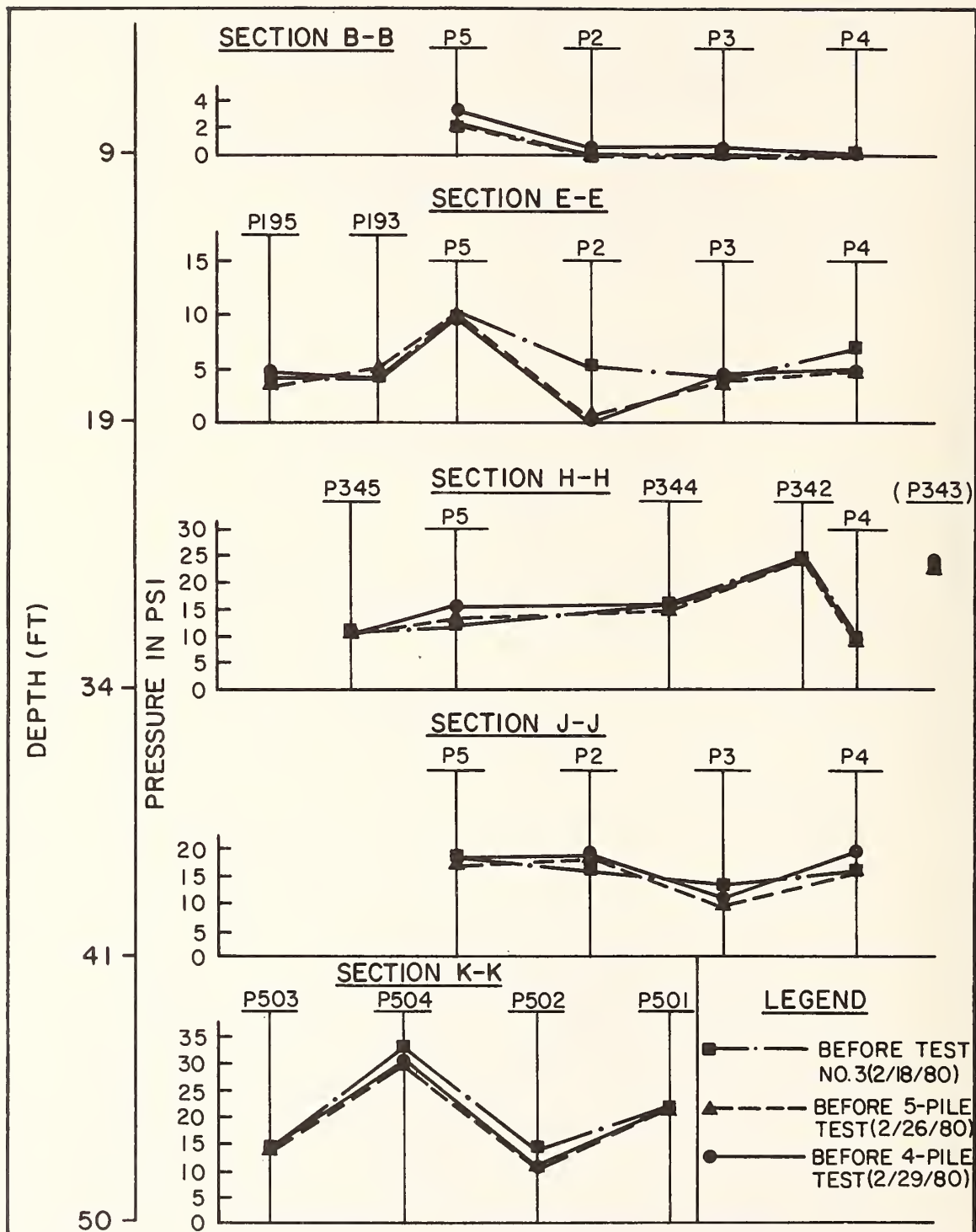


FIGURE 2.31. HORIZONTAL VARIATION IN PORE PRESSURE IN SOIL AND ON GROUP PILES PRIOR TO SUBGROUP TESTS (1 ft = 0.305 m; 1 psi = 6.89 kN/m²)

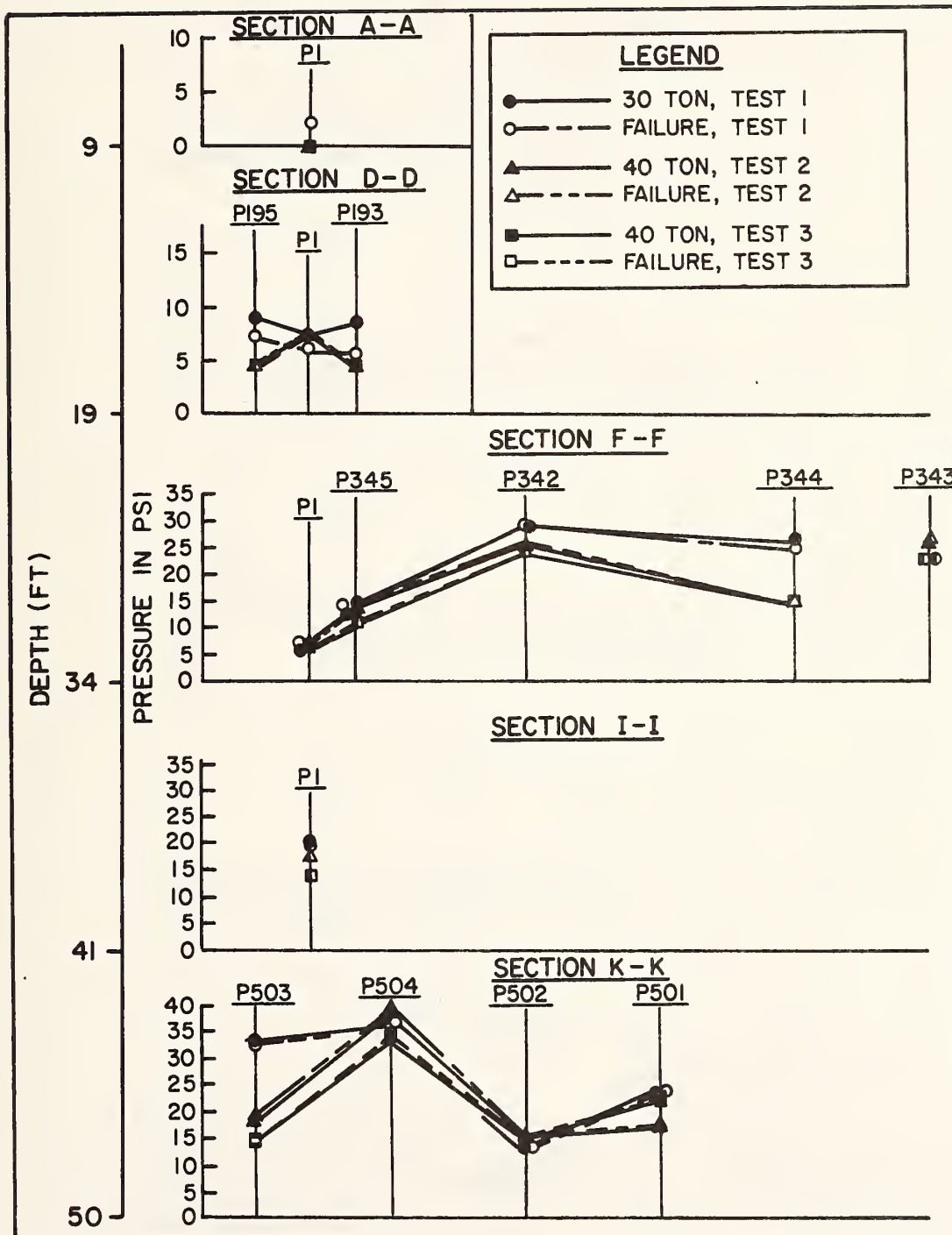


FIGURE 2.32. HORIZONTAL VARIATION IN PORE PRESSURE DURING REFERENCE PILE TESTS (1 ft = 0.305 m; 1 psi = 6.89 kN/m²; 1 ton = 8.9 kN)

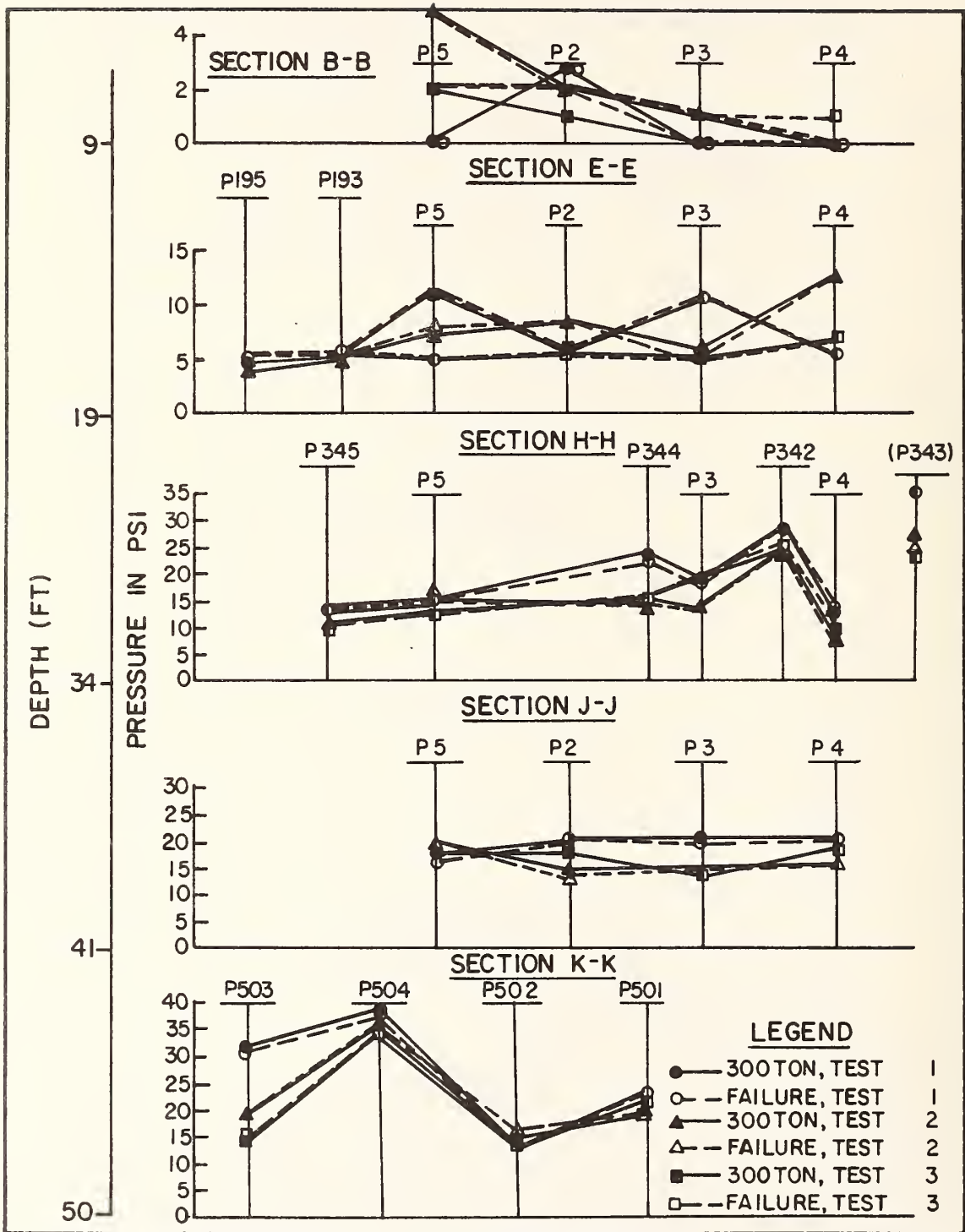


FIGURE 2.33. HORIZONTAL VARIATION IN PORE PRESSURE DURING 9-PILE TESTS
 (1 ft = 0.305 m; 1 psi = 6.89 kN/m²; 1 ton = 8.9 kN)

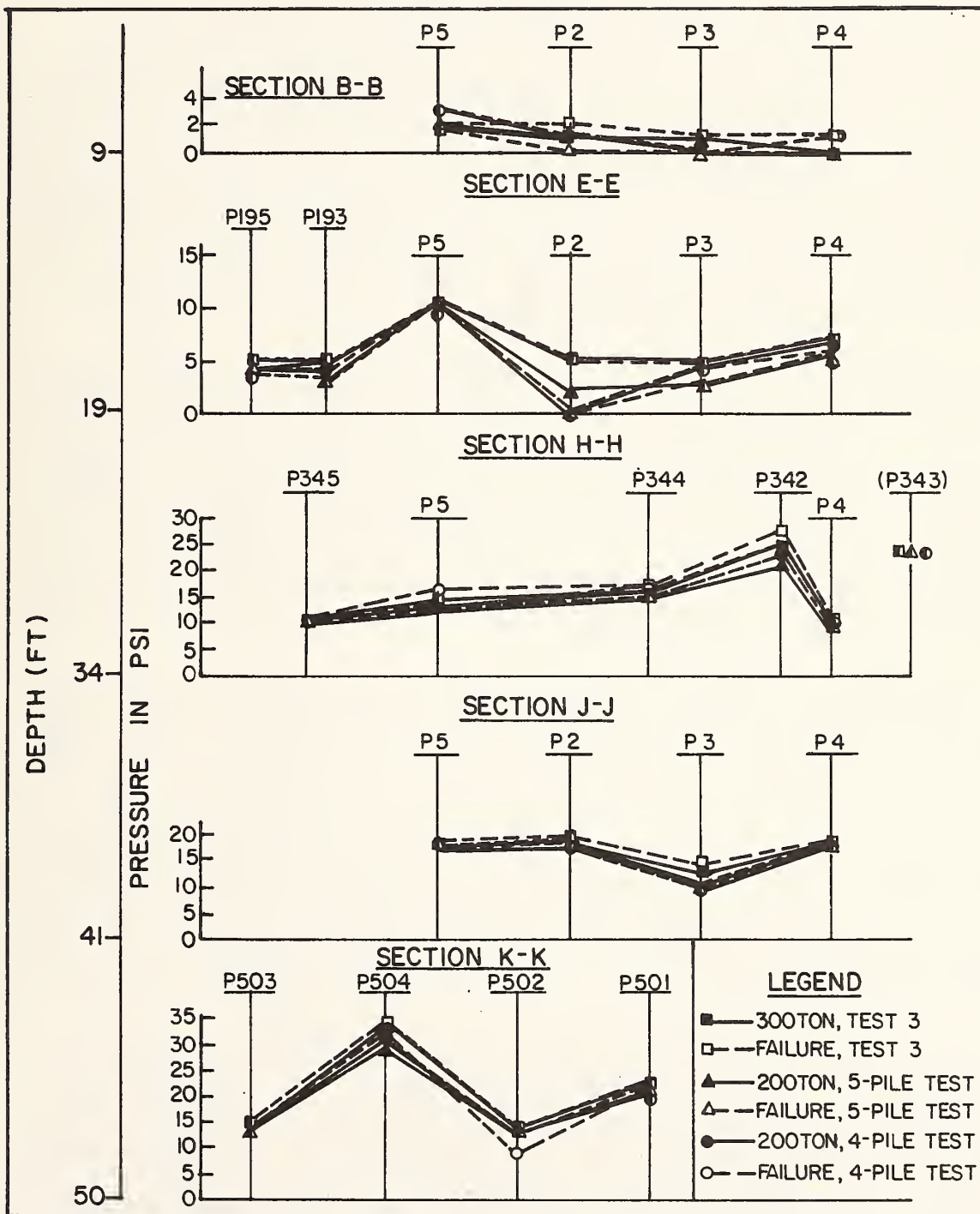


FIGURE 2.34. HORIZONTAL VARIATION IN PORE PRESSURE DURING SUBGROUP TESTS
 (1 ft = 0.305 m; 1 psi = 6.89 kN/m²; 1 ton = 8.9 kN)

pore pressure conditions in and around the group before the 9-pile tests; and Fig. 2.31 pertains to the conditions preceding the subgroup tests. Pore pressure variations for the third (final) 9-pile group test are also included in Fig. 2.31 for purposes of comparison.

A fairly significant scatter in the absolute values of pore pressure can be seen from point to point in these figures. Analyzed in total, however, the average pore water pressures on the piles and in the soil at the two common depths, 19 ft. and 34 ft. (5.8 m and 10.4 m), at which pile and ground piezometers were placed did not differ significantly prior to the tests, which is a further indication that excess pore pressures generated during driving had almost fully dissipated through-out the entire mass of soil controlling the behavior of the group. The pressure gradients implied in the various figures under consideration probably do not have much physical significance.

Figures 2.32-2.34 show measured pore pressures at about one-half the failure load and at failure for the reference pile tests, 9-pile group tests, and subgroup tests, respectively. The pore water pressure changes in the soil mass, as on the faces of the piles, were very small during both reference pile and group tests. At some soil instrument locations the changes were negative, while at others the changes were positive, but almost all changes recorded in the soil mass, as on the piles, from prior to a test until failure were less than about 2 psi (14 kN/m²). Pore pressure changes during load test in the soil surrounding Pile 1 were not significantly different from those in the soil mass surrounding the group piles.

Depthwise Variations of Lateral Pressures on Piles. The observed vertical variation in pore water pressure on the face of Pile 1, the reference pile, prior to each compression load test and at failure is plotted in Fig. 2.35. That figure, as well as the following figures on vertical pore pressure variation, also shows a "hydrostatic line" that is a graph of pore pressure variation based on a constant piezometric surface at a depth of 7.5 ft. (2.3 m), which was the average free water surface depth in the soil borings as well as in the anchor casings. Some trend toward slightly lower pressures with each succeeding test can be observed, and the small pressure changes developed during loading, described previously, are evident. The low pore pressure value at the third level is believed to be unrepresentative.

The average vertical pore water pressure variation with depth for the four instrumented group piles is shown in Figs. 2.36 and 2.37. These figures represent the 9-pile and subgroup compression tests, respectively. On the latter figure, the pore pressure variation for the third 9-pile test is shown for purposes of comparison. Average results for the three tests reported in Fig. 2.37 consider only the piles actually being loaded. Hence, different numbers of piezometers are included in each average, so that conclusions concerning apparent profile changes between the 9-pile group and subgroup tests should not

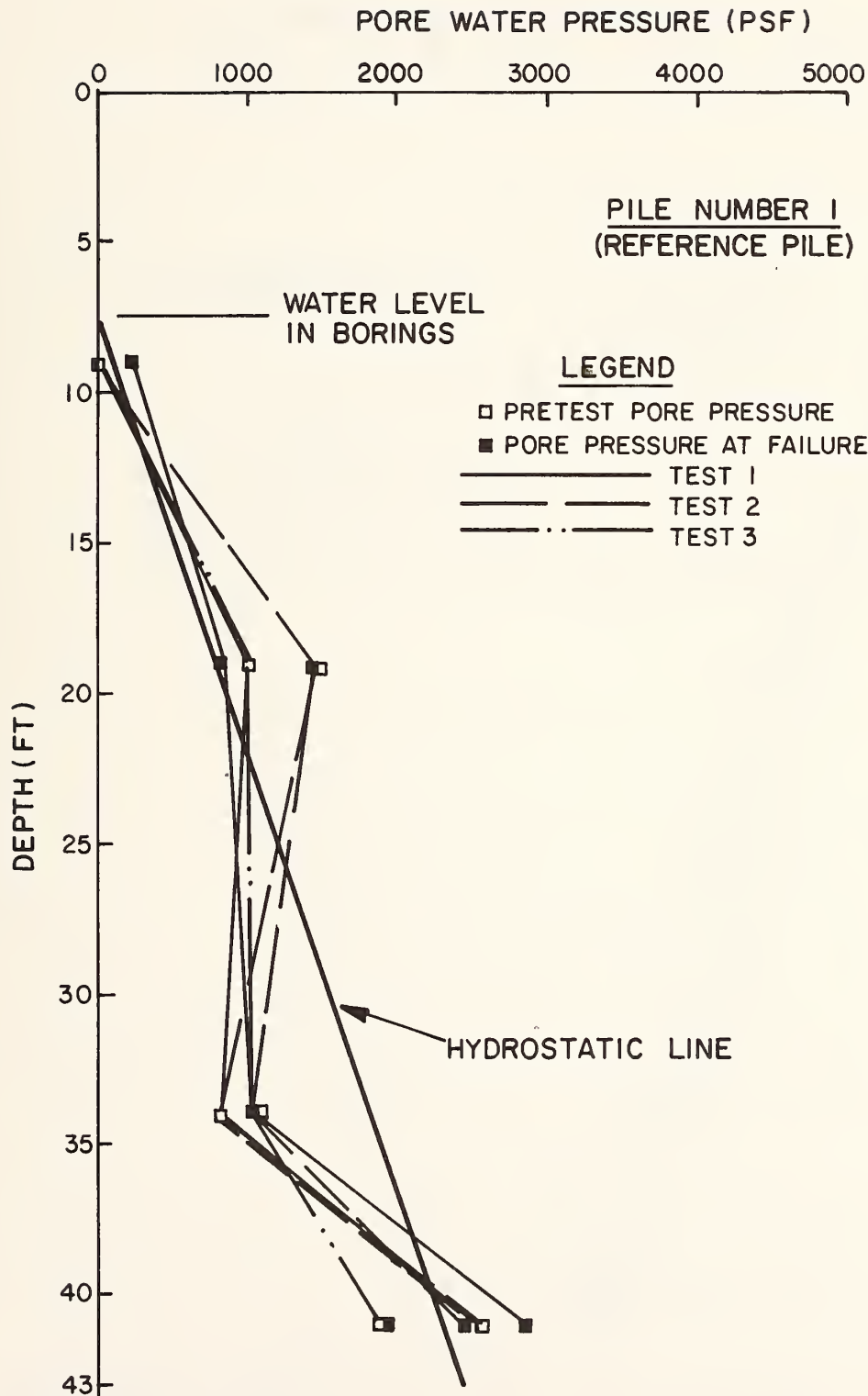


FIGURE 2.35. VERTICAL VARIATION IN PORE PRESSURE ON REFERENCE PILE 1
(1 ft = 0.305 m; 1 psf = 47.9 N/m²)

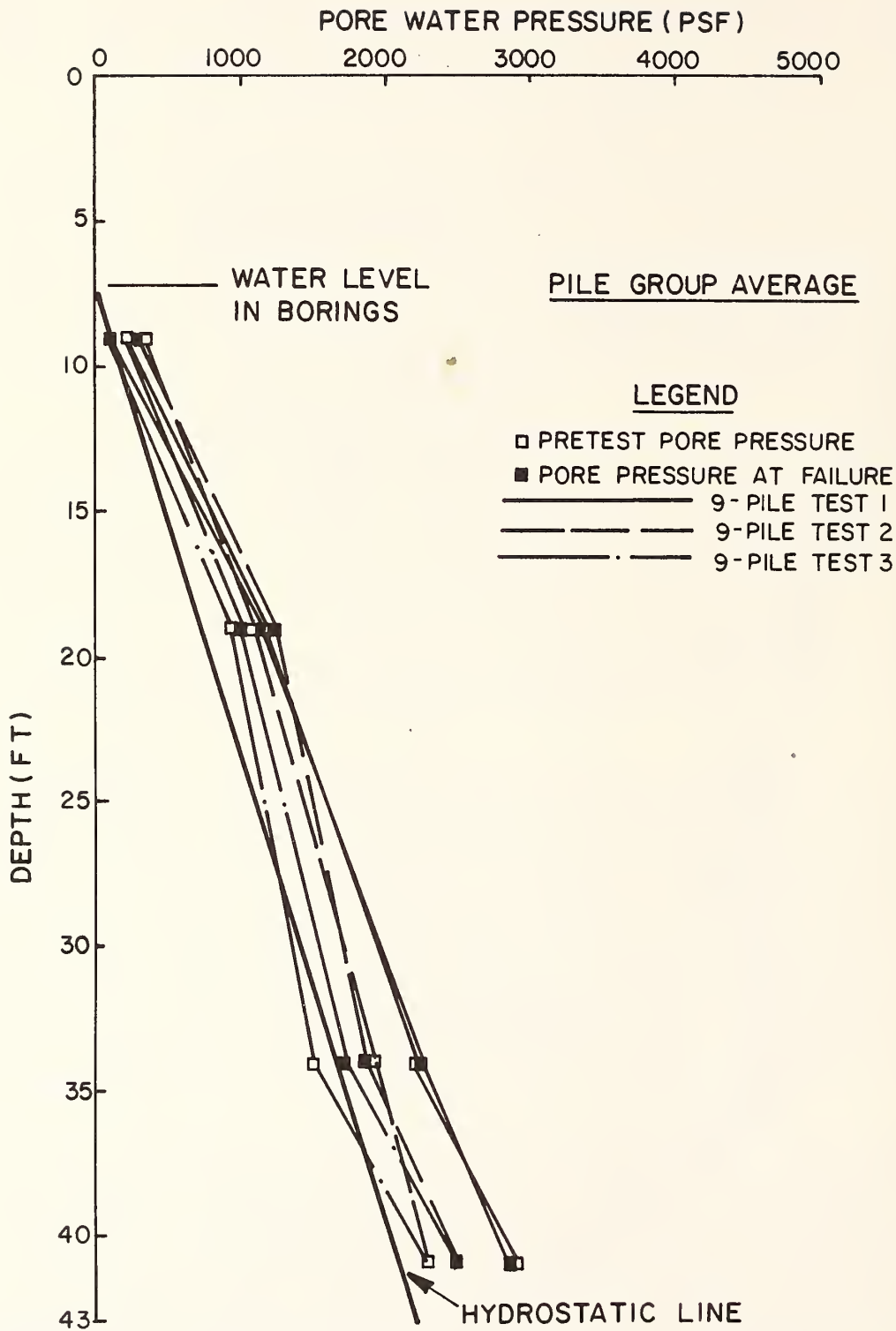


FIGURE 2.36. VERTICAL VARIATION IN AVERAGE PORE PRESSURE ON GROUP PILES;
9-PILE TESTS (1 ft = 0.305 m; 1 psf = 47.9 N/m²)

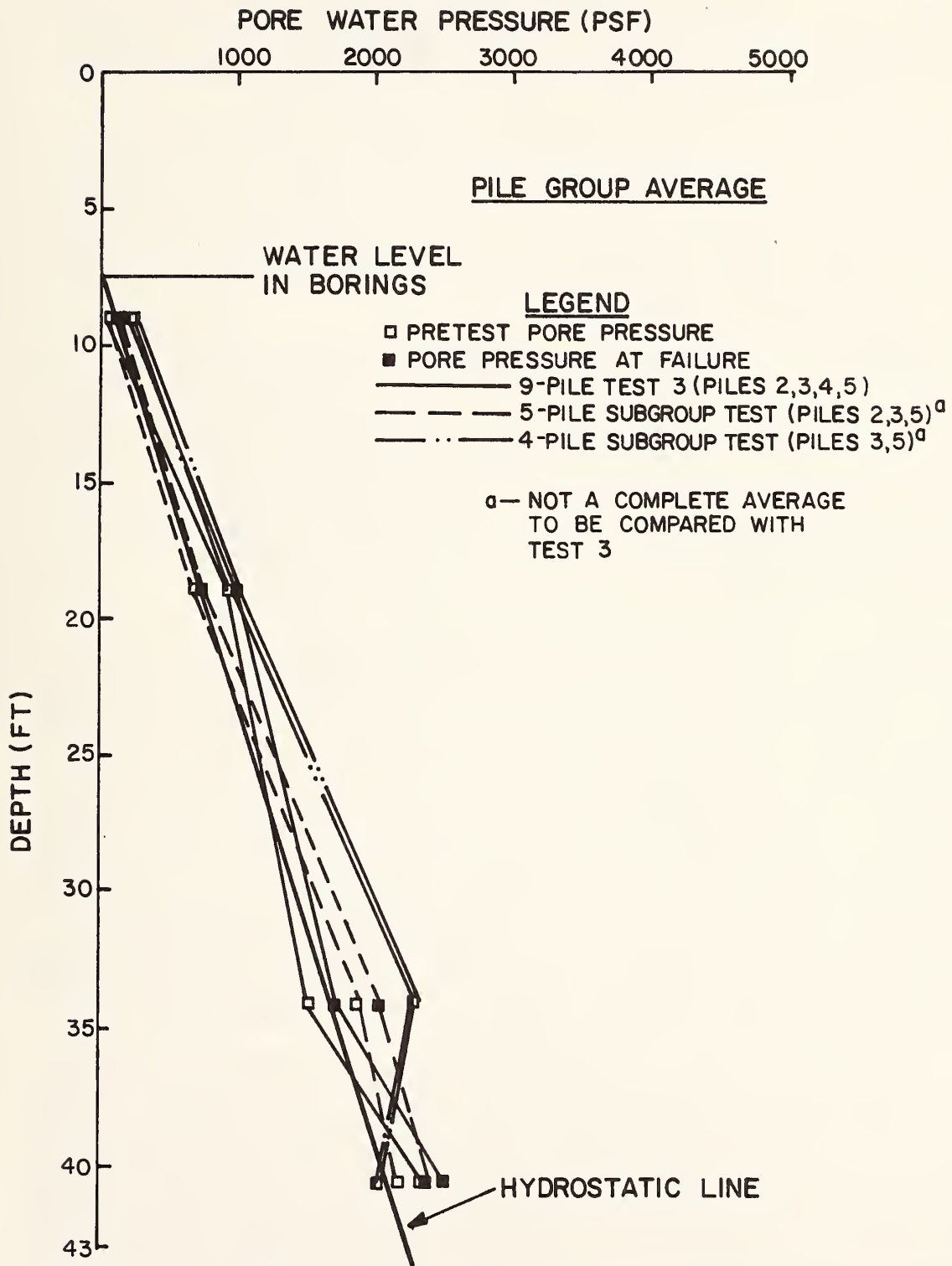


FIGURE 2.37. VERTICAL VARIATION IN AVERAGE PORE PRESSURE ON GROUP PILES; SUBGROUP TESTS (1 ft = 0.305 m; 1 psf = 47.9 N/m²)

be drawn. It is evident, however, that the vertical variation of pore pressure against the group piles was essentially hydrostatic, both prior to each group test and at failure. Some slight trend toward reduction in pore pressure between 9-pile tests can be observed in Fig. 2.36.

Figure 2.38 shows the vertical pore pressure variation on the four piles subjected to individual uplift tests that were instrumented for lateral pressure measurement. Again, for the uplift tests, pressure variation was essentially hydrostatic, with only small changes developing during loading. On all piles pore pressure changes were slightly positive at the upper two levels and essentially zero at the lower two levels during uplift loading.

Graphs of total pressure variation with depth, corresponding to the graphs of pore water pressure variation with depth that were shown in Figs. 2.35-2.38, are presented in Figs. 2.39-2.42. The observed patterns in the reference pile (Fig. 2.39) and for the average of the group piles (Fig. 2.40) are discernably different, with the total stresses at the first three levels being much higher in the group piles than in the reference pile. This difference is attributed to the effects of data scatter, discussed elsewhere. Pressures on the group piles are probably more reliable than those shown for the reference pile because each point is the average of readings on several piles.

Indicated total pressures decreased slightly, but relatively uniformly, at all depths on the group piles between Nov. 5, four days after completion of driving, and Nov. 16, the date of the first load test. No such behavior was observed for Pile 1. This effect could not be attributed to any operational problem but may be related to temperature correction methods. After Test No. 1, there was a general increase in indicated total stress in the upper level in the reference pile and in the upper three levels in the group piles. The evidence compiled through analysis of maximum side load transfer in the various tests (Appendix D) does not support an increase in total (and consequently effective) lateral normal stresses of the magnitude indicated in Figs. 2.39 and 2.40. Therefore, the total stress values in Figs. 2.39 and 2.40 should be considered as general trends and not precise representations of the states of total stress. This statement also applies to the calculated effective stress variations shown later.

Total lateral pressure variation on the group piles in the subgroup tests approximated those in the third 9-pile test, as shown in Fig. 2.41. Total pressure profiles for the uplift tests are shown in Fig. 2.42. Note that the total stress variation in uplift for the piles that were in the group does not include data from Pile 3, which was not subjected to an uplift test. The absence of data for that pile caused the average indicated total pressures for the uplift tests to differ significantly from those for the earlier compression tests on the group at the upper two levels.

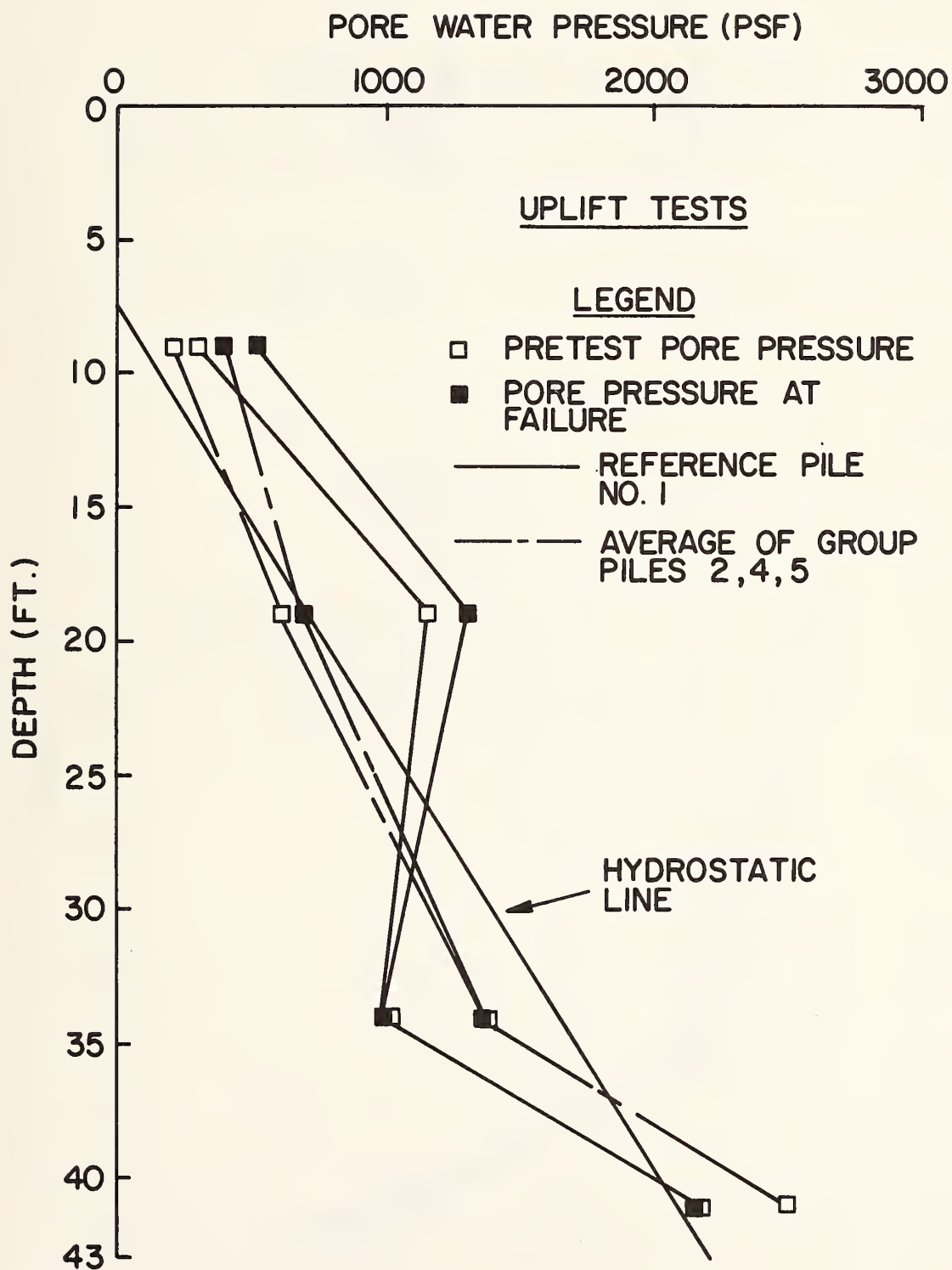


FIGURE 2.38. VERTICAL VARIATION IN PORE PRESSURE ON PILES DURING UPLIFT TESTS (1 ft = 0.305 m; 1 psf = 47.9 N/m²)

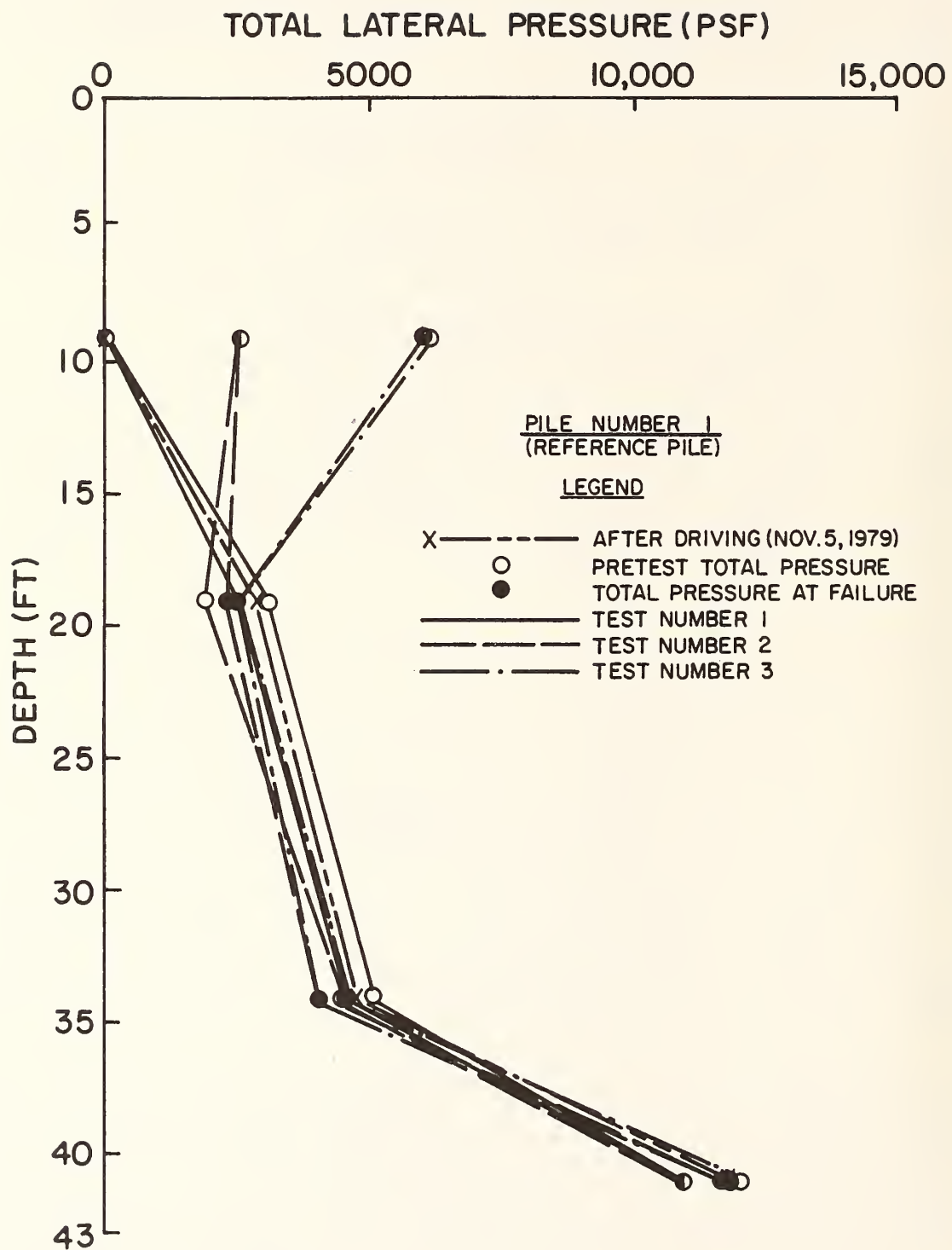


FIGURE 2.39. VERTICAL VARIATION IN TOTAL LATERAL PRESSURE ON REFERENCE PILE 1 (1 ft = 0.305 m; 1 psf = 47.9 N/m²)

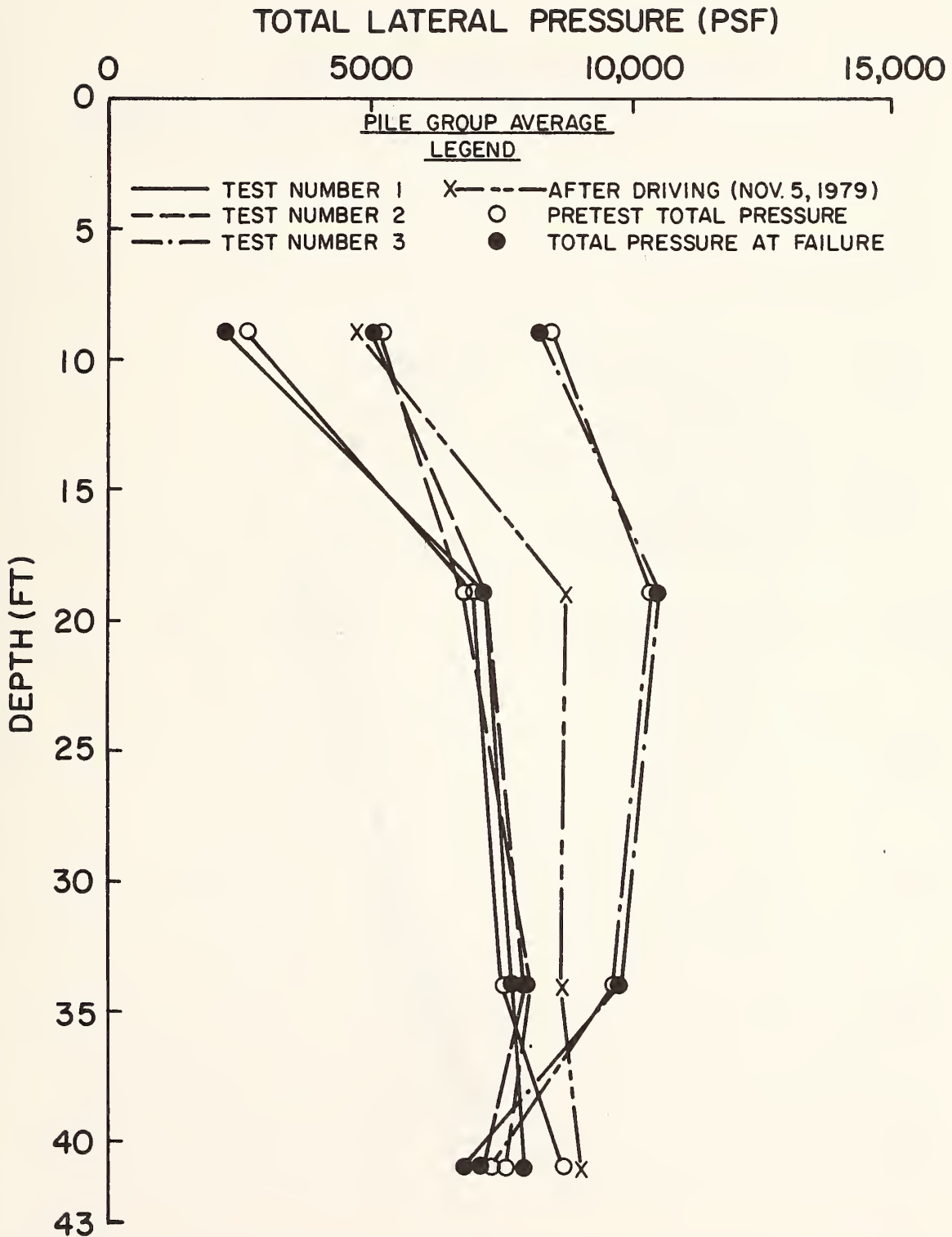


FIGURE 2.40. VERTICAL VARIATION IN AVERAGE TOTAL LATERAL PRESSURE ON GROUP PILES (2, 3, 4, 5) (1 ft = 0.305 m; 1 psf = 47.9 N/m²)

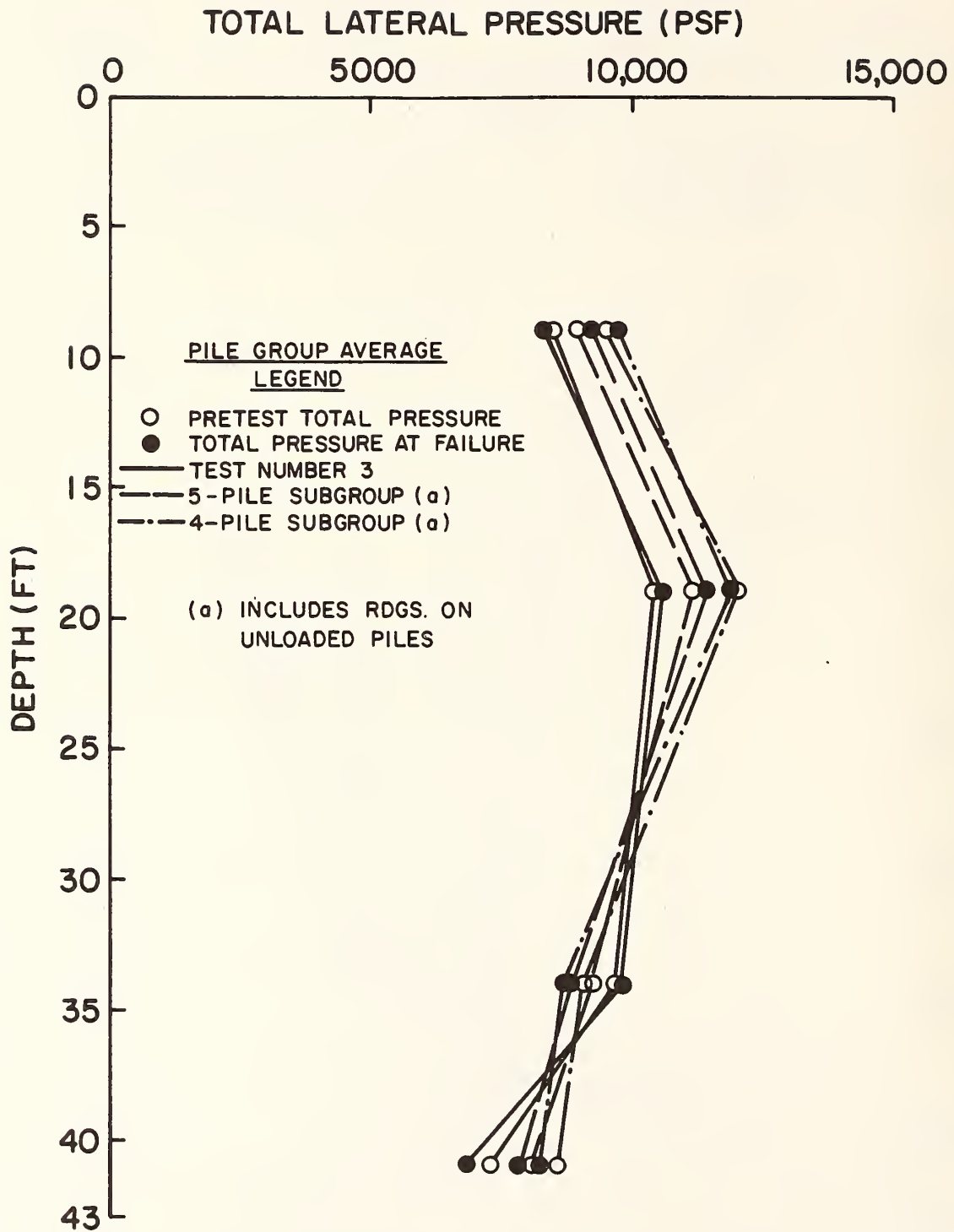


FIGURE 2.41. VERTICAL VARIATION IN AVERAGE TOTAL PRESSURE ON PILES IN SUBGROUP TESTS (2, 3, 5) (1 ft = 0.305 m; 1 psf = 47.9 N/m²)

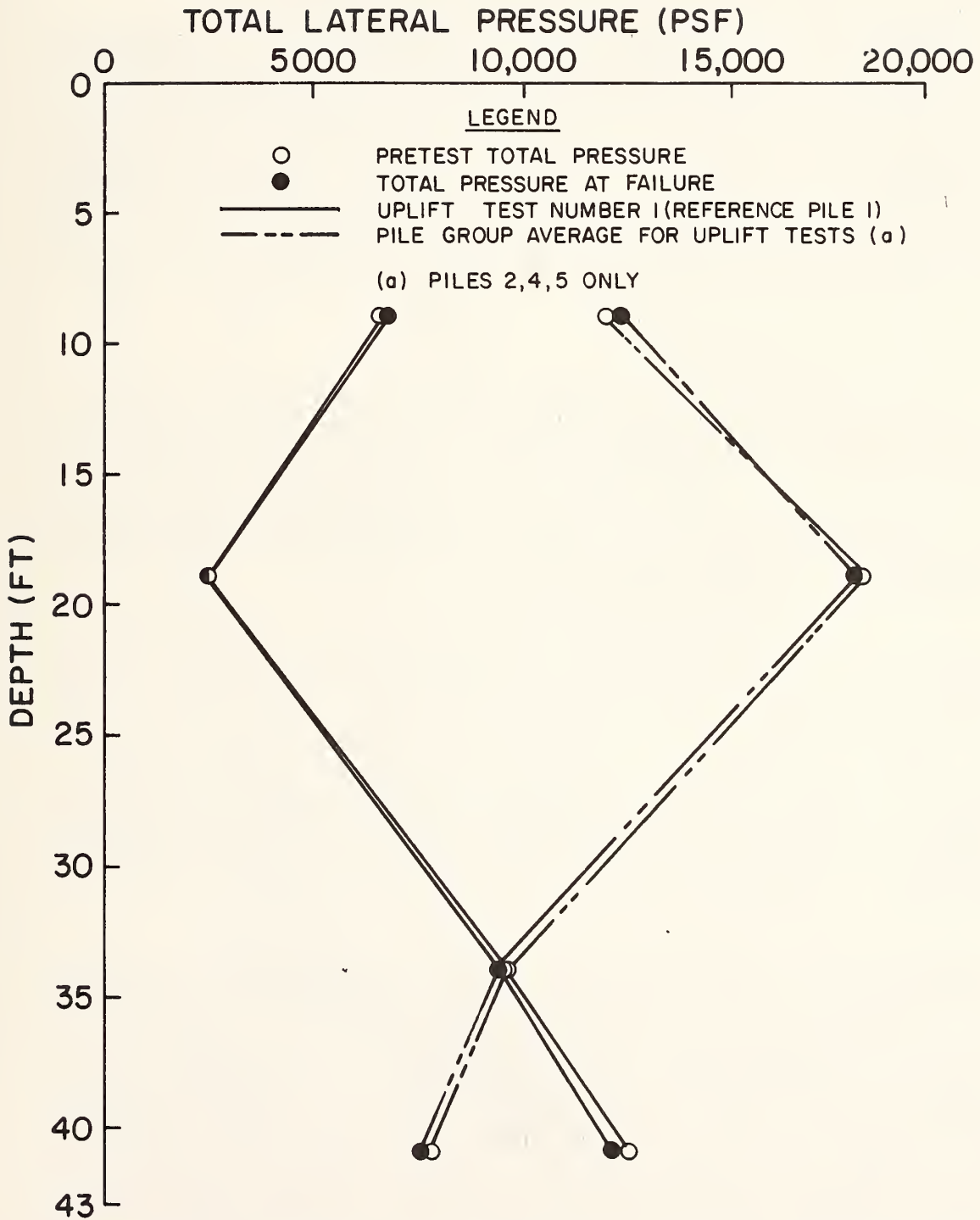


FIGURE 2.42. VERTICAL VARIATION IN TOTAL PRESSURE FOR UPLIFT TESTS
 (1 ft = 0.305 m; 1 psf = 47.9 N/m²)

Figures 2.39-2.42 clearly demonstrate, in profile form, that total pressure changes generated on the pile surfaces due to loading were uniformly small.

Finally, normal effective stresses against the faces of the piles were calculated by subtracting the pore water pressure readings detailed in Figs. 2.35-2.38 from the total pressure values given in Figs. 2.39-2.42. The resulting effective stress variations, for pretest and failure conditions for all tests, are given in Figs. 2.43-2.46 in a format corresponding to the pore and total stress variations described previously. The patterns of effective stress are dominated by the observed total stress patterns, and the combination of the small measured pore and total pressure changes during loading result in small normal effective pressure changes.

Ground Movements During Tests

Vertical soil movements at several points on the surface of the soil and at several depths were monitored during the load tests to provide a means of verifying the mode of failure (punching of individual piles versus failure of the group as a block), to obtain information on the lateral extent of the zone of surface soil deformations produced by loading the pile groups, and to obtain deformation data that could be used by others to calibrate mathematical models which calculate soil deformations (e.g., the finite element model).

Some irregularities due to ambient temperature changes, "bumping" of gages, and similar effects, were observed when the raw ground settlement readings were plotted as functions of time. Plots of raw ground movement data versus applied load for the 5-minute reading set are contained in Appendix F. The raw data plots for each settlement point were first smoothed by a procedure outlined in Appendix F to correct for false readings produced by rapid ambient temperature changes. A separate study, documented in Appendix E, was conducted to evaluate the expected range of false readings to be expected from temperature fluctuations, and this information was used in correcting the data.

Several other considerations in interpreting the ground movement data included (1) discarding the data for the first reference pile test due to inadequate shading of the dial gages stands; (2) discarding the data for the subgroup tests for the 600 inch (15.2 m) depth due to unexplained inconsistencies; and (3) combining and averaging the data for each settlement point in groupings according to reference tests, 9-pile group tests, and subgroup tests without considering individual tests. Analysis of the raw data revealed that very minor differences existed between the soil deformations in the first and third test sets for both the reference and group piles and between the two subgroup tests and that measured settlements were essentially recoverable.

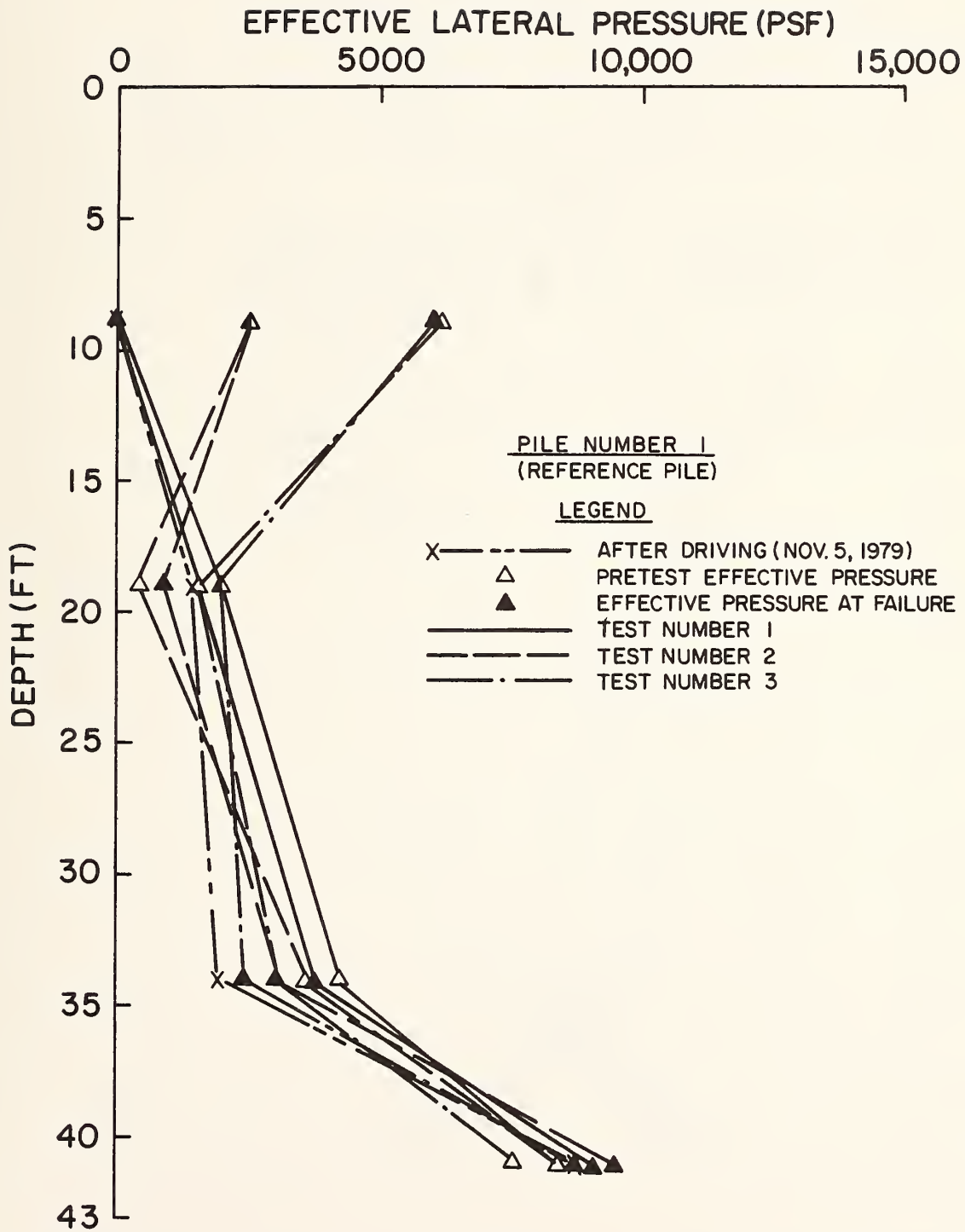


FIGURE 2.43. VERTICAL VARIATION IN LATERAL EFFECTIVE STRESS ON REFERENCE PILE 1 (1 ft = 0.305 m; 1 psf = 47.9 N/m²)

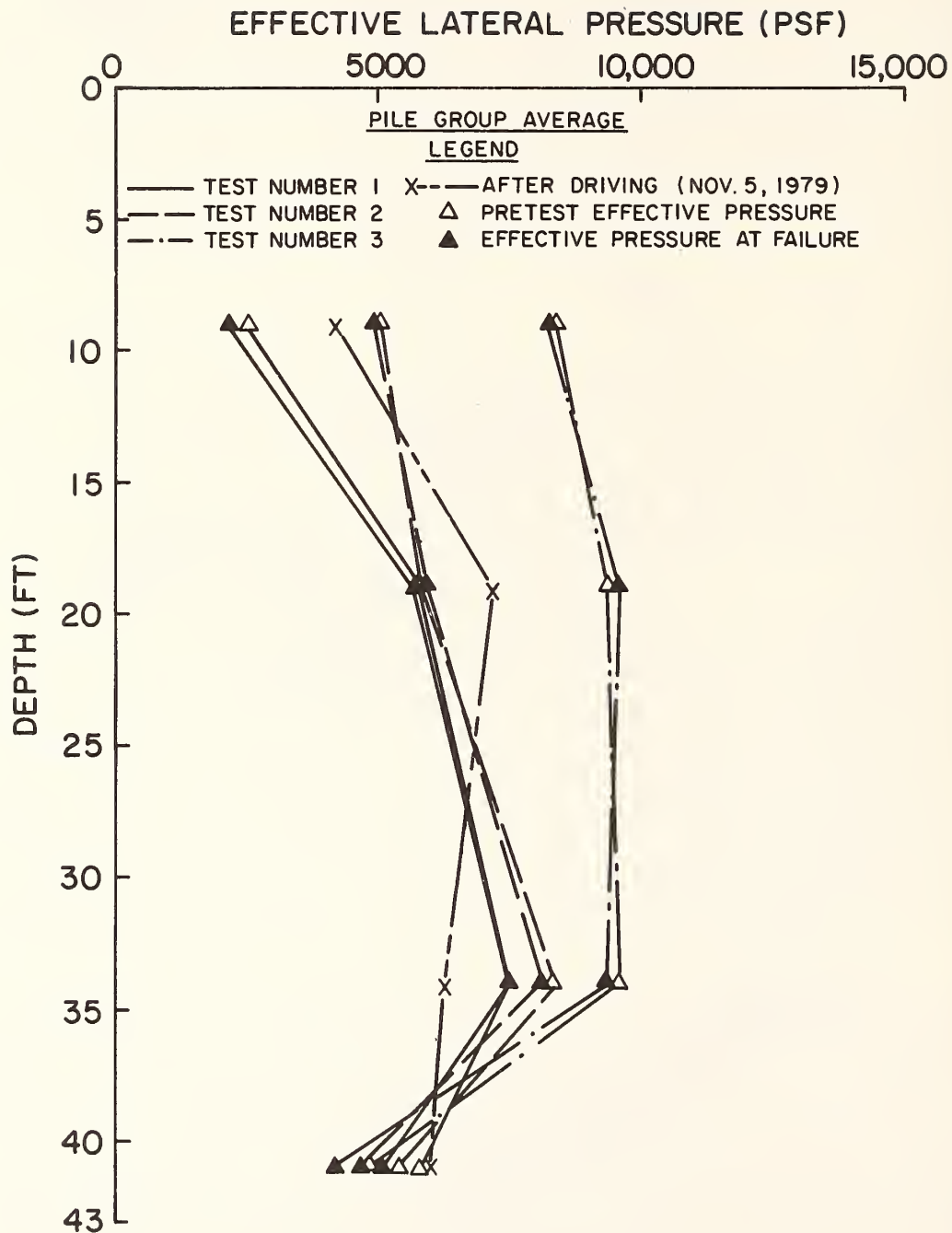


FIGURE 2.44. VERTICAL VARIATION IN AVERAGE LATERAL EFFECTIVE STRESS ON GROUP PILES (2, 3, 4, 5) (1 ft = 0.305 m; 1 psf = 47.9 N/m²)

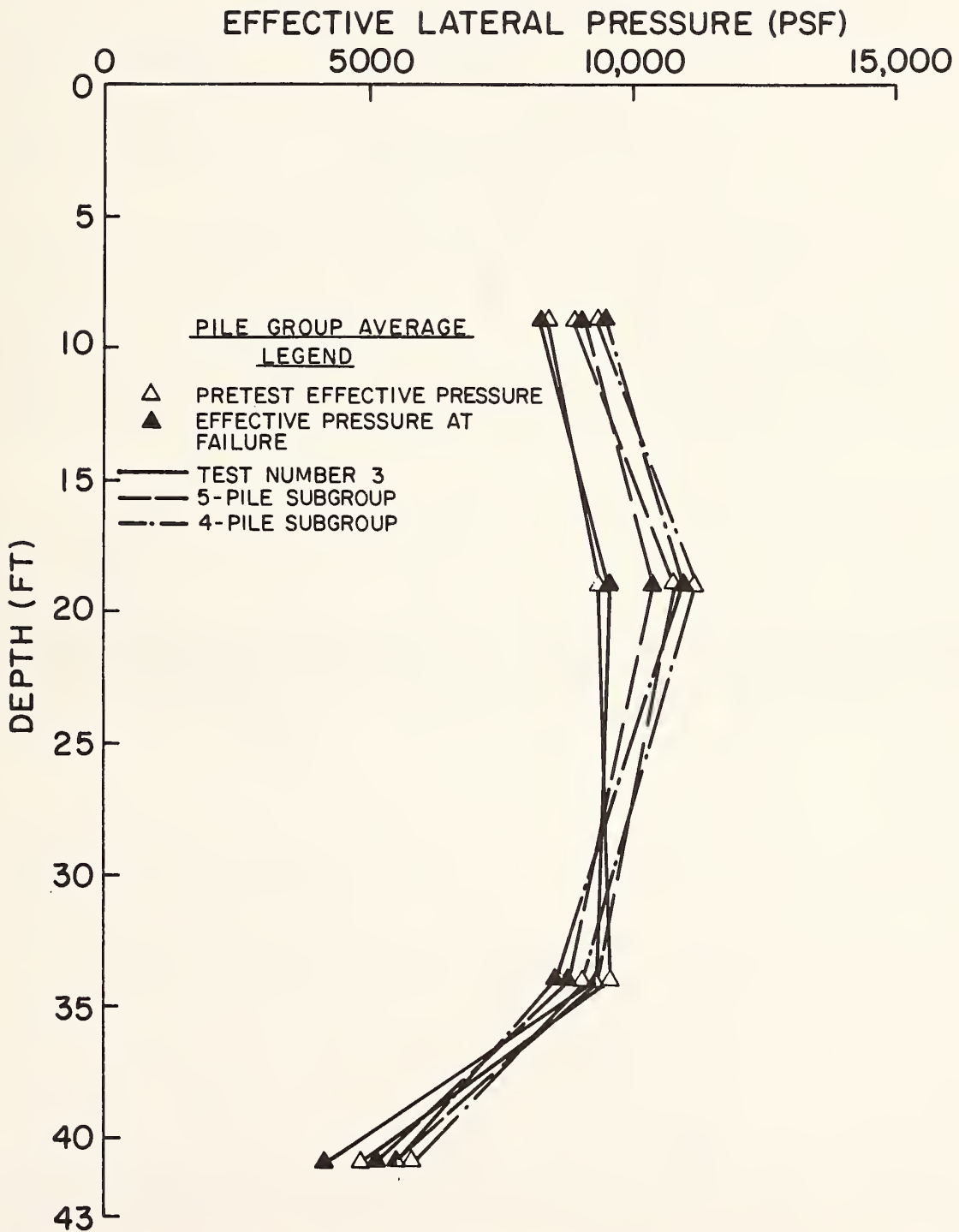


FIGURE 2.45. VERTICAL VARIATION IN AVERAGE LATERAL EFFECTIVE STRESS IN SUBGROUP TESTS (PILES 2, 3, 5) (1 ft = 0.305 m; 1 psf = 47.9 N/m²)

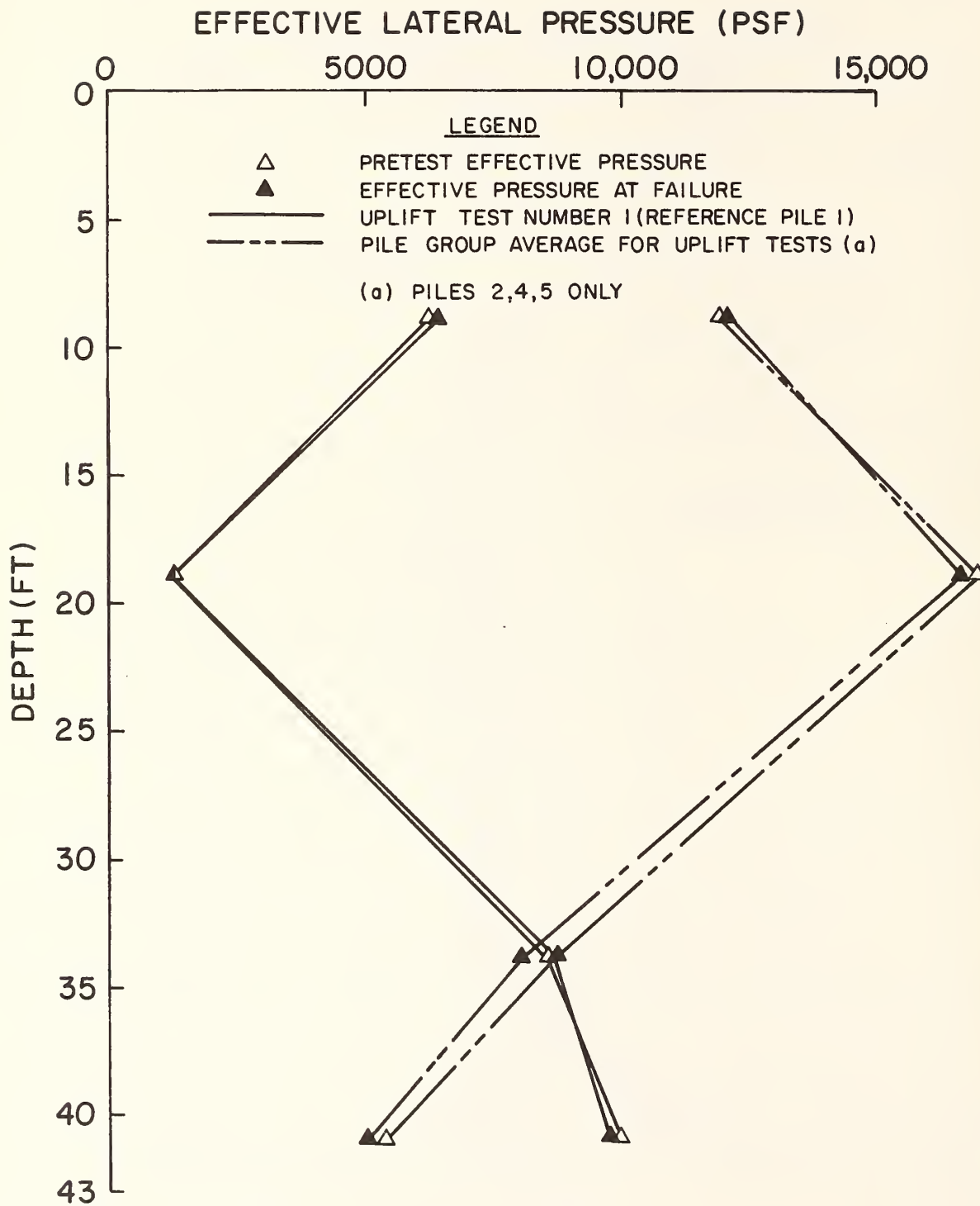


FIGURE 2.46. VERTICAL VARIATION IN LATERAL EFFECTIVE STRESS FOR UPLIFT TESTS (1 ft = 0.305 m; 1 psf = 47.9 N/m²)

The corrected and averaged readings are presented in graphical form in Figs. 2.47-2.54. In these figures the settlement points are arranged in order according to their distance from either the reference pile (Pile 1) or the center of the pile group, which are assumed to be points of symmetry. This arrangement, considered without regard to direction of the settlement point from the assumed point of symmetry, may be the cause of the reading variations that are seen in these figures. Assessment of errors by the authors indicate a reliability of about ± 0.005 in. (0.13 mm) in the plotted results.

Figure 2.47 shows soil surface displacements for the last two reference pile tests at a distance interval of about 40 to 80 in. (1.0 to 2.0 m) from the center of the pile, which had a radius of 5.375 in. (137 mm), and pile displacements. The distance from the center to the edge of the pile is represented by the shaded zone on the figure. The displacements measured in the reference tests (Fig. 2.47) indicate (1) that virtually all of the surface soil deformation occurred within less than one meter (about 4 diameters) of the face of the pile, and (2) that no heave or otherwise unusual soil movements occurred at failure.

Figure 2.48 depicts the surface soil movements in the soil mass in and around the 9-pile group. Several facts are evident in this figure: (1) failure was of the punching type, i.e., the soil near the piles, both inside and outside the group, did not move down with the piles as the piles failed; (2) soil-pile deformations were essentially horizontally continuous up to an applied load of about 400 kips (1780 kN); and (3) no surface heave accompanied failure. Soil surface movements at failure did not exceed about 0.02 in. beyond a distance of 170 in. (4.3 m) from the center of Pile 2. The predominant zone of soil straining was observed to be within about 3 in. (75 mm) of the faces of the piles.

Similar soil surface deflections are seen for the average of the two subgroup tests in Fig. 2.49. However, soil settlements in the vicinity of the piles can be seen to be only about one-half of those generated in the 9-pile tests at equivalent loads. Lateral gradients of deflection are also notably lower.

Movements at two locations in the soil at depths of 300 in., 516 in., and 600 in. (25 ft., 43 ft., and 50 ft.) (7.6 m, 13.1 m, and 15.3 m) for the 9-pile group and for the average of the subgroups are shown in Figs. 2.50-2.54. (No graph is shown for the lowest level for the subgroup tests, as no reliable data were acquired.) The trends in subsurface deflections are very similar to the trends in surface deflections. Examination of the data indicates that the average shear strains in the soil between DSP1 and DSP2, situated between about 10 and 60 inches (250 and 1520 mm), respectively, from the face of edge Pile 9, were in the order of 0.04 per cent at and above a depth of 25 ft. (7.6 m) and in the order of 0.01 percent at the 43 and 50 ft. (13.1 and 15.3 m) depths for a nominal load value of 800 kips (3560 kN) in the 9-pile group. This load would probably be somewhat in

SETTLEMENT AT DEPTH OF 24 IN. (IN.)
RELATIVE TO REFERENCE SYSTEM SUPPORTS AVG. OF TESTS 2 AND 3 (REF. PILE NO. 1)

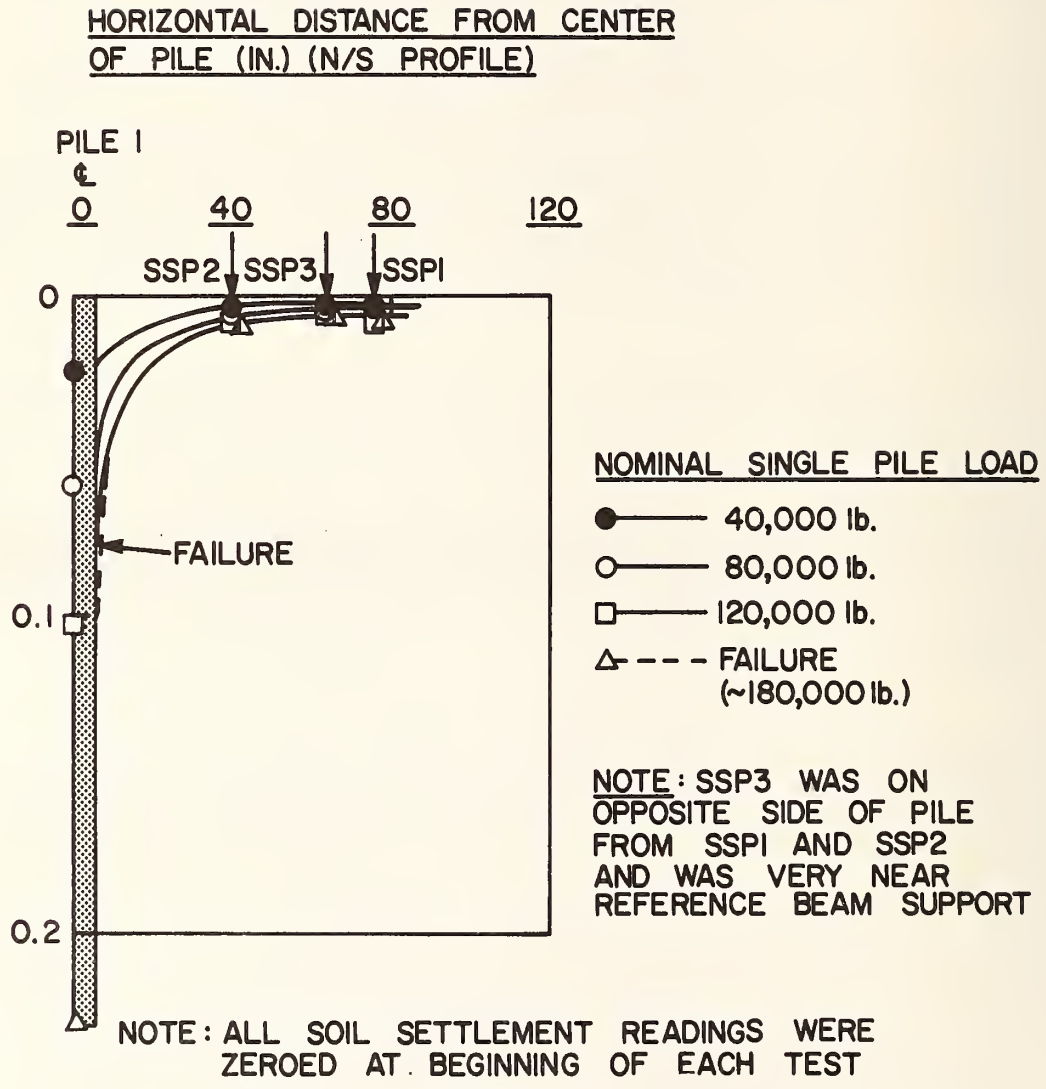


FIGURE 2.47. SURFACE SOIL MOVEMENTS NEAR PILE 1; REFERENCE TESTS
(1 lb = 4.45 N; 1 in = 25.4 mm)

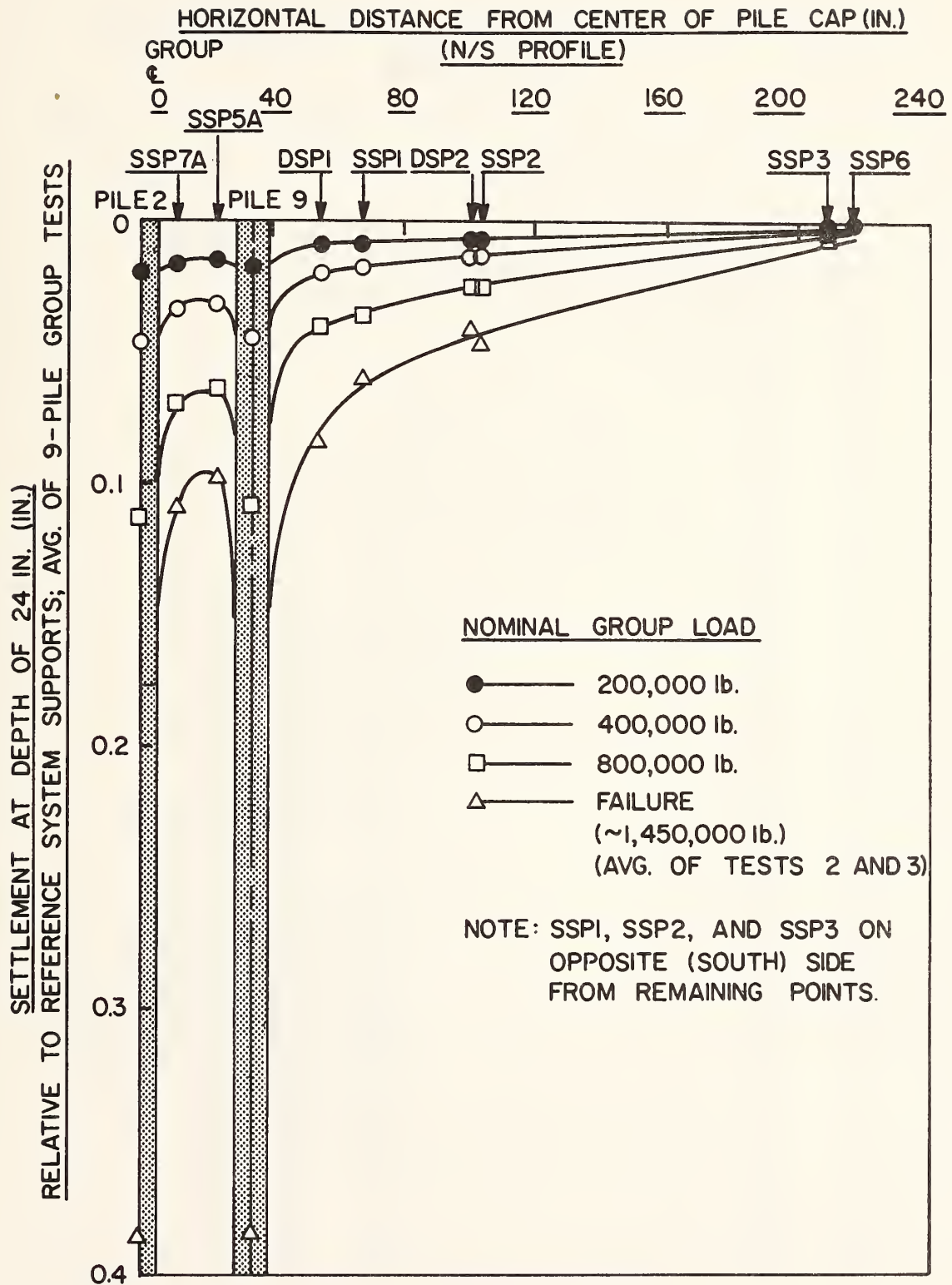


FIGURE 2.48. SURFACE SOIL MOVEMENTS FOR 9-PILE GROUP TESTS
(1 lb = 4.45 N; 1 in = 25.4 mm)

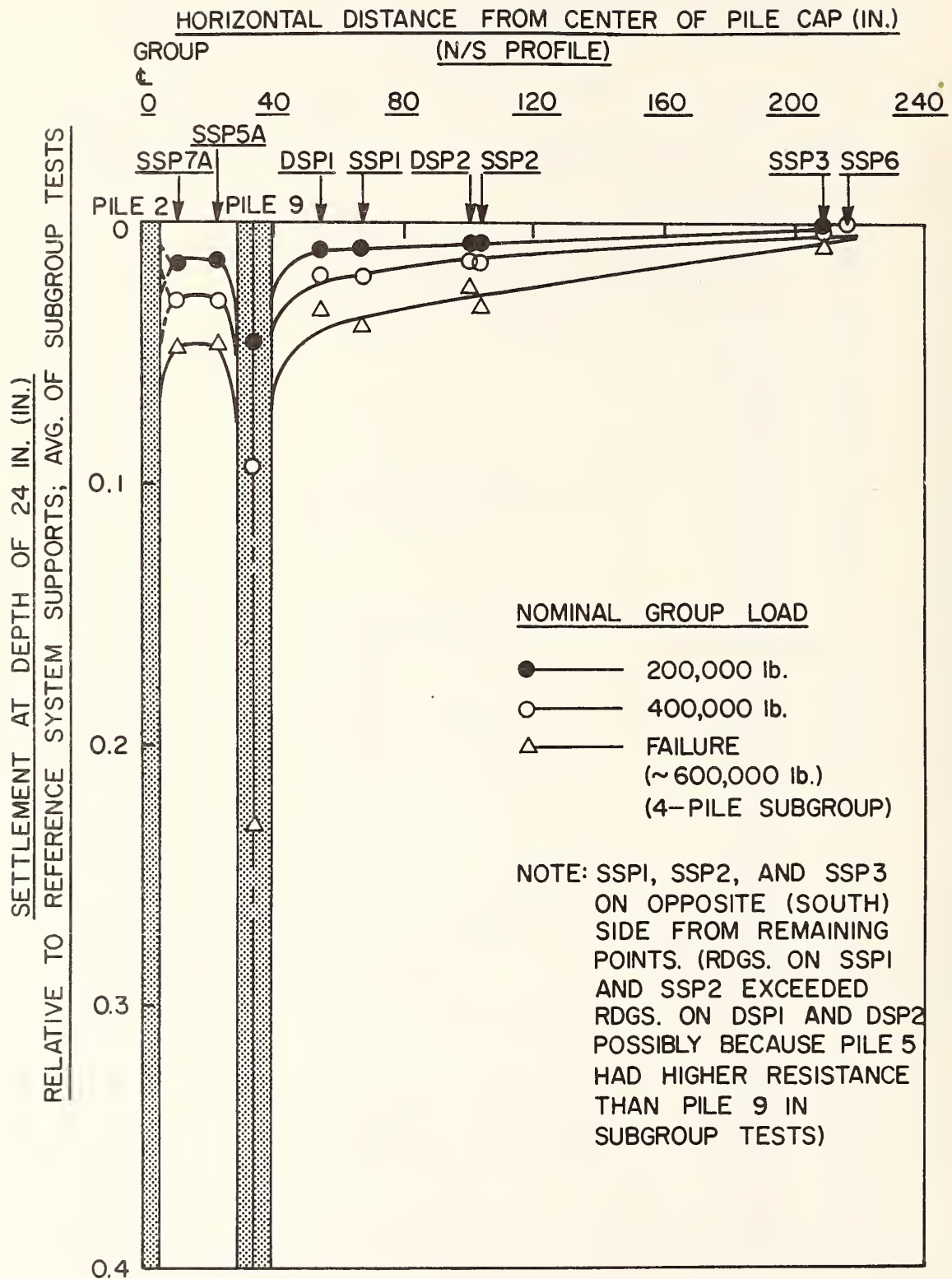


FIGURE 2.49. SURFACE SOIL MOVEMENTS FOR AVERAGE OF SUBGROUP TESTS
(1 lb = 4.45 N; 1 in = 25.4 mm)

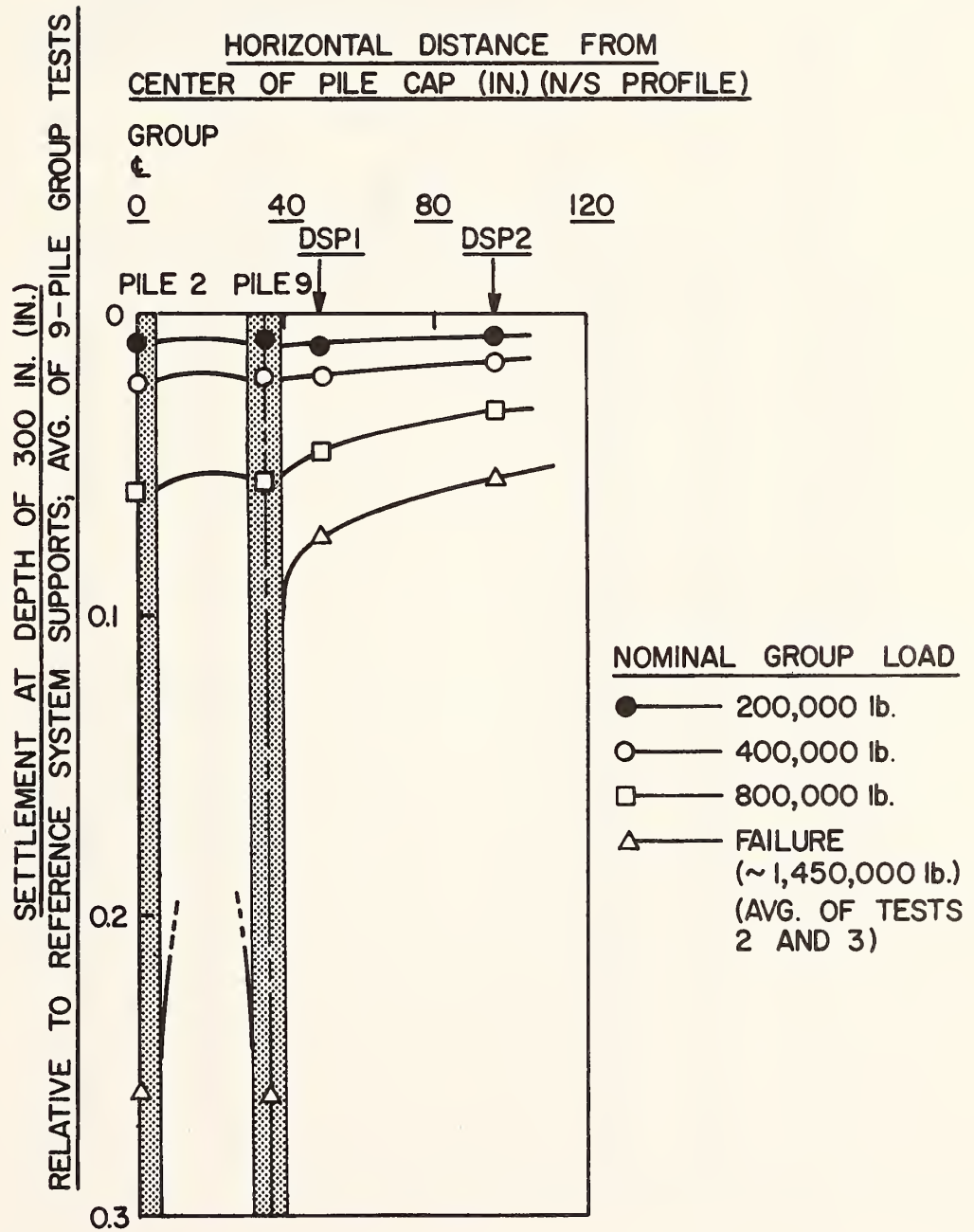


FIGURE 2.50. SOIL MOVEMENTS; 300 INCH (7.6 M) DEPTH: 9-PILE GROUP TESTS (1 lb = 4.45 N, 1 in = 25.4 mm)

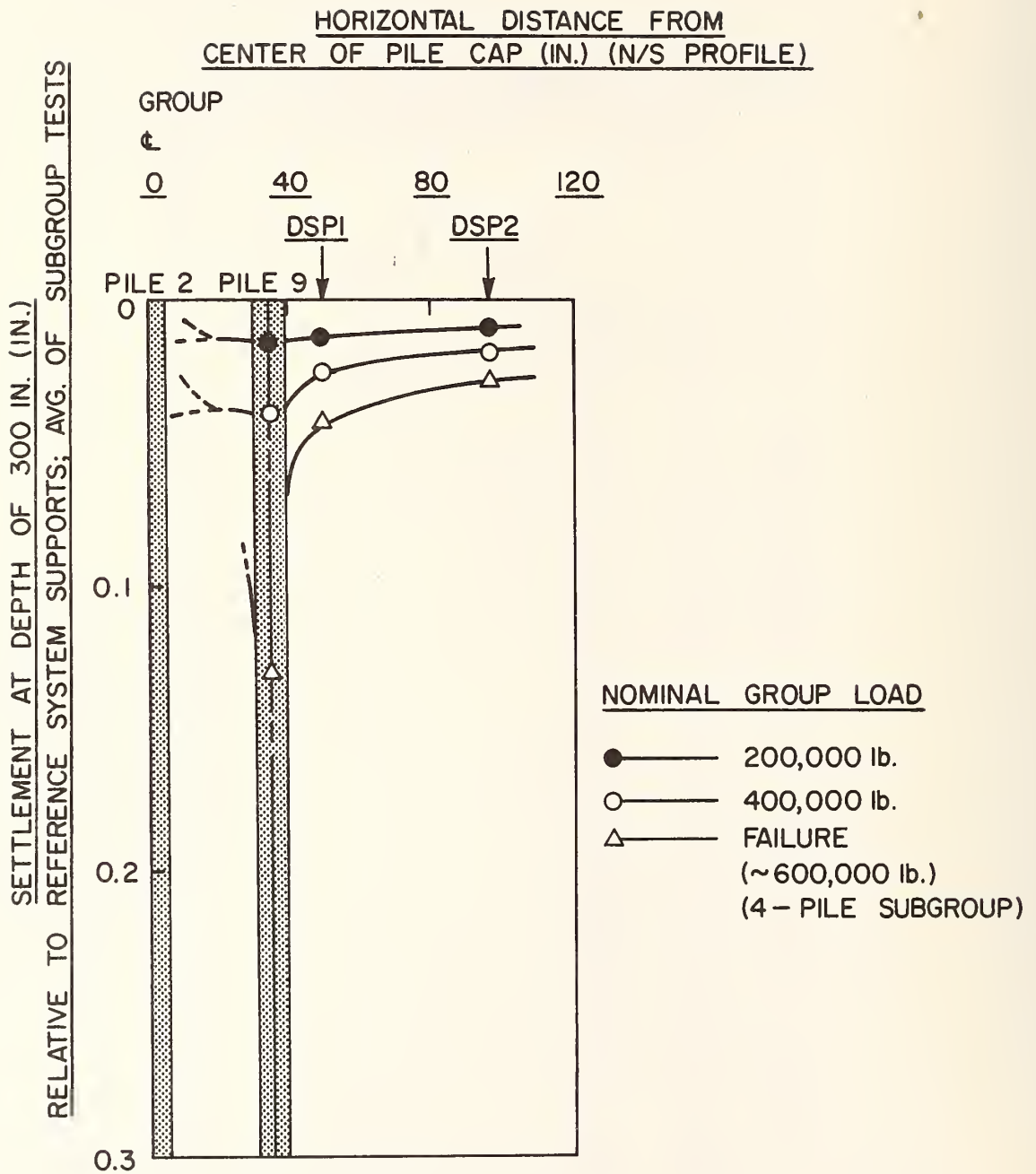


FIGURE 2.51. SOIL MOVEMENTS; 300 INCH (7.6 M) DEPTH; AVERAGE OF SUBGROUP TESTS (1 lb = 4.45 N; 1 in = 25.4 mm)

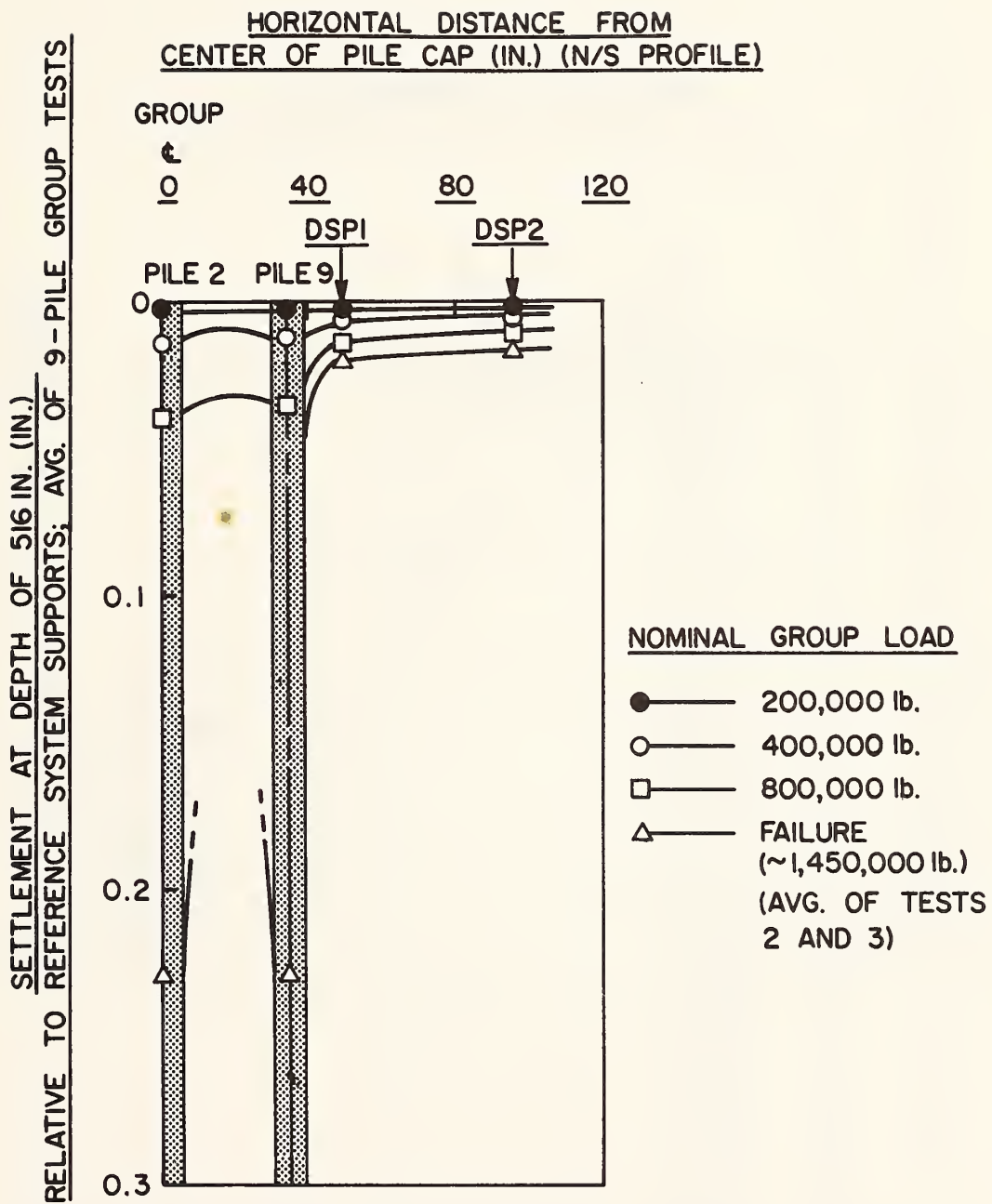


FIGURE 2.52. SOIL MOVEMENTS; 516 INCH (13.1 M) DEPTH; 9-PILE GROUP TESTS (1 lb = 4.45 N; 1 in = 25.4 mm)

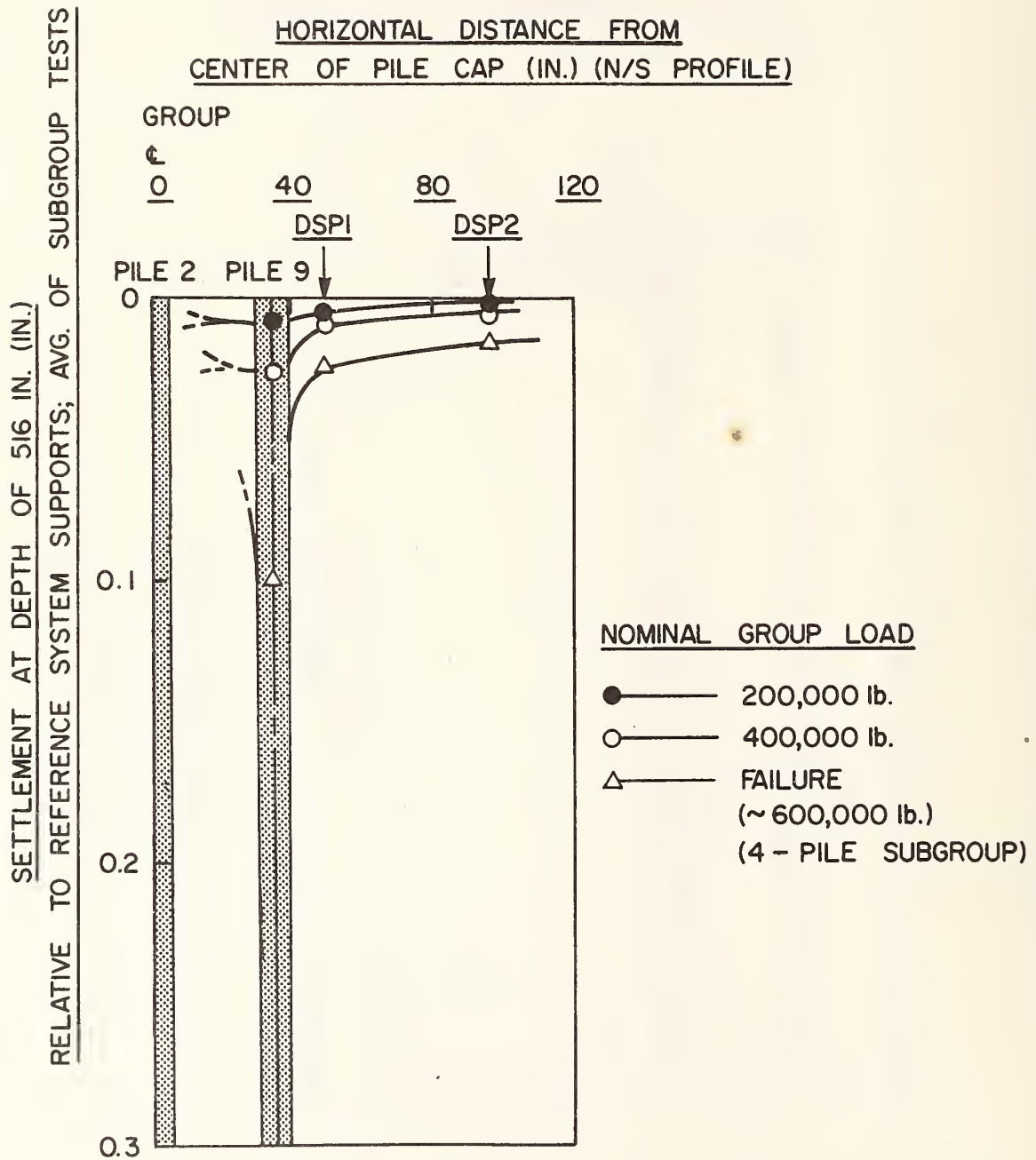


FIGURE 2.53. SOIL MOVEMENTS; 516 INCH (13.1 M) DEPTH; AVERAGE OF SUBGROUP TESTS (1 lb = 4.45 N; 1 in = 25.4 mm)

SETTLEMENT AT DEPTH OF 600 IN. (IN.)
RELATIVE TO REFERENCE SYSTEM SUPPORTS;

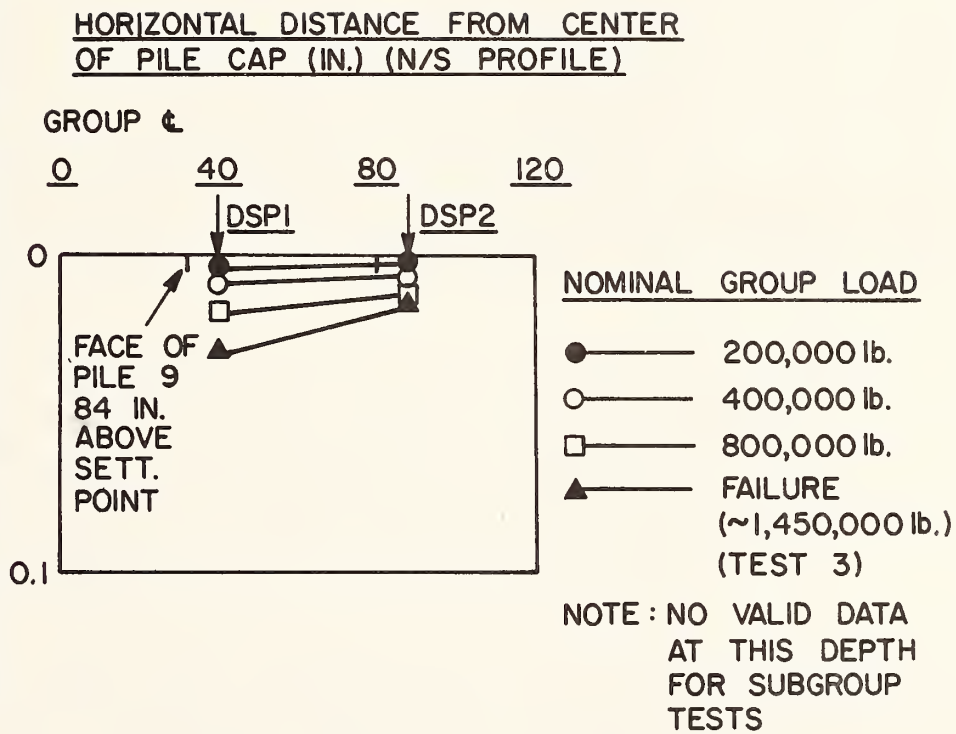


FIGURE 2.54. SOIL MOVEMENTS; 600 INCH (15.3 M) DEPTH; 9-PILE GROUP TESTS (1 lb = 4.45 N; 1 in = 25.4 mm)

excess of a working load for this group. These strain values are based on the assumption that all soil movement is vertical in the vicinities of settlement monuments, and, while such an assumption may not be completely correct, particularly near the pile tips, the quoted shear strain magnitudes suggest that the elastic modulus to be selected for pile-soil-pile interaction calculations in the hybrid model should be taken at very low strain amplitudes, preferably at less than 0.1% principal normal strain in heavily overconsolidated clays of the type encountered at this test site if triaxial or pressuremeter tests are used to evaluate soil deformability.

Chapter 3. Load Transfer

General

The objectives of this chapter are to present detailed information on measured load transfer, to compare load transfer patterns for reference and group piles, to assess the effects of residual stress on load transfer, and to correlate load transfer with measured soil properties. With regard to these objectives, comments are made concerning certain basic phenomena thought by the authors to be involved.

Load Transfer Patterns for Reference Piles and for Group Piles by Position

The average distributions of load along the reference piles, center group pile, edge group piles, and corner group piles are plotted in Figs. 3.1 - 3.10 for the three 9-pile test sets, for the 5-pile subgroup test, and for the 4-pile subgroup test. Comparative graphs are presented for a load value in the working load range and for the average peak failure condition. These figures, which do not include the effects of residual loads (discussed later) or cap weight, also show the corresponding relationships of developed unit side shear (f) to depth (d), which were obtained by differentiation of the load distribution curves assuming that the shearing surface coincided with the pile surface.

The load distribution curves were derived from the raw load data using a piecemeal second degree least-squares fitting procedure, described in Appendix E, which also gives an example of the differences between raw and fitted load distributions. In general these differences were very small except at the points in the f - d curves where the greatest curvature exists, where the fitted f values were somewhat smaller than the raw f values in the 20 ft. (6.1 m) depth range and larger in the 28 ft. (8.5 m) depth range.

While only average values of load and unit side shear have been plotted in Figs. 3.1 - 3.10, a sense of the scatter of the data can be obtained by consulting the load transfer correlation tables given later in this chapter. Appendix D presents an extensive set of load-settlement, load-distribution, f - d , and f - z (unit load transfer vs. relative deformation curves) for all tests beyond 9-pile Set 1, which is covered in this chapter.

Reference to Figs. 3.1, 3.3, and 3.5 reveals that the group piles developed substantially different load transfer patterns than occurred in the reference piles at an average load per pile of about 60 kips (267 kN). The reference piles, at that load, developed considerably higher rates of load transfer in Zones A and B (Fig. 1.1) than did any of the group piles, while greater side load transfer was registered in the group piles in Zone D and in end bearing. Observation of the f - d

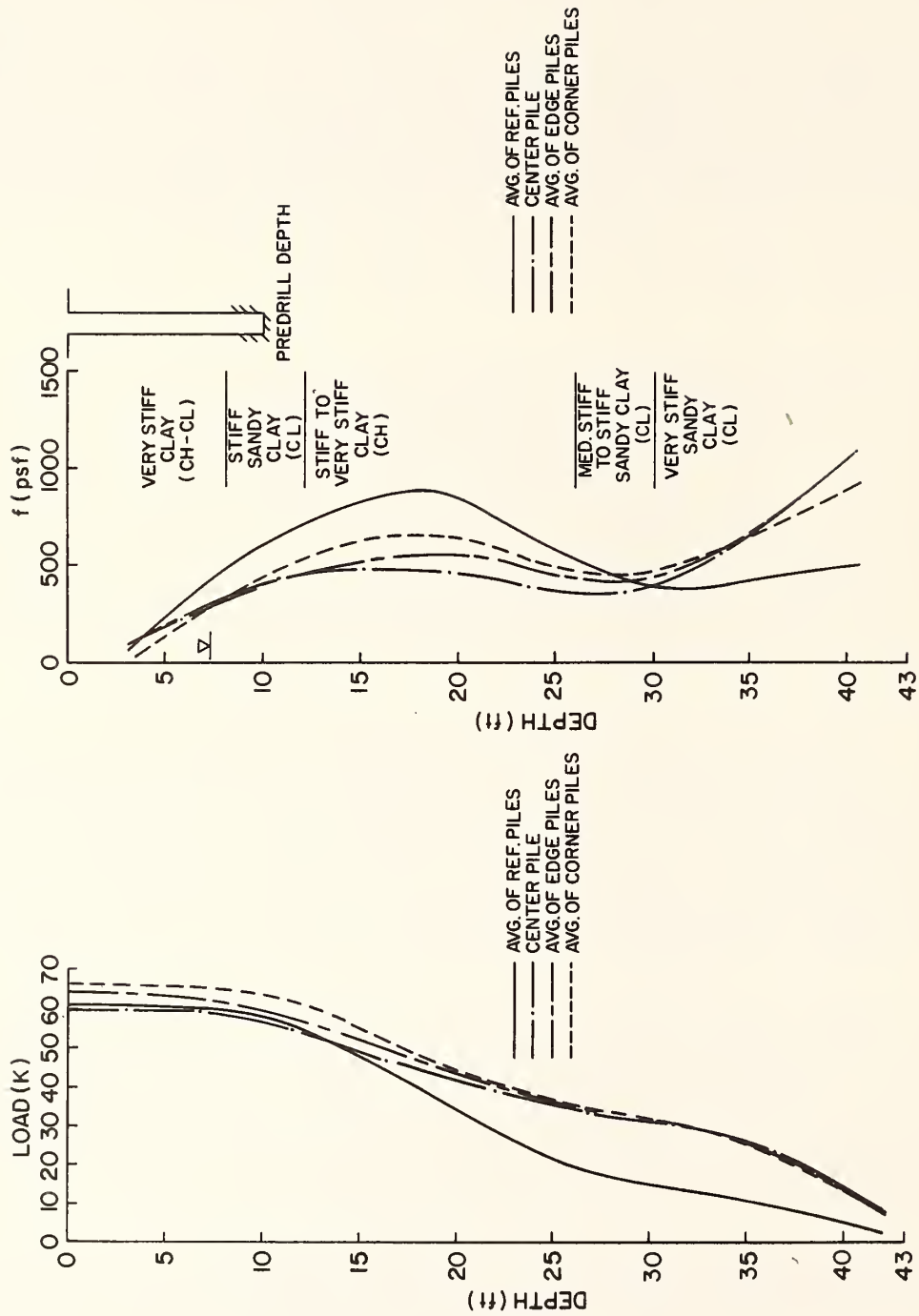


FIGURE 3.1. LOAD DISTRIBUTION AND F-D DIAGRAMS; SUBFAILURE; 9-PILE TEST 1 (1 ft = 0.305 m; 1 k = 4.45 kN; 1 psf = 47.9 N/m²)

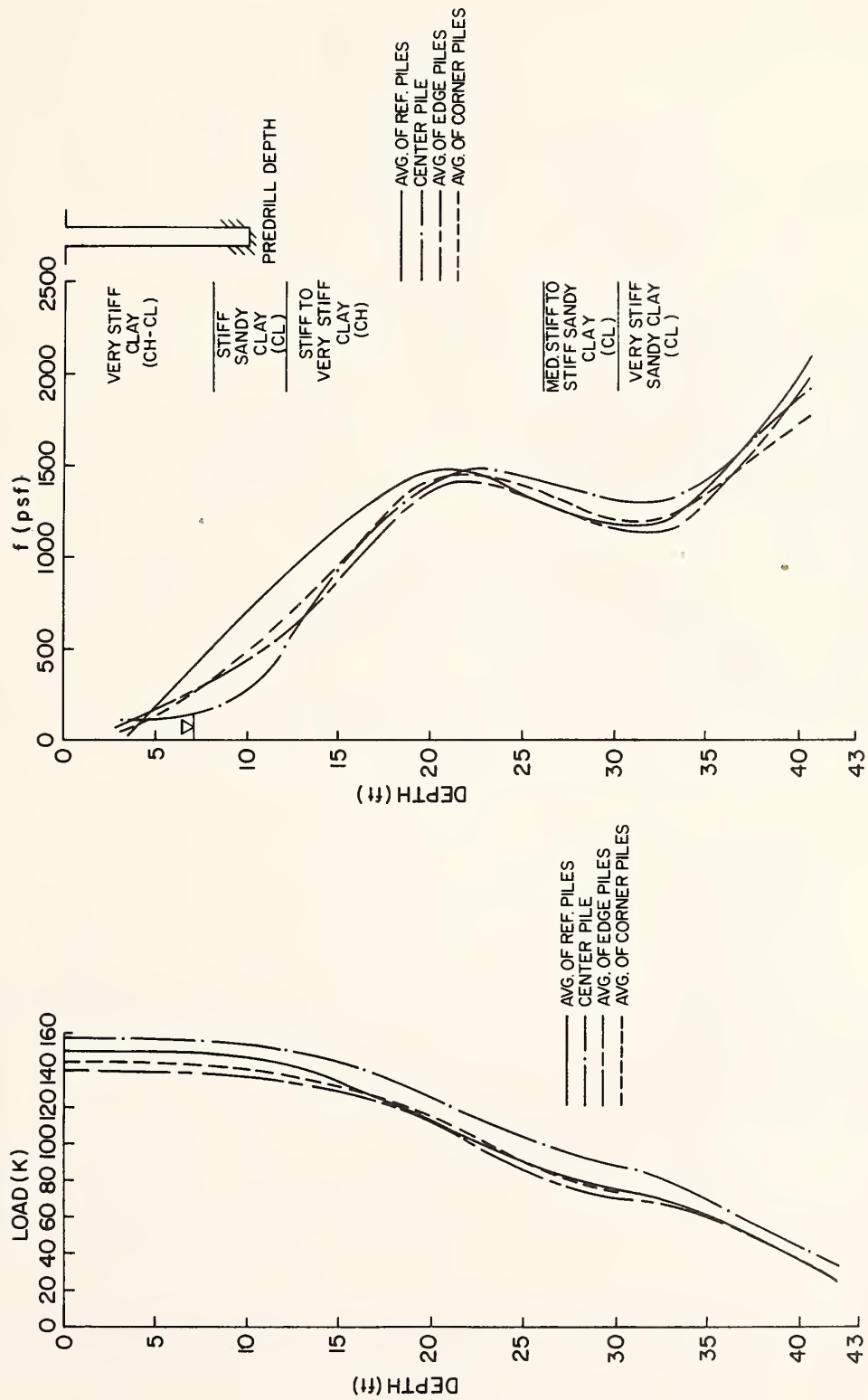


FIGURE 3.2. LOAD DISTRIBUTION AND F-D DIAGRAMS; FAILURE; 9-PILE TEST 1
 (1 ft = 0.305 m; 1 k = 4.45 kN; 1 psf = 47.9 N/m²)

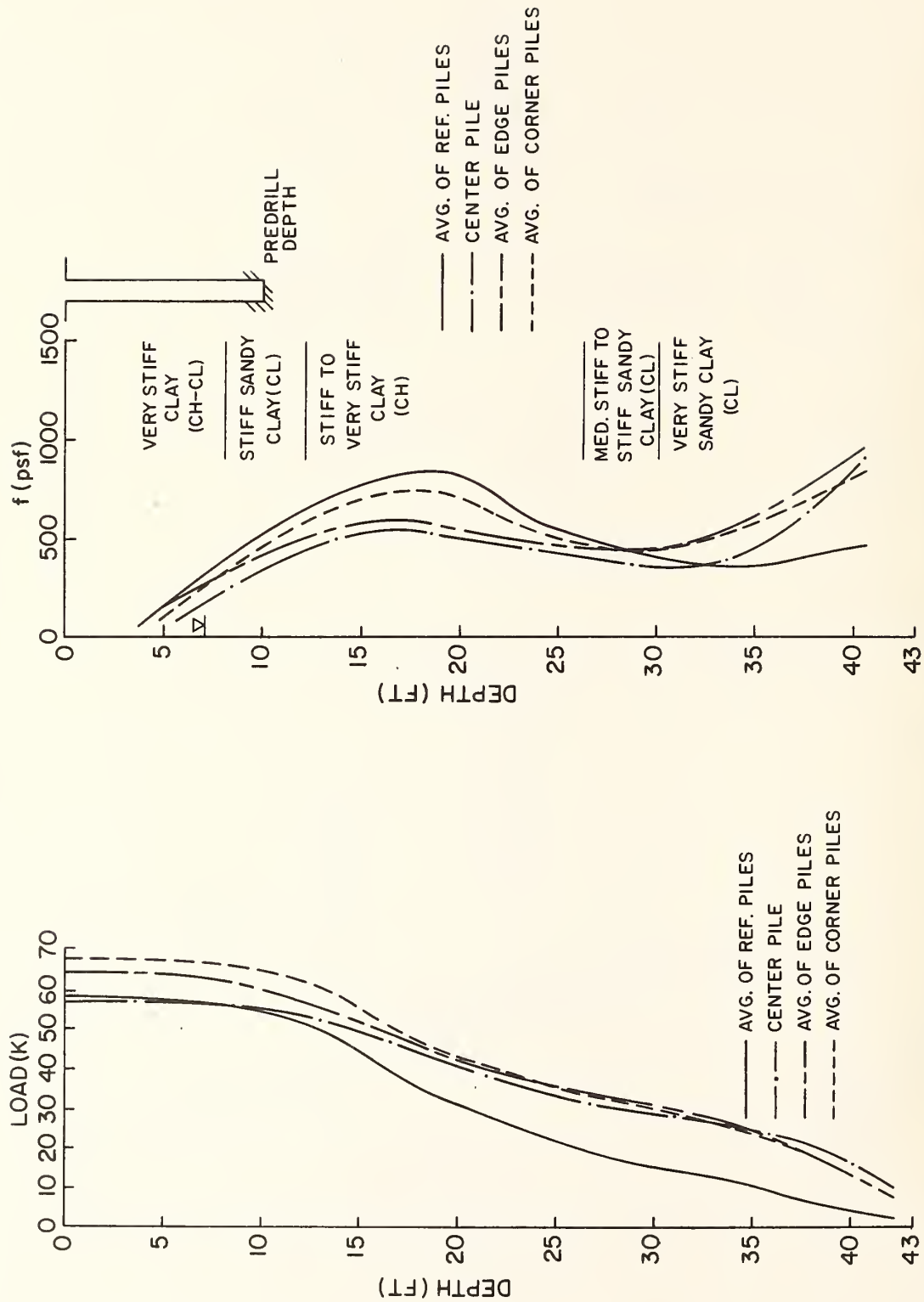


FIGURE 3.3. LOAD DISTRIBUTION AND F-D DIAGRAMS; SUBFAILURE; 9-PILE TEST 2 (1 ft = 0.305 m; 1 k = 4.45 kN; 1 psf = 47.9 N/m²)

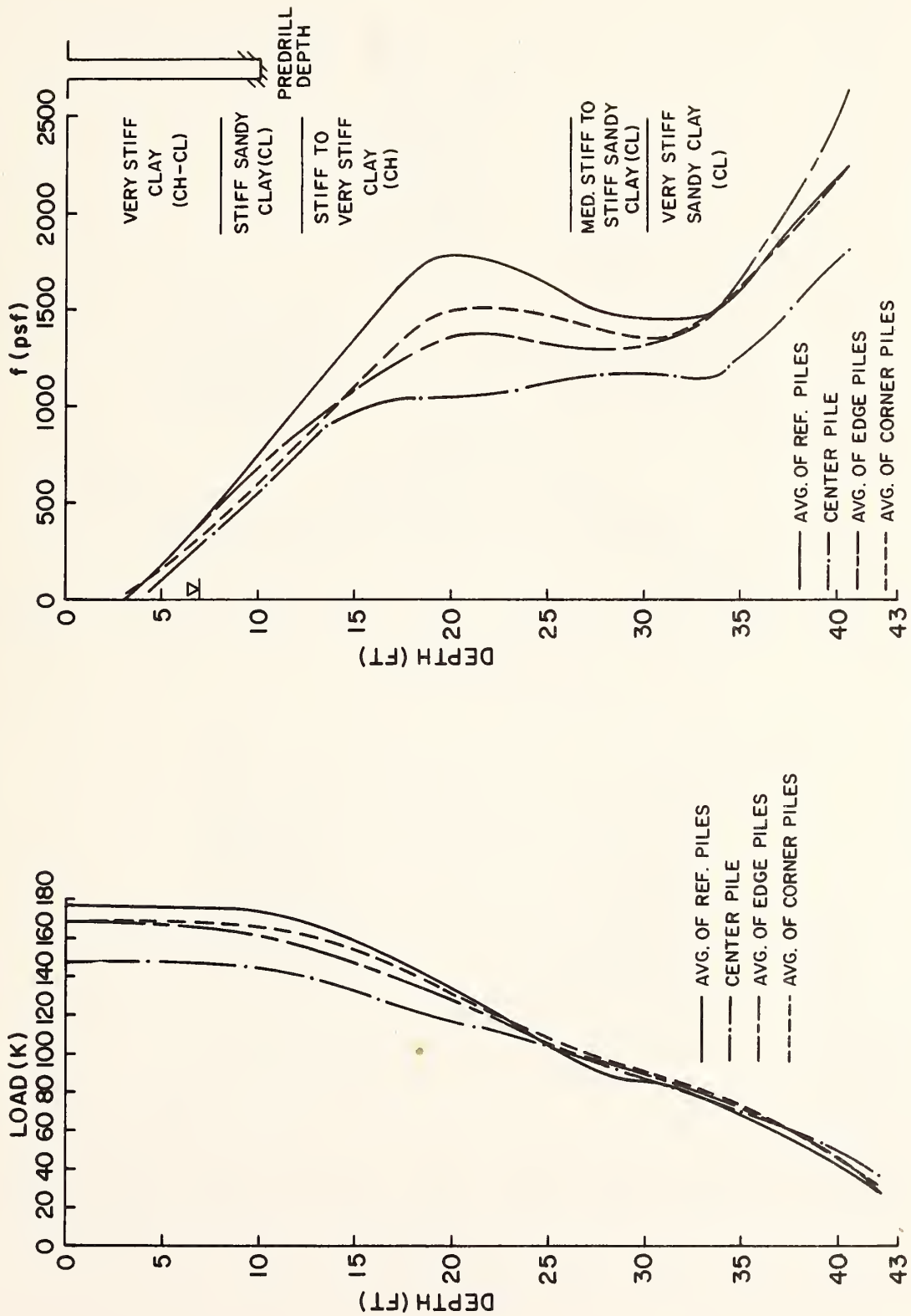


FIGURE 3.4. LOAD DISTRIBUTION AND F-D DIAGRAMS; FAILURE; 9-PILE TEST 2
 (1 ft = 0.305 m; 1 k = 4.45 kN; 1 psf = 47.9 N/m²)

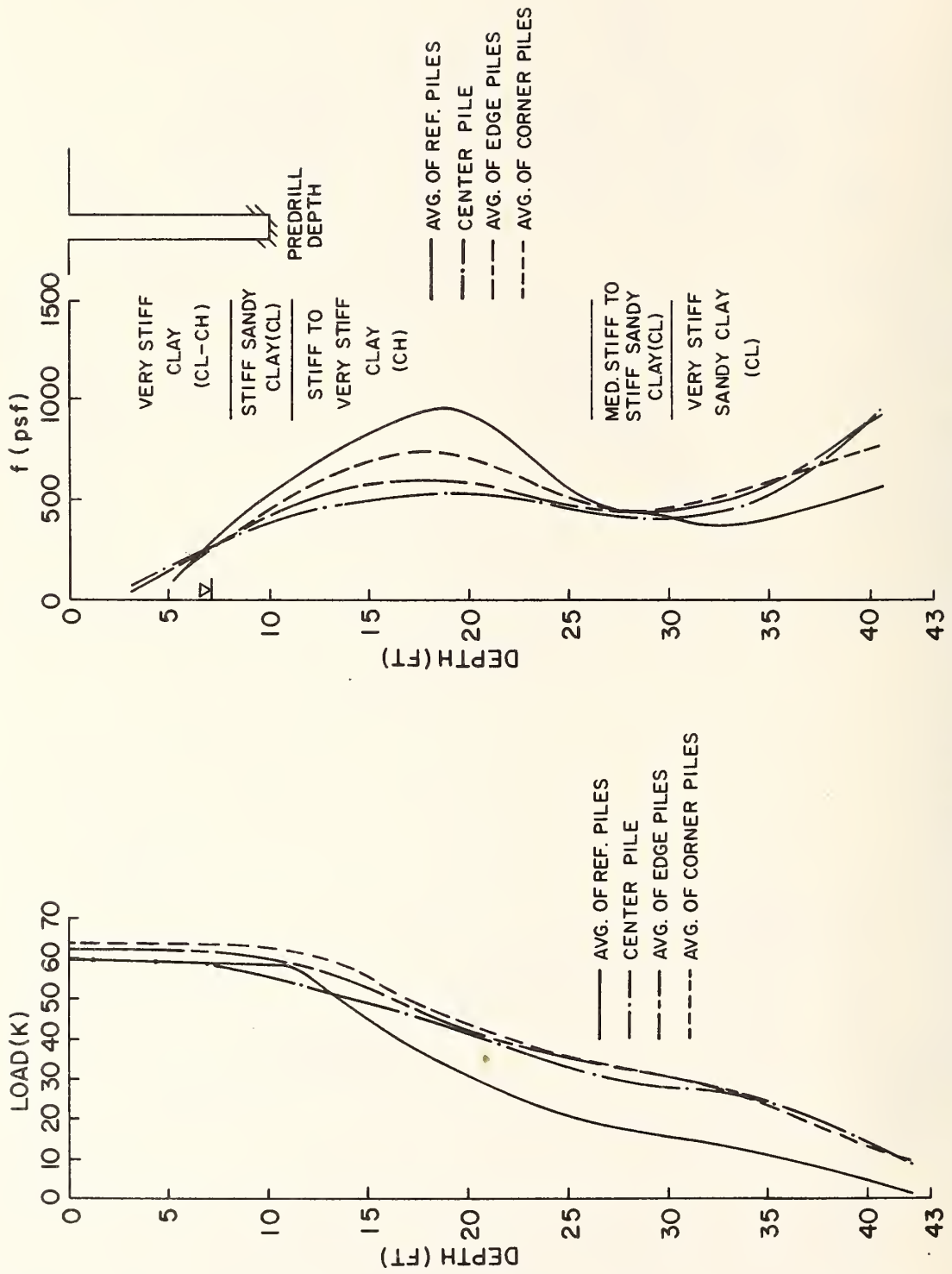


FIGURE 3.5. LOAD DISTRIBUTION AND F-D DIAGRAMS; SUBFAILURE; 9-PILE TEST 3 (1 ft = 0.305 m; 1 k = 4.45 kN; 1 psf = 47.9 N/m²)

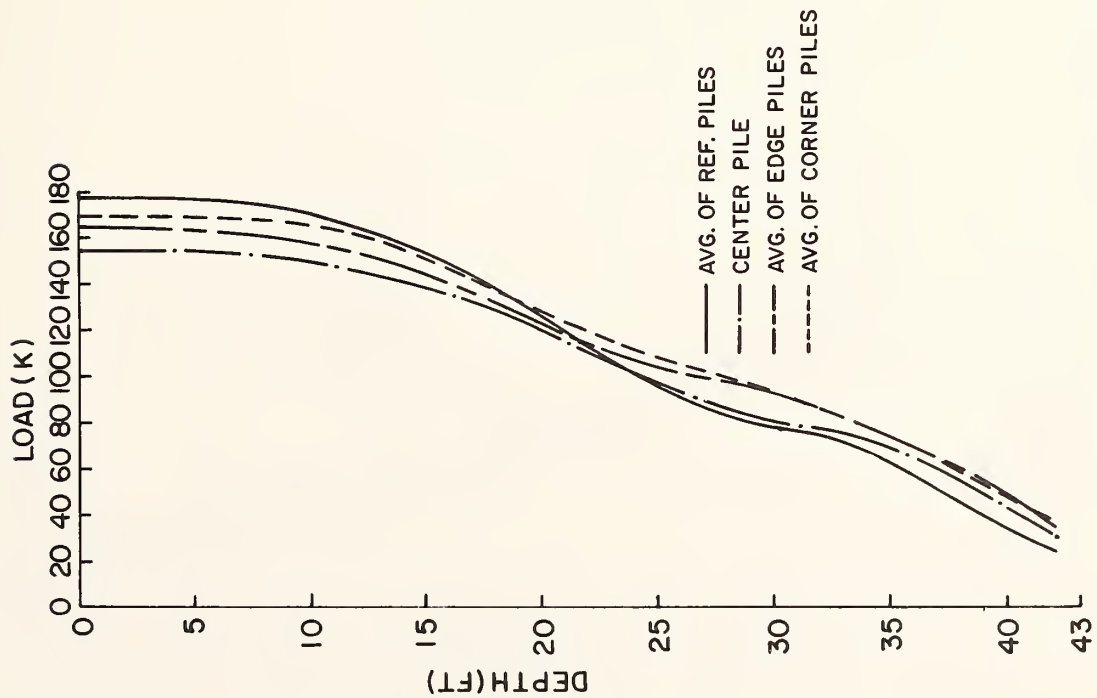
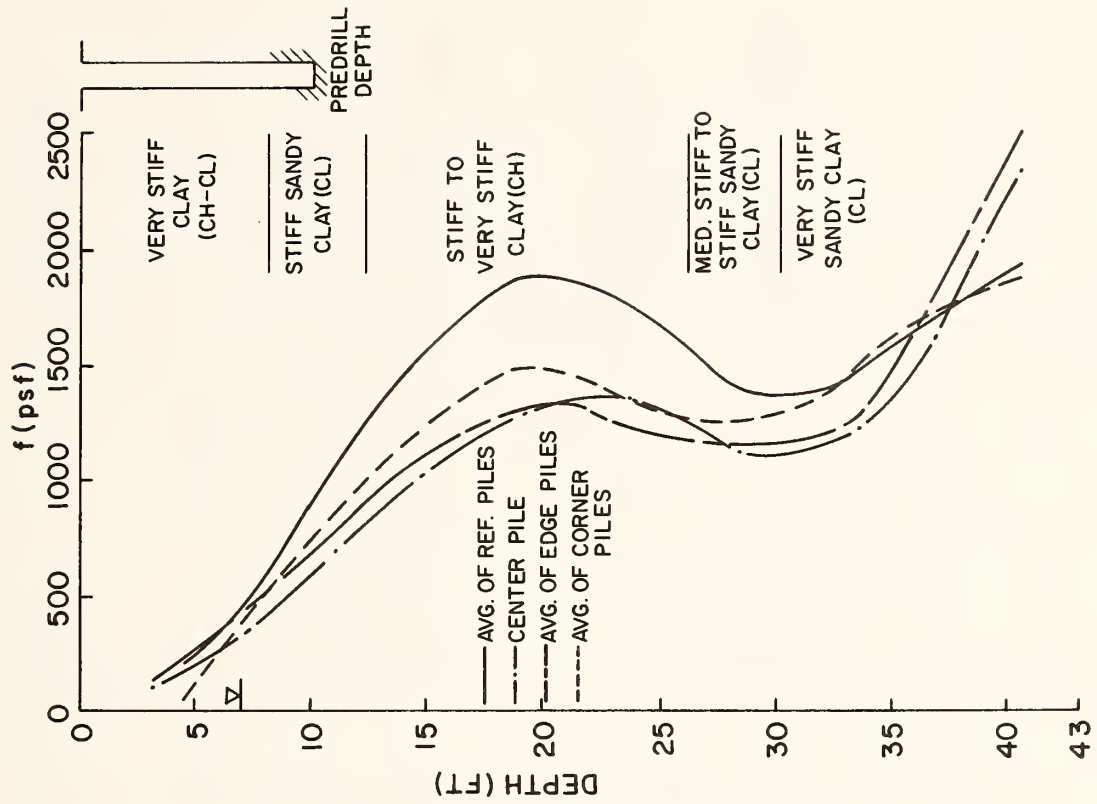


FIGURE 3.6. LOAD DISTRIBUTION AND F-D DIAGRAMS; FAILURE ; 9-PILE TEST 3
 (1 ft = 0.305 m; 1 k = 4.45 kN; 1 psf = 47.9 N/m²)

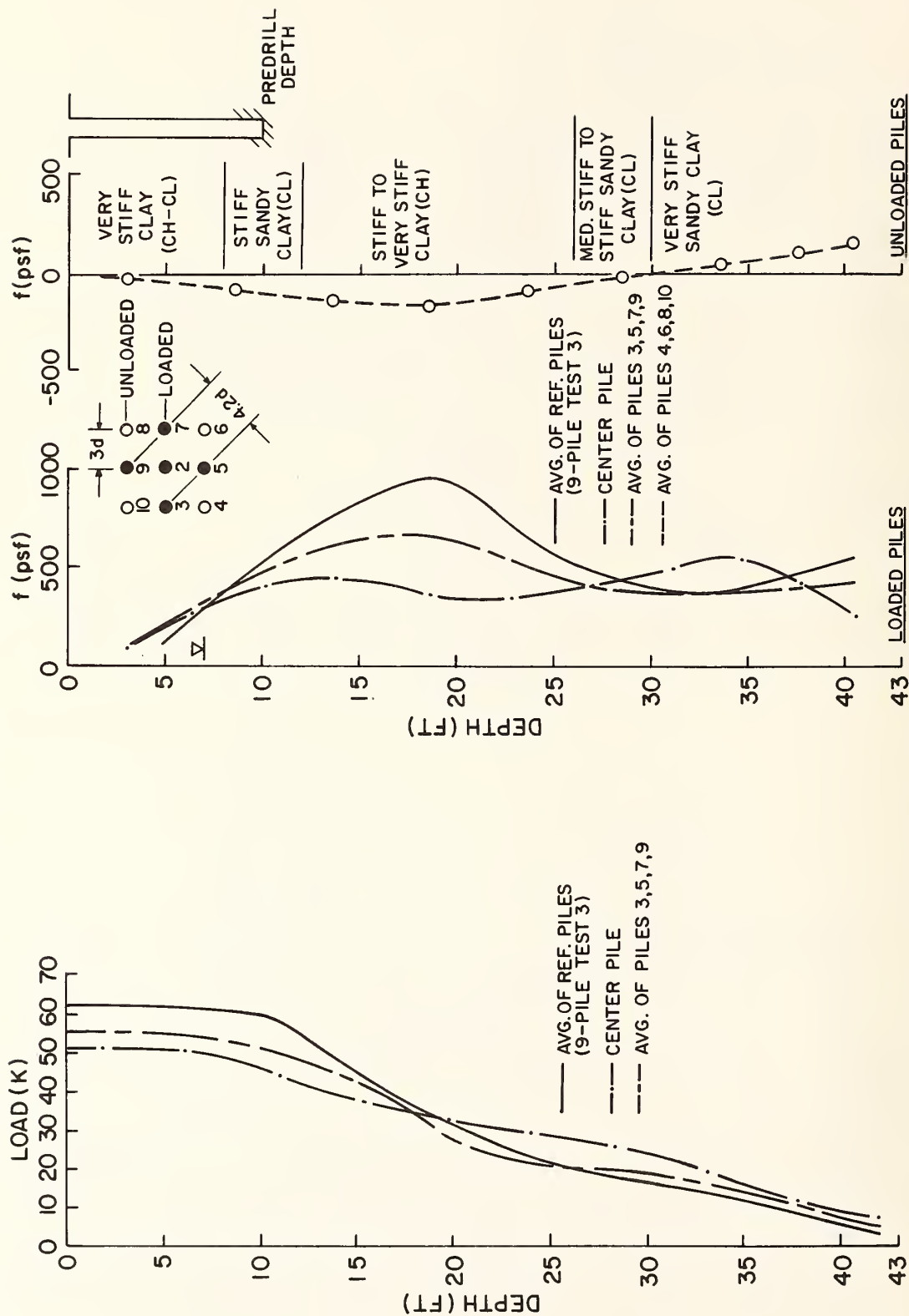


FIGURE 3.7. LOAD DISTRIBUTION AND F-D DIAGRAMS; SUBFAILURE; 5-PILE TEST
 (1 ft = 0.305 m; 1 k = 4.45 kN; 1 psf = 47.9 N/m²)

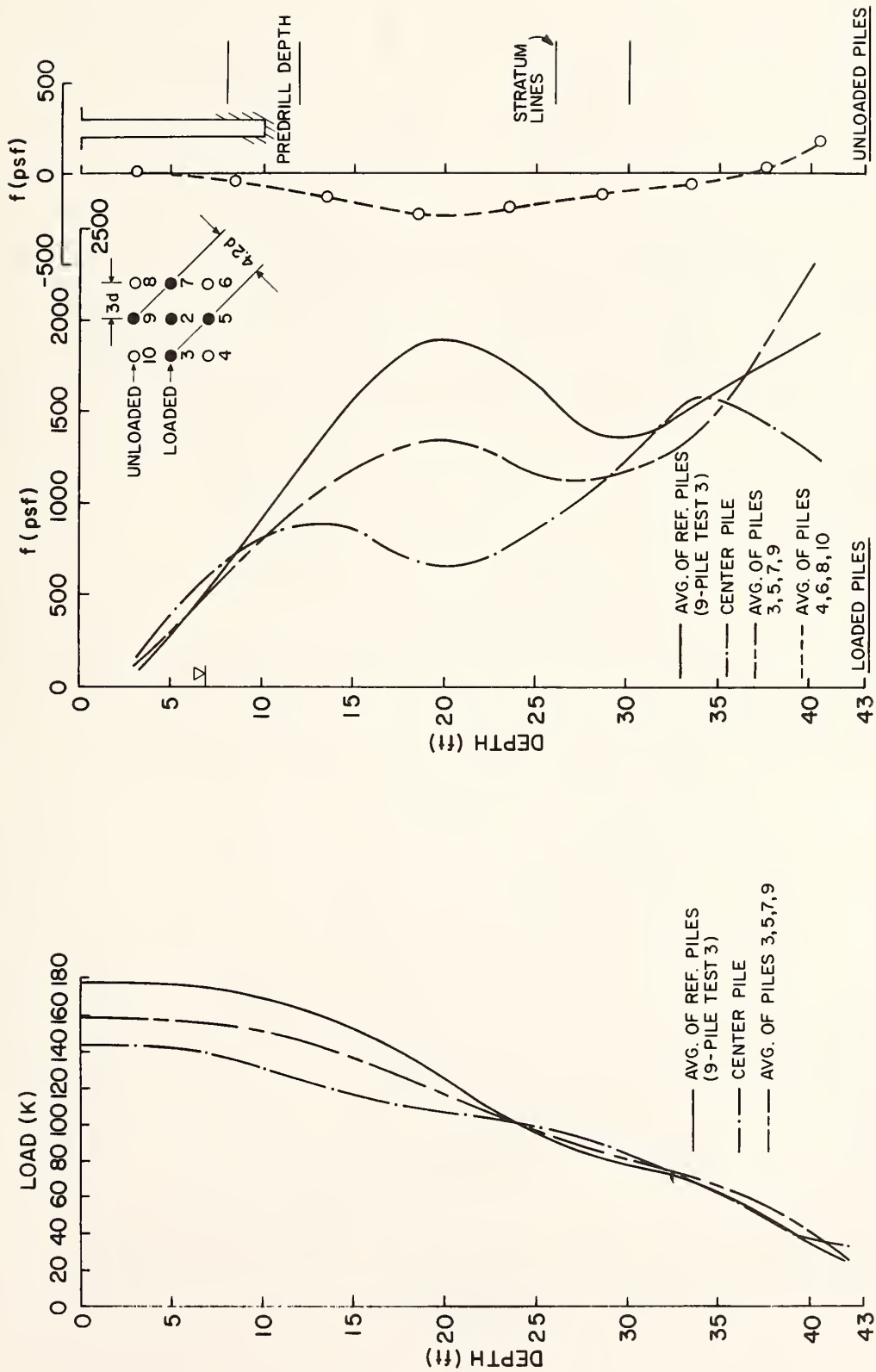


FIGURE 3.8. LOAD DISTRIBUTION AND F-D DIAGRAMS; FAILURE; 5-PILE TEST
 (1 ft = 0.305 m; 1 k = 4.45 kN; 1 psi = 47.9 N/m²)

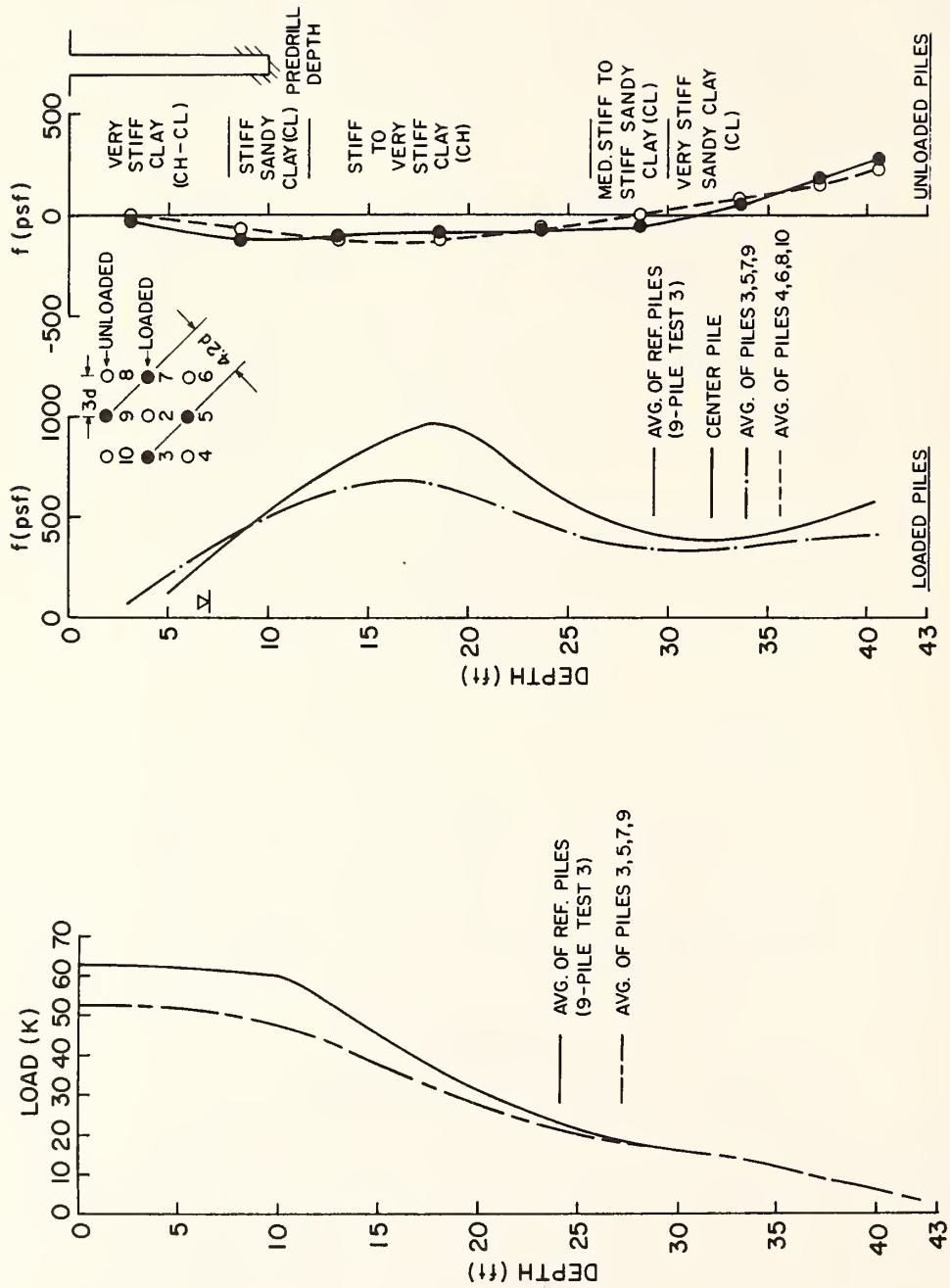


FIGURE 3.9. LOAD DISTRIBUTION AND F-D DIAGRAMS; SUBFAILURE; 4-PILE TEST (1 ft = 0.305 m; 1 k = 4.45 kN; 1 psi = 47.9 N/m²)

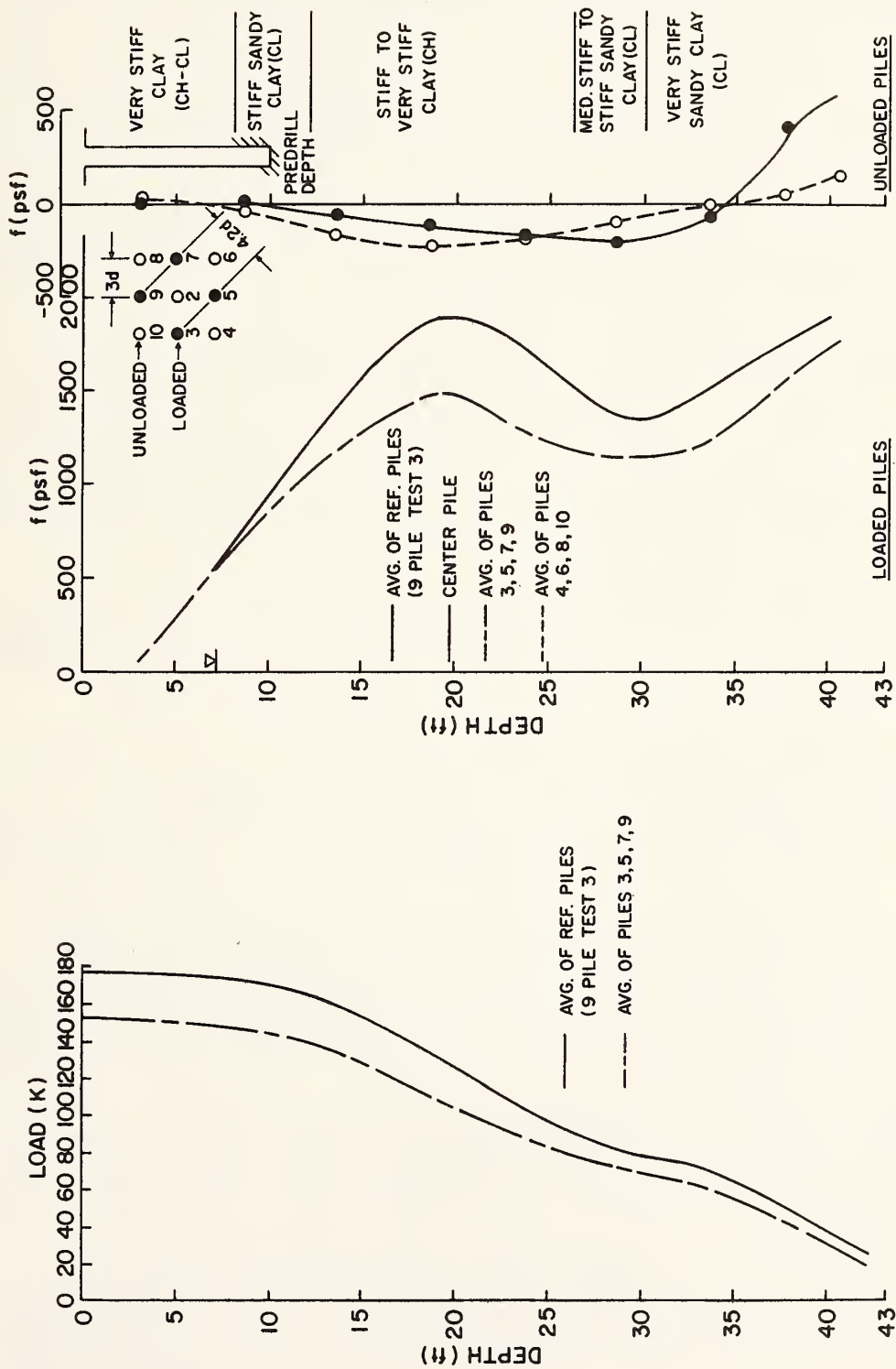


FIGURE 3.10. LOAD DISTRIBUTION AND F-D DIAGRAMS; FAILURE; 4-PILE TEST (1 ft = 0.305 m; 1 k = 4.45 kN; 1 psi = 47.9 N/m²)

curves shows a clear trend toward decreasing load transfer in Zone B with increasing "protection" of the pile. That is, the center pile transferred less load than the edge piles, which in turn transferred less load than the corner piles.

The trend is not so clear among the group piles near the bottoms of the piles, but the group piles as a whole clearly transferred more load there than did the reference piles simply because of the lack of ability to transfer load at a higher level.

The above phenomena have been observed by others in both full scale and model tests and are believed to be a general characteristic of pile group behavior, although the extent to which differences between load transfer in isolated and group piles exists is expected to be a function of relative pile-soil flexibility. The trend toward load transfer occurring farther down the piles at subfailure loads for piles in groups and to occur at the greatest depth for the most protected (interior) piles is due to the decreased opportunity for relative deformation to occur between the group piles and soil near the surface because near-surface soils have been forced to settle to a greater extent than the corresponding soils around an isolated pile due to stress overlaps produced by the group piles.

It should be observed that essentially no load was transferred in the upper 5 ft (1.5 m) of any of the piles tested. This was within the depth of predrilling but was also in the zone of highest OCR and greatest lateral pile motion, both during driving and testing.

Other aspects of the shapes of the subfailure f-d curves can be explained qualitatively in terms of measured soil properties. The peaks observed at a depth of approximately 20 ft. (6.1 m) correspond to a zone of high lateral in-situ pressures (Fig. 1.4), while the reduced load transfer in the vicinity of 28 ft. (8.5 m) is associated with Zone C (Fig. 1.1), which is a softer (and probably less overconsolidated) soil than that in the zones above and below. The high load transfer in Soil Zone D is most probably associated with depthwise increasing sand content in the sandy clay comprising that zone, depthwise increasing in-situ lateral earth pressures, and the low volumetric compressibility of the soil in Zone D, as expressed in Fig. 5.6 of the Interim Report.

The patterns of load transfer in the subgroup tests at loads approximately equal to one-half of failure load, shown in Figs. 3.7 and 3.9, reveal, as expected, somewhat smaller differences between reference pile and group pile behavior, especially in the 4-pile test where loaded pile spacing was 4.2 diameters. In fact, the differences appear as large as they are in these figures principally because comparisons had to be made at significantly different pile head loads due to the fact that coincidental reference and group pile-head loads were not achieved in the subgroup tests.

Figures 3.7 and 3.9 also depict the patterns of load transfer induced in the unloaded piles during the subgroup tests. The developed unit side shear patterns resembled side shear patterns for piles undergoing downdrag, with negative side resistance (downdrag) above about 30 ft. (9.2 m) and positive side resistance below that depth. The zone of maximum negative load transfer occurred about 1 m below the depth of maximum positive load transfer in the loaded piles. Only minor differences in load transfer in the original center and corner piles existed at this load level in the 4-pile subgroup test. Depthwise maximum negative side shear stresses induced in the unloaded piles for the configuration shown in the figures were about 20 percent of the depthwise maximum positive side shear stresses in the loaded group piles in the 4-pile test and about 25 percent in the 5-pile test.

Distributions of loads along piles at failure and values of f versus d at peak load are described in Figs. 3.2, 3.4 and 3.6 for the 9-pile group tests and in Figs. 3.8 and 3.10 for the subgroup tests. These load transfer curves were derived by averaging the load distributions in the indicated piles (e.g., corner group piles) at the maximum pile-head load developed for each pile. Such maximum loads were not always developed simultaneously on all piles in a set. The curves also do not represent the absolute maximum value of f achieved at every level because side resistance failure was distinctly progressive, as will be described subsequently. They do represent the available side resistance at failure, however, which is the quantity of interest to designers.

A more uniform f - d pattern existed among the various group and reference piles at failure than existed at 60 kips (267 kN) per pile. This is especially true for the first 9-pile load test, depicted in Fig. 3.2. An increasing dissimilarity of load transfer pattern occurred with further testing, especially in Zone B, possibly because of the degrading effects of multiple loading in this soil.

The shapes of the f - d curves at failure were similar to those at the 60-kip (267 kN) load level, except for the sharp increase in unit side resistance near the bottoms of the piles. High unit side shear did not exist in the lower portions of the piles at the lower loads because relative pile-soil movement had not yet occurred that was sufficient to develop as high a percentage of maximum unit side resistance at that level as was developed farther up the piles, especially in the reference piles. This phenomenon, well-known from tests on instrumented single piles, is associated with the compression that takes place within flexible piles, which results in larger downward movements in the piles near the tops than near the tips for a given applied load.

The depths of median side load transfer, tabulated in Table 3.1, were smaller in the reference piles at subfailure loads than were the corresponding depths for the group piles. At failure, however, all median load transfer depths were essentially equal at slightly above the two-thirds depth.

TABLE 3.1. VARIATION OF DEPTH OF MEDIAN SIDE LOAD TRANSFER AMONG TESTS
 (1 ft = 0.305 m; 1 k = 4.45 kN)

DEPTH OF MEDIAN SIDE LOAD TRANSFER (FT)

TEST	LOAD LEVEL	AVG. OF REFERENCE PILES	CENTER PILE	AVG. OF EDGE PILES	AVG. OF CORNER PILES
9-PILE TEST 1	60K/PILE FAILURE	21	26	27	26
		26	27	25	26
9-PILE TEST 2	60K/PILE FAILURE	21	25	25	23
		25	28	26	27
9-PILE TEST 3	60K/PILE FAILURE	20	25	25	24
		24	26	27	26
5-PILE SUBGROUP	60K/PILE FAILURE	—	25	19	—
		—	29	26	—
4-PILE SUBGROUP	60K/PILE FAILURE	—	—	20	—
		—	—	24	—

NOTE: MIDDEPTH OF PILES = 21.5 FT.
 2/3 OF PILE PENETRATION = 28.7 FT.

No discernable "tip effect" was observed for either the group piles or the reference piles at loads up to and including those producing shaft failure or total failure, which occurred simultaneously except for reduction in unit load transfer near the tip of a pile caused by the influence of the stress field generated in the soil at the pile tip on the stress field in the zone around the pile just above the tip. In this regard it should be emphasized that the lowest two load transducer levels were situated 1 ft. (0.305 m) and 4 ft. (1.22 m), respectively, above the bottoms of the boot plates. Therefore, the center of the lowest increment of pile load measurement was 2.5 ft. (0.76 m) or 2.8 diameters above the pile tips, which should be considered the lowest level at which the f-d data are applicable, so that some undetected tip effect may have existed before or at shaft failure. Tip movements were very small at failure. However, further tip penetration was accompanied by relaxation of load transfer in the bottom few feet of the piles. This may have been a manifestation of tip effect.

In the subgroup tests, the magnitudes of the side shear stresses induced in the unloaded piles at failure were greater than those reported for the 60 kip (267 kN) per pile load condition. Transition from negative to positive load transfer also occurred at a greater depth at failure than at the lower load. This resulted in a corresponding higher induced tip load in the unloaded piles. Consideration of the induced load transfer (f-d) patterns provides a clear phenomenological explanation of the reasons for the differences in load transfer patterns in single piles and in piles within groups.

Apparent Peak Load Transfer by Soil Layer

If the average peak load transfer values depicted in Figs. 3.2, 3.4, 3.6, 3.8, and 3.10 are tabulated by soil zone or layer, Table 3.2 results. The word "apparent" is used here because the side shear stresses tabulated are only the stresses mobilized upon application of external load and do not consider side shear stresses that existed due to residual loads in the piles. It is significant to observe that all apparent peak load transfer values (denoted f_{\max}) below a depth of 11 ft. (3.4 m) exceed 1 ksf (47.9 kN/m²), a value sometimes considered as a limiting value for skin friction in overconsolidated clay. In fact, f_{\max} exceeded 1.5 ksf (71.9 kN/m²) in Zone D. There was also a trend toward increasing values of f_{\max} in each layer with repeated compression loading, except in Pile 2, the interior pile, where a trend toward side shear degradation is evident in Zones B and C.

The only significant differences in apparent peak load transfer between the reference and group piles occurred in Layers A and B. In both layers the reference piles produced slightly higher apparent load transfer values. An anticipated large increase in the load transfer value in the group piles in the zone of predrilling did not materialize, indicating that installation of nearby piles had no discernable effect on

TABLE 3.2. VARIATION OF PEAK UNIT SIDE LOAD TRANSFER BASED ON PRETEST
 ZEROS (1 ft = 0.305 m; 1 psf = 47.9 N/m²)

LAYER	AVG. PEAK LOAD TRANSFER IN PSF									
	AVG. OF REF. PILES			AVG. OF ALL GROUP PILES			PILE 2 (CENTER PILE IN GROUP)			
	TEST 1	2	3	TEST 1	2	3	TEST 1	2	3	
0 - 11' (A)	334	272	399	241	256	281	226	131	288	
11' - 26' (B)	1326	1546	1673	1196	1229	1236	1288	1002	1179	
26' - 31' (C)	1204	1479	1385	1239	1319	1225	1308	1162	1112	
31' - 42' (D)	1605	1803	1757	1593	1947	1921	1752	1693	1735	

radial lateral pressures around the upper parts of piles driven in shallow pilot holes.

Progressive Failure Patterns

The soil at the test site can be described as "brittle" and "strain softening." (Refer to Appendix C for typical laboratory stress-strain relationships.) Because of this fact pile failure was progressive in two ways: (1) progressive failure occurred along the shaft of each pile, and (2) progressive failure occurred among the piles of the group. After the soil near the bottoms of the piles failed, some relaxation occurred, possibly due to the tip effect described earlier. As a result of this phenomenon and of the small relative deformations needed to mobilize peak load transfer in Zone D, failure often progressed from the bottoms of the piles toward the tops at the same time failure was progressing from the tops toward the bottoms. This phenomenon is presented diagrammatically in Figs. 3.11 and 3.12, which show by means of vertical black bars the range over which shaft failure had progressed in each pile as a function of applied load for Test Set 1. No shear failure was observed anywhere along the shafts at loads lower than those described. All piles, except for Piles 3 and 11, show upward progression of failure from near the pile tips beginning at loads below the failure load. It is suggested that the load at which depthwise progressive failure begins would be the approximate load at which the group or reference piles would have failed under long-term sustained loading.

Figure 3.12 also shows how shaft failure (and total failure, which corresponded to complete shaft failure) progressed from pile to pile during the first 9-pile test, in which tipping of the cap toward the north row of piles (8, 9, and 10), along with some rotation about a vertical axis and northward, translation, occurred. See Fig. 2.8. Pile 8, the northeast corner pile, failed first, followed by Piles 9 and 10 and the piles in the middle row. Pile 6, shown as having incomplete shaft failure in Fig. 3.12, did fail for all practical purposes during the one-hour load hold at 700 tons (6.23 mN).

Effects of Residual Stresses on Load Transfer

Measured variations in the residual loads within the reference piles before and after Test 1 are shown in Fig. 3.13. These loads are based on zeros taken while the piles were in an unstressed condition in the calibration beds. It can be observed that the residual loads induced by load testing the piles to failure exceed by a significant amount the residual loads induced during driving. This residual side shear stress pattern was computed by differentiation of the graph of residual load before Test 1 versus depth.

Figure 3.14 shows the average residual side shear stress distribution corresponding to the residual load distribution patterns observed prior to Test 1. Negative residual stresses (downward directed on piles) of

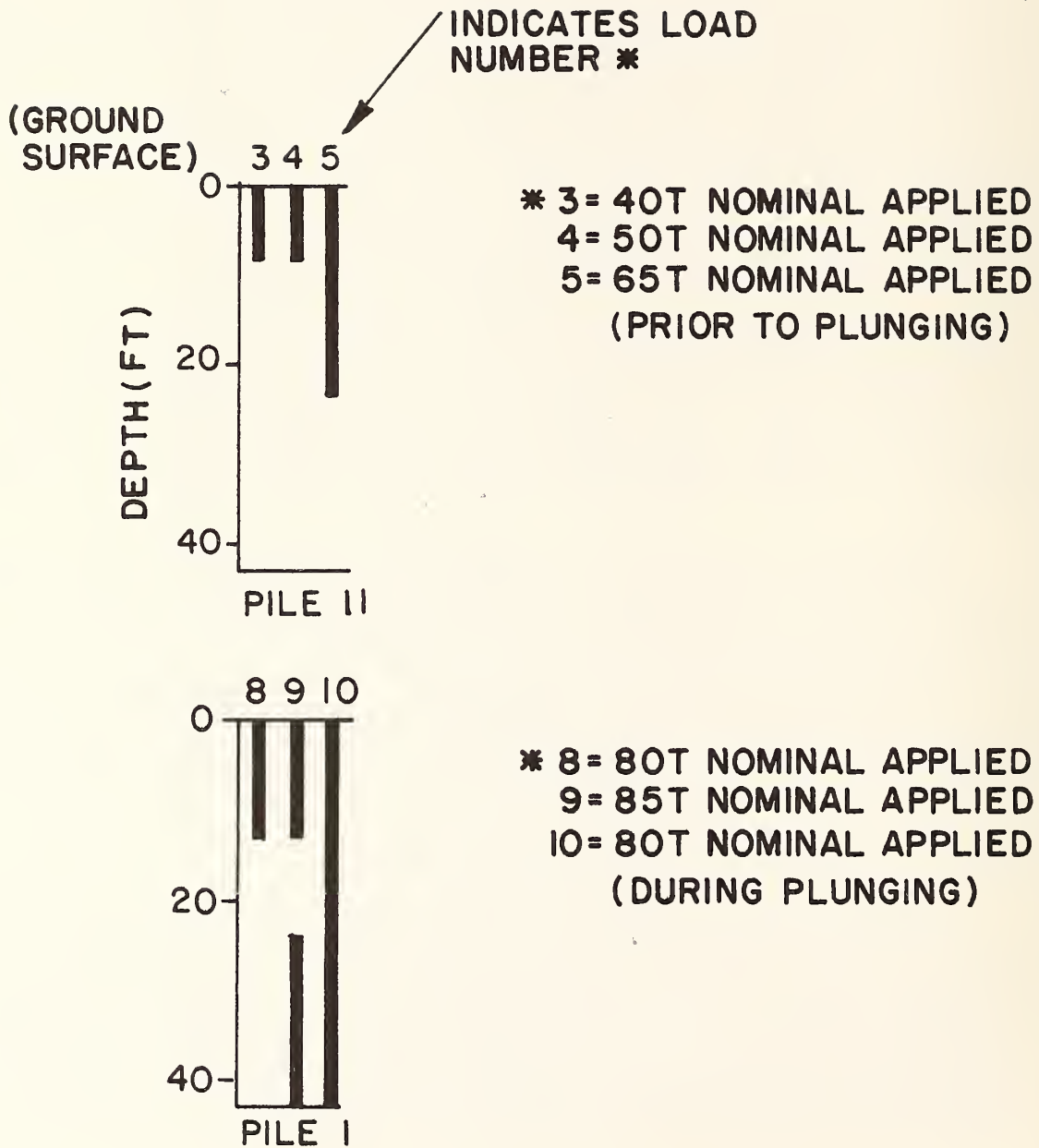


FIGURE 3.11. PROGRESSIVE FAILURE IN REFERENCE PILES; TEST 1
 (1 ft = 0.305 m; 1 ton = 8.9 kN)

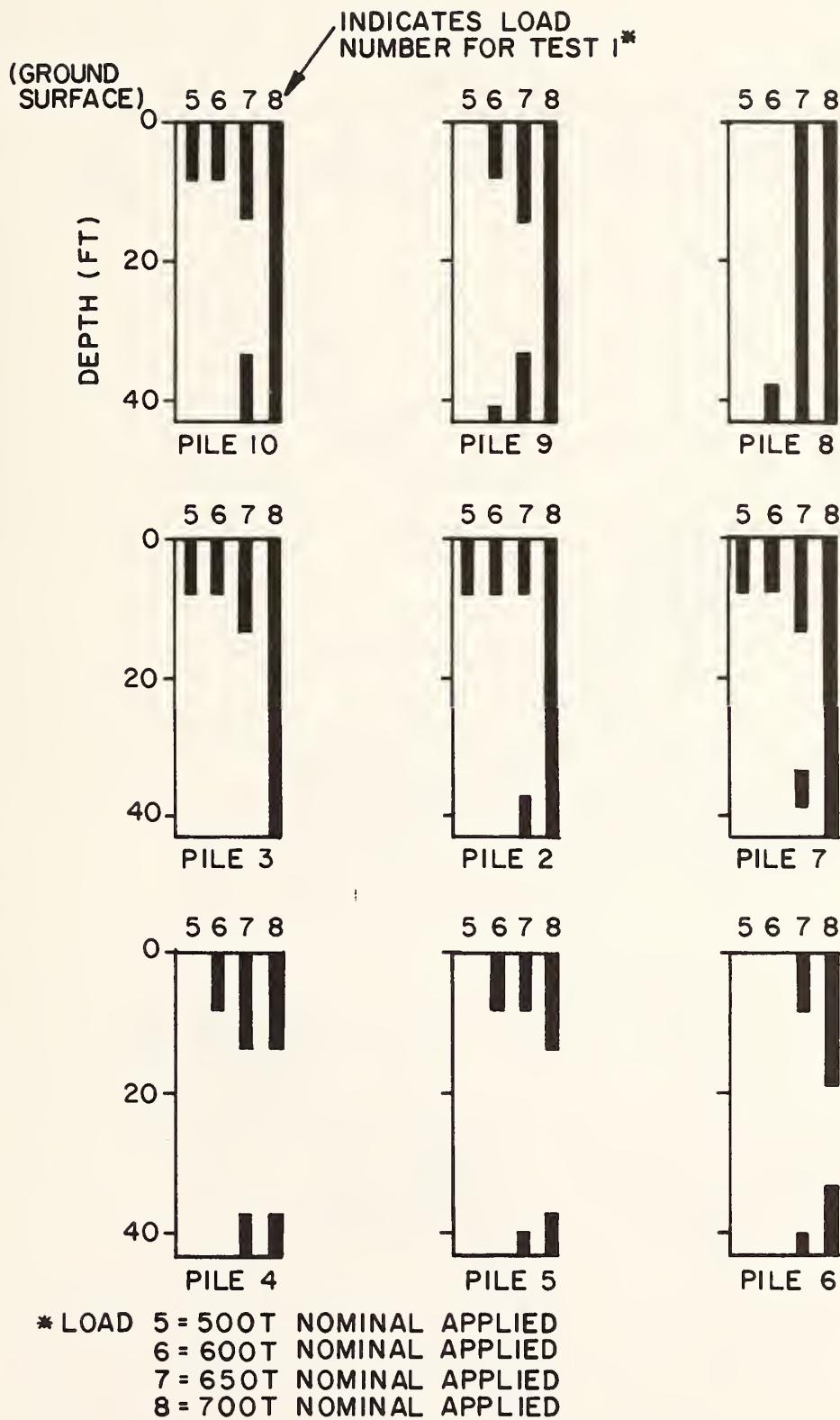


FIGURE 3.12. PROGRESSIVE FAILURE IN GROUP PILES; 9-PILE TEST 1
 (1 ft = 0.305 m; 1 ton = 8.9 kN)

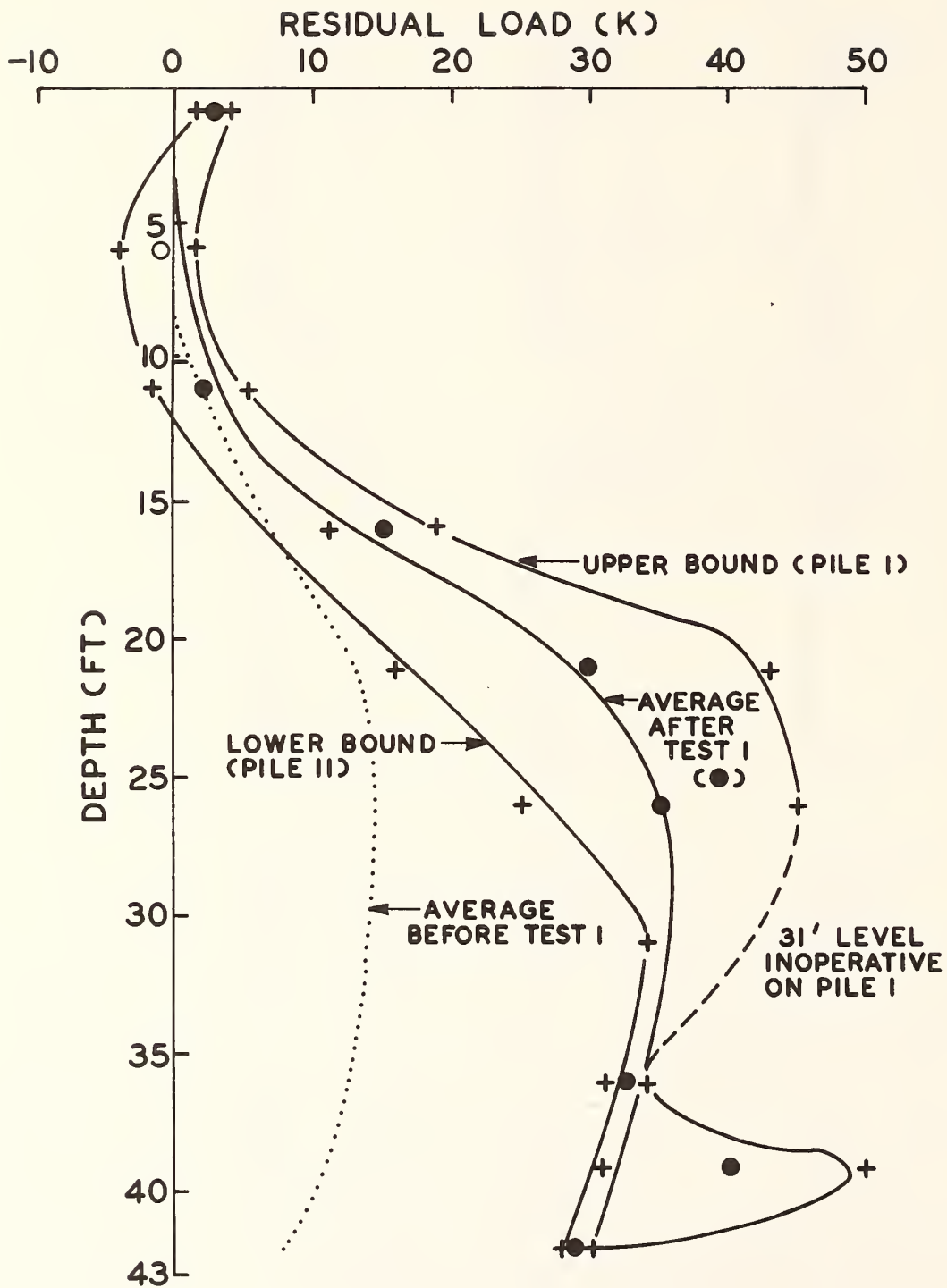


FIGURE 3.13. RESIDUAL LOADS IN REFERENCE PILES; TEST 1
 (1 ft = 0.305 m; 1 k = 4.45 kN)

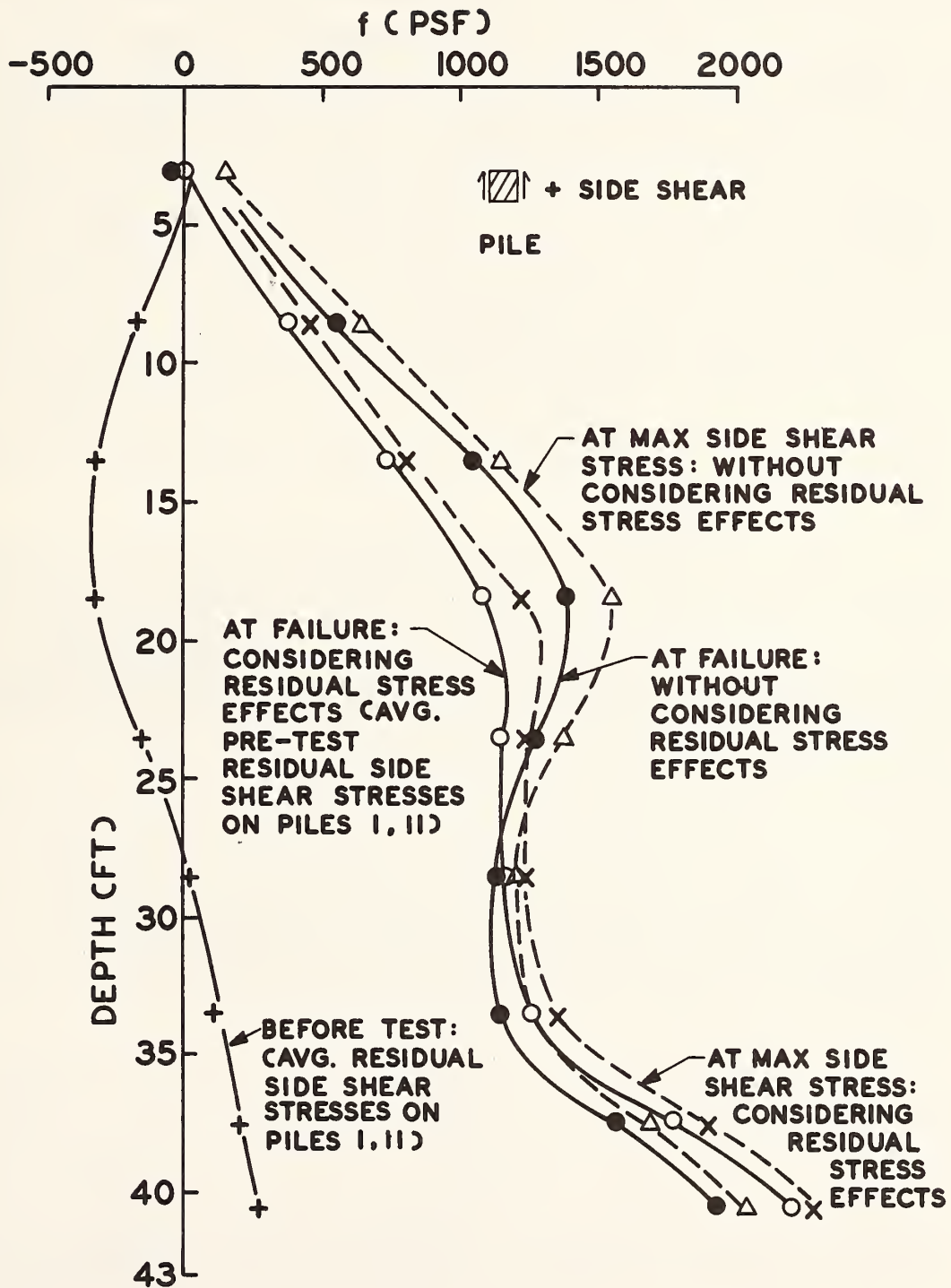


FIGURE 3.14. F-D RELATIONSHIPS FOR REFERENCE PILES; TEST 1
 (1 ft = 0.305 m; 1 psf = 47.9 N/m²)

up to 400 psf (19 kN/m²) were observed in the top two-thirds of the piles, while lesser positive values existed in the bottom one-third.

Figure 3.14 also shows graphs of maximum apparent side shear distributions (without considering group effects) based on the average side shear stresses in Piles 1 and 11 in Test 1 at the time of total pile failure. It also shows curves based on the average maximum value of measured side shear stresses at each level, irrespective of whether those values occurred at the time of total failure. The average measured initial residual side shear stress distribution was then added to these apparent f-d curves to produce "true" f-d curves. The true f-d curves represent the actual variation of peak stress with depth experienced by the soil at the time the reference piles failed and the variation of maximum peak shear stress, respectively. It can be seen that consideration of residual stresses tends to linearize the graphs of f_{\max} versus depth, suggesting in a preliminary way that side shear development was essentially frictional. This speculation is reinforced by the observation that excess pore pressures were very small throughout the test.

A similar set of curves was developed for the average of the group piles. These curves are displayed in Figs. 3.15 and 3.16. (Only the average variation of residual stress among group piles was considered due to scatter in the data. See Chapter 1 and Appendix E.) Statements concerning residual stress effects relevant to the reference piles are also generally valid for the group piles. The negative residual shear stresses in the upper portions of the piles tended to be lower in the group piles than in the reference piles. In the upper 15 ft. (4.6 m) the residual side shear stresses were positive, presumably due to shearing resistance produced by the weight of the cap. In the bottom several feet of the group piles the residual side shear was higher than at the corresponding depths in the reference piles. When this residual stress is added to the apparent stresses, the true maximum shear stresses and shear stresses at pile failure are seen to be higher for the group piles than for the reference piles below 35 ft. (10.7 m). This phenomenon is believed to be due to the increasingly granular nature of the sandy clay in Zone D below that depth.

The no-load zeros could not be maintained beyond Test 1 due to drift in the data collection system, thought to be due primarily to intrusion of minute amounts of water into the lead wire. See Appendix E. In order to attempt to estimate the variation of true unit side resistance by soil layer between the first and last compression tests, the true load distributions, including the effects of residual stresses, at failure were calculated for the last compressive loading by using a procedure suggested by Hunter and Davisson (Ref. 32, Interim Report). In this procedure an apparent load-depth curve at failure is corrected by subtracting from a given measured apparent load value at failure the apparent load value at that level observed upon unloading and adding to the result the absolute value of the apparent load remaining in the pile at the same level after conducting an uplift load test to failure and

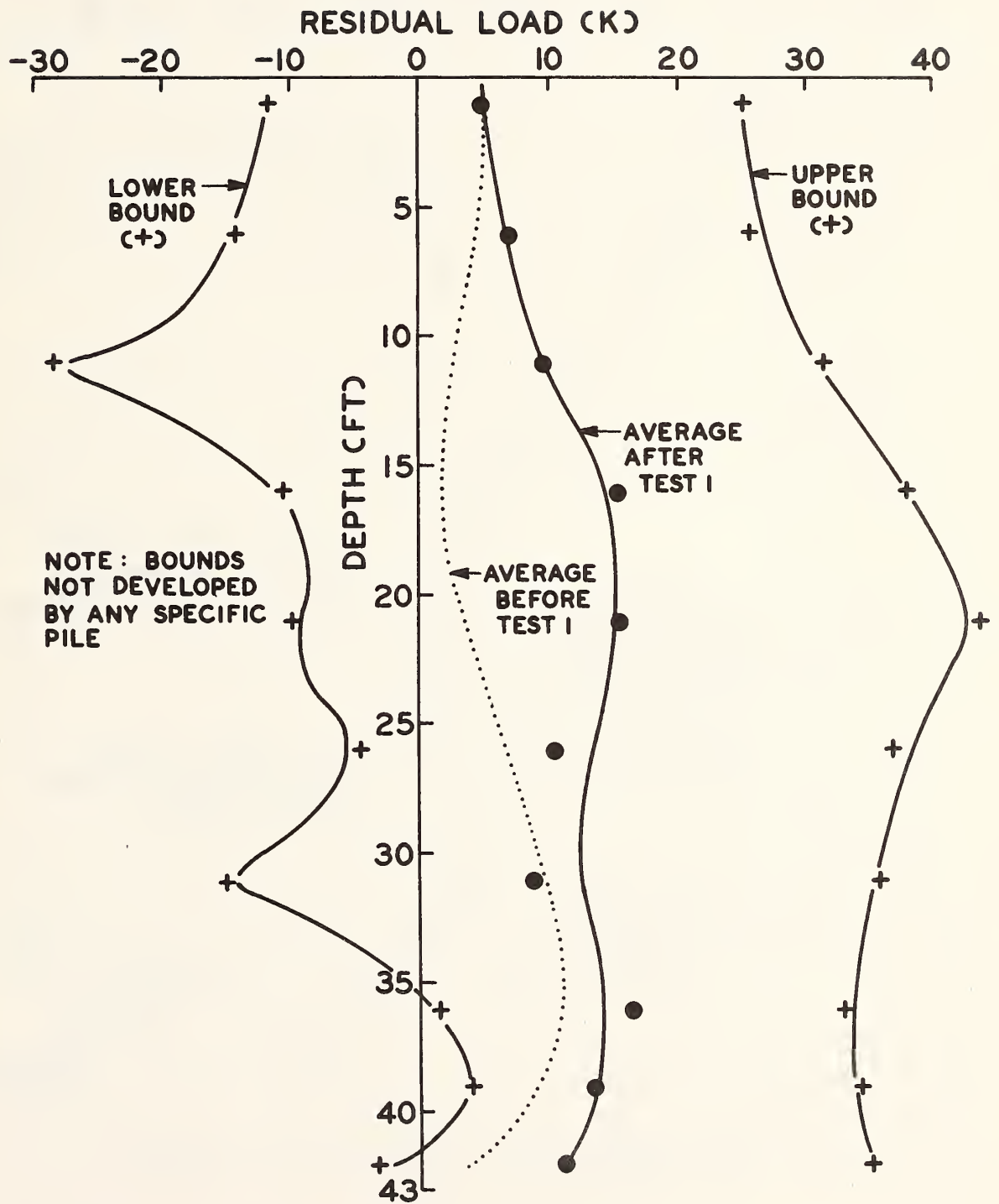


FIGURE 3.15. AVERAGE RESIDUAL LOADS IN GROUP PILES; TEST 1
 (1 ft = 0.305 m; 1 k = 4.45 kN)

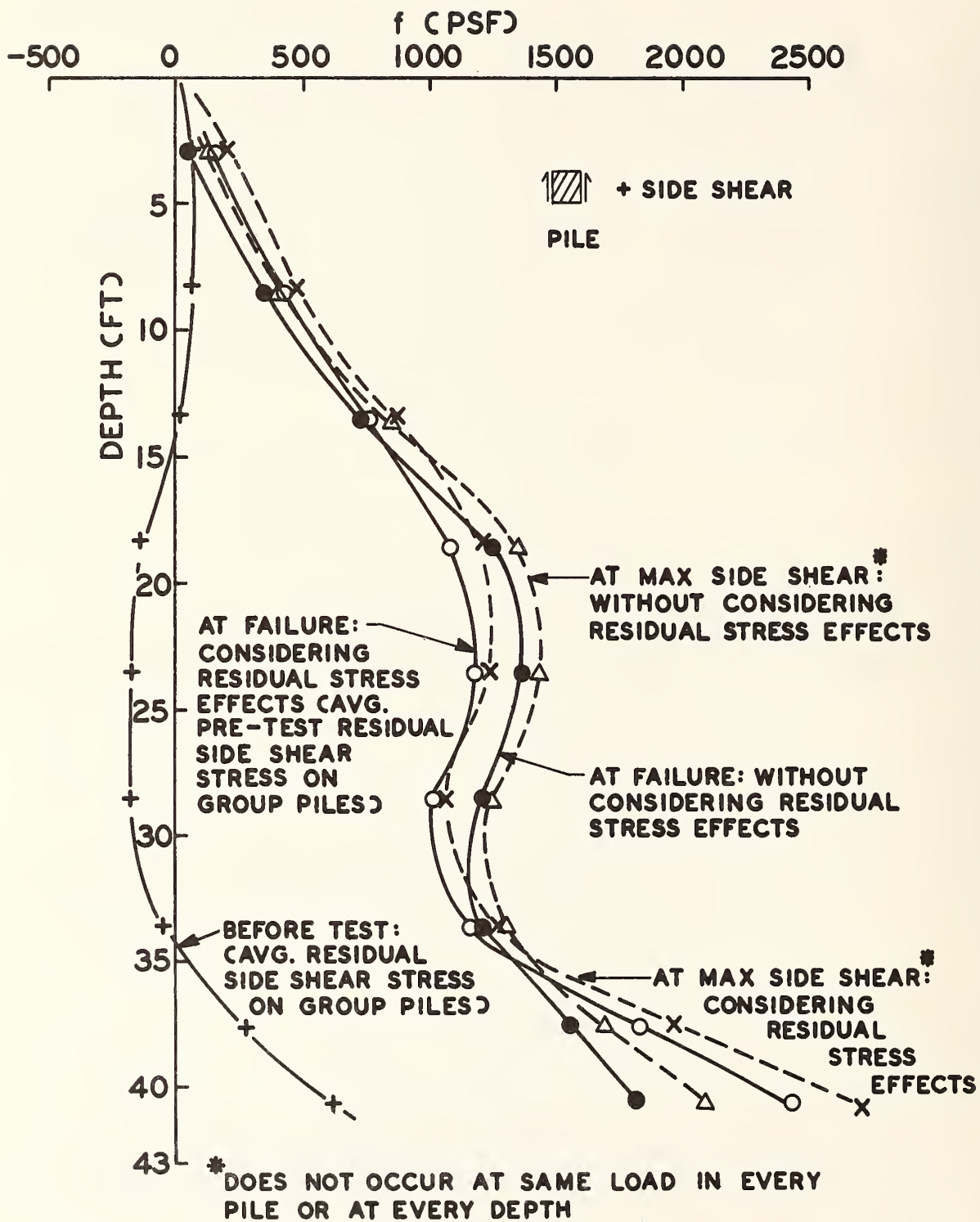


FIGURE 3.16. AVERAGE F-D RELATIONSHIPS FOR GROUP PILES; TEST 1
(1 ft = 0.305 m; 1 psf = 47.9 N/m²)

unloading. Loads are zeroed before the uplift test. The resulting adjusted load distribution diagram should approximate the true load distribution at failure. A similar type of correction procedure was used to adjust the apparent load distribution diagrams at failure in uplift to produce a true load distribution diagram for uplift behavior.

The average apparent and adjusted load distribution diagrams for the two reference piles are given in Fig. 3.17. The compression tests represented are the last tests, conducted in conjunction with the final 9-pile test. Similar average diagrams for Group Piles 2, 4, 5, and 9 (those tested in uplift) are given in Fig. 3.18. In the case of the group piles the compression load-depth diagram for each individual pile was taken as that corresponding to the last compression test conducted (e.g., last 9-pile test for Pile 4; 4-pile test for Pile 5).

Differentiation of the load distribution diagrams in Figs. 3.17 and 3.18 yields the unit side shear distribution at total pile failure for the last compressive loading of each pile and for uplift loading that followed the several cycles of compression loading. The results of this differentiation, expressed as average values of unit side shear at failure, are tabulated in Table 3.3. For purposes of comparison, values obtained from direct measurement on Piles 2, 4, 5, and 9 for the first compressive loading (first 9-pile test) are also shown.

Conclusions that can be drawn from this table are that (1) no significant changes occurred in the reference piles in true (adjusted) unit side resistance in any of the four soil zones between the first and last (third) compressive loadings; (2) significantly reduced true side load transfer occurred in the reference piles in the more granular soils below a depth of 26 ft. (7.9 m) in uplift as compared to the last compressive loading and (3) reduction in true unit side shear stresses at failure occurred in the group piles between the first and last compressive loading in Zones B and C, in the depth range of 11 to 31 ft. (3.4 to 9.5 m). Unexpectedly, these losses in Zones B and C were recovered when the group piles were subjected to uplift tests. This phenomenon may be due to fabric reorientation in the highly plastic Beaumont clay that results from a reversal of the direction of applied shearing strain. The group piles developed slightly higher true side shear stresses at failure than did the reference piles in the more granular deeper soil zones.

It should be emphasized that the side shears actually available to the piles to resist applied load are those tabulated in Table 3.2 and not the true values in Table 3.3. Table 3.3 does, however, provide some insights into the way in which the true shear strength of the soil varies with loading cycle and direction of loading.

Unit Load Transfer Curves

Graphs of average developed side shear stress versus downward pile deflection (f-z curves) are presented for the four principal soil zones for the reference and group piles, respectively, in Figs. 3.19-3.22.

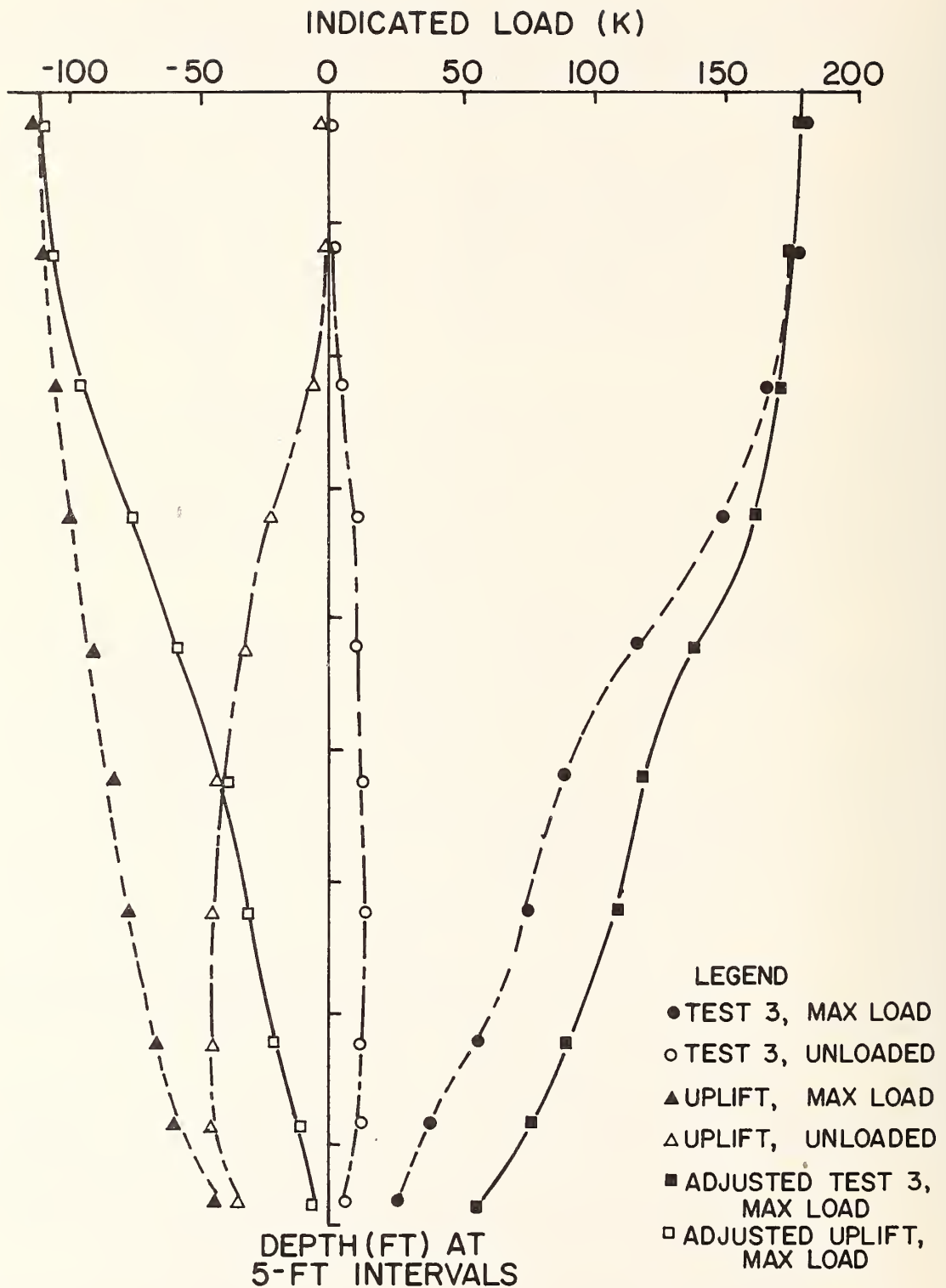


FIGURE 3.17. AVERAGE APPARENT AND ADJUSTED LOAD DISTRIBUTION DIAGRAMS AT FAILURE FOR REFERENCE PILES (1 ft = 0.305 m; 1 k = 4.45 kN)

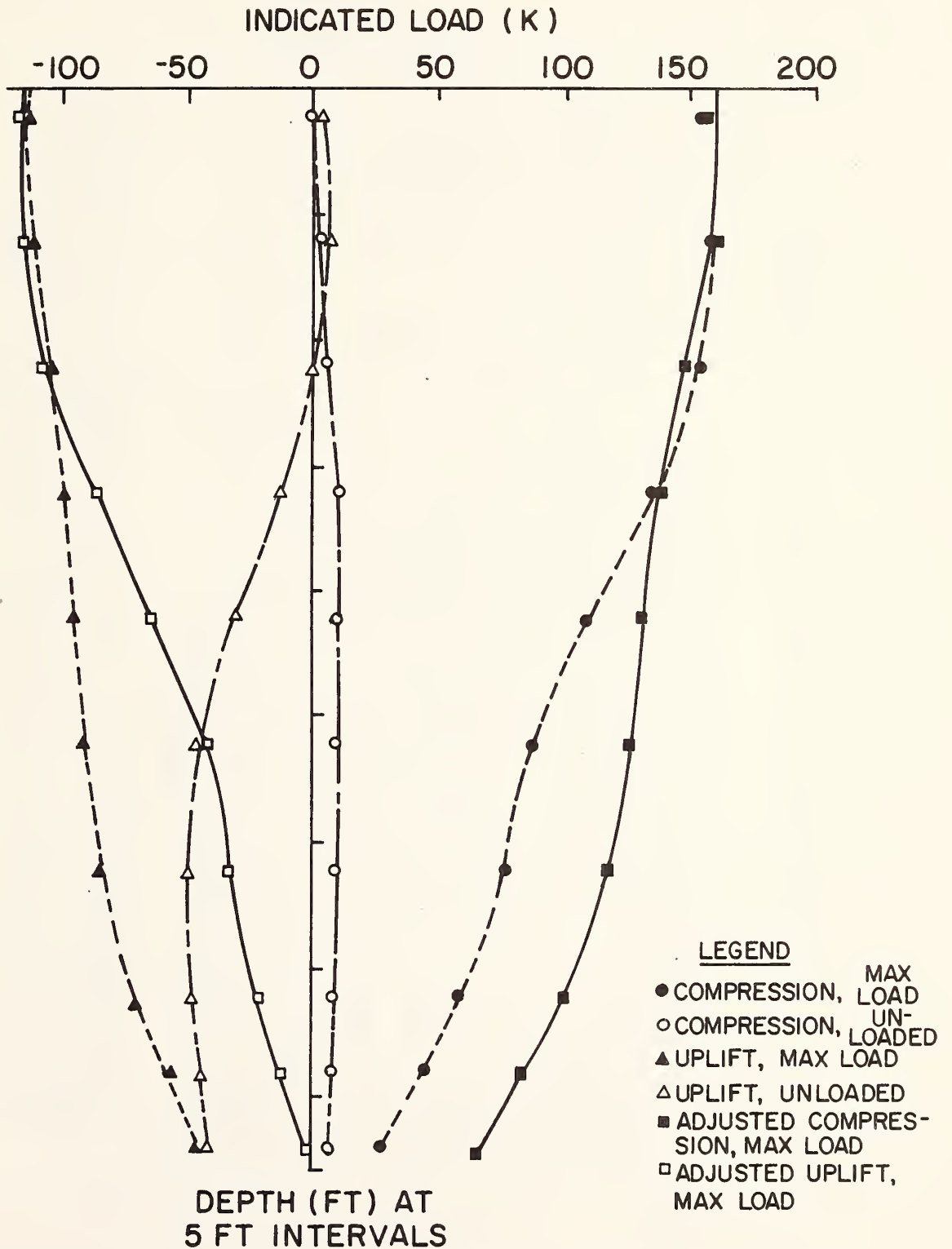


FIGURE 3.18. AVERAGE APPARENT AND ADJUSTED LOAD DISTRIBUTION DIAGRAMS AT FAILURE FOR GROUP PILES 2, 4, 5, AND 9 (1 ft = 0.305 m; 1 k = 4.45 kN)

TABLE 3.3. ADJUSTED AND UNADJUSTED PEAK LOAD TRANSFER IN PSF BY SOIL LAYER FOR COMPRESSION AND UPLIFT TESTS (1 ft = 0.305 m; 1 psf = 47.9 N/m²)

DEPTH (ft)	FIRST COMPRESSIVE LOADING			LAST COMPRESSIVE LOADING			UPLIFT LOADING			
	REFERENCE PILES		GROUP PILES(a)	REFERENCE PILES		GROUP PILES(a)	REFERENCE PILES		GROUP PILES(a)	
	U (b)	A (c)	U	U	A	U	U	A	U	
0-11	330	270	250	400	290	230	260	500	250	400
11-26	1330	1070	1220	1670	1110	1370	500	1220	340	1270
26-31	1200	1230	1240	1390	1120	1210	550	840	570	990
31-42	1600	1780	1630	1760	1790	1650	1130	800	1310	1080

(a) AVERAGE ONLY OF GROUP PILES SUBJECTED TO UPLIFT TESTS: 2, 4, 5, 9.

(b) UNADJUSTED FOR RESIDUAL STRESSES.

(c) ADJUSTED FOR RESIDUAL STRESSES.

NOTE: FIRST COMPRESSIVE LOADING WAS TEST NO.1. LAST COMPRESSIVE LOADING: TEST NO.3 (9-PILE) FOR PILES 1,11 (REFERENCE) AND 2,4; FOUR-PILE SUBGROUP TEST FOR PILES 5,9. ADJUSTED RESULTS FOR TEST 1 INCLUDED MEASURED RESIDUAL STRESSES. THE REMAINDER OF ADJUSTED RESULTS ARE DEDUCED FROM UPLIFT TESTS.

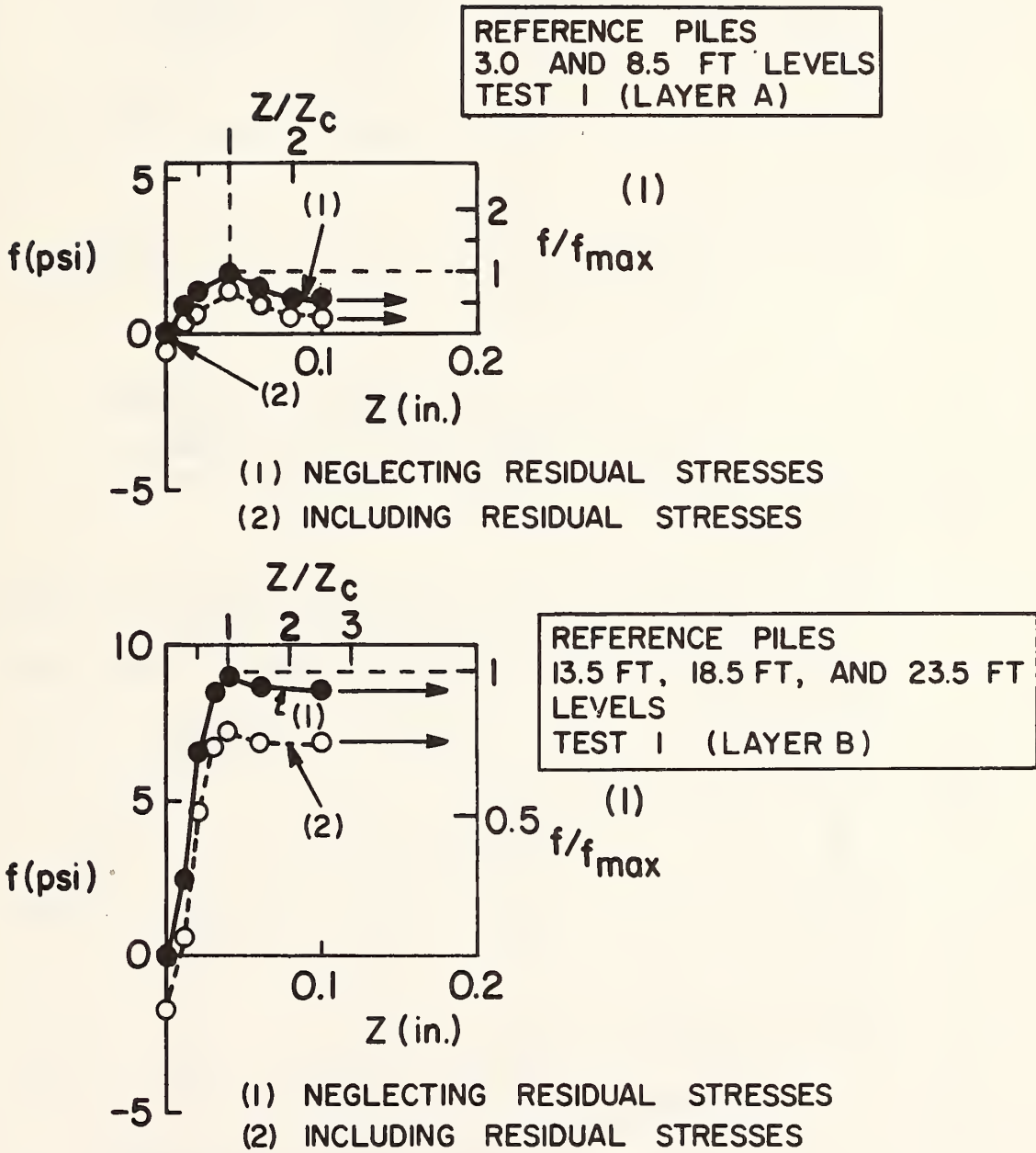
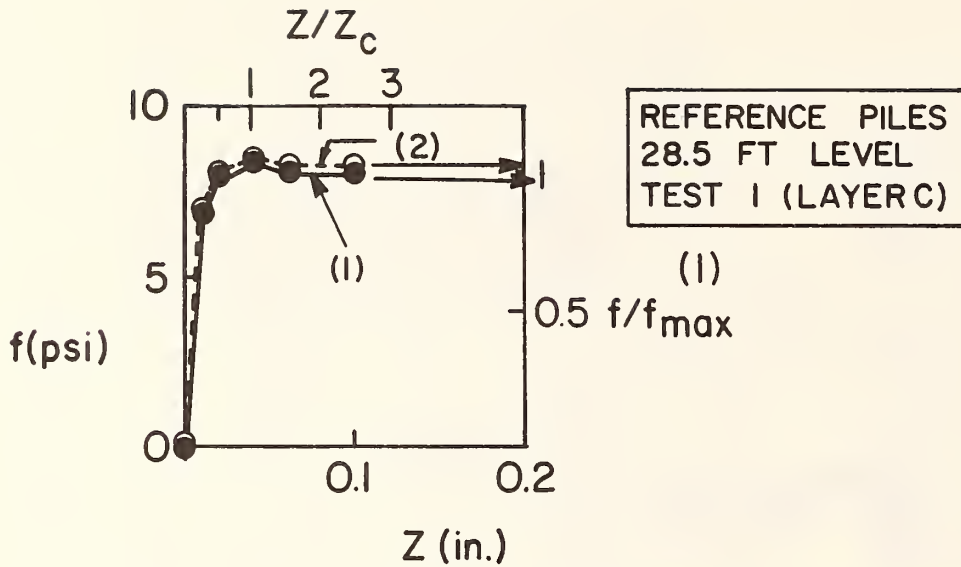
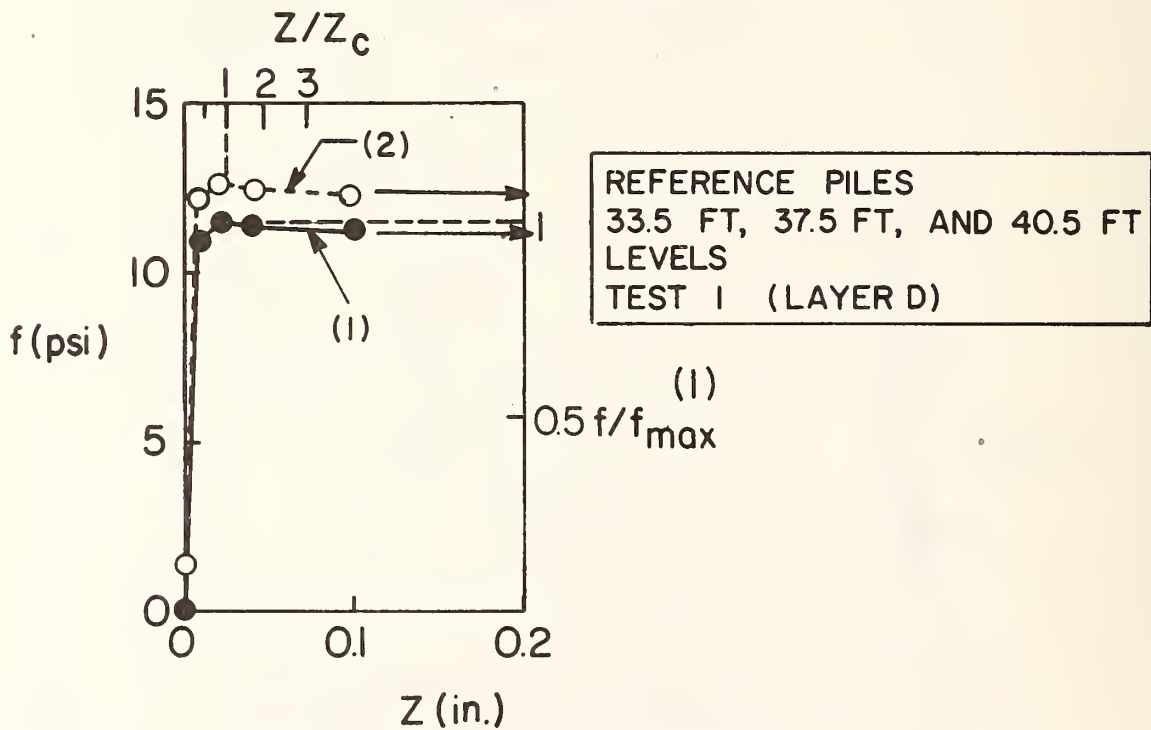


FIGURE 3.19. F-Z CURVES; SOIL ZONES A AND B; REFERENCE PILES; TEST 1
 (1 ft = 0.305 m; 1 in = 25.4 mm; 1 psi = 6.89 kN/m²)

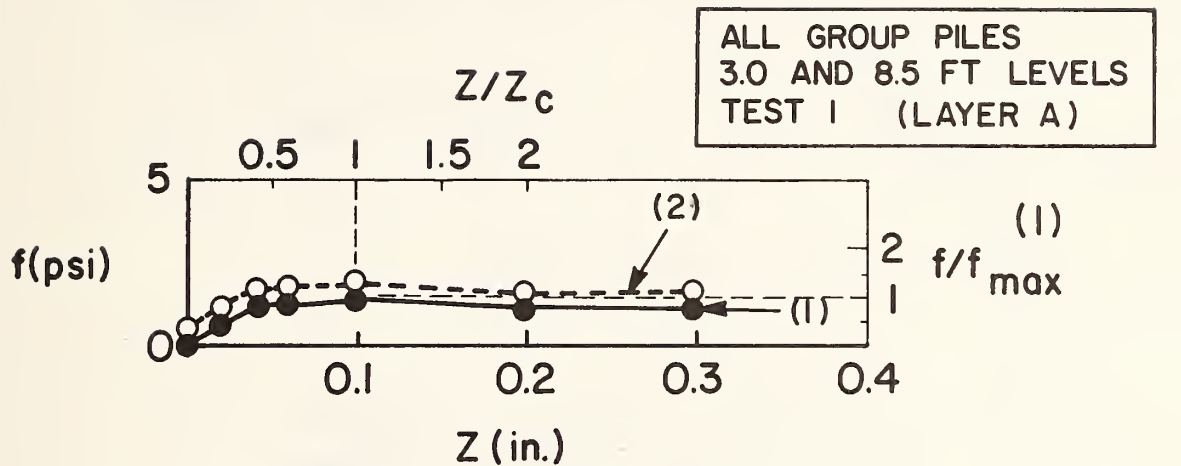


(1) NEGLECTING RESIDUAL STRESSES
(2) INCLUDING RESIDUAL STRESSES

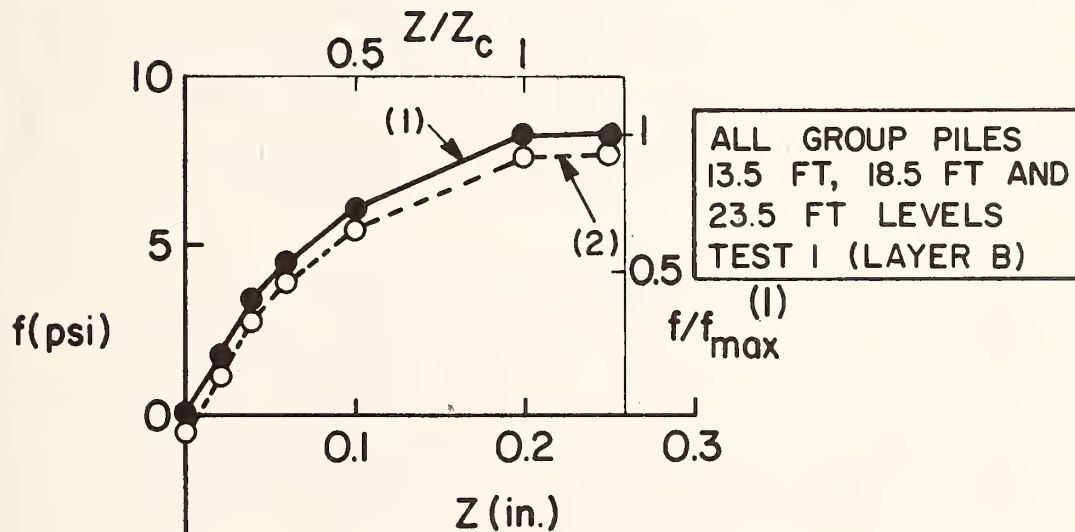


(1) NEGLECTING RESIDUAL STRESSES
(2) INCLUDING RESIDUAL STRESSES

FIGURE 3.20. F-Z CURVES; SOIL ZONES C AND D; REFERENCE PILES; TEST 1
(1 ft = 0.305 m; 1 in = 25.4 mm; 1 psi = 6.89 kN/m²)



- (1) NEGLECTING RESIDUAL STRESSES
- (2) CONSIDERING RESIDUAL STRESSES (POSITIVE VALUES AT THIS LEVEL DUE TO CAP WEIGHT)



- (1) NEGLECTING RESIDUAL STRESSES
- (2) CONSIDERING RESIDUAL STRESSES

FIGURE 3.21. F-Z CURVES; SOIL ZONES A AND B; GROUP PILES; TEST 1₂
 (1 ft = 0.305 m; 1 in = 25.4 mm; 1 psi = 6.89 kN/m²)

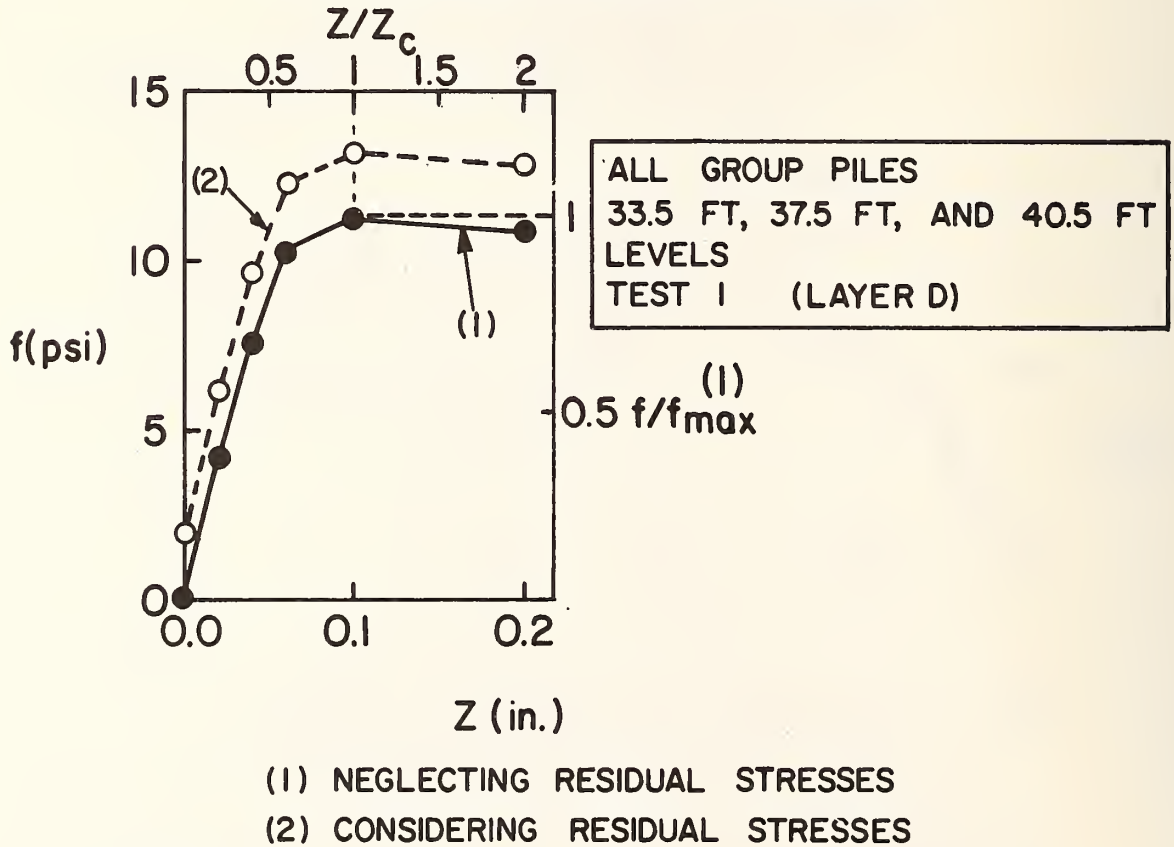
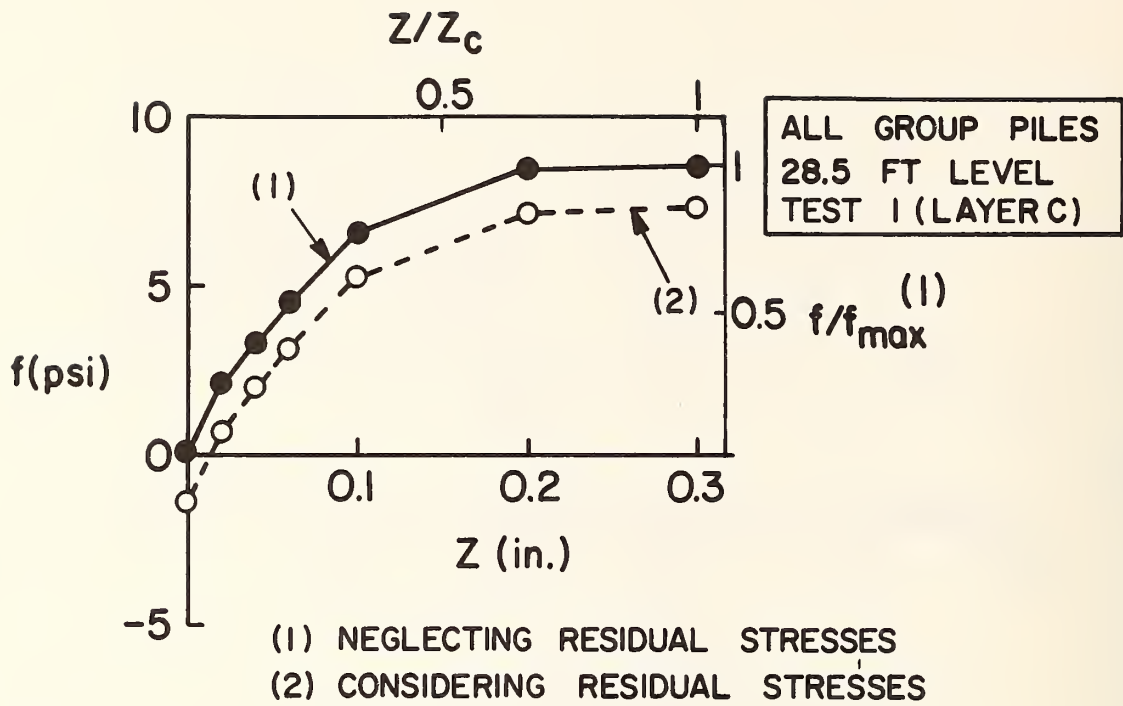


FIGURE 3.22. F-Z CURVES; SOIL ZONES C AND D; GROUP PILES; TEST 1,
(1 ft = 0.305 m; 1 in = 25.4 mm; 1 psi = 6.89 kN/m²)

These graphs refer to the first test set on the reference piles and 9-pile group, and in general each represents the average of f - z relationships developed at two or three stations between strain gage levels. Similar relationships for the remaining tests may be found in Appendix D. The f -values were obtained by differentiating fitted f - d curves at a given depth (e.g., 3.0 ft. (0.92 m)) for each value of applied load. Corresponding z -values were obtained by subtracting the elastic compression between the level of the settlement gages and the depth in question from the average settlement gage reading for the pile under consideration. The elastic compression was computed from the area under the partial measured load distribution versus depth curve divided by elastic stiffness.

These curves are instructive in visualizing the buildup of unit side shear with pile displacement in the various zones of soil, defined in Fig. 1.1. The curves for the reference piles are also necessary inputs into the pile group behavior model described in Chapter 4. The various f - z curves have been plotted considering both pretest zeros (apparent curves, which neglect residual stresses) and predrive zeros (true curves, which include the effects of residual stresses) and have also been plotted in normalized form, in which z_c is the displacement corresponding to peak load transfer. Several observations may be made concerning these curves: (1) the critical displacements in the reference piles are much smaller than had been anticipated, ranging from about 0.05 in. (1.3 mm) in Zones B and C to about 0.02 in. (0.5 mm) in Zone D, near the bottoms of the piles; (2) the average critical displacements for the piles in the 9-pile group ranged from about 0.2 in. (5.1 mm) in Zones B and C to about 0.1 in. (2.5 mm) in Zones A and D; (3) the differences between the curves which include residual stresses and those which neglect residual stresses could be classified as relatively minor.

Tip load versus tip movement curves (Q - z curves) for Test 1, derived from measured tip load (Q) and values of tip movement (z) computed by the method employed for computing z -values for the f - z curves, are shown in Fig. 3.23. Corrections to the z -values were made for the reference pile tests because of the very small movements associated with small tip loads coupled with small errors in measuring pile settlement (and thereby z at the tip) produced by surface temperature variations and computed pile flexibility.

Load Transfer Correlations

Correlations of apparent measured maximum unit side resistance values to soil shear strength obtained by several methods are presented in Table 3.4 for Test 1. Similar correlations for the other tests are presented in Appendix F. The correlations, which do not include residual stress effects, are ratios of maximum observed side shear stress to:

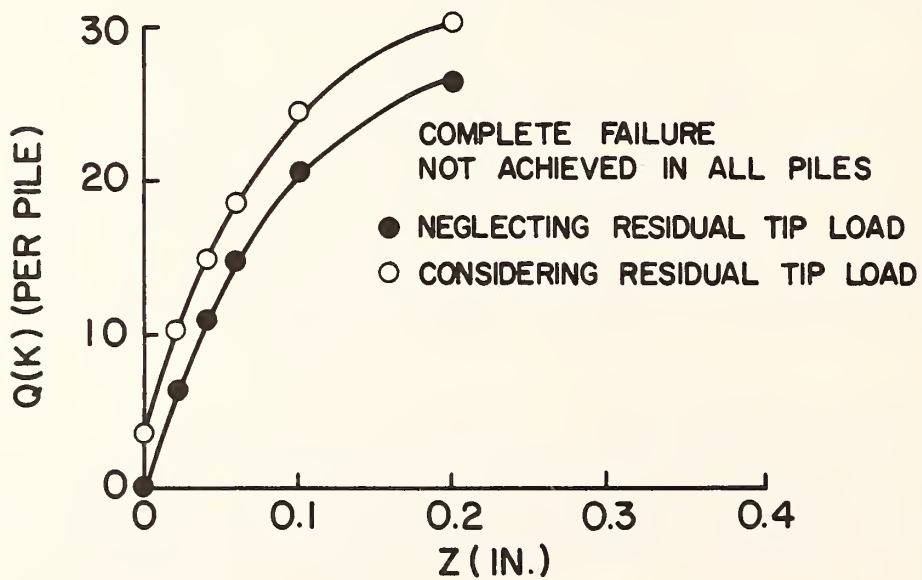
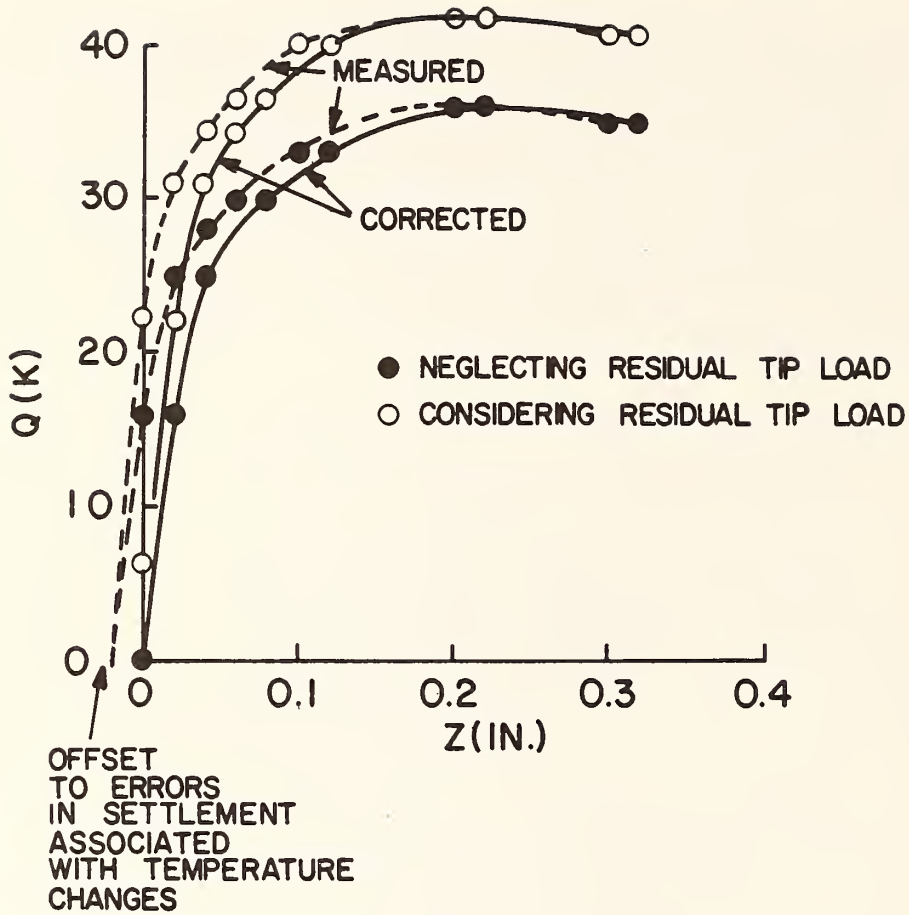


FIGURE 3.23. Q-Z CURVES FOR TEST 1; REFERENCE PILES (ABOVE); GROUP PILES (BELOW) (1 k = 4.45 kN; 1 in = 25.4 mm)

TABLE 3.4. SIDE RESISTANCE CORRELATION FACTORS,
9-PILE TEST 1 (1 FT = 0.305 m)

FACTOR (REFERENCE SOIL TEST)	AVERAGE OF REFERENCE PILES	AVERAGE OF GROUP PILES
α (UU TRIAX.)		
STRATUM A	0.08	0.07
B	0.65	0.58
C	0.67	0.68
D	0.54	0.45
OVERALL	0.48	0.44
α_{RC} (REMOLEDDED UU TRIAX.)	0.47	0.43
α (CONE SLEEVE)		
STRATUM A	0.16	0.16
B	0.96	0.86
C	1.21	1.23
D	1.48	1.37
OVERALL	0.95	0.88
α_{LP} (LIMIT PRESSURE)	0.0252	0.0234
α (CU TRIAX. W/ MEASURED PRETEST EFF. STRESS)		
DEPTH 9'	1.89	0.25
19'	1.61	0.57
34'	0.33	0.27
41'	0.47	0.58
$\bar{\alpha}$ (\overline{CU} TRIAX. W/ MEASURED EFF. STRESS AT FAILURE)		
DEPTH 9'	1.66	0.30
19'	2.37	0.54
34'	0.61	0.33
41'	0.60	1.23
λ (UU TRIAX.)	0.174	0.162
f_{max} (measured)		
$\frac{f_{max}}{f_{max}^{(GESM)}}$		
DEPTH 10'	0.49	0.32
20'	0.87	0.76
35'	0.64	0.68
40'	0.92	0.92

NOTE: Residual Stress Effects and Cap Weight Not Considered in Computations.

1. Shear strengths from UU triaxial compression tests on undisturbed samples (Fig. 1.2), resulting in the α factor.
2. Shear strengths from UU triaxial compression tests on remolded samples (Interim Report), resulting in the α_{RC} factor.
3. Shear strengths as indicated by sleeve friction on the static cone penetrometer.
4. The average limit pressure to a depth of 43 ft. (13.1 m) from the self-boring pressuremeter, yielding the α_{LP} factor.
5. The peak shear strengths inferred from the CU triaxial compression tests, in which the confining pressure equals the measured pretest lateral effective stress on the pile face. CU Mohr-Coulomb envelopes from Appendix C were used to assess these strengths.
6. The peak shear strengths inferred from the \overline{CU} triaxial compression tests, in which the confining pressure equals the lateral effective stress measured at failure. Composite effective stress Mohr-Coulomb envelopes for each zone from Appendix C were used to obtain these shear strengths. The ratio obtained from this correlation is denoted the $\bar{\alpha}$ factor.
7. The average UU triaxial shear strength to a depth of 43 ft. (13.1 m) plus twice the average vertical quasi-effective stress between the surface and that depth, denoted the λ factor.

The ratio of maximum measured side shear stress to maximum side shear stress computed by a version of the General Effective Stress Method (GESM) (Ref. 5 of Appendix A) is also given in Table 3.4.

Correlations 1, 3, 5, 6, and the GESM correlation were made for the reference tests and the group test for each of the four principal soil zones or at four distinct depths. For Correlations 5 and 6, they were made using the measured effective stresses on the piles at the indicated depths and the shear strength parameters shown in Table 3.5, which were interpreted from the data in Appendix C (although they are not exactly equal to the cohesion and internal friction values tabulated in that Appendix). The remaining three correlations were average correlations over the entire embedded lengths of the reference and group piles.

The following comments are offered concerning the correlations:

1. The best overall correlation was with the cone sleeve, although it overpredicted load transfer in Zone (Stratum) A near the top of the pile and underpredicted load transfer in Zones C and D, near the bottoms of the piles.

TABLE 3.5. INTERPRETED PEAK COHESION (c) AND ANGLE OF INTERNAL FRICTION (ϕ) VALUES USED FOR LOAD TRANSFER CORRELATIONS
 (1 ft = 0.305 m; 1 psf = 47.9 N/m²)

Depth (ft)	Cohesion (psf)		Angle of Internal Friction (degrees)	
	c (CU)	\bar{c} ($\bar{C}U$)	ϕ (CU)	$\bar{\phi}$ ($\bar{C}U$)
9	440	500	25	22
19	300	0	19	23
34	2,500	200	20	28
41	2,500	0	20	27

2. The α (UU triaxial) correlation was near the median value of 0.45 to 0.50 currently used in stiff to very stiff clay by designers. Correlation to the remolded undrained shear strength was almost identical to that for undisturbed undrained strength due to the characteristically underrepresented undisturbed values produced by sample disturbance and preferential failure along fissure planes.
3. The λ correlation was below the nominal value of 0.22 generally recommended for a 43 ft. (13.1 m) penetration.
4. The correlations with measured preload effective stresses and effective stresses at failure were not especially good. This may be due largely to the fact that the soil strength at failure may better be represented by a residual strength from a direct or simple shear test than by peak strengths obtained from triaxial compression tests.
5. The GESM predicted values of load transfer that were generally too large, although the depthwise accuracy achieved was generally equivalent to that achieved with the cone sleeve.

An additional rational correlation, not addressed in Table 3.4 but referred to above, is the ratio of measured maximum unit side load transfer to shear strength computed by the product of the measured effective stress times the tangent of the residual angle of internal friction. This was not done because the residual friction angles reported in Appendix C are unrepresentative of the soils at the site, possibly because complete residual conditions had not been achieved in the laboratory tests. Representative values are believed to be approximately as follows:

$$\begin{aligned} \bar{\phi} &= 17 \text{ deg. at } 9 \text{ ft. (2.75 m) depth} \\ &= 13 \text{ deg. at } 19 \text{ ft. (5.80 m) depth} \\ &= 22 \text{ deg. at } 34 \text{ ft. (10.37 m) depth} \\ &= 25 \text{ deg. at } 41 \text{ ft. (12.51 m) depth.} \end{aligned}$$

If the tangents of the above angles are multiplied times the average measured effective stress at failure at each depth in all five piles instrumented for lateral effective stress and the result divided into the average measured apparent unit side resistances in those five piles for the first load test, the following dimensionless correlation factors result:

$$\begin{aligned} &0.90 \text{ at } 9 \text{ ft. (2.75 m) depth} \\ &1.27 \text{ at } 19 \text{ ft. (5.80 m) depth} \\ &0.49 \text{ at } 34 \text{ ft. (10.37 m) depth} \\ &0.82 \text{ at } 41 \text{ ft. (12.51 m) depth.} \end{aligned}$$

The above factors do not consider effects of residual stress, which if included, should cause the factors to tend more toward unity. The

generally good correlations indicate that assessment of pile capacity in overconsolidated clay based on estimated lateral effective stress and measured residual shear strength could conceivably be reliable.

Other correlations of possible interest to designers could be developed from the available data, including correlations with unconfined compressive strength, pocket penetrometer strength, and standard penetration test results. Such correlations, however, have not been included in this report. The unconfined compression and normalized parameter strengths should yield α factors in the same order as those developed using UU triaxial test results.

Variability of Load Transfer

The load transfer correlation factors shown on Table 3.4 and on the corresponding tables in Appendix F are average values for the reference or group piles for the soil zones (strata) indicated. The variability of the α factors based on UU triaxial and static cone test results from pile to pile and layer to layer can be assessed by multiplying the δ factors from Table 3.6 times the average α factor (for reference or group pile, as appropriate) given for the stratum of concern in Table 3.4. For example, the α factor (UU triaxial) for Pile 3, a group pile, in Stratum B was 0.96 (Table 3.6) times 0.58 (Table 3.4), or 0.56. Analysis of Table 3.6 reveals that the α factors (and therefore unit side load transfer) was relatively uniform among the group piles, except in Stratum A.

Load Transfer Correlation Factors at Pile Tips

Correlations of maximum average developed tip load in the reference and group piles to UU triaxial shear strength and to peak static cone tip resistance in the soil immediately below the pile tips are given in Table 3.7.

End bearing correlations, which yield end bearing capacity factors with respect to the tests mentioned, were made with and without consideration of residual tip loads. Measured residual tip loads were used for Test 1; computed loads based on the procedure described earlier for assessing residual side shear were used for Test 3 for the reference piles and for the last compressive loading on the group piles. The tip loads used to develop these factors are actual loads measured one ft. (0.305 m) above the tips. It has been tacitly assumed that no side resistance existed in the bottom one ft. (0.305 m) (approximately one diameter) of the piles. If load were in fact transferred in this zone, the factors given in Table 3.7 would be too high.

Correlations with UU triaxial test results yielded unrealistically high factors, probably due to two effects: (1) sample disturbance and (2) frictional behavior along with full or partial drainage in the soil beneath the pile tips, due to the high sand content of that soil, that

TABLE 3.6. FACTORS (δ) FOR COMPUTING α CORRELATIONS FOR INDIVIDUAL PILES AND LAYERS, 9-PILE TEST 1 (1 ft = 0.305 m)

PILE	STRATUM A (0 - 10')	STRATUM B (10' - 26')	STRATUM C (26' - 30')	STRATUM D (30' - 43')
1 (REF)	1.07	1.10	1.11	1.16
2	0.82	0.99	1.07	1.04
3	1.59	0.96	0.90	0.91
4	1.70	1.06	0.93	0.90
5	0.73	0.90	0.87	1.24
6	0.29	0.90	1.12	1.27
7	0.82	0.93	1.00	1.02
8	1.22	0.94	0.78	0.79
9	1.12	1.12	1.14	0.83
10	0.71	1.20	1.20	0.99
11 (REF)	0.93	0.90	0.89	0.84

NOTE: α for a particular pile and layer = δ from above table times α from Table of Average Correlation Factors. This does not apply to α_{LP} (LIMIT PRESSURE) or λ .

$$\delta = \frac{\text{MEASURED LOAD TRANSFER FOR PILE/STRATUM}}{\text{AVG. LOAD TRANS. FOR STRATUM FOR REF. OR GROUP PILES}}$$

TABLE 3.7. AVERAGE END BEARING CAPACITY FACTORS FOR REFERENCE AND GROUP PILES

Test, Piles	UU Triaxial, ⁽¹⁾ Neglecting Residual Tip Load	Cone Tip, ⁽²⁾ Neglecting Residual Tip Load	UU Triaxial, ⁽¹⁾ Including Residual Tip Load	Cone Tip, ⁽²⁾ Including Residual Tip Load
1, Reference Piles	31.8	0.65	37.5	0.77
1, Group ⁽³⁾ Piles	31.8	0.65	35.0	0.72
2, Reference Piles	24.3	0.50	----	----
2, Group Piles	32.2	0.66	----	----
3, Reference Piles ⁽⁴⁾	21.6	0.42	47.2	0.93
Last Loading ^{(4) (5)} Group Piles	23.1	0.45	56.4	1.11

- (1) Peak unit end bearing stress divided by undrained cohesion at 43-45 ft. (13.1-13.7 m) from UU triaxial test.
- (2) Peak unit end bearing stress divided by average peak tip bearing stress at 43-45 ft. (13.1-13.7 m) registered by static cone.
- (3) Includes only those piles where tip failure occurred.
- (4) Residual load values obtained by adjustment procedure involving uplift tests.
- (5) Includes only group piles subjected to uplift tests (2, 4, 5, 9). Last Loading taken as 4-pile Subgroup test for Piles 5 and 9 and third 9-pile Test for Piles 2 and 4.

could not be properly represented by the undrained triaxial tests. The cone tip correlations were much better. A correlation factor of about 0.65 (measured on pile / cone tip reading) appears appropriate for apparent capacity upon first loading for both the group and reference piles. The correlation factor approached 1.0 after several loadings (total gross tip movement of 20-40 percent of pile diameter) when residual load effects were considered.

Chapter 4. Reanalysis of Performance Using Hybrid Model

Introduction

The hybrid method of pile group analysis has been described in some detail in the Interim Report and in Appendix A of this report. Chapter 4 of the Interim Report contained a prediction of the response of the test group, assuming certain ideal conditions and preliminary estimates of pile penetrations and soil properties using Program GP3B, an early algorithmic version of the hybrid model. An improved version of the hybrid model, Program PILGP1 (described in Appendices A and B), was used to model the performance of the test group upon completion of the field tests. This analysis, which is described in this chapter, used results of the site investigation performed for the study and as-built pile penetrations. Two solutions were obtained: (1) Using unit load transfer curves measured from the reference piles and complete as-built geometry (including inadvertant batters and true pile spacing) as inputs (hereafter called the "reanalyzed" solution) and (2) Using unit load transfer curves developed from criteria and ideal (as-planned) spacing and zero batters as inputs, hereafter called the "criterion" solution. The criterion solution represents a solution that could be made by a designer with minimal data. For the criterion solution, the following criteria (refer to Appendix A) were applied:

$$\underline{f-z \text{ Curves:}} \quad f = f_{\max} [2(z/z_c)^{0.5} - z/z_c]$$

$$\text{where} \quad f_{\max} = \alpha c_u$$

$$z_c = \frac{f_{\max} r}{G} [0.67 + \ln \frac{2\rho l(1-\nu)}{r}]$$

in which

f = unit side resistance

f_{\max} = maximum unit side resistance

z = pile deflection

z_c = pile deflection corresponding to f_{\max}

c_u = undrained shear strength from triaxial compression tests

α = proportion factor (=0.5 for most of soil profile)

r = pile radius

- ν = Poisson's ratio of soil (=0.5)
- G = Shear modulus of soil
- l = Pile penetration (=43 ft or 13.1 m)
- ρ = G at middepth of pile/ G at pile tip.

For this analysis G was taken as that value given by the self-boring pressuremeter at the various depths at which f - z curves were input. G was observed to be about 450 times the UU triaxial shear strength of the soil.

Q-z curve: $Q = Q_{\max} (z/z_c)^{0.33}$

where Q = end bearing force

Q_{\max} = bearing capacity
 $= 9 \times \text{tip area} \times \text{UU triaxial shear strength of soil at elevation of pile tips}$

z = tip deflection

z_c = 0.03 x tip diameter.

Tests Modeled

For purposes of examining the capabilities of the model to predict pile group performance, 9-pile Test 1, the 5-pile Subgroup Test, and the 4-pile Subgroup Test were modeled. The former test was modeled with the reanalyzed and the criterion solutions, while the latter tests were modeled only with the reanalyzed solution.

Geometric Inputs

A coordinate system was established with its origin (O) at the geometric center of the bottom of the pile cap, as shown in Fig. 4.1. Coordinates in the X-Z plane were then established for the pile heads, assumed to be at the base of the rigid cap. These coordinates for the reanalyzed solution, also shown in Fig. 4.1, were taken to be identical to the coordinates at the actual pile tops, reported in Chapter 1. For the reanalyzed solution, the direction angles for the piles, as projected onto the X-Z plane, were taken as shown in Fig. 4.2 and are based on measurements reported in Chapter 1. The true batter slopes, or base offsets divided by pile lengths, also input into PILGP1, are tabulated in Table 4.1, which additionally gives tabular values of pile head coordinates and direction angles. For the criterion solution, the center of the pile cap coincided with Pile 2, and the unbattered piles were taken to be on a 32.25 in. (819 mm) grid.

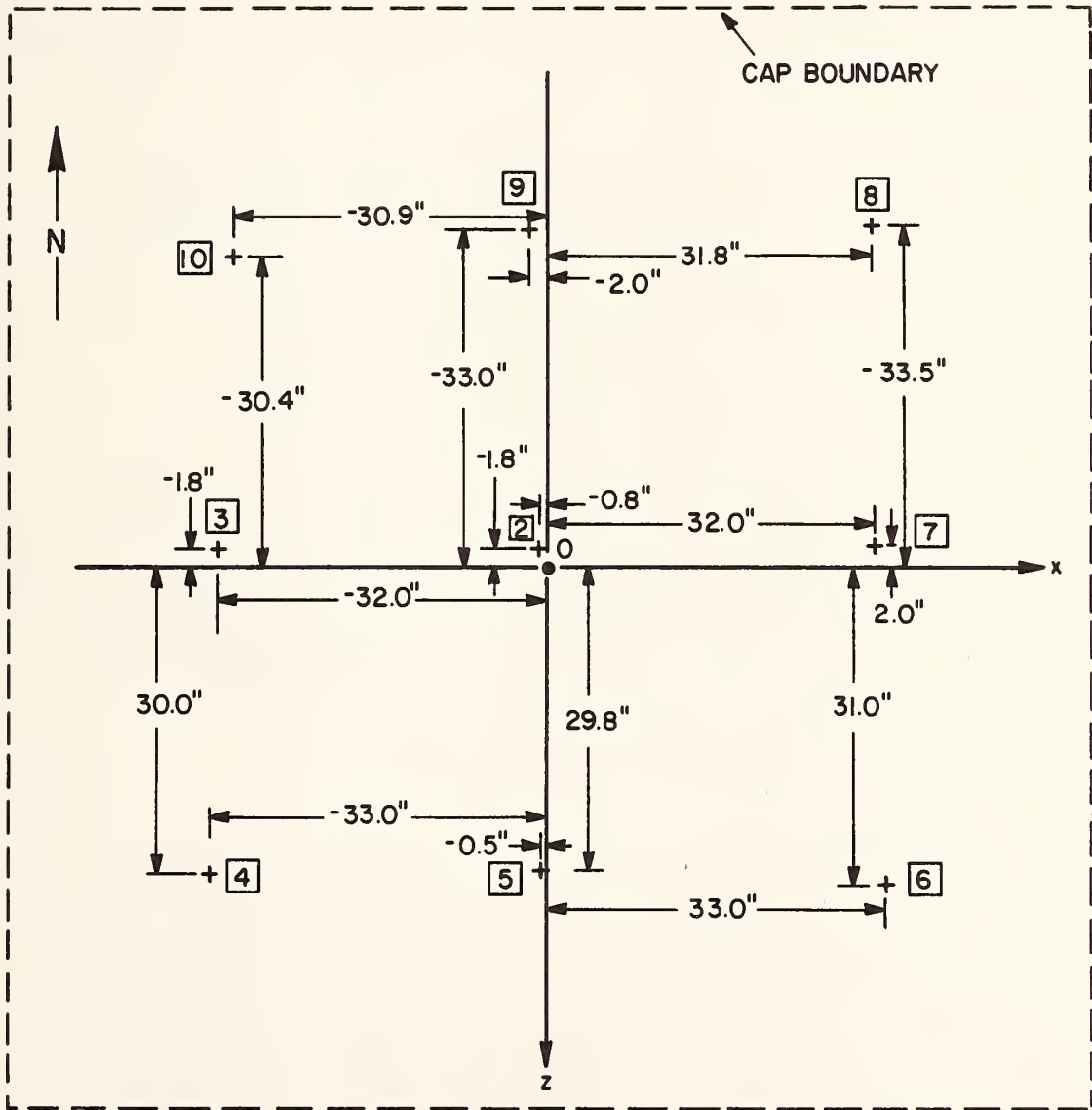


FIGURE 4.1. PILE HEAD COORDINATES FOR PILGP1 ANALYSIS (1 in = 25.4 mm)

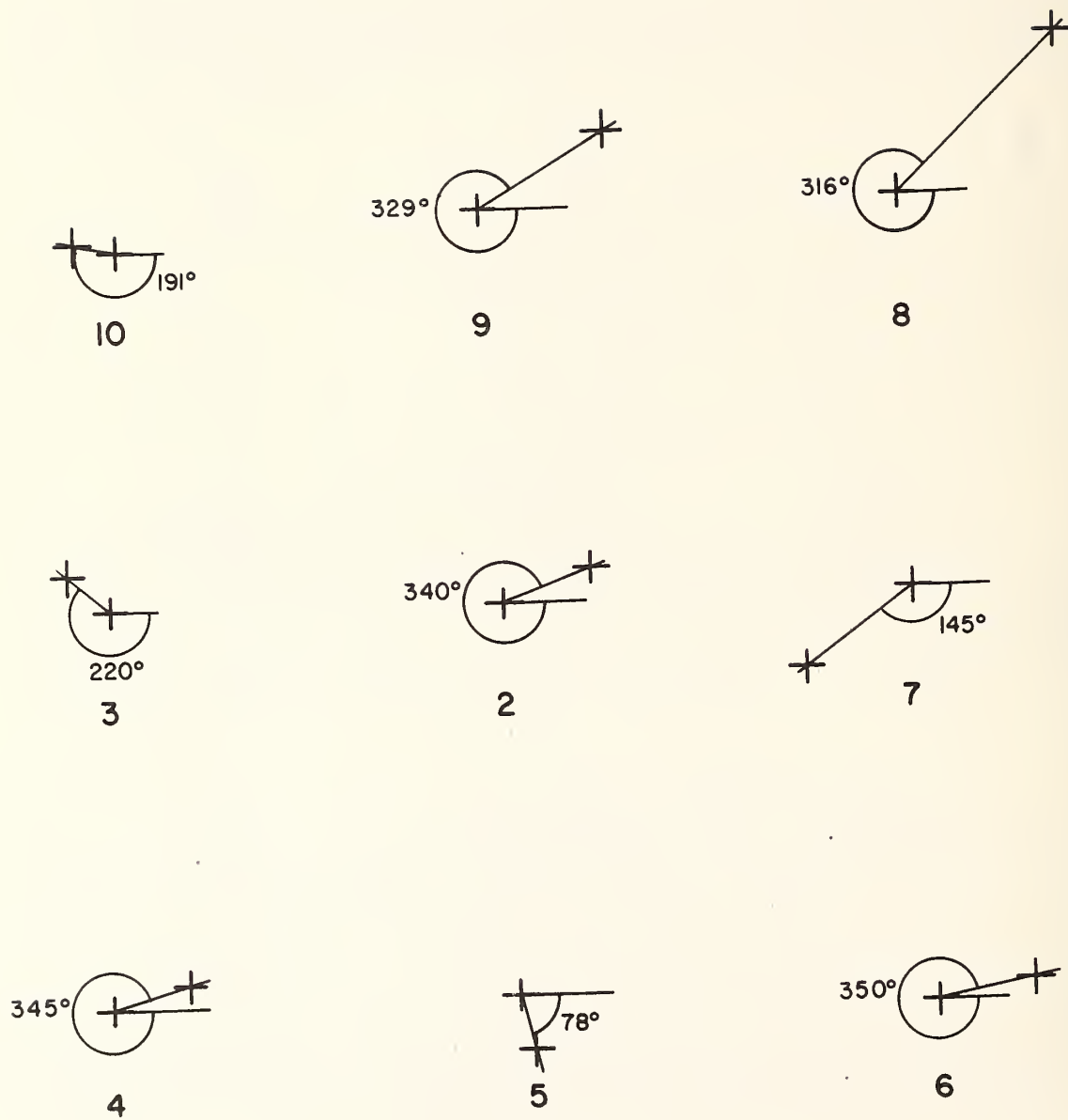


FIGURE 4.2. DIRECTION ANGLES

TABLE 4.1. PILE GEOMETRY FOR PILGP1 REANALYSIS (1 in. = 25.4 mm)

Pile	Direction angle α (deg.)	True batter slope	Pile head coordinates (in.)		
			X	Y	Z
2	340	0.014	- 0.8	0.0	- 1.8
3	220	0.009	-32.0	0.0	- 1.8
4	345	0.013	-33.0	0.0	30.0
5	78	0.008	- 0.5	0.0	29.8
6	350	0.014	33.0	0.0	31.0
7	145	0.020	32.0	0.0	- 2.0
8	316	0.033	31.8	0.0	-33.5
9	329	0.022	- 2.0	0.0	-33.0
10	191	0.007	-30.9	0.0	-30.4

Loadings

The loading inputs for the reanalyzed solution were developed from the loads measured at each of the four jack locations. Variation of load from jack to jack and slight positioning anomalies for the jacks were taken into account by also inputting moments about the X and Z axes equal to the sums of the products of the jack loads and the moment arms depicted in Fig. 4.3. Multiple loadings, not associated with measured loads, were also run in order to develop the entire load-settlement curve. Cap weight was not included in the applied loads. Similar considerations were made for the criterion solution, except that no load eccentricity was used.

Structural Properties

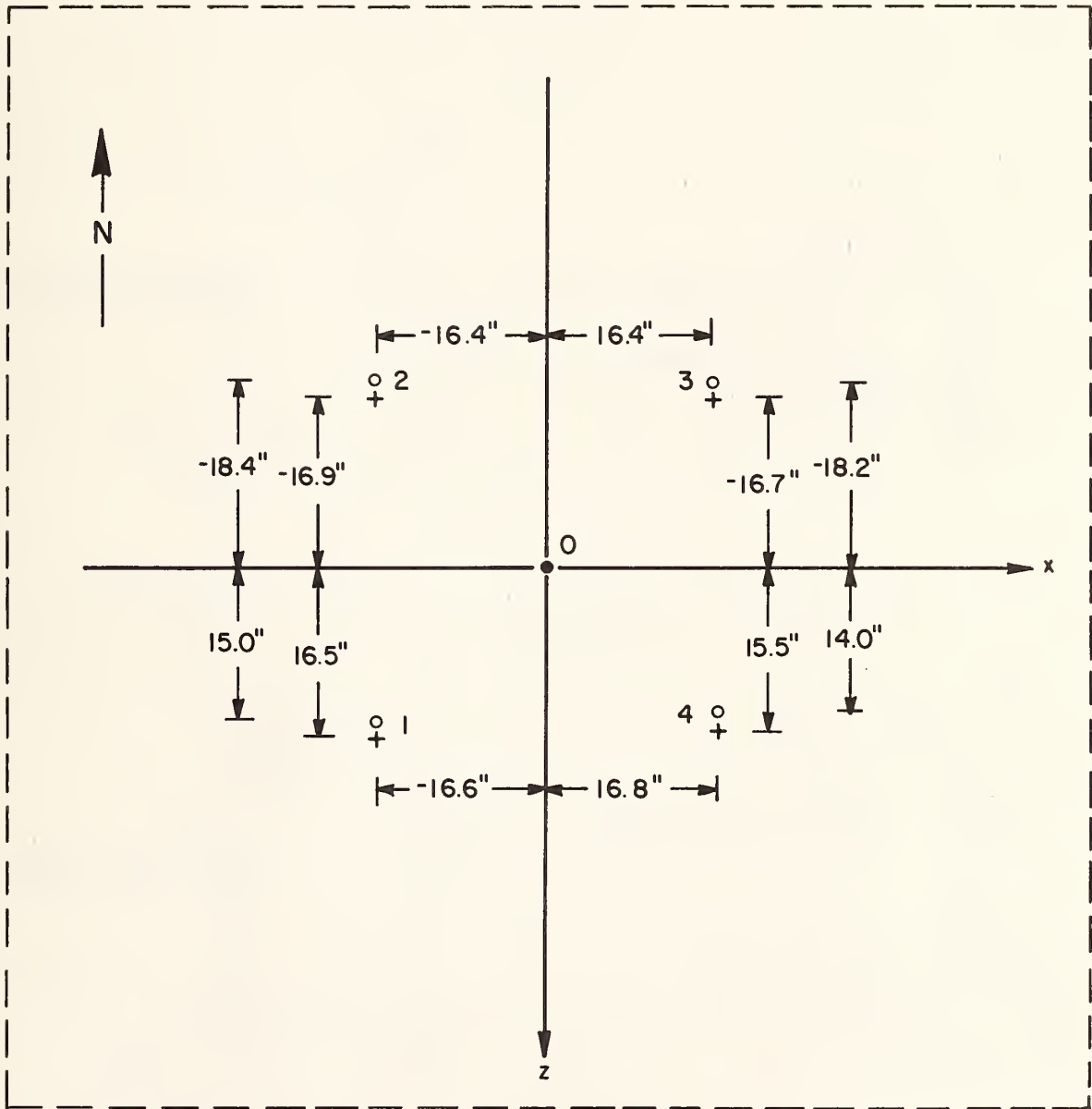
Each pile was assigned a cross-sectional area of 11.91 square in. (7884 square mm) and a Young's modulus of 30,000,000 psi (206,000 mN/m²). Moments of inertia were computed internally within the program from the inside and outside diameters of the piles (10.02 and 10.75 in., respectively) (255 and 273 mm, respectively). Each pile was specified to protrude 3 ft. (0.915 m) above the ground surface. Forty-six discrete elements were used to represent the piles.

Soil Inputs

For unit side shear, four f-z curves were assumed to represent soil response. These curves are shown in Fig. 4.4. Each specific curve for the reanalyzed solution was developed by averaging the experimental f-z curves (obtained at 5-ft. (1.53 m) depth intervals beginning at a depth of 3 ft. (0.92 m)) within the depth intervals noted from Piles 1 and 11. The Q-z curve for the reanalyzed solutions, Fig. 4.5, is the average corrected curve for the reference piles. Soil inputs for the criterion solution are described on pp. 169-170. Exact inputs for the unit load transfer curves are tabulated in Tables 4.2 and 4.3.

Since the piles were nearly vertical, lateral unit soil resistance curves (p-y curves) were not input, except for one run to compare results obtained with and without inputting these curves. For this special run the non-cyclic stiff clay criteria described in Appendix A were employed to develop p-y curves.

For purposes of making group effect calculations the Poisson's ratio of the soil was taken at 0.5 (incompressible soil) and the variation of Young's modulus (E) with depth was taken in accordance with the relationship shown in Fig. 1.3 for the in-situ pressuremeter. Several other, constant values of E were also input in order to assess the sensitivity of the solution to the choice of E and to obtain the optimum value with respect to prediction of load-settlement and load transfer.



○ Position for subgroup tests

⊕ Position for 9-pile test no. 1

FIGURE 4.3. JACK COORDINATES (1 in = 25.4 mm)

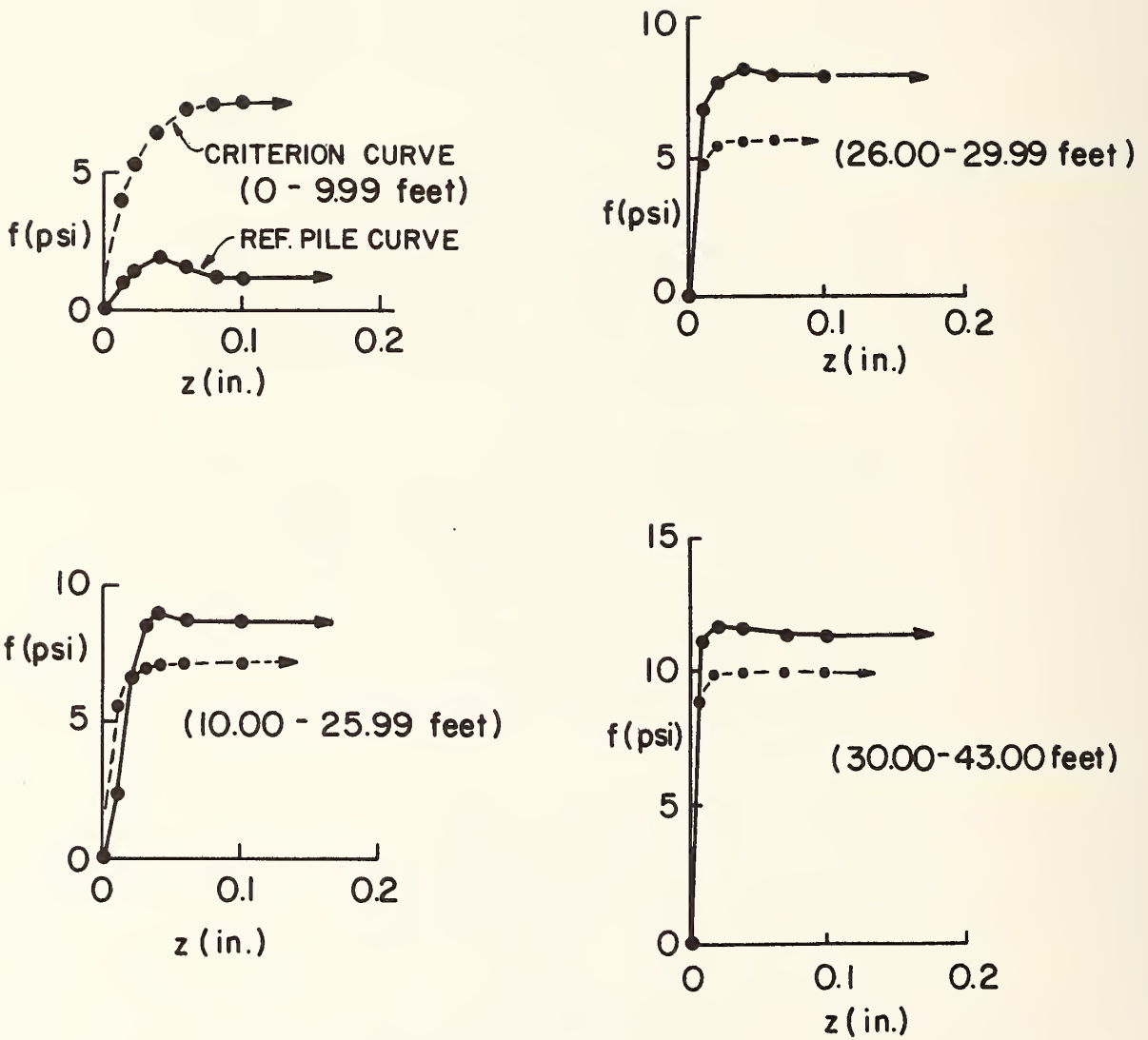


FIGURE 4.4 F-Z CURVES FOR PILGP1 INPUT (1 psi = 6.89 kN/m² ;
 1 ft. = 0.305 m ; 1 in. = 25.4 mm)

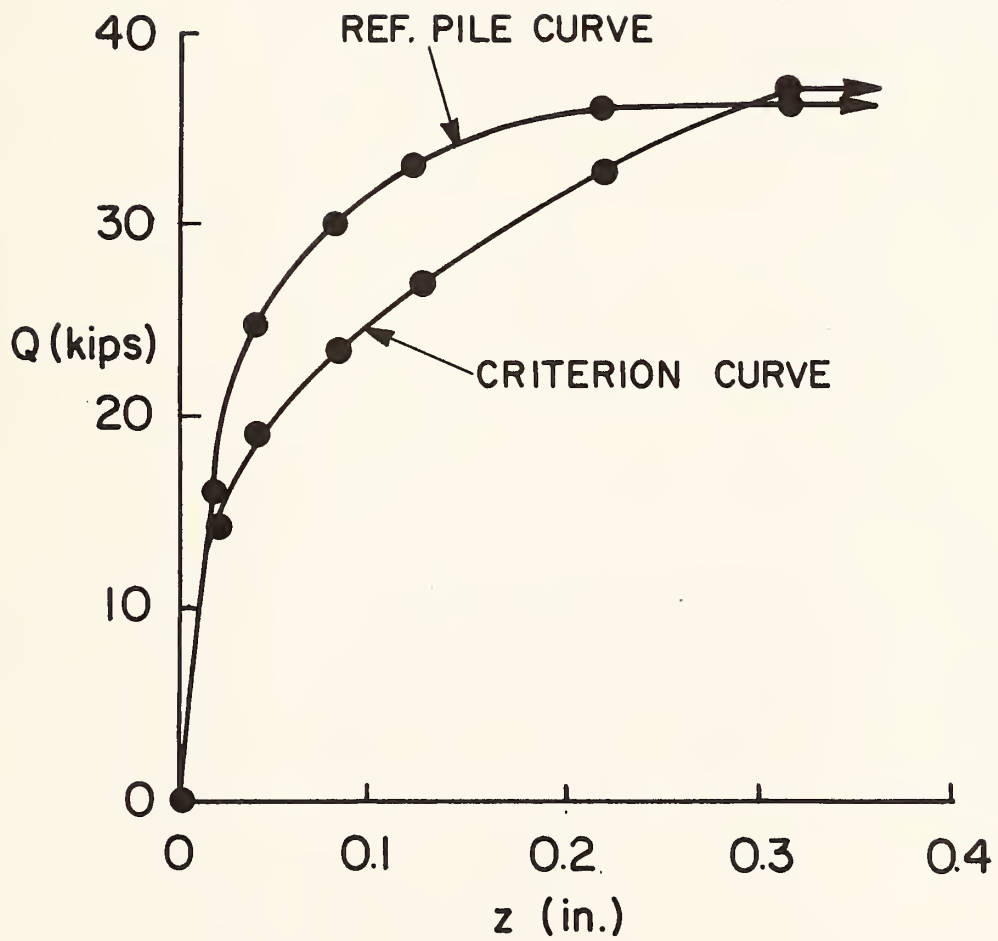


FIGURE 4.5. Q-Z CURVE FOR PILGP1 INPUT
 (1 k = 4.45 kN; 1 in. = 25.4 mm)

TABLE 4.2. f-z CURVES FOR PILGP1 SOLUTIONS: REANALYZED AND CRITERIA (1 in. = 25.4 mm, 1 ft. = 0.305 m, 1 psi = 6.89 kN/m²)

z (in.)	f (rean.) f (crit.) (psi) (psi) (0-2.99 ft.)	f (rean.) f (crit.) (psi) (psi) (3.00-12.99 ft.)	f (rean.) f (crit.) (psi) (psi) (13.00-28.99 ft.)	f (rean.) f (crit.) (psi) (psi) (29.00-32.99 ft.)	f (rean.) f (crit.) (psi) (psi) (33.00-46.00 ft.)
0.00	0 0	0.00 0.00	0.00 0.00	0.00 0.00	0.00 0.00
0.01	0 0	0.80 3.90	2.35 5.42	5.00 4.75	11.00 8.89
0.02	0 0	1.30 5.14	6.55 6.38	6.70 5.20	11.55 9.72
0.04	0 0	1.85 6.43	8.45 6.60	7.70 5.20	11.40 9.72
0.06	0 0	1.45 7.12	8.85 6.60	8.20 5.20	11.30 9.72
0.08	0 0	1.05 7.47	8.65 6.60	7.95 5.20	11.25 9.72
0.10	0 0	1.05 7.62	8.50 6.60	7.95 5.20	11.25 9.72
1.00	0 0	1.05 7.64	8.50 6.60	7.95 5.20	11.25 9.72

NOTE: PILE PROPERTIES:

Inside diameter: 10.02 in. Young's Modulus = 30 x 10⁶ psi

Outside diameter: 10.75 in. Area = 11.908 sq. in.

TABLE 4.3. Q-z CURVES FOR PILGP1 SOLUTIONS
 (1 in. = 25.4 mm, 1 kip = 4.45 kN)

z (in.)	Q (rean.) (Kips)	Q (crit.) (Kips)
0.00	0.00	0.00
0.02	16.00	14.40
0.04	24.80	18.40
0.08	29.60	22.80
0.12	33.00	26.40
0.22	35.00	32.00
0.32	35.70	36.40
1.00	35.70	36.40

NOTE: Q (crit.) values were obtained by assigning cohesion values equal to 4 times 'U' triaxial values, since observation of profile reveals that UU triaxial strengths significantly underpredict in-situ strength in sandy clay near pile tips.

Results - Single Pile

The single (reference) pile behavior produced by PILGP1 from the input described previously is represented in Figs. 4.6 and 4.7, which compare measured and predicted pile head load-settlement behavior and load distribution along the piles. In each case the "measured" values are averages of Piles 1 and 11. The "computed" values are for the reanalyzed solution and the "computed (cr)" values are for the criterion solution. The slight overprediction of capacity observed in Fig. 4.6 for the reanalyzed solution is due to the use of average f-z curves over the depth regions defined in Fig. 4.4 instead of using separate f-z curves for each of the 46 discrete elements. Some further error was introduced by using f-z curves that were derived from fitted, rather than raw, load distribution diagrams. The same general comments apply to the comparisons of load distribution shown in Fig. 4.7, which was made only for the reanalyzed case. Theoretically, the measured and computed load distribution curves should be identical since the program is modeling the test from which the inputs were derived.

Based on the comparisons shown in Figs. 4.6 and 4.7, the unit load transfer inputs were judged appropriate to model the group tests. Since the computed single pile capacity from the reanalyzed case exceeded the average measured failure load by an amount almost equal to the set-up that occurred between the first and final tests, no alterations in the f-z or Q-z curves were made for purposes of modeling the two subgroup tests.

Results - Pile Groups

9-Pile Test 1. Comparative plots of the load-settlement curves obtained for 9-pile Group Test 1 are presented in Fig. 4.8. The curves shown on that figure are the measured load-settlement curve, the reanalyzed load-settlement curve obtained by using the previously described f-z and Q-z curves and no p-y curves for the variation in soil modulus indicated by the pressuremeter, the reanalyzed load-settlement curve obtained by using a uniform soil modulus of 25 ksi (172 mN/m²) and no p-y curves, and a repeat of the 25 ksi (172 mN/m²) run for the reanalyzed case including p-y curves developed according to the stiff clay criteria. The criterion case is also shown for E=25 ksi (172 mN/m²).

It is obvious that inputting an elastic modulus (E) variation equivalent to that measured in-situ with the self-boring pressuremeter (2.5 ksi (17.2 mN/m²) at the surface, varying linearly to 11.5 ksi (79.2 mN/m²) at the depth of the pile tips) produced a softer load-settlement relationship than that which was measured. Use of modulus values from the UU triaxial or normalized strength triaxial tests would have resulted in even greater discrepancies. The best match occurred when E use taken as a depthwise uniform value of 25 ksi (172 mN/m²), which is slightly greater than twice the in-situ modulus in the soil immediately

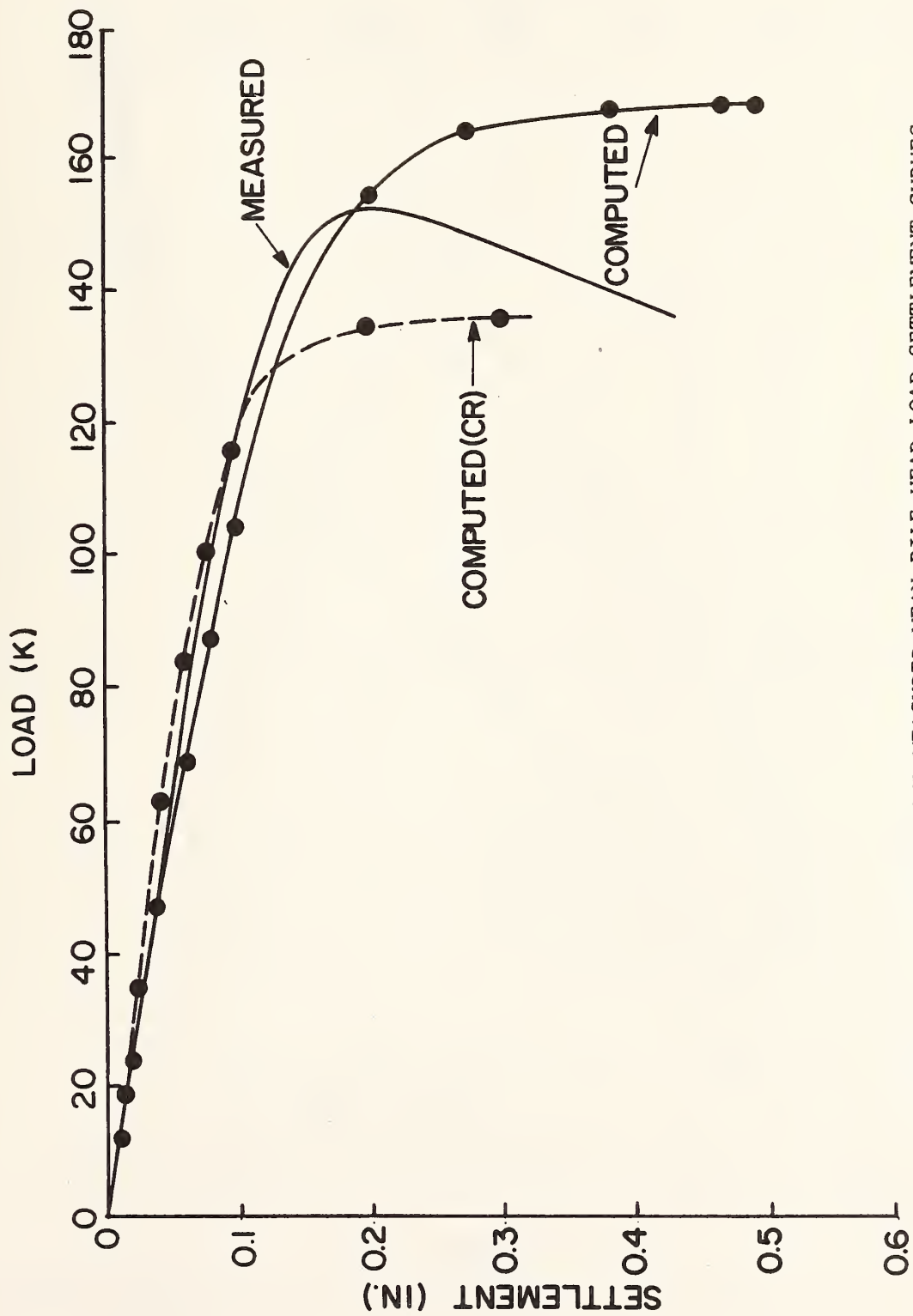


FIGURE 4.6. COMPUTED AND MEASURED MEAN PILE HEAD LOAD-SETTLEMENT CURVES; REFERENCE PILES; TEST 1; PILGP1 (1 k = 4.45 kN; 1 in = 25.4 mm)

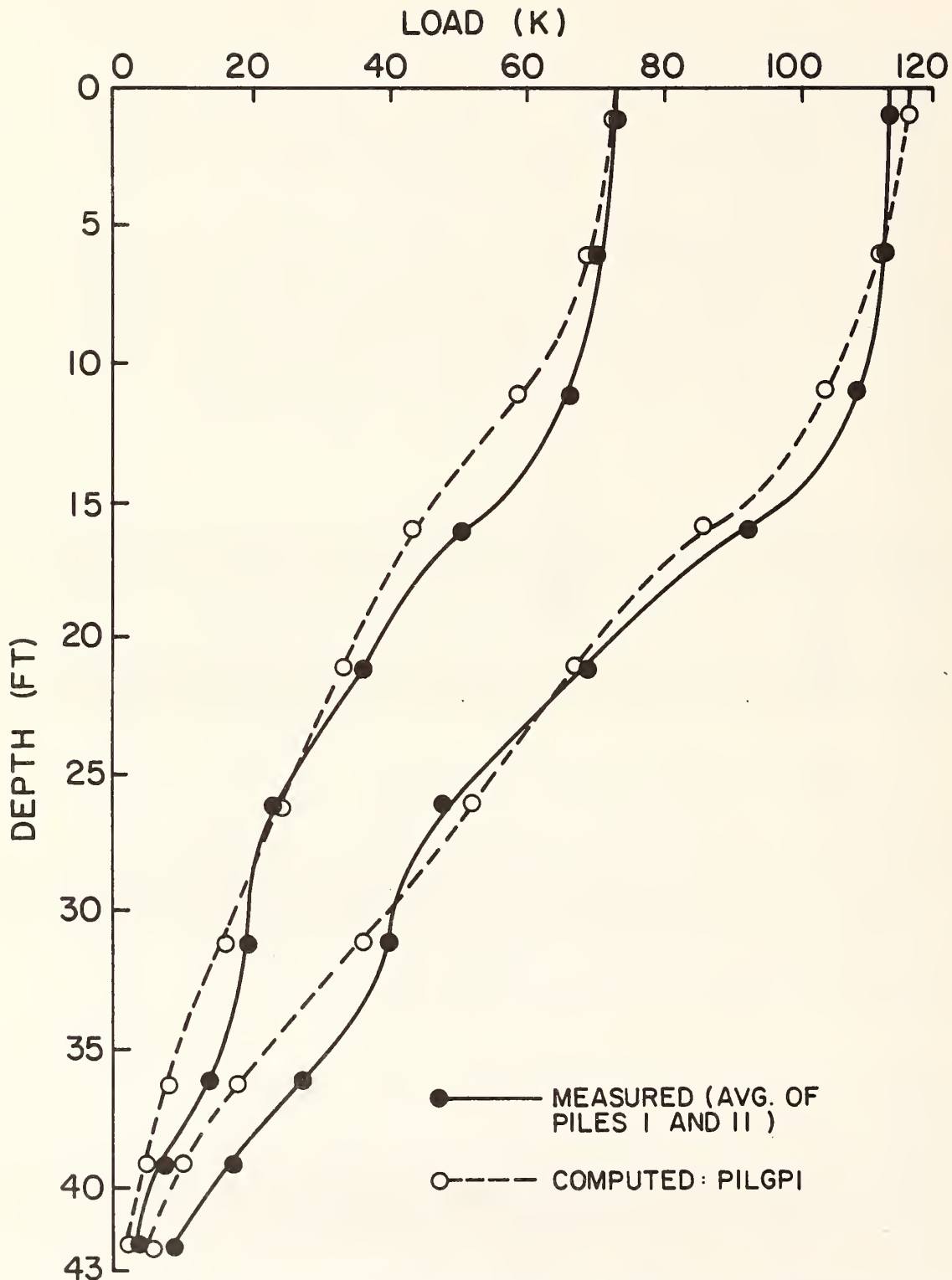


FIGURE 4.7. COMPUTED AND MEASURED MEAN DISTRIBUTION OF LOAD; REFERENCE PILES; TEST 1; PILGP1 (1 k = 4.45 kN; 1 ft = 0.305 m)

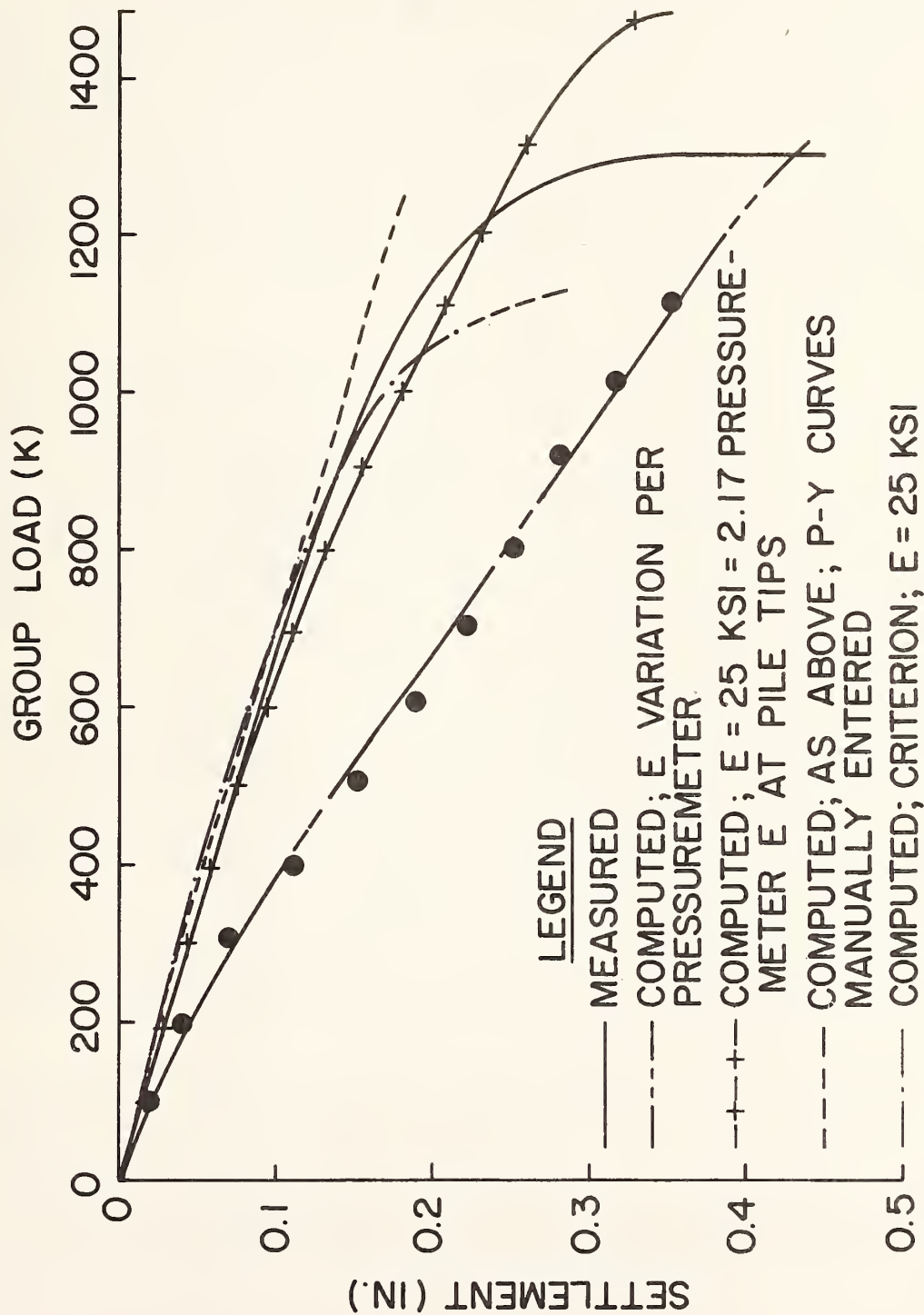


FIGURE 4.8. MEASURED AND COMPUTED LOAD-SETTLEMENT CURVES; 9-PILE TEST 1
 (1 k = 4.45 kN; 1 psi = 6.89 kN/m²; 1 in = 25.4 mm)

below the pile tips as indicated by the pressuremeter but less than either the average E along the depth of the piles or the E just below the tips of the piles indicated by the crosshole seismic tests. The appropriateness of such a high value for E can be explained in terms of the low strain values measured in the soil around the group, the reinforcing effects of the piles on the soil not accounted for explicitly in the hybrid model, and the influence of the relatively stiffer soils beneath the pile tips on the load-settlement behavior. With respect to the low measured strain values, even the self-boring-type pressuremeter used in the field study requires some lateral straining to seat the expanding membrane firmly against the sides of the borehole, so that the reported moduli were not obtained at strain amplitudes as low as those produced in the soil outside the immediate vicinity of the individual piles in the group.

The best-fit E value corresponds to an average E/c of 1400 when c is based on average UU triaxial test results to a depth of 45 ft. (13.7 m). This ratio is consistent with the general range of values observed in the Interim Report for the BRE and AREA tests, which were also conducted in overconsolidated clay. Since the measured settlements may have been too low by perhaps 10 to 20 percent at low load values due to small movements of the reference system relative to the group, it may be assumed that a more appropriate E/c for predicting true load-settlement behavior for the soil at this site would be about 1200. This compares with the range of 400 to 800 originally assumed in the first analysis reported in Chapter 4 of the Interim Report.

The dashed curve in Fig. 4.8 is also for a uniform E of 25 ksi (172 mN/m²), but p-y curves were included as inputs for the computations employed to develop that curve. It can be seen that the inclusion of p-y curves in a case where the piles are slightly battered, as occurred here, influences the vertical load-settlement behavior. When p-y curves are not input the model must generate pile-head stiffness terms artificially whenever battered piles exist. In the case of the stiff soil at this site these stiffnesses were slightly too soft.

The overestimation of capacity in the reanalyzed solution was the result of the overestimation of single pile capacity produced by the use of average f-z curves, discussed earlier.

Computed and measured settlement ratios are shown in Fig. 4.9. Program PILGP1 does not output settlement ratios directly but they can easily be deduced from the non-interactive axial mode curve (load-settlement tabulation for an isolated pile) and the computed group settlement. The value of computed settlement ratio is somewhat dependent on the exact formulation used for the f-z and Q-z curves, as can be seen by comparing criteria and reanalyzed results. Better matches in both the settlement ratios and load-settlement plots could have undoubtedly been obtained by manipulation of the input parameters. However, this was not the objective of this analysis.

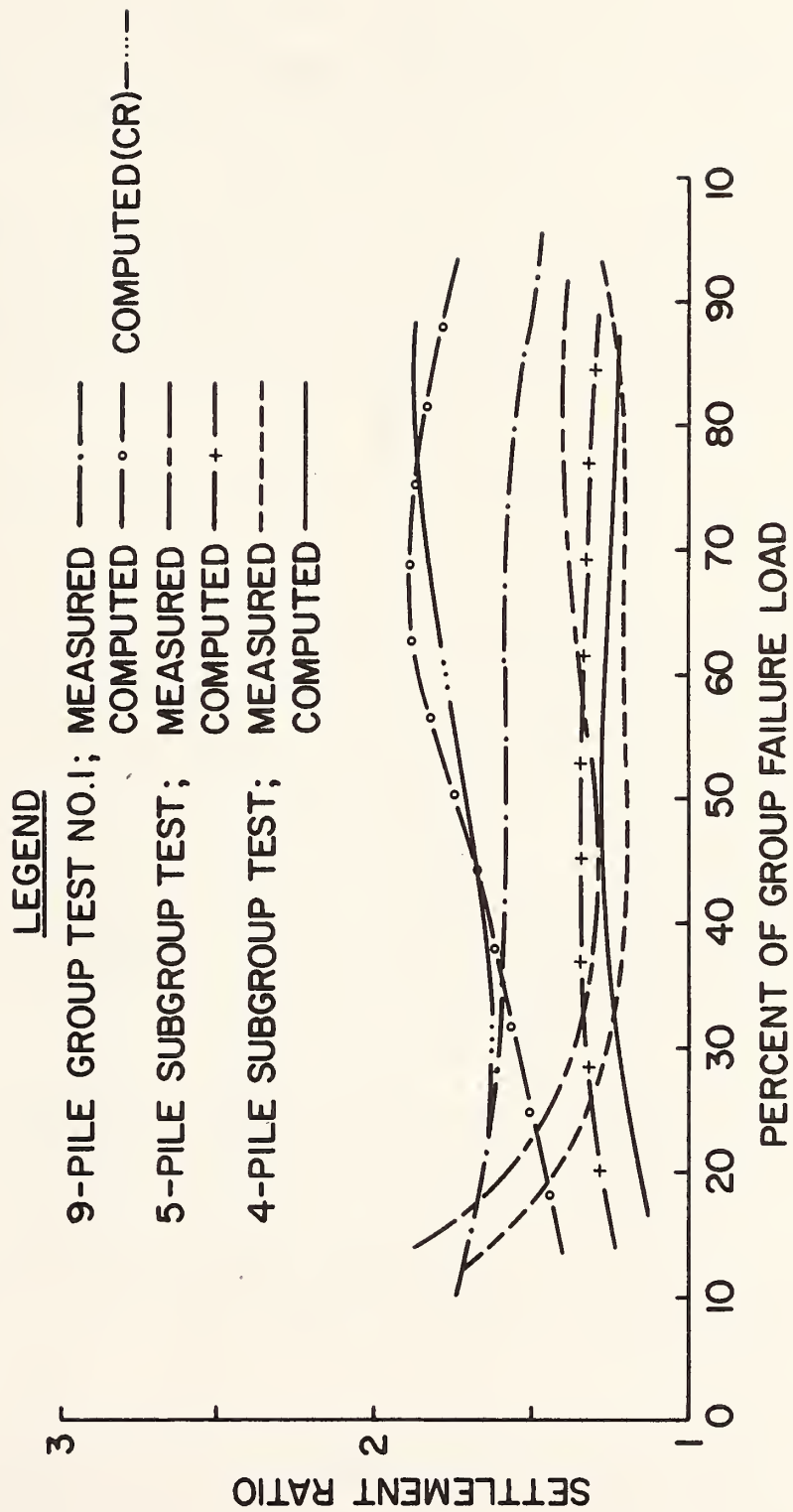


FIGURE 4.9. MEASURED AND COMPUTED SETTLEMENT RATIOS; 9-PILE TEST 1

Computed distributions of loads to the pile heads are tabulated for the case of $E = 25$ ksi (172 mN/m^2) and no p-y input in Table 4.4, which also gives the measured values. In general, the correspondence is good, although some differences exist at a load of 1274.7 k (5.67 mN), which was the measured failure load. The computed loads for the reanalyzed case are not symmetric because the program has accounted for pile batter and eccentricity of applied load.

Computed distributions of load along the piles for the reanalyzed case are shown in Figs. 4.10 and 4.11 for applied group loads of 581.4 kips (2.59 mN) and 1274.7 kips (5.67 mN), respectively. The largest deviations from measured behavior appear to be general underestimation of tip load by the model and failure of the model to replicate the high load (primarily high tip load) produced in the center pile at the failure load, which is represented in Fig. 4.11.

It should be emphasized that the loads shown in Figs. 4.10 and 4.11 are apparent loads that do not include residual loads that existed prior to loading.

Subgroups. Analysis was made only for the reanalyzed case. Computed and measured load-settlement curves are shown for the two subgroup tests in Fig. 4.12. The PILGP1 soil inputs were exactly as for the 9-pile test, and the load-settlement curves displayed are for E (uniform) = 25 ksi (172 mN/m^2). Good agreement was achieved with these parameters for the 5-pile group. Settlements for the 4-pile group were slightly excessive, suggesting that E should have been slightly greater for this group. It is speculated that the requirement for a higher E for the 4-pile group may be the result of wider pile spacing ($4.2 d$ compared with $3 d$ for the 9-pile group) and to the effects of prior loads to failure on the behavior of the 4-pile subgroup, which was tested after the 9-pile group and the 5-pile subgroup. The measured and best computed load-settlement curves for the 9-pile test are also shown in Fig. 4.12 for purposes of comparison.

Computed and measured settlement ratios for the subgroups may be compared by referring to Fig. 4.9, and distribution of loads to the pile heads at load values representative of working loads may be seen in Table 4.4. Computed and measured load distributions along piles for an applied load of 278.9 k (1241 kN) on the 5-pile subgroup are plotted in Fig. 4.13. Figure 4.14 shows similar plots for an applied load of 287.6 k (1280 kN) on the 4-pile subgroup. The computed relationships of load to depth deviate from the measured relationships in a manner similar to that observed for the 9-pile test.

Observations

The hybrid model, in the algorithmic form of Program PILPG1, appears to have yielded satisfactory results for this field test study when unit soil resistance curves developed from reference piles and

TABLE 4.4 DISTRIBUTION OF LOADS TO PILES FROM PILGPI ANALYSES (1 k = 4.45 kN)

TEST	PILE	AXIAL PILE HEAD LOADS (K)									
		LOAD = 581.4 K		LOAD = 1166.1 K		LOAD = 1274.7 K					
		MEASURED	COMPUTED	MEASURED	COMPUTED	MEASURED	COMPUTED				
9-PILE GROUP	2	59.9	61.9	62.1	128.8	125.0	154.4	137.7			
	3	68.6	64.4	64.1	124.6	130.5	135.1	143.4			
	4	65.7	64.9	65.8	132.8	129.3	140.9	135.9			
	5	62.2	64.1	64.1	127.3	128.2	139.4	135.2			
	6	64.3	65.7	65.8	130.5	129.1	144.9	134.8			
	7	61.0	64.9	64.1	116.6	130.9	126.0	144.7			
	8	67.5	65.8	65.8	131.8	130.4	131.0	146.5			
	9	64.1	63.8	64.1	135.8	128.8	152.2	145.5			
	10	68.0	65.8	65.8	137.8	133.8	150.9	150.9			
	5-PILE SUBGROUP		LOAD = 278.9 K								
2		50.5	54.3								
3		58.2	54.9								
5		55.9	59.2								
7		56.2	57.4								
9	53.4	53.1									
4-PILE SUBGROUP		LOAD = 287.6 K									
	3	76.5	69.9								
	5	75.4	75.3								
	7	71.2	73.9								
9	64.7	68.7									

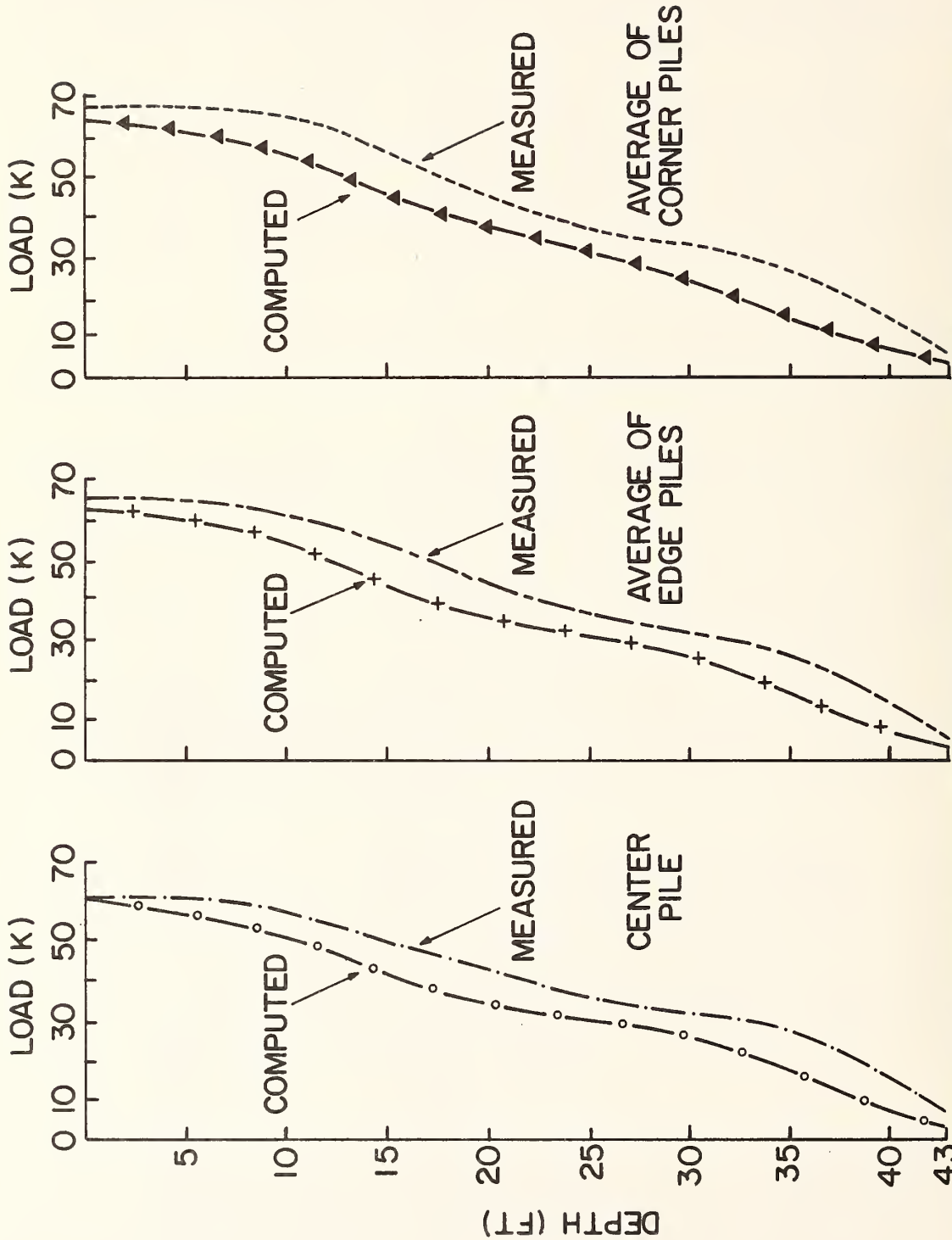


FIGURE 4.10. MEASURED AND COMPUTED DISTRIBUTIONS OF LOADS ALONG PILES; 9-PILE TEST 1;
 LOAD = 581.4 K (1 k = 4.45 kN; 1 ft = 0.305 m)

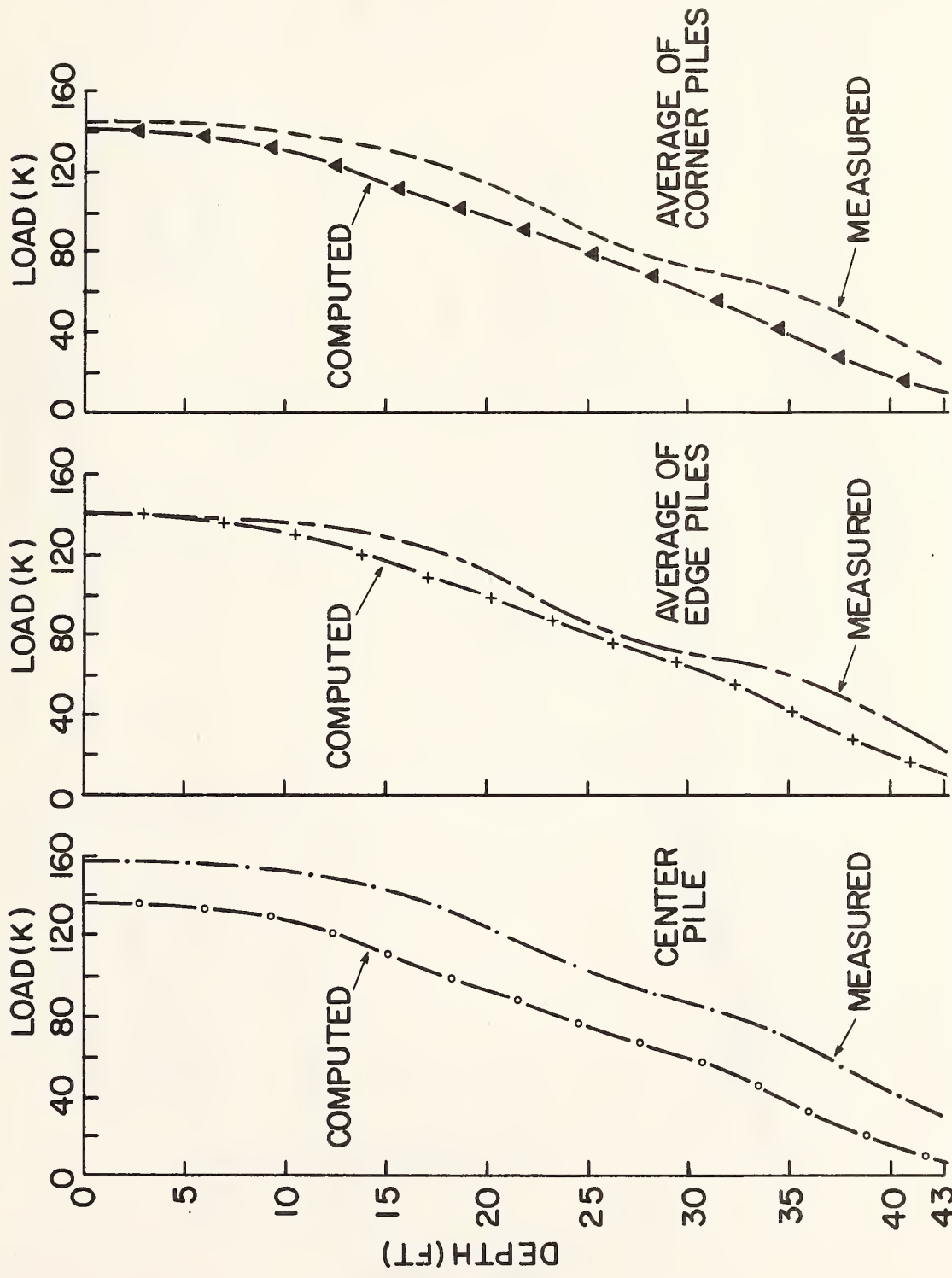


FIGURE 4.11. MEASURED AND COMPUTED DISTRIBUTIONS OF LOADS ALONG PILES; 9-PILE TEST, 1;
 LOAD = 1274.7 K (1 k = 4.45 kN; 1 ft = 0.305 m)

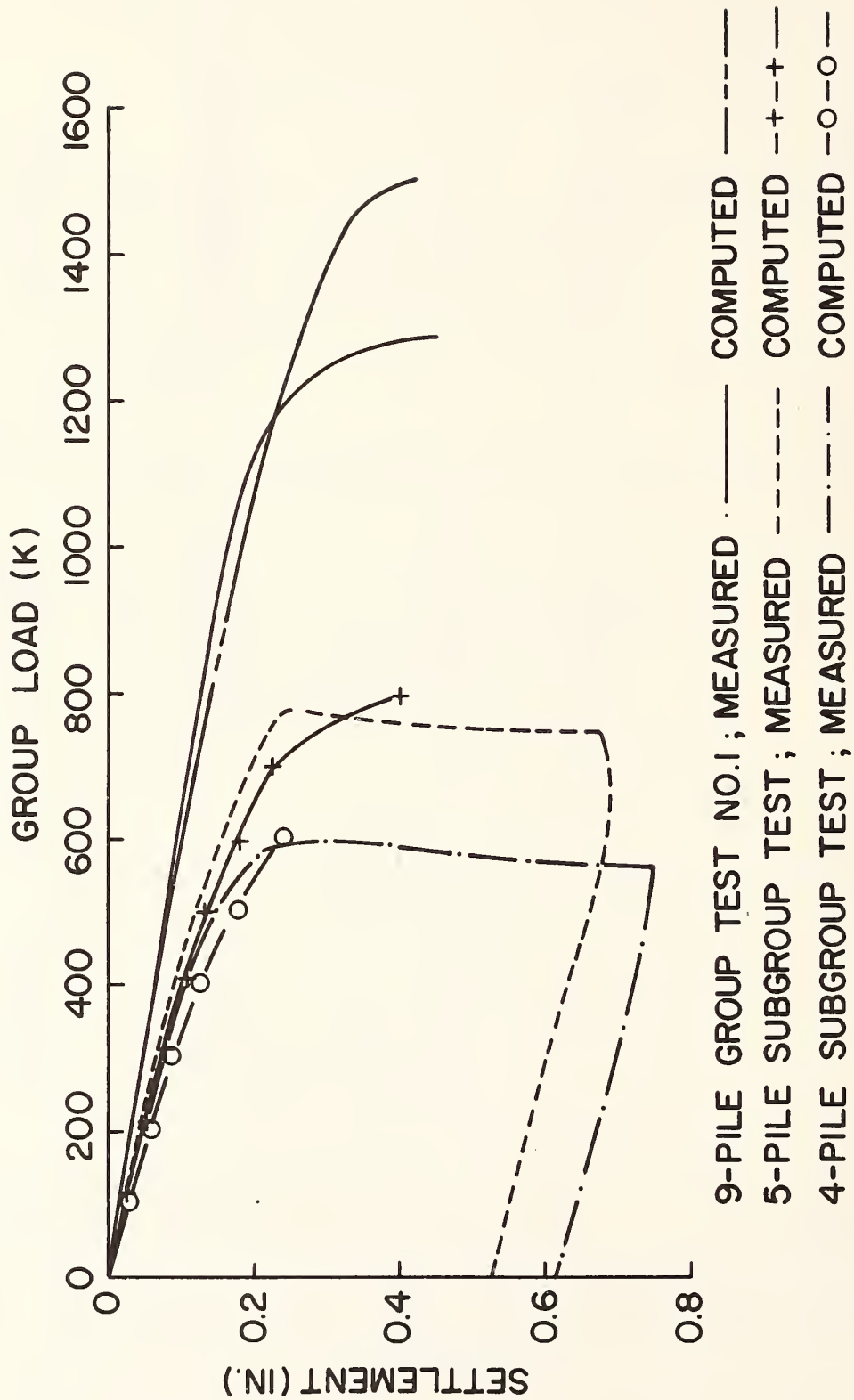


FIGURE 4.12. MEASURED AND COMPUTED LOAD-SETTLEMENT CURVES; SUBGROUP TESTS
 (1 k = 4.45 kN; 1 in = 25.4 mm)

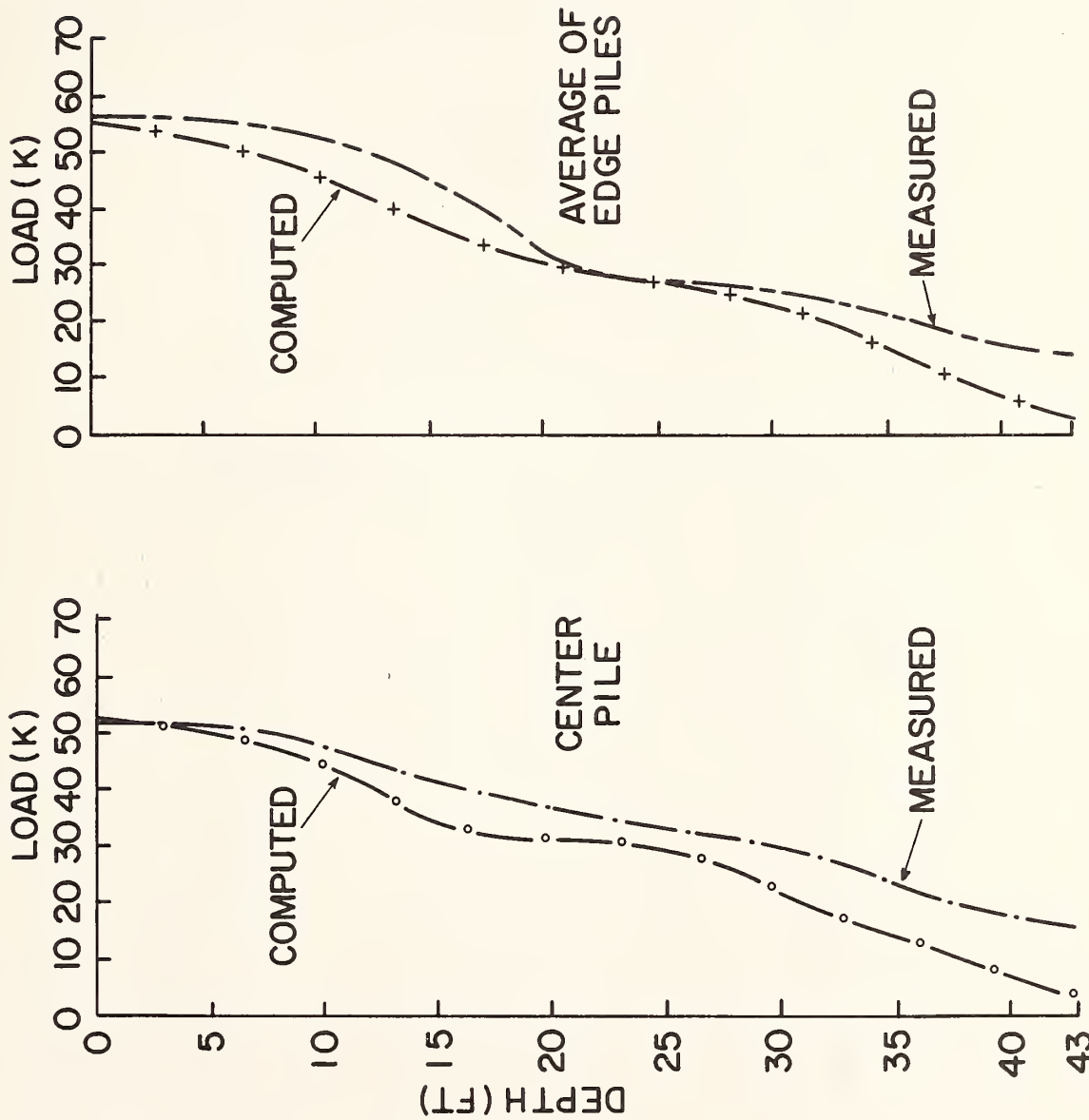


FIGURE 4.13. MEASURED AND COMPUTED DISTRIBUTIONS OF LOADS ALONG PILES; 5-PILE TEST; LOAD = 278.9 K (1k = 4.45 kN; 1 ft = 0.305 m)

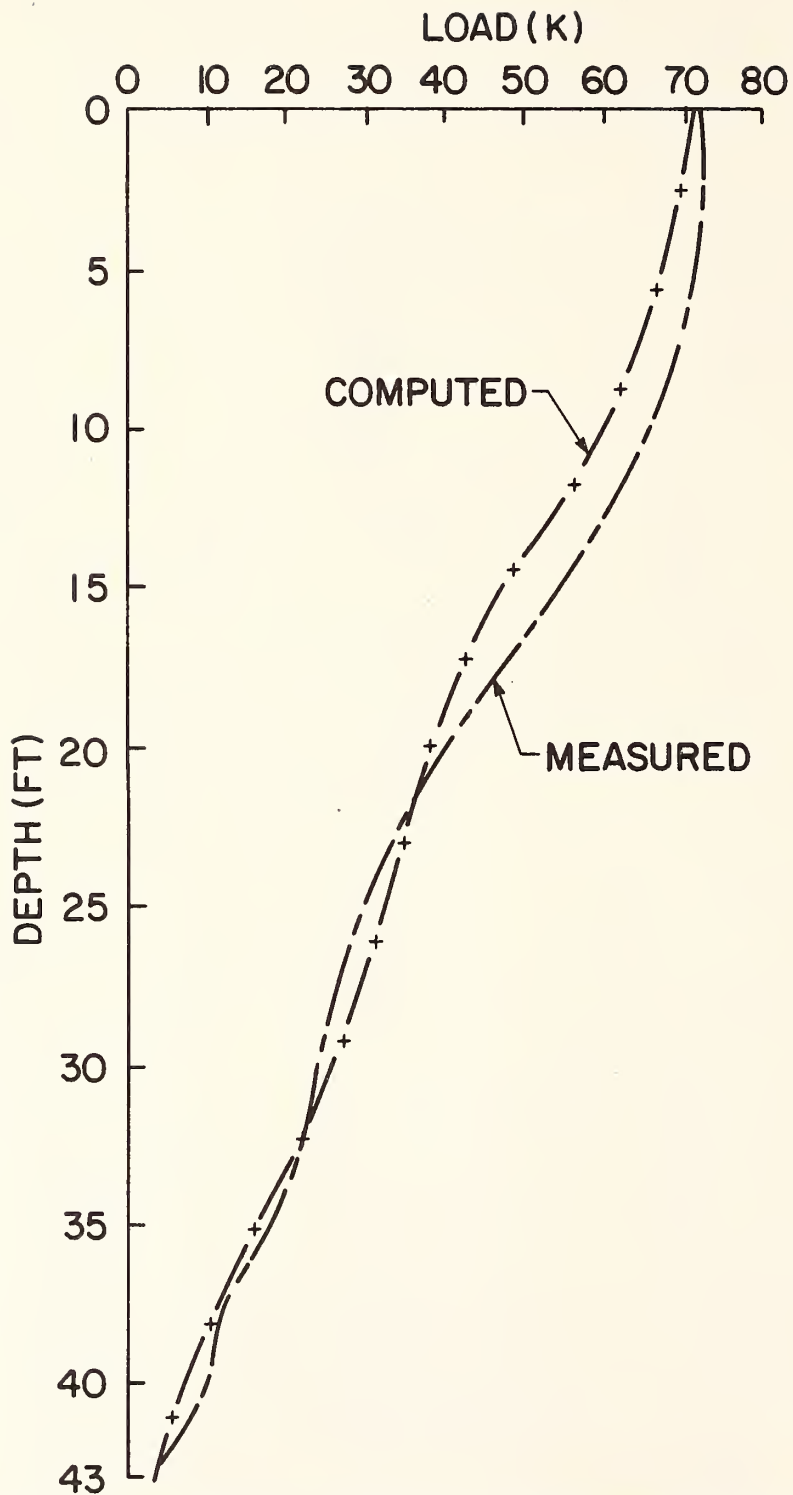


FIGURE 4.14. MEASURED AND COMPUTED DISTRIBUTION OF LOADS ALONG PILES;
 4-PILE TEST; LOAD = 287.6 K (1 k = 4.45 kN; 1 ft = 0.305 m)

elastic soil properties representative of incompressible soil behavior (Poisson's ratio = 0.5) and of very low strain levels (constant Young's modulus approximately twice the value of the modulus measured by the self-boring pressuremeter at the level of the pile tips) are used. The authors realize that use of the term "satisfactory" implies an element of judgment on their part and that the reader may wish to interpret the term in light of specific criteria that he or she might have for assessing modeling accuracy.

Use of criteria load transfer curves and ideal geometry also appear satisfactory, although less accurate.

Chapter 5. Recommendations for Future Study

Based upon observations that the authors have made during this study, the following general recommendations for further research into the behavior of statically, vertical loaded pile groups are offered.

1. While the study reported herein is believed to represent an important step in the understanding of pile group behavior, direct application of the experimental findings is limited, as discussed earlier. Further full-scale tests are necessary to develop a similar level of understanding in other soils. In particular, there exists a general paucity of data for pile groups in sand, and the existing test data are contradictory with respect to factors needed by designers, including efficiency and settlement ratio. These apparent anomalies may be primarily the result of installation effects (pre-drilling, partial jetting, order of driving, installation of all piles simultaneously) and of the in-situ conditions of the sand (density, compressibility, degree of overconsolidation, piezometric conditions, stratigraphy). The "mechanical" interaction effect, that is, the settlement and load transfer induced in one pile in a group by loadings on other piles, is probably less important and can probably be handled adequately by existing analytical procedures (e.g., by one or more of the models described in the Interim Report) once the effects of installation on load transfer and load-settlement for various individual piles in a group are known.

Therefore, a full-scale field study should be undertaken to test individual instrumented piles within groups of various sizes and spacings, and for appropriate reference piles, in which installation techniques are varied. Sand stratigraphy variations should also be considered. Such a study should yield practical, statistically significant information and would be cost-effective compared to conducting tests on complete groups of piles. Full-scale, or near full-scale, tests would be warranted because of difficulty in the physical modeling of certain important effects such as arching and grain crushing within the sand. In this regard the program of physical model testing at various scales now being undertaken by Mr. Carl Ealy of the FHWA should provide useful insight into the minimum size of piles required for such a field study. Measurement of residual stresses in the field should be emphasized because it is believed that the "critical depth" (depth at which ultimate unit side resistance ceases to increase linearly with depth) may be strongly dependent on the residual stress distribution and that such distribution may be considerably different in pile groups than in isolated piles.

2. The effects of cyclic and long-term loading for groups in sands and in normally or slightly overconsolidated clays can best be studied by instrumentation and careful observation of in-service pile groups. In order for such studies to be effective, considerable

attention must be given to details of load and settlement measurements, particularly with respect to long term stability, and to coordination of activities with the bridge construction contractor. High quality soil compressibility data must also be obtained.

3. The bearing capacity of the pile cap and the cap's effect on load-settlement response may be important for bridge foundations that can settle enough for consistent cap capacity to develop. It is the authors' opinion that at working load (low-settlement) levels, cap resistance is too unpredictable to be relied upon in design, but at settlements of greater than perhaps 1 in. (25.4 mm) cap resistance may become predictable. Several analytical studies (see Interim Report) have been published regarding cap-soil interaction in pile groups. Experimental verification or modification of the analytical results could be developed best through physical (not full-scale) testing because numerous parameters, including method of preparation of the cap bearing surface, degree of cap overhang, moisture content changes in the surface soils, and effects of cyclic and vibratory loading should be systematically studied. Such studies can be justified in a practical sense only if FHWA's and other research into tolerable movements of structures indicates that settlements exceeding about 1 in. (25.4 mm) are acceptable in significant numbers of structures.

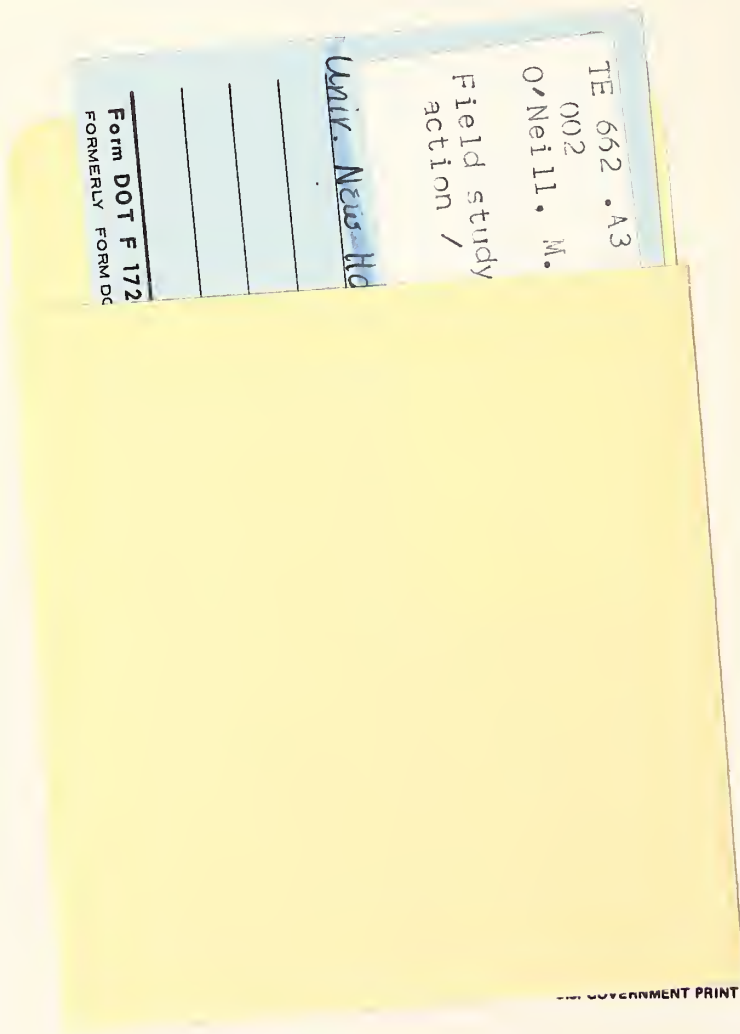
4. Research into the development of purely theoretical approaches to the assessment of single pile and pile group capacity and load-settlement characteristics should be continued if installation of extremely long piles is contemplated for transportation-related structures.

Behavior of such piles (e.g., piles longer than about 150 ft. (45.8 m)), especially in groups, is largely beyond the limit of empirical knowledge. This may continue to be the case because of the expense involved in conducting full-scale load tests on instrumented piles of that length. A strong effort should be made to validate newly developed theories by comparing predictions to measurements acquired recently in several notable tests, including tests conducted for the FHWA at Ellis Island, Mo., the tests conducted at the Keehi interchange, Oahu, Hawaii, and the tests reported herein.

5. With regard to Recommendation 4, future field test experiments should be designed to measure effective stresses against the faces of friction piles and at points within the soil mass. This recommendation is made because new completely theoretical models will likely involve the direct or implied usage of effective stresses. Before such measurements can be made reliably, further development of total stress and/or effective stress cells should be undertaken.

6. No prediction of single pile or pile group behavior can be made reliably unless proper soil information is available. The results of this study and of other experiences by the authors suggest that soil

properties derived from in-situ testing procedures should lead to enhanced prediction of pile shaft and tip capacities and of deformations in the soil mass. Research into the development of in-situ test methods should therefore be continued with an emphasis on simple methods that will be implemented by potential users.



FEDERALLY COORDINATED PROGRAM (FCP) OF HIGHWAY RESEARCH AND DEVELOPMENT

The Offices of Research and Development (R&D) of the Federal Highway Administration (FHWA) are responsible for a broad program of staff and contract research and development and a Federal-aid program, conducted by or through the State highway transportation agencies, that includes the Highway Planning and Research (HP&R) program and the National Cooperative Highway Research Program (NCHRP) managed by the Transportation Research Board. The FCP is a carefully selected group of projects that uses research and development resources to obtain timely solutions to urgent national highway engineering problems.*

The diagonal double stripe on the cover of this report represents a highway and is color-coded to identify the FCP category that the report falls under. A red stripe is used for category 1, dark blue for category 2, light blue for category 3, brown for category 4, gray for category 5, green for categories 6 and 7, and an orange stripe identifies category 0.

FCP Category Descriptions

1. Improved Highway Design and Operation for Safety

Safety R&D addresses problems associated with the responsibilities of the FHWA under the Highway Safety Act and includes investigation of appropriate design standards, roadside hardware, signing, and physical and scientific data for the formulation of improved safety regulations.

2. Reduction of Traffic Congestion, and Improved Operational Efficiency

Traffic R&D is concerned with increasing the operational efficiency of existing highways by advancing technology, by improving designs for existing as well as new facilities, and by balancing the demand-capacity relationship through traffic management techniques such as bus and carpool preferential treatment, motorist information, and rerouting of traffic.

3. Environmental Considerations in Highway Design, Location, Construction, and Operation

Environmental R&D is directed toward identifying and evaluating highway elements that affect

the quality of the human environment. The goals are reduction of adverse highway and traffic impacts, and protection and enhancement of the environment.

4. Improved Materials Utilization and Durability

Materials R&D is concerned with expanding the knowledge and technology of materials properties, using available natural materials, improving structural foundation materials, recycling highway materials, converting industrial wastes into useful highway products, developing extender or substitute materials for those in short supply, and developing more rapid and reliable testing procedures. The goals are lower highway construction costs and extended maintenance-free operation.

5. Improved Design to Reduce Costs, Extend Life Expectancy, and Insure Structural Safety

Structural R&D is concerned with furthering the latest technological advances in structural and hydraulic designs, fabrication processes, and construction techniques to provide safe, efficient highways at reasonable costs.

6. Improved Technology for Highway Construction

This category is concerned with the research, development, and implementation of highway construction technology to increase productivity, reduce energy consumption, conserve dwindling resources, and reduce costs while improving the quality and methods of construction.

7. Improved Technology for Highway Maintenance

This category addresses problems in preserving the Nation's highways and includes activities in physical maintenance, traffic services, management, and equipment. The goal is to maximize operational efficiency and safety to the traveling public while conserving resources.

0. Other New Studies

This category, not included in the seven-volume official statement of the FCP, is concerned with HP&R and NCHRP studies not specifically related to FCP projects. These studies involve R&D support of other FHWA program office research.

* The complete seven-volume official statement of the FCP is available from the National Technical Information Service, Springfield, Va. 22161. Single copies of the introductory volume are available without charge from Program Analysis (HRD-3), Offices of Research and Development, Federal Highway Administration, Washington, D.C. 20590.

DOT LIBRARY



00057035

